AD NUMBER

AD827947

NEW LIMITATION CHANGE

TO

Approved for public release, distribution unlimited

FROM

Distribution authorized to U.S. Gov't. agencies and their contractors; Critical Technology; JAN 1968. Other requests shall be referred to Army Mobility Equipment Research and Development Center, Attn: SMEFB-EP, Fort Belvoir, VA 22060.

AUTHORITY

USAMERDC notice, dtd 24 May 1971

U2-202452-2

15-kW HYDROCARBON-AIR FUEL CELL ELECTRIC POWER PLANT DESIGN

FINAL REPORT

by

J.K. Truitt

January 1968

U. S. ARMY MOBILITY EQUIPMENT
RESEARCH AND DEVELOPMENT CENTER
Fort Belvoir, Virginia

Prepared Under Contract DA-44-009-AMC-1806(T)

by

TEXAS INSTRUMENTS INCORPORATED
13500 North Central Expressway
Dallas, Texas 75222

NOTICES

AVAILABILITY

This document is subject to special export controls and each transmittal to foreign governments or foreign nationals may be made only with prior approval of Mobility Equipment Command Research and Development Center, Power Equipment Division, SMEFB-EP, Fort Belvoir, Va. 22060.

DISCLAIMERS

The findings in this report are not to be construed as an official Department of the Army position, unless so designated by other authorized documents.

The citation of trade names and names of manufacturers in this report is not to be construed as official Government indorsement or approval of commercial products or services referenced herein.

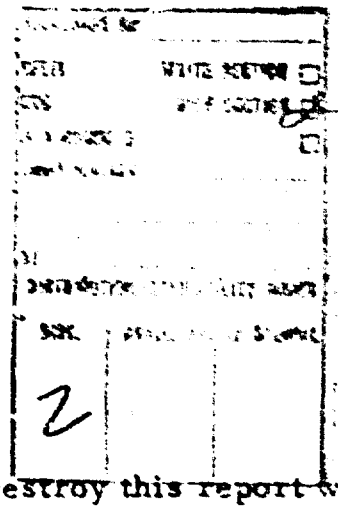

DISPOSITION

Destroy this report when it is no longer needed. Do not return it to the originator.

AD

U2-202452-2

15-kW HYDROCARBON-AIR FUEL CELL ELECTRIC POWER PLANT DESIGN

FINAL REPORT

by

J.K. Truitt

[redacted]

Prepared Under Contract DA-44-009-AMC-1806(T)

by

TEXAS INSTRUMENTS INCORPORATED
13500 North Central Expressway
Dallas, Texas 75222

TABLE OF CONTENTS

TABLE OF CONTENTS (Continued)

LIST OF ILLUSTRATIONS

LIST OF ILLUSTRATIONS (Continued)

LIST OF ILLUSTRATIONS (Continued)

LIST OF TABLES

SUMMARY

This final report covers the development, construction, and testing of breadboard representations of critical subsystems and components as required in the designed 15-kilowatt fuel cell power supply, described in the interim report of Contract No. DA-44-009-AMC-1806(T), dated October 1966. The experimental work described herein is a part of the same contract.

The critical subsystems and components, as designated by the interim technical report, were as follows:

A. Cell stack or module, 1-kilowatt size

B. Partial oxidizer, 1-kilowatt size

C. Liquid fuel dispersion, 3-kilowatt size

D. Startup burner system, 15-kilowatt size

E. Gaseous fuel scrubber, 1-kilowatt size

F. Spent fuel recycle blower, 1-kilowatt size.

Demonstration of the 1-kilowatt module stack breadboard has been delayed by establishment of startup procedures for the 100-cell modules, but will be completed shortly. Achievement of this demonstration will now be followed by integration with other components to form a complete 1-kilowatt prototype system.

Partial-oxidation development was demonstrated in combination with the liquid fuel dispersion breadboard since, during the experimental work period, a simple vaporization technique was found very satisfactory, thus eliminating the need for continued development of the ultrasonic atomizer. It was the latter which indicated the 3-kilowatt size. Numerous test periods, including two continuous 100-hour tests, were successfully carried out on both combat gasoline and CITE fuel.

Although called for at the 15-kilowatt size, the startup burner breadboard was executed at the 1-kilowatt level because it was determined, following the preparation of the interim report that lightweight burners of suitable design were available covering the size range called for. Therefore, development work was carried out at the smaller size in order to be able to incorporate the unit into the now planned 1-kilowatt prototype unit. The modified aircraft cabin heater was operated repeatedly on combat gasoline and CITE fuel.

The least critical of the subsystems selected for investigation was the gaseous fuel scrubber. The efficiency of a molten salt scrubber and the use of dispersed nickel on a support was demonstrated, but demonstration at the 1-kilowatt, 50-hour level has not been completed. This work is being continued to completion.

Spent fuel recycle blowers were designed and fabricated with the assistance of Torrington, an experienced vendor of larger, high-temperature blowers. Testing for more than 100 hours under operating conditions has been carried out successfully.

Continued module development effort during the period reported has resulted in considerable advances in cell performance and operating life. The most recent of these has not yet been incorporated into large-module fabrication but will be the basis for the 3-inch by 8-inch cells being investigated in the period covered by the contract modification. The recent tests have demonstrated greater than 500-hour operating life capability and greater than 40 watts per square foot stable output, lending considerable reassurance to the projections called for in the establishment of a qualified 15-kilowatt field power unit.

Tests, as executed, indicate that the 15-kilowatt unit design as projected can be attained with continued development.

SECTION I

PROGRAM OBJECTIVES

The purpose of this contract is to perform a systems analysis and furnish a design of a 15-kilowatt fuel cell electric power plant based on the Texas Instruments molten carbonate concept, utilizing designated military fuels. This analysis covers the complete system and the major interrelated components, designed basically to meet the requirements of the U. S. Army Engineer Research and Development Laboratories' "Purchase Description for 15-kilowatt Hydrocarbon-Air Fuel Cell Electric Power Plant," dated 28 January 1966. The contract work is further intended to prove the practicality of this engineering design through fabrication, assembly, and testing of critical subsystems and/or components. An Interim Report, dated October 1966, relates the results of the systems analysis and establishes the critical subsystems and/or components to be experimentally evaluated. Results of these experimental evaluations and the influence of these results on the design of the total systems, as shown in Figure 1-1, are the subject of this report.

The contract has been modified to permit additional work on enlarged cell modules and to alter the deliverable items from the separate experimental subsystem test units to a single 1-kilowatt Prototype Demonstration Unit. An additional report covering this additional work will be prepared at the conclusion of the modified contract.

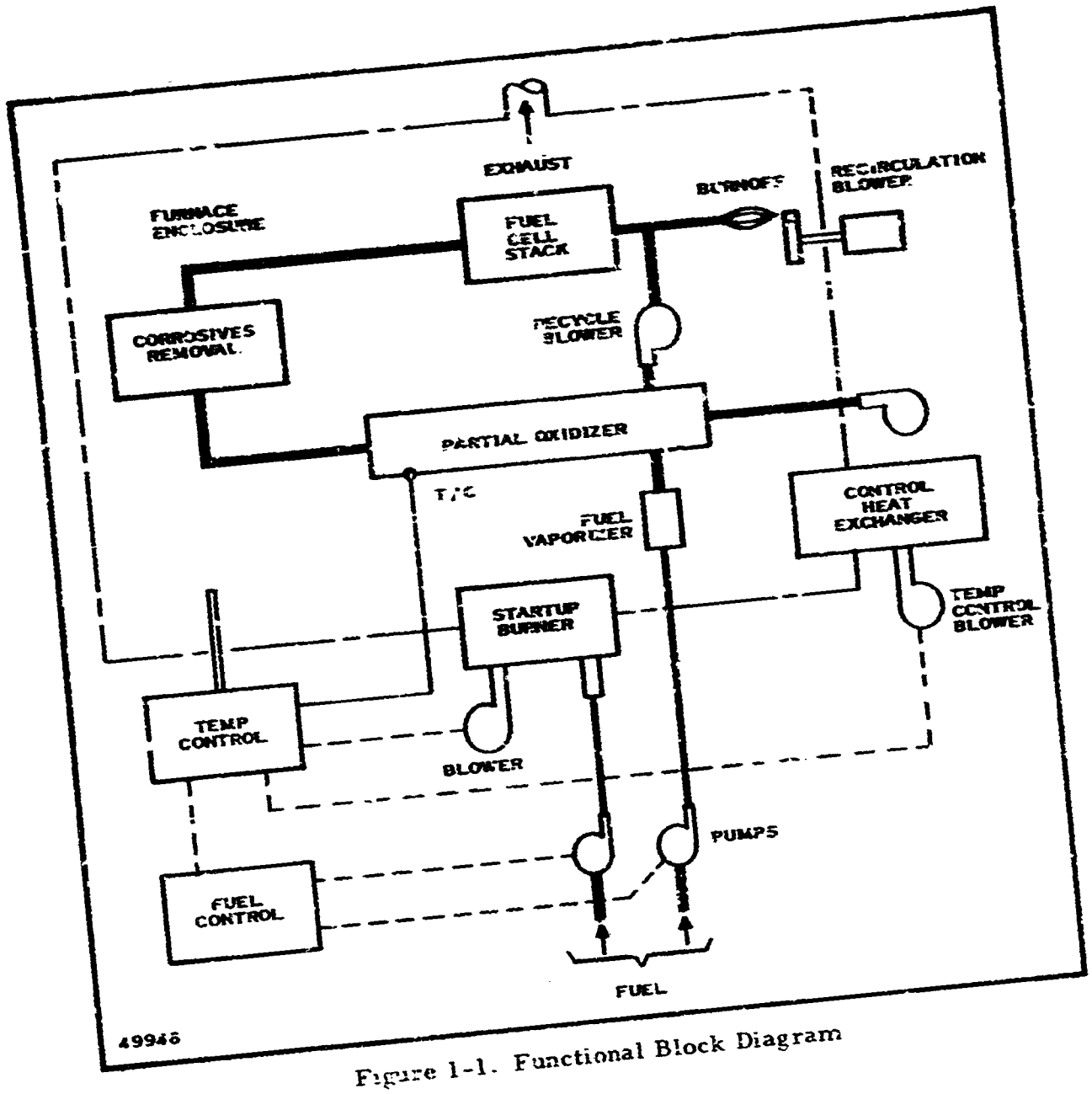

Figure 1-1. Functional Block Diagram

SECTION II

INVESTIGATION OF CRITICAL SUBSYSTEMS

A. INTRODUCTION

The operational unit, based on the combined use of air–partial oxidation of liquid hydrocarbon fuels–and the molten carbonate fuel cell, has been investigated by experimental evaluation of subsystems that were thought to be critical. Figure 1-1 is a functional schematic of the total system, exclusive of the converter.

Study of the total system during the initial phase of the contract indicated the following subsystems needed experimental demonstration and development.

Cell stack or modules

Partial oxidizer

Liquid fuel dispersion

Startup burner

Gaseous fuel scrubber

Spent fuel recycle blower

Establishment of these as critical subsystems was the subject of the Interim Technical Report, dated October 1966.

The following sections report the experimental work carried out in the development of each of these and, in addition, the control system and electric output conditioning are discussed.

B. FUEL CELL MODULE

1. Design Basis

The basis of the Texas Instruments fuel cell module design is practicality. The ideal cell might consist of two invariant electrodes, both exhibiting active areas typical of catalysts, separated by an electrolyte of zero resistance. The actual cell should consist of (1) electrodes which do not flood easily, (2) electrode materials which exhibit a minimum of nonproductive corrosion, (3) a matrix which is opaque to gases but transparent to ions when saturated with electrolyte, and (4) a method of assembly which minimizes nonproductive weight and volume.

The design criteria for the present module were:

Maximum packing density (i.e., maximum active electrode area per unit volume)

Minimum specific weight (i.e., minimum weight per unit active electrode area)

Resistance to deleterious effects of temperature cycling

Resistance to corrosion

Adaptable to mass production techniques

Capable of considerable cost reduction in high quantity production.

Figure 1-1 shows the basic crossflow configuration (the apparent similarity to heat exchanger construction has led some to label it the heat exchanger design) with the active cell area separating the fuel and air sides. Theoretically, the width of the air and fuel passages can be decreased until the pressure drop becomes significant. Actually, the gas flow channels must be wide enough to accommodate the welding electrodes used in the assembly of the modules. The height of the cell is limited by the degree and distribution of the molten electrolyte. A limit has not been set. Most test cells have been 4 or 5 inches in height. Preliminary results indicate that 8 inches is not excessive. As with the width of the gas passages, it is probable that the practical height will be that which can be assembled economically. The cell length (horizontal dimension) depends on the voltage required (number of cells in series), the gas flow rate, and the expected utilization. In addition, since the current increases proportionally to the length, the ohmic power loss may limit the dimension.

The necessary sealing and interconnection structure requires about 3/8 inch to be added to the height and length of the cell. Thus, a cell with an active area of 1 by 4 inches will occupy an area of 1.375 by 4.375 inches, and the active area will be about 67 percent of the total area. Similarly, the active area of a 3- by 8-inch cell will be about 85 percent of the total area. Obviously, to maximize the packing density, the cells should be as large as possible in area and the gas passage width should be minimized.

Specific weight relates to system size. System components other than the module exhibit relatively little change as system size changes. For example, the weight of auxiliaries in a 15-kilowatt system is only three times the weight of those in a 1-kilowatt system (not 15 times). Conversely, the module weight is nearly linear. Thus, an absolute minimum specific weight can be approached only as system size increases.

A practical fuel cell power system must be capable of repeated startups (from cold condition) without loss of performance or effective life. Experience has shown that ceramic (alumina) insulators and spacers cannot endure repeated temperature cycling. The present design eliminated ceramic parts by utilizing the matrix as a structural member as well as a retainer for the electrolyte. During assembly the matrix is compressed between the anode and cathode structures. The resulting friction provides a cell assembly with the anodes and cathodes electrically isolated, yet which exhibits sufficient structural integrity at operating temperatures. Actual module tests have shown no performance loss after 12 complete temperature cycles. Further tests are planned for series modules which might be more susceptable to temperature-cycling damage. The classic description of a fuel cell involves the electrochemical combination of fuel and oxygen on "invariant" electrodes. Actually, both electrodes (and structural members) are contacted by electrolyte. At operating temperature the cell can operate as a battery. It may be that even in the fuel cell operating mode there will still be a small contribution from battery action (corrosion). In any case, any (and every) molten carbonate fuel cell has shown some evidence of corrosion.

Corrosion on the cathode side seems to be controlled somewhat by keeping the oxygen-carbon dioxide ratio at about 1:2. Unfortunately, the CO_2 available in actual systems is only about 10 percent. The cathode side mixture of 5 percent O_2 and 10 percent CO_2 does not afford the protection realized in the laboratory where the O_2 can be about 15 percent and the CO_2 about 30 percent.

Serious corrosion of the anode is probably more common than corrosion on the cathode side. Actually, a certain amount of corrosion (activation) seems indicated to improve cell performance. Another facet of anode corrosion involves utilization. It is probable that anode corrosion increases as the H_2 content of the fuel decreases due to utilization. The limit or threshold utilization has not been established.

It is characteristic of fuel cells that increased power demands, in proportion, increased area. Thus, at an arbitrary 30 watts per square foot, a 15-kilowatt system will require about 600 square feet of active area or about 3600 cells, each 3 by 8 inches. A 1500-kilowatt system would require 60,000 square feet, and a central station size system would require 200 acres or more of electrode active area. Whether such a requirement

exists in one large system or many smaller systems, it is obvious that uniformity of cell structure and design for easy assembly are paramount. The present design utilizes die cut and die formed parts which can be assembled in proper fixtures and automatically welded. The application of the matrix remains a hand operation at present and considerable development work remains to automate this process.

The cost of fuel cell modules is intimately tied to the degree of automated production attained. In addition, the choice of materials and the power density have obvious relationships with cost. For example, the use of 446 stainless steel as a structural material will decrease material cost and improve corrosion resistance, but difficulties with welding may increase assembly costs unduly.

It is axiomatic that the optimization of any rather complicated system or structure involves compromises in component selection. These compromises will depend on the choice of the primary goal (minimum weight, maximum life, minimum cost, etc.). Such compromises are difficult to make even when complete component information is available. In the case of the fuel cell, where much information is lacking and the balance is rather uncertain, the necessary compromises must be made arbitrarily and may not result in an optimum module or system.

2. Fabrication Techniques

The design of the Texas Instruments fuel cell was specifically aimed at creating a product which could be manufactured at a reasonable cost while achieving the required performance level. This design involves the assembly of the three basic fuel cell elements (anode, cathode and matrix electrolyte) into arrays of cells to achieve the desired power and voltage. The cell elements were designed to be completely interchangeable so that the same parts could be used to construct any size modules.

The manufacturing philosophy which results from the basic design considerations listed above is as follows:

Hold close tolerances in those areas where demanded by interchangeability

Automate as many operations as possible to produce interchangeable parts with minimum labor

Develop prototype fixtures and tooling capable of achieving the production rates necessary to meet the needs of a 15-kilowatt development program, estimate the production costs accurately and determine the manufacturing problem areas which may exist.

Each of the manufacturing operations related to the three basic parts will be discussed showing the fixtures and tooling developed and assembly operations. In most cases possible new techniques will be discussed which would lead to either lower cost or higher production.

a. Anode Fabrication

A composite drawing of the anode is shown in Figure 2-1 and includes information from drawings number 106004, 106009, 106012, 106019, and 106026. The flange, which is shown in Detail 3, is made up of two pieces spot-welded together to form the part. Consideration was given to deep drawing to eliminate the weld, but this would have required progressive die tooling which would cost approximately $20.000. This expenditure was not warranted for the number of parts which were to be produced in this contract and may not be warranted in the 15-kilowatt development program. Figure 2-2 shows the two separate parts and a completed part with the welding fixture used to assemble them. The anode primary, made from 80 mesh nickel screen wire, is die-cut to exact dimension. The primary is then bent on both ends in a fixture to form the shape shown in Detail 1 of Figure 2-1. The anode secondary does not require the close tolerances required of the anode primary and is therefore shear-cut in strips to length. The strips are then corrugated in a gear tooth fixture shown in Figure 2-3. The anode is then cut to length in a fixture which holds the end-to-end dimension, the number of corrugations and the location of the cut by cutting out exactly one lobe of the corrugation (Figure 2-4). This allows the parts to be inserted into a fixture which controls all the pertinent dimensions and allows both the flange-to-primary weld and primary-to-secondary weld to be made on two different welding machines without additional fixturing. The overall width of the anode subassembly is controlled by a series of copper fingers which fit inside each corrugation and are later used as one electrode in the primary-to-secondary welder. This fixture with parts is shown in Figure 2-5.

Three different weld operations are required to make the anode assembly: anode flange, anode flange-to-primary screen, primary-to-secondary screen. All parts are cleaned in Freon cleaning solvents, using both boiling solvents and ultrasonic bath. This cleaning removes all traces of oil and water soluble soils from the parts. After this operation, the parts are handled with gloves or finger cots. The cleaned parts are assembled and placed in the anode flange-to-primary screen spot-weld machine. The weld is made with a stored energy spot welder which is fired every 0.050 inch through a set of rollers. Figure 2-6 shows this machine. The part is removed from this machine and placed on the table of the primary-to-secondary screen welder machine shown in Figure 2-7. This machine welds each secondary corrugation in five places with five stored energy spot welders. The weld electrodes fit into the slots on the fixture and index from corrugation to corrugation. The cycle to weld one side takes about ten seconds;

the part is then turned over and the opposite corrugations are welded similarly.

At the start of this program it took over an hour of assembly time in all operations to produce one anode. With the machines and fixtures shown here, this time has been reduced to about ten minutes per anode. Additional time and cost savings could be made if the anode screen could be changed to expanded metal. This would eliminate the edge-fraying problem with screen and produce a more rugged and dimensionally stable part, while at the same time, making the parts easier to handle.

b. Matrix Application

The matrix is applied to the anode in the form of a paste. The material must be applied in a uniform thickness of 0.024 inch to each face of the anode primary screen and 0.040 inch to the ends of the anode primary screen. Since the anode primary screen is nickel, it must be protected from high-temperature oxidation at the point at which the Type 446 stainless steel flange is welded to the screen. A nonporous protective oxide coat is applied to the screen along the anode flange and at the anode primary ends before application of the matrix. The paste matrix must be kept from extruding through the screen wire anode since the oxide particle size is smaller than the screen mesh opening. A water slurry of powdered sodium-lithium carbonate electrolyte is spread over the anode primary, allowed to dry, and then scraped off to expose the tops of the screen wire. The matrix is applied like concrete and trowelled off as shown in Figure 2-8. The fixture is two-sided with the matrix thickness and total thickness controlled by the fixture. Matrix is applied to the ends in a similar manner with the fixture shown in Figure 2-9. The anode thickness and flatness are controlled at this stage to ±0.005 inch. The ends of the anode assembly with matrix applied is then sanded square to locate the edges of the anode primary screen. This helps ensure that thin spots in the matrix will not result in anode-to-cathode electronic shorts during operation.

The techniques described above require about 45 minutes total time considering all phases of the matrix application. This is one phase of the assembly operation which has not been automated. With the present techniques this will probably not go below 35 minutes per anode. Automation of this process has not been successful to date because of the limited time in which the matrix can be worked and the large number of separate tasks. The short working time for the matrix means that in the process we now use, only a few anodes can be processed per batch. The total time is split up into many small operations followed by periods of air-drying with many stages of visual inspection and gaging. The most successful approach to decreasing assembly time for the matrix will probably result from modifications to the matrix itself, anode construction, and material which eliminates many of the steps now necessary.

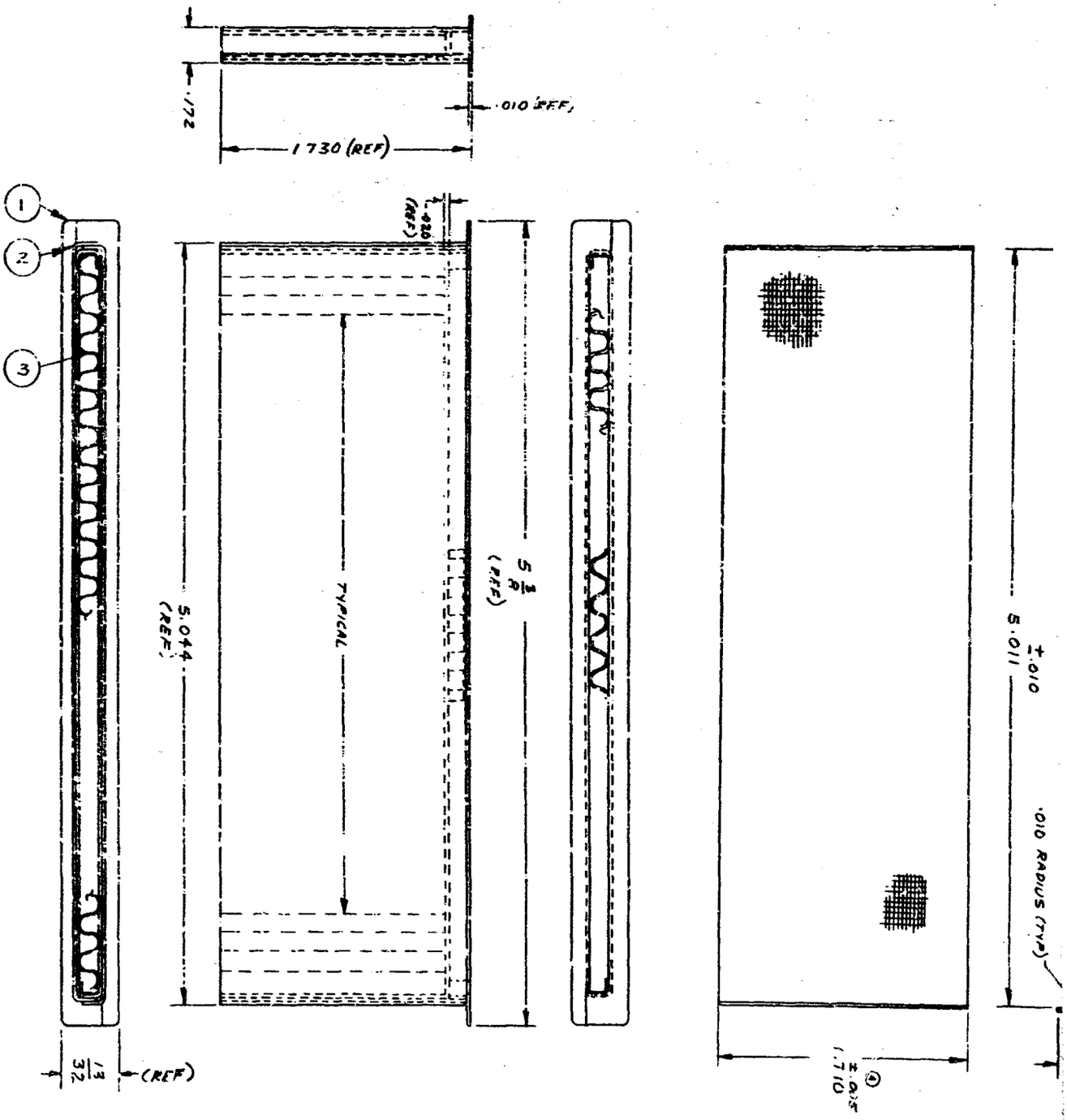
.172
.010 (REF)
1.730 (REF)
1
2
3
.020 (REF)
5.044 (REF)
TYPICAL
5 1/2 (REF)
13/32 (REF)
±.010
5.011
.010 RADIUS (TYP)
±.015
1.710

50363

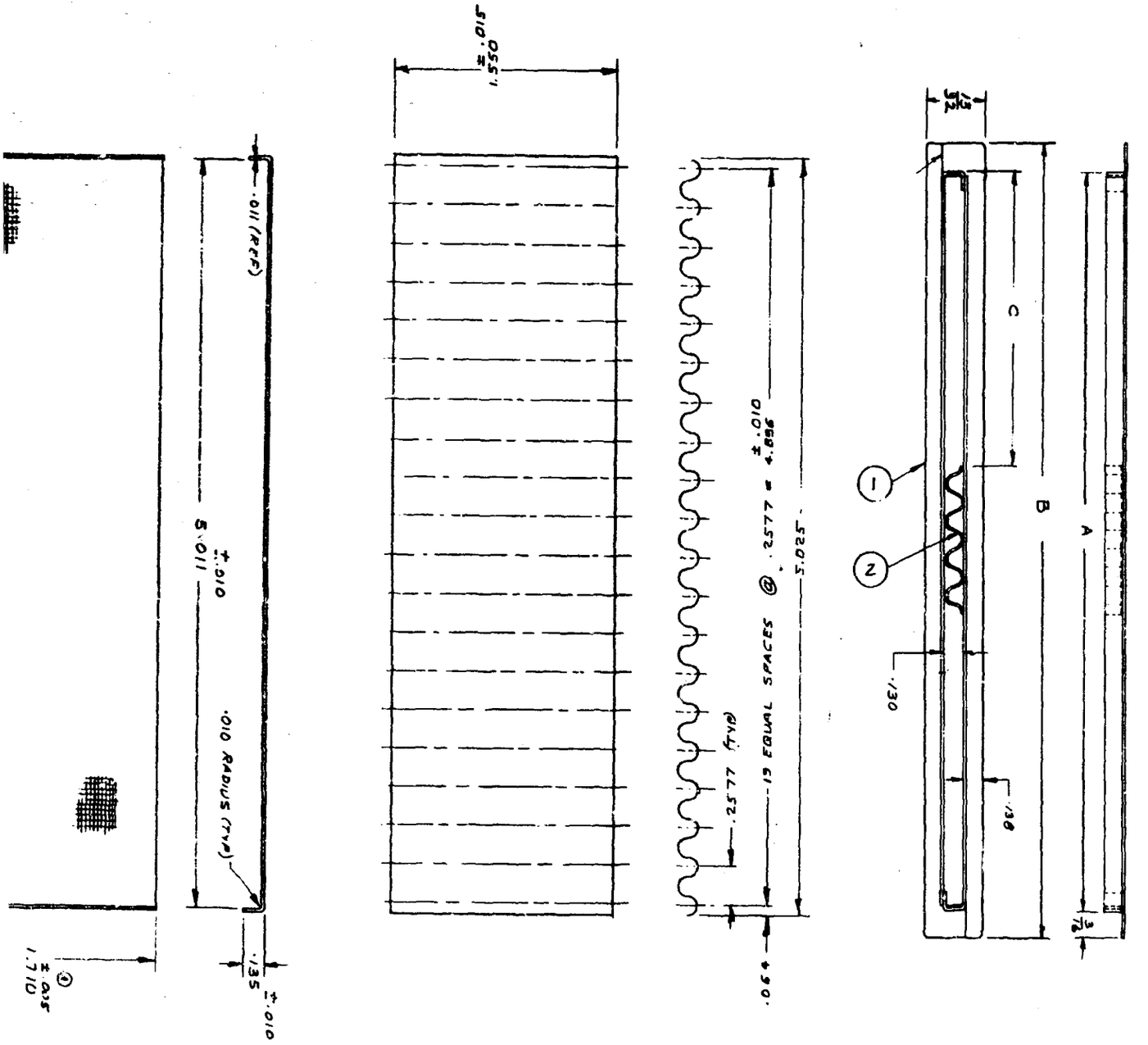

Figure 2-1. Anode Construction

B.

Figure 2-2. Anode Flange Parts and Fixture

Figure 2-3. Anode Secondary Corrugator

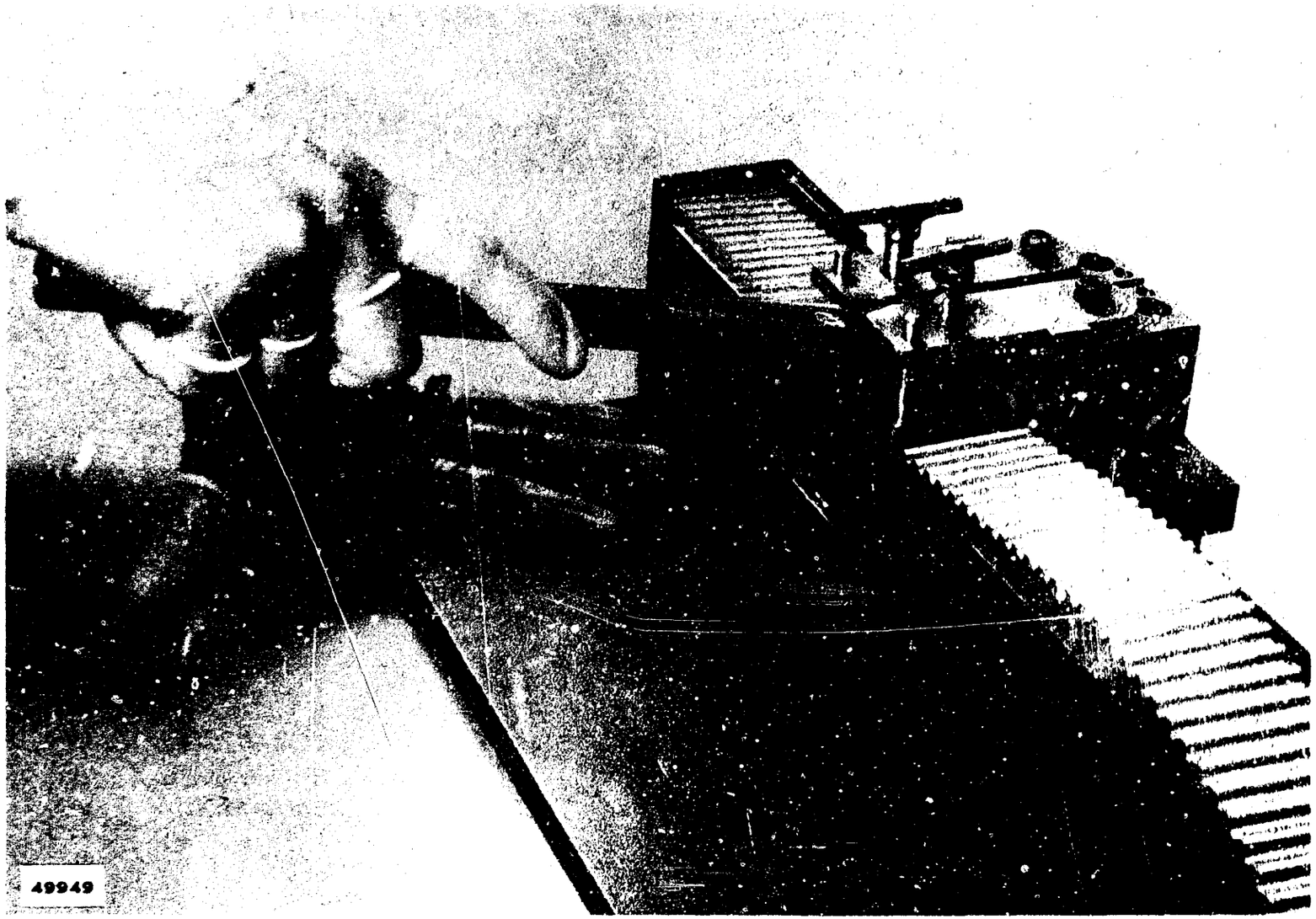

Figure 2-4. Anode Secondary Cutting Fixture

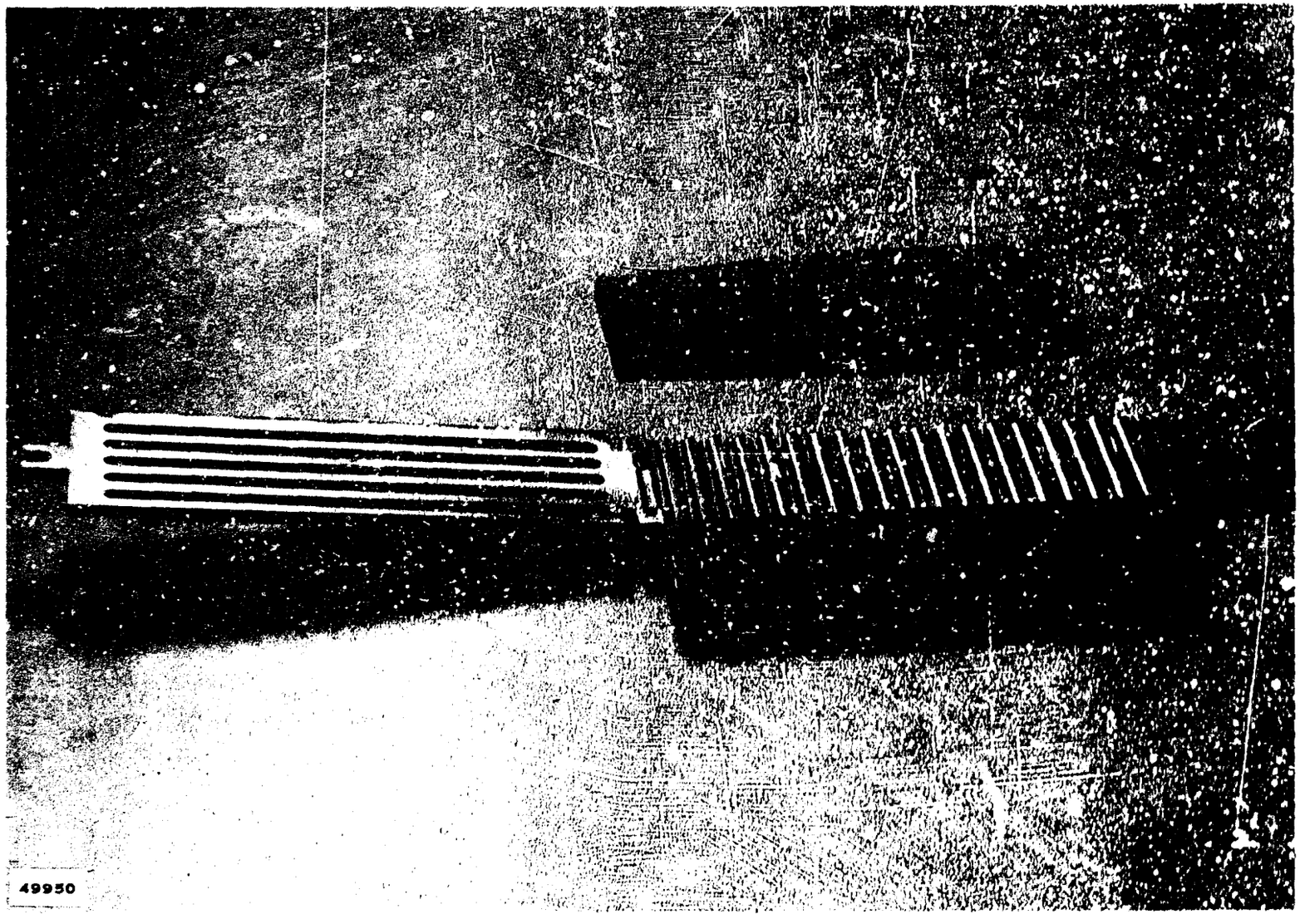

Figure 2-5. Anode Assembly Welding Fixture

Figure 2-6. Anode Flange-to-Primary Weld Machine

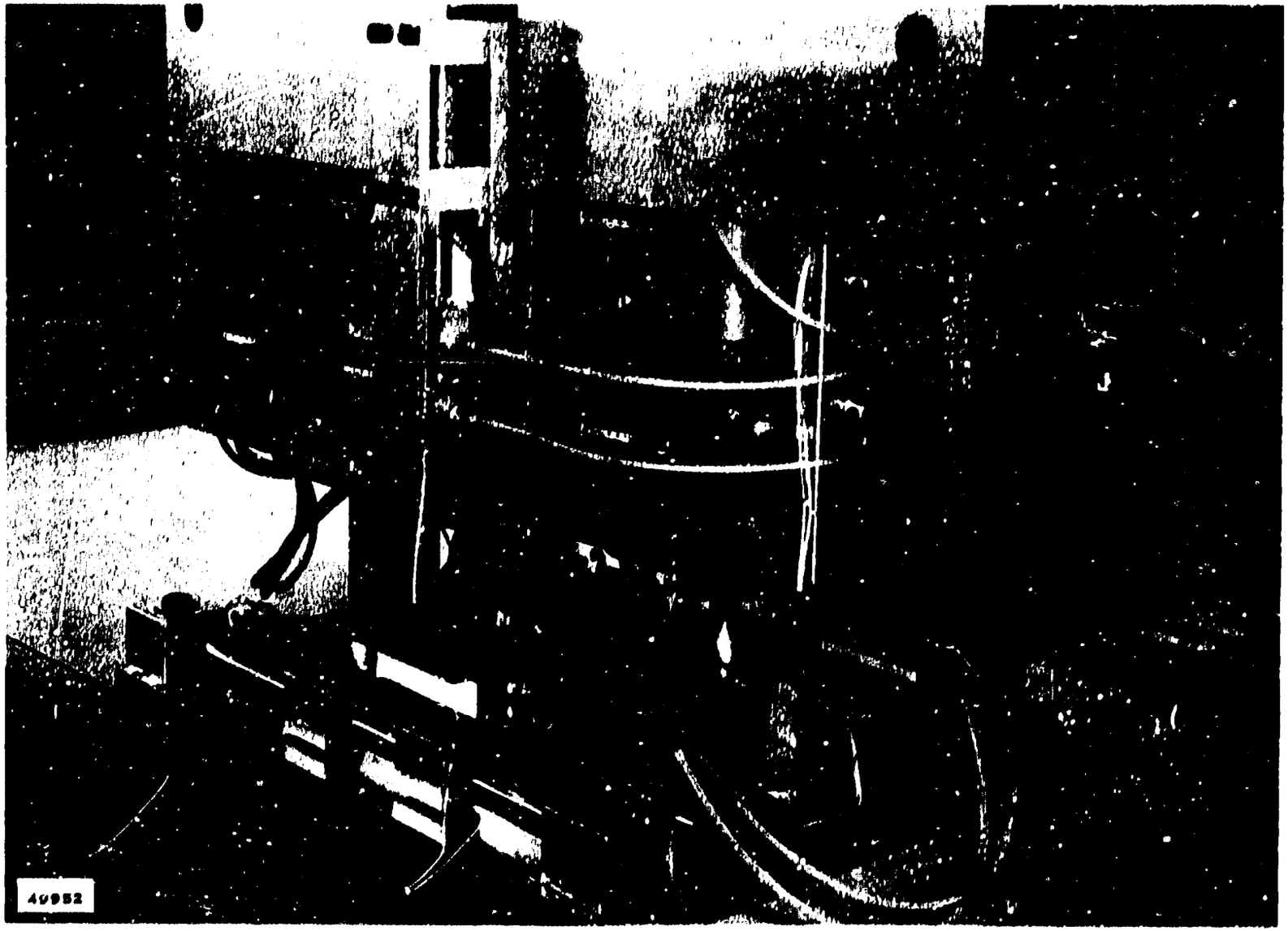

Figure 2-7. Anode Primary-to-Secondary Screen Welder

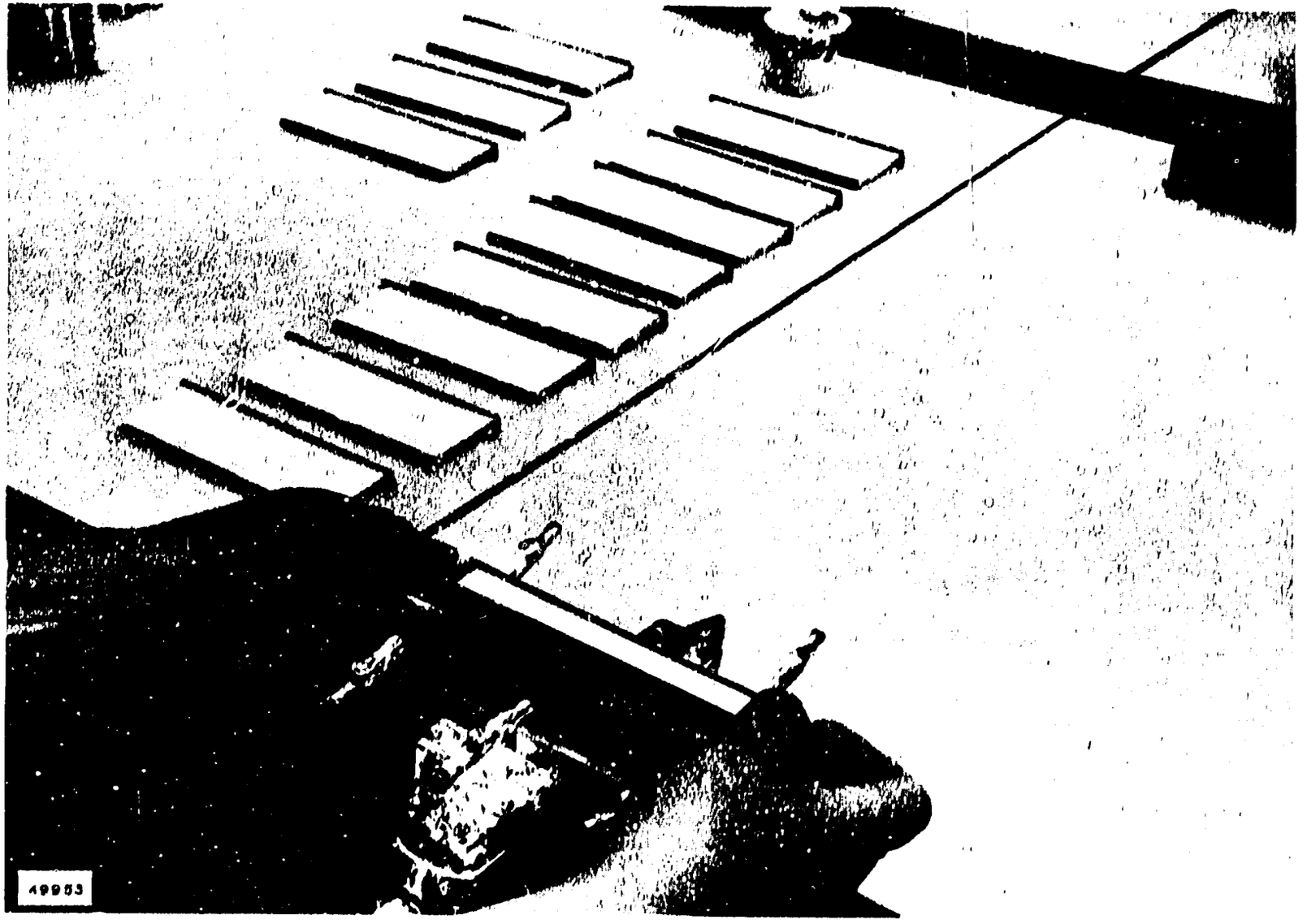

Figure 2-8. Matrix Application Fixture

Figure 2-9. End Matrix Application Fixture

c. Cathode Fabrication

A composite drawing of the cathode is shown in Figure 2-10 and includes information from drawings number 106000, 106002, 106010, and 106020. The cathode primary screens are die-cut to exact dimensions. The cathode secondary does not require close tolerance except on the dimensions across the corrugations. The cathode is corrugated in a manner similar to the anode and then cut to length by hand. The parts are inserted into a cathode holding fixture (shown in Figure 2-11) which is similar to that used on the anode but allows both the top and the bottom channels to be welded simultaneously.

Two weld operations are required to complete the cathode, cathode primary-to-channel and cathode primary-to-secondary. All parts are cleaned in Freon cleaning solvents before welding and thereafter handled with finger cots or gloves. The cleaned parts are assembled into the cathode holding fixture as shown above and placed in the cathode welder shown in Figure 2-12. This tool welds both the top and bottom channels simultaneously. At the present time the part is removed from the holding fixture, a cathode secondary is inserted and each cathode corrugation is welded in four places with a hand-operated tweezer welder. Total assembly time per dual anode is now about 15 minutes. A modification to the anode primary-to-secondary weld machine is being made which will allow the cathode primary-to-secondary weld to be made automatically. In a manner similar to the anode, a set of copper fingers (and the cathode secondary) are inserted inside the cathode fixture. After the cathode flanges are welded, the part and fixture are removed and placed on the modified anode primary-to-secondary weld machine. The secondaries will then be welded once every 0.25 inch. The additional welds will not take as long as is now required to hand-weld four places on each corrugation and will result in a flatter and more rigid part. Total time per part should decrease to less than ten minutes. The parts are then inspected for squareness, straightened and then plated with silver to a thickness of 0.0005 inch.

d. Parallel Assembly of Cells

Five dual anodes and six dual cathodes are assembled into an electrically paralleled assembly of cells as shown in Figure 2-13, drawing number 106023. The outer two cathodes are not active and thus a ten-cell parallel array of cells requires ten anodes and 12 cathodes. The cells are assembled in an assembly fixture shown in Figure 2-14. Each part must be inspected and cleaned before the assembly operation. Starting with a cathode, the parts are stacked sequentially in the fixture with anodes pulled to one side and cathodes to the opposite side by a series of springs on the fixture. A movable ram is then forced down on the stack of parts so that the dimension between the fixture jaws is 2.312 inches. The spring clips

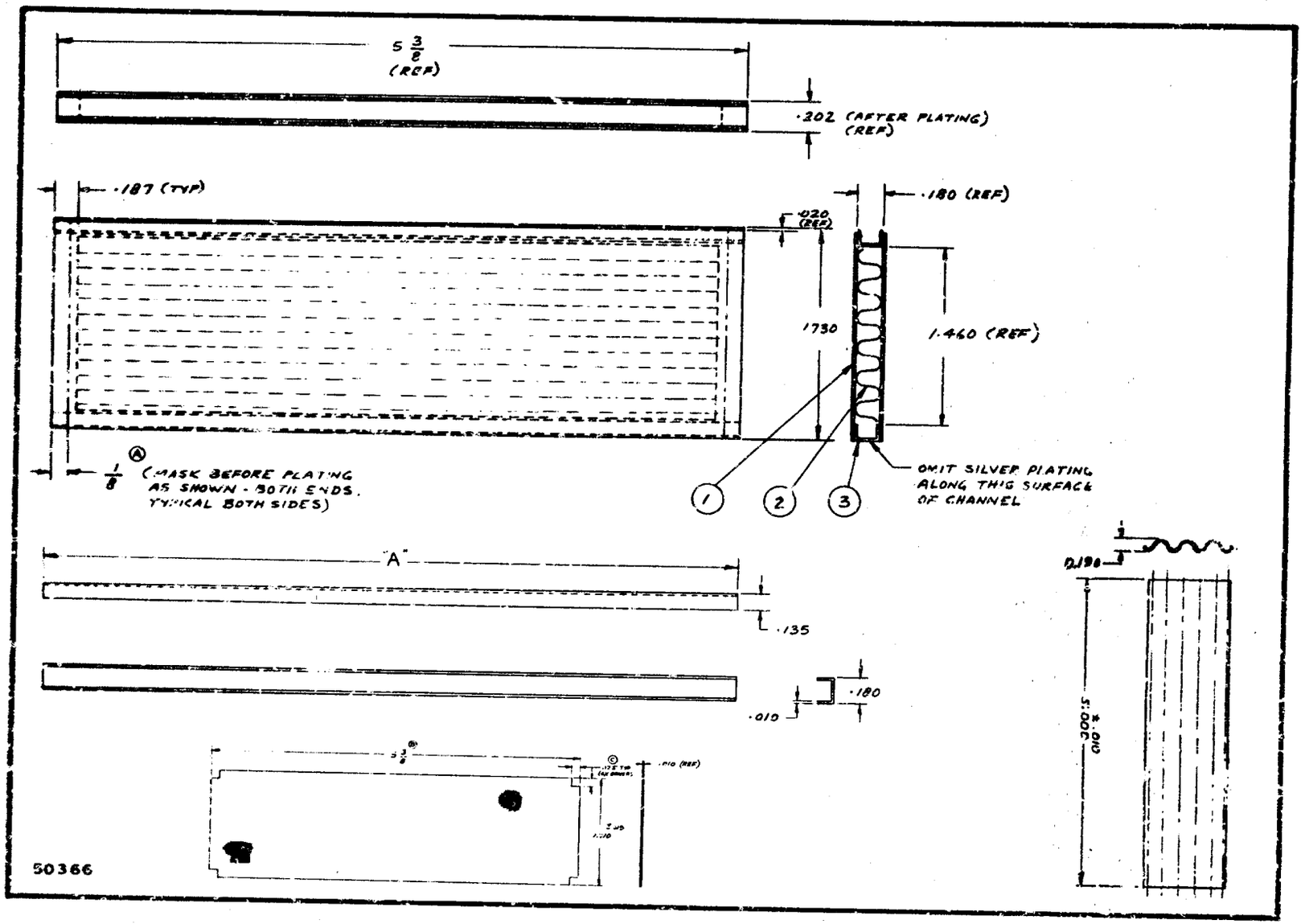

Figure 2-10. Cathode Construction

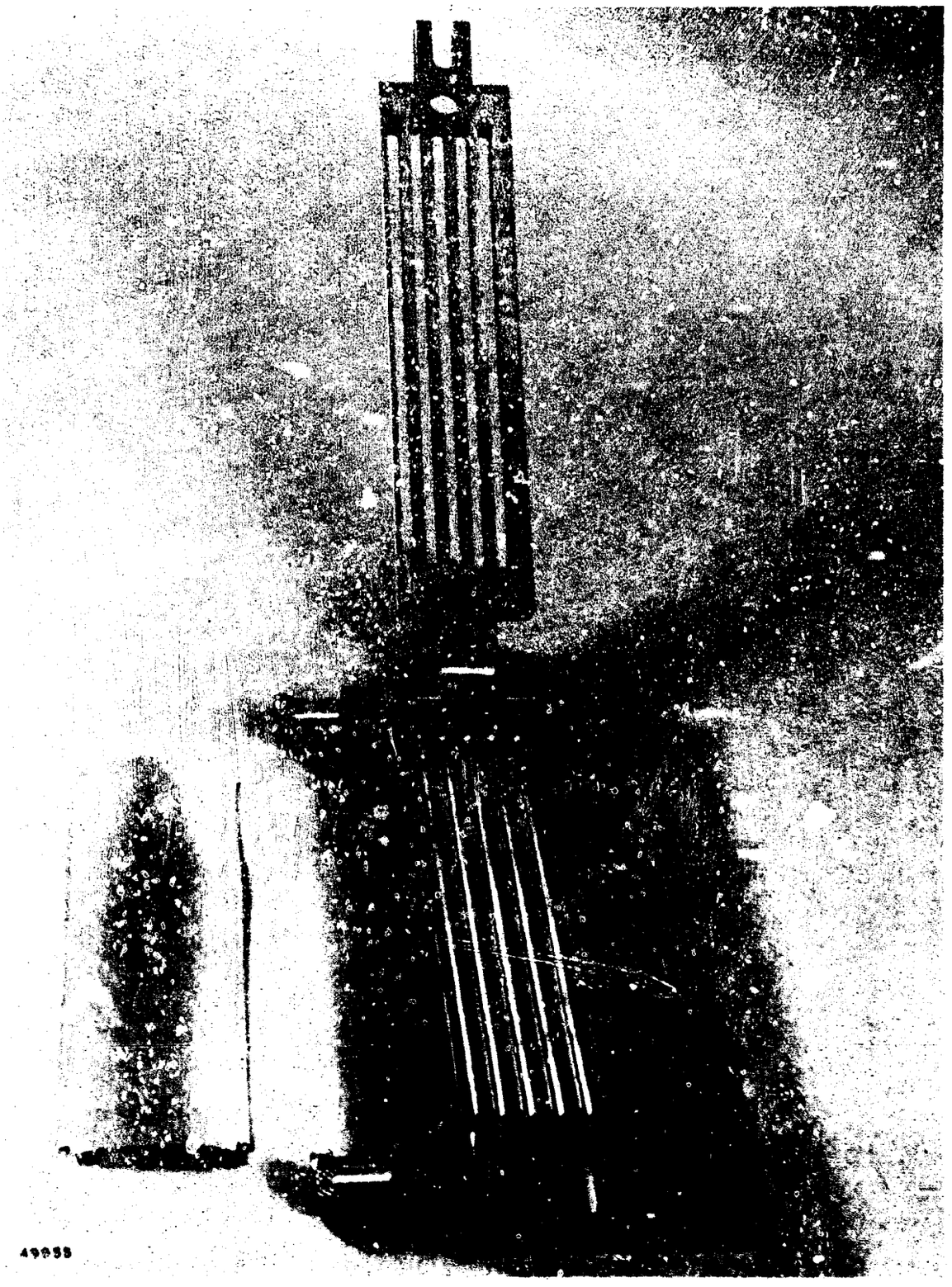

Figure 2-11. Cathode Holding Fixture

Figure 2-12. Cathode Primary-to-Channel Welder

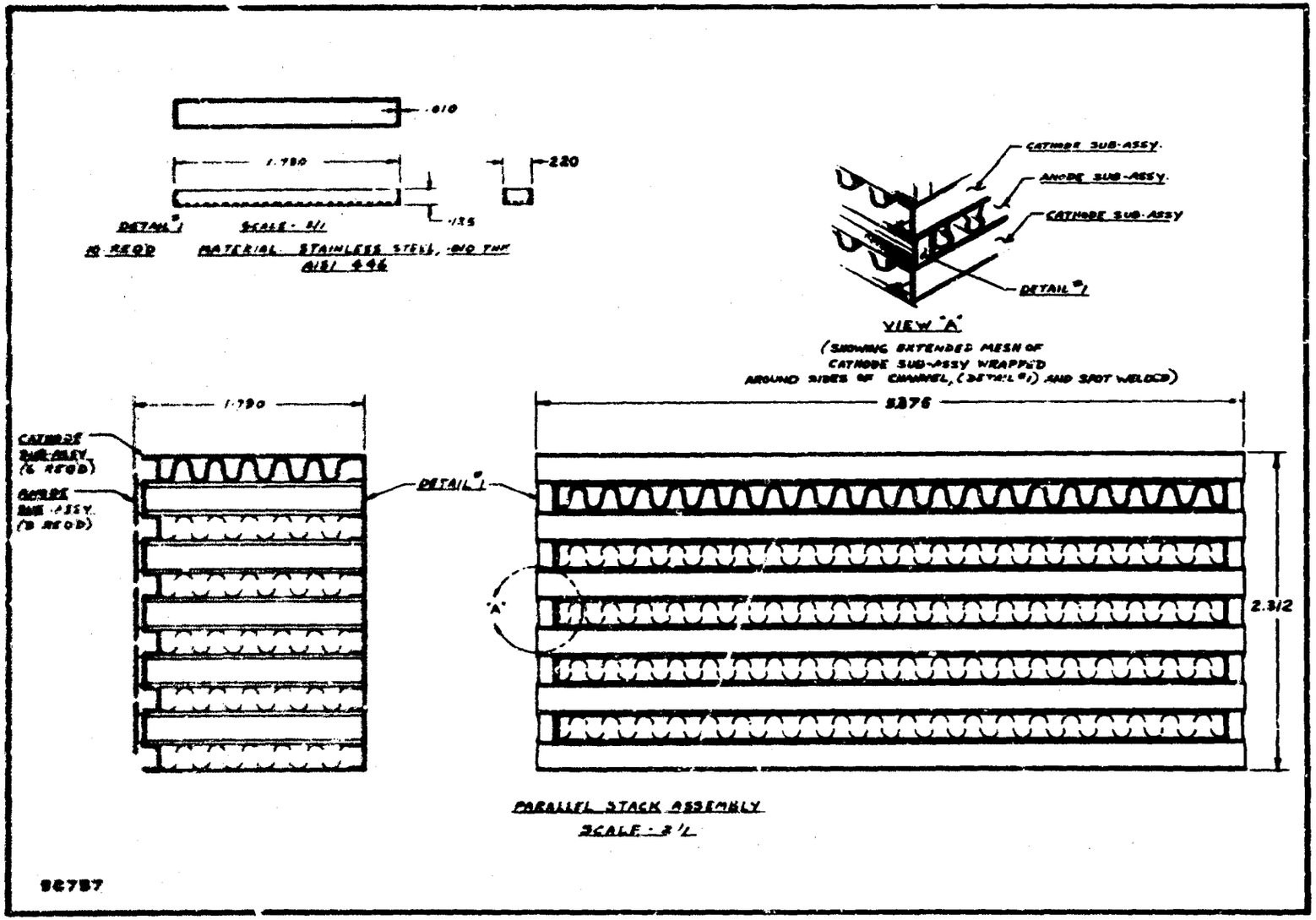

Figure 2-13. Parallel Stack Assembly

Figure 2-14. Parallel Assembly Fixture

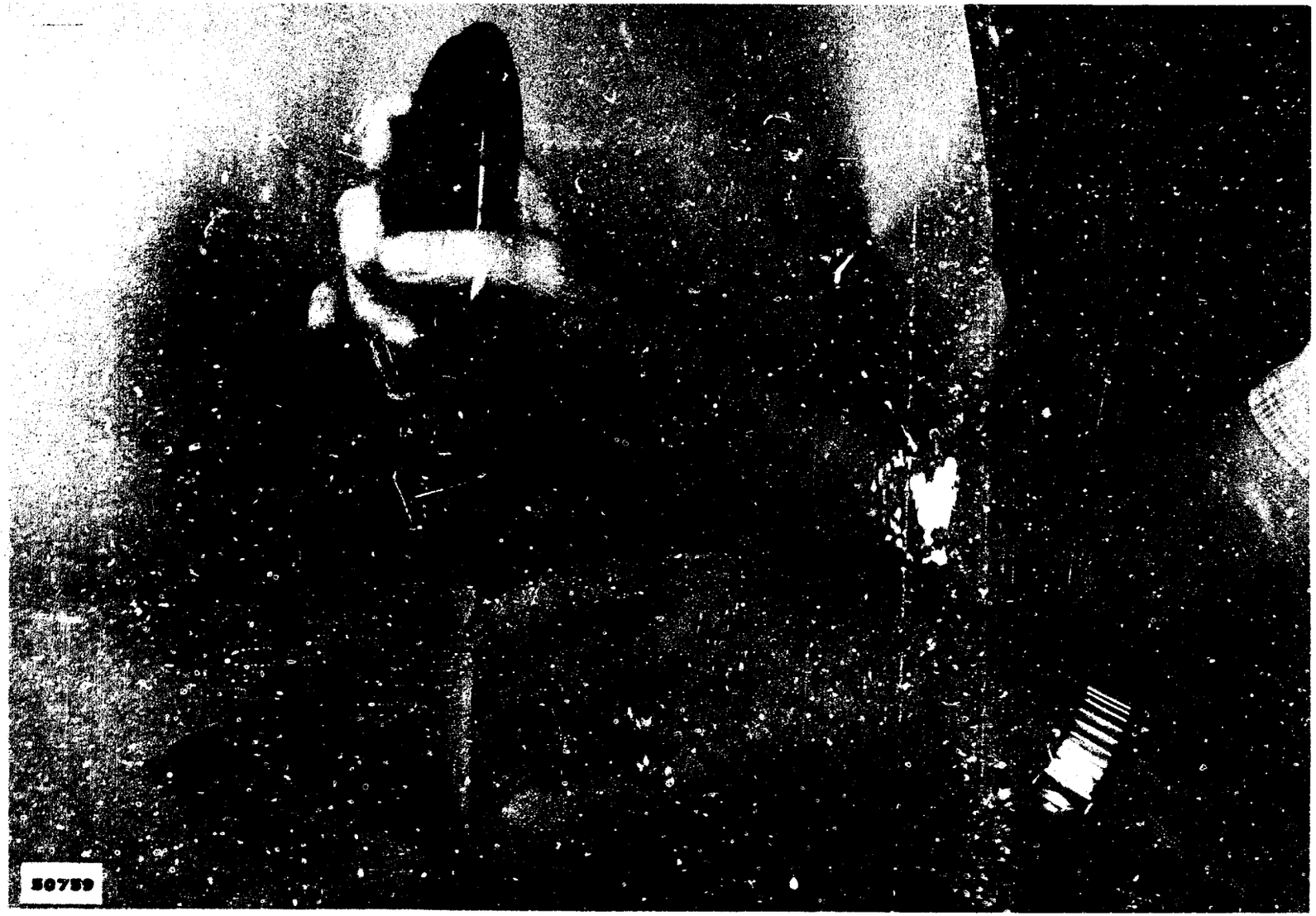

Figure 2-15. Welding of Cathode End Channel

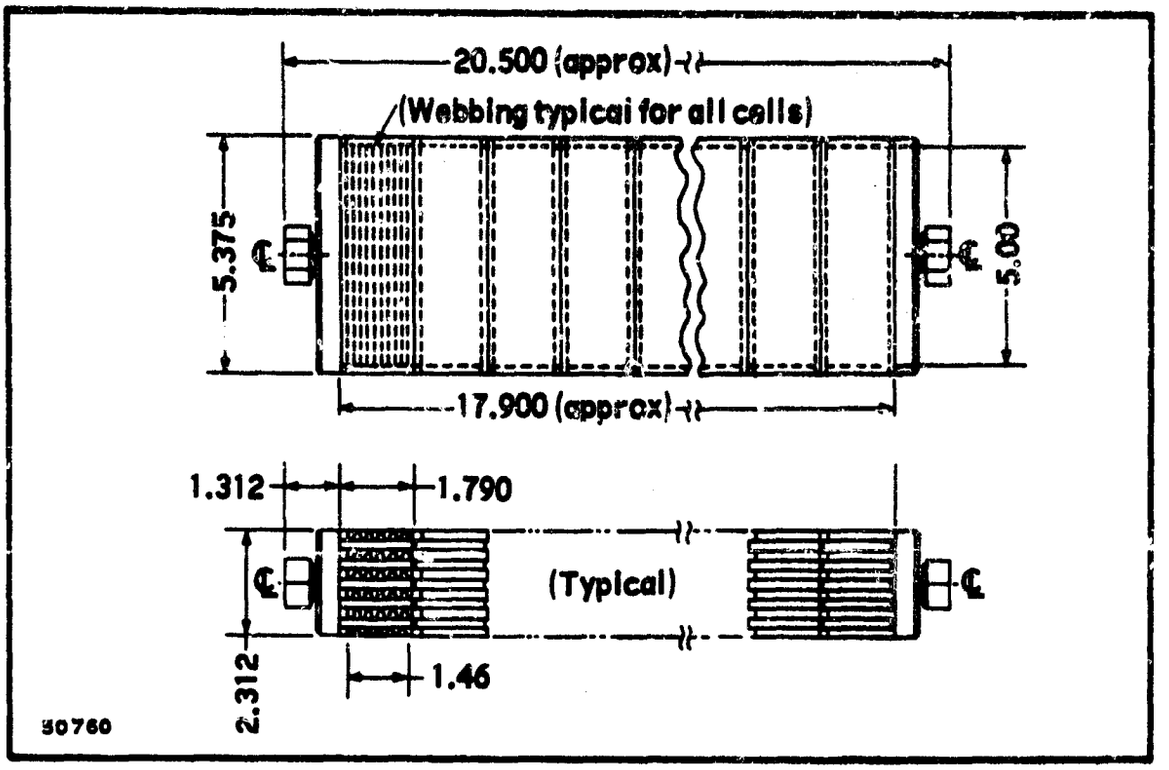

Figure 2-16. 10 by 10 Module

are then removed and the 1 by 10 assembly is checked with an ohmmeter to be sure that no short circuit exists between anode and cathode. The fixture is turned on its side, and the cathode end channel shown in Detail 1 of Figure 2-13 and drawing number 106007 is inserted between adjacent cathodes and spot-welded. Each part is individually checked and shimmed to fit. This operation is shown in Figure 2-15 and View A of Figure 2-13. When all cathode end channels are welded, the ram is retracted and the part removed from the fixture. Again, a check is made for shorts. A sealer is applied to the joint where the open anode end lies against the cathode channel to seal the anode compartment and stop fuel gas communication from anode to cathode. The sealer is allowed to dry and the part is checked to be sure no shorts exist. This operation takes about four hours per assembly. This time will be reduced by eliminating many of the checking and fitting jobs now performed, by better control of part tolerances.

e. Series Assembly

Ten parallel assemblies are now joined together in electrical series by welding the anode flange of each cell to the adjacent series cathode to form a 10 by 10 module (Figure 2-16). This weld is made with a

muitiple head welder (Figure 2-17) which reaches down inside the cathode channel and across the anode flange to weld two anode flanges to one cathode. The welder electrodes reach halfway into the module, a distance of about 3 inches. The electrodes are preloaded to a constant force during the weld cycle. The electrodes are bent slightly in the unrestrained position and straightened out by a force applied at their base during the electrode insertion operation. This force is applied by air cylinders on each side of the weld head, which closes to straighten out the electrodes. The separate 1 by 10 assemblies are loaded into a rack and then held firmly from the top and ends by compression. All the welds are made on one side, the module removed and turned over, and the welds made on the other side. This welding operation requires about four to six hours per 10 by 10 module. When all series welds are made, the module is removed from the welding fixture and checked for shorts. A thin distributor plate (drawing number 106047) is then welded to both the anode and cathode ends of the 10 by 10 module. The manifold shown in Figure 2-18 (drawing number 106049) is then attached to the distributor plate by spot welds along its outside edge.

Since only spot welds are used in the series weld operation, the anode compartment is not gas tight. If the joints were all sufficiently close then electrolyte would eventually seal all the spaces between the welds. To achieve a gas-tight module, even without the electrolyte, a sealer is applied to all welded joints. This sealer is applied to the joint with the anode compartment under a slight vacuum. The vacuum helps to pull the sealer into any leaks and the viscosity of the sealer is such that it will seal wet against a few inches of water vacuum. In the long run, a technique must be developed to obtain a hermetic seam weld at all joints so that sealer is not required. This possibly can be achieved by allowing the weld nuggets to overlap, or by changing the joining technique to obtain a brazed assembly.

f. Large Electrode Sizes

Scale-up of the present 1.4- by 5-inch electrodes to 3 by 8 electrodes involves changes in most of the fixtures and tools to accommodate the larger dimensions. This is presently being done with all of the simple fixtures, the anode flange-to-primary welder and the cathode channel welder. A heavier gage material (0.019 inch) will be used to obtain greater structural rigidity. The biggest unknown in the scale-up is whether a reliable series weld can be made on the 8-inch cell, since the weld electrode must reach over 4 inches into the cell and make a reliable weld. To help ensure a better weld, a material change to Type 316 stainless steel from Type 446 stainless steel will be made. With a Type 446 anode flange and a Type 316 cathode channel, the resulting spot weld is strong, ductile and requires less pressure and lower weld current settings.

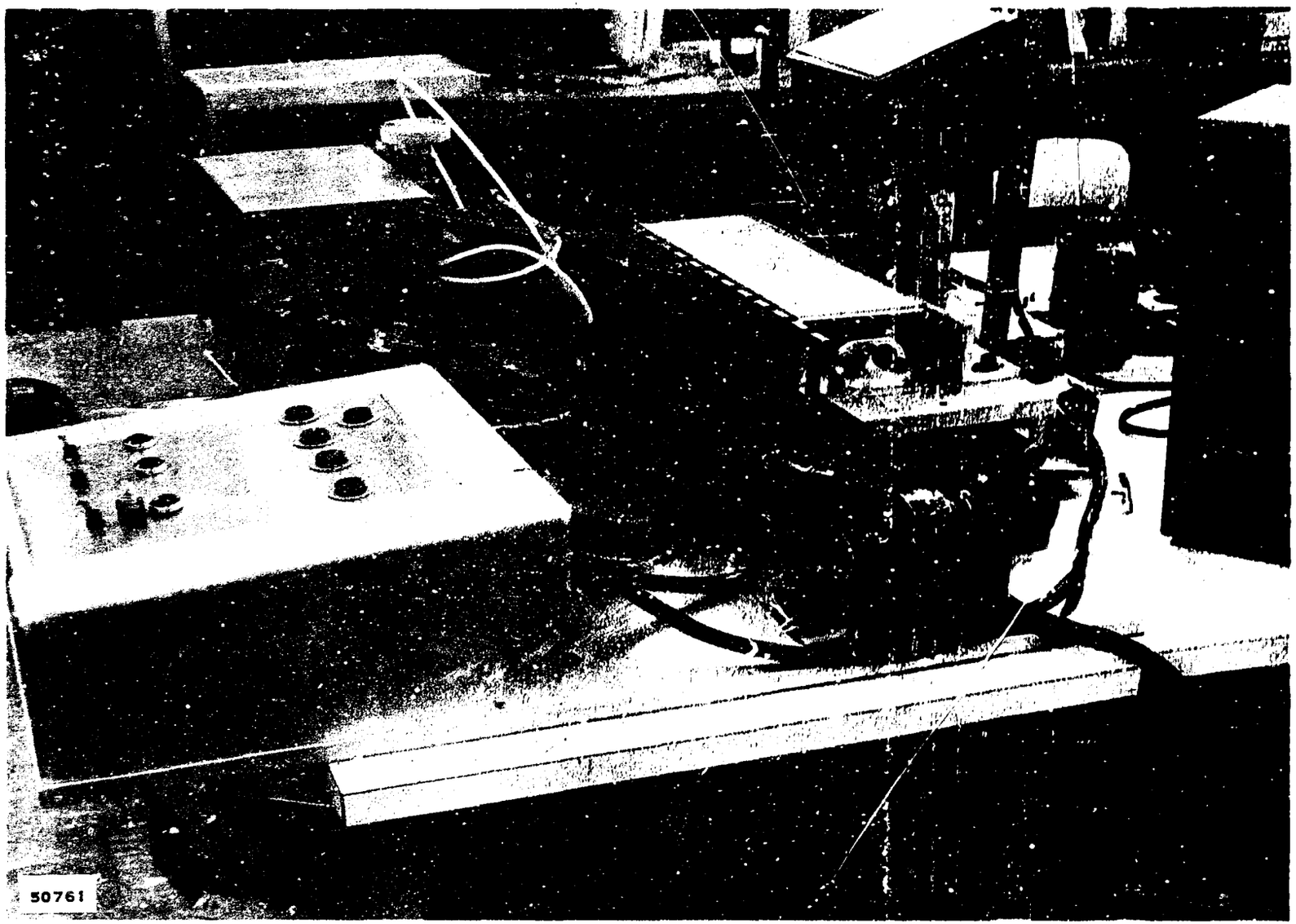

Figure 2-17. Multiple Head Series Welding Machine

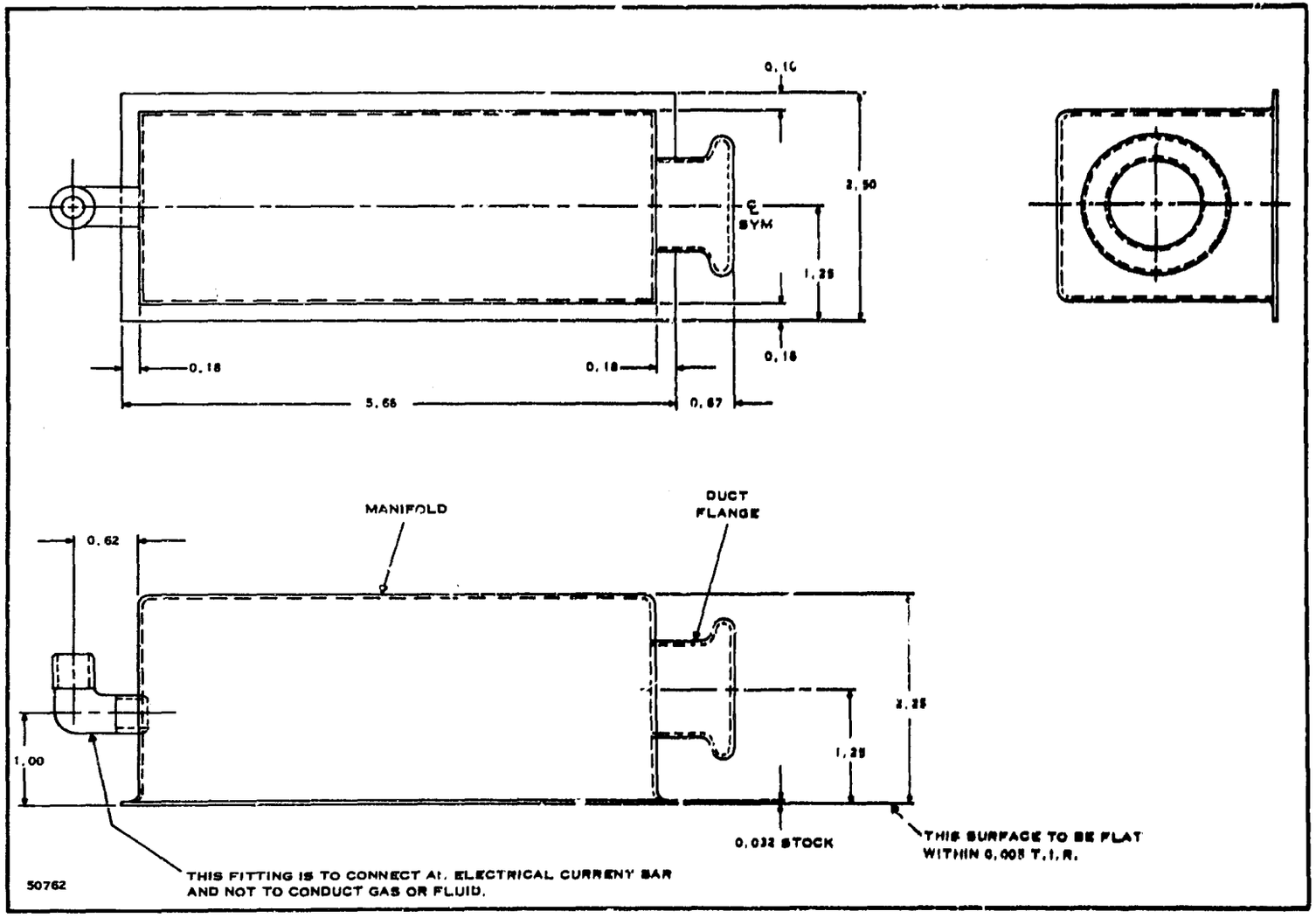

Figure 2-18. 10 by 10 Manifold

3. Performance

a. Trends During Contract Period

In a very general way, the performance of fuel cells refers to how well they run. Actually, most workers refer to performance in terms of watts per square foot of projected electrode surface. Performance may also refer to volume, weight, lifetime, cost, etc., depending on the relative importance of these factors to the customer.

In addition, the performance (on any basis) of a cell will depend on the length and manner of operation and on the degree of activation. Also, since the fuel cell exhibits a response lag when the load is changed, the level of performance depends on the manner in which performance is measured.

One popular method of determining performance is by taking a plot of cell voltage versus cell current (E-I plot). This method uses a device to load progressively the cell, simultaneously recording cell current and potential. The E-I product gives the watts produced by the cell under essentially instantaneous conditions (plot time is generally less than 10 minutes). Based on experience, it is not realistic to expect stable operation at performance levels deduced from E-I plots.

Another method of obtaining performance figures is to obtain a time record of the load carrying ability of the cell at some chosen cell voltage level (usually 0.7 volt). Cells operated in this way still may not be directly comparable, since wide variations in cathode and anode voltages can combine to give the chosen cell voltage. In general, however, cathode polarizations have proved to be reasonably uniform from cell to cell, thus making the anode (and cell) nearly comparable. Figure 2-19 is a graph of recent cell performance and open circuit voltages plotted against time of start-up. Each point is the average of the maximum performance and the open circuit voltage of cells started during that week. Performance figures represent watts per square foot at 0.7 volt per cell, as recorded over a period of more than two hours.

The increase in the open circuit voltage seems to indicate improved sealing of the cells, thus reducing gas communication. The improvement in performance probably is due to improved activation techniques. It is interesting to note that the performance decrease during the weeks of March 13 and April 10 coincided with the operation of several 3 by 10 modules, rather than single cells.

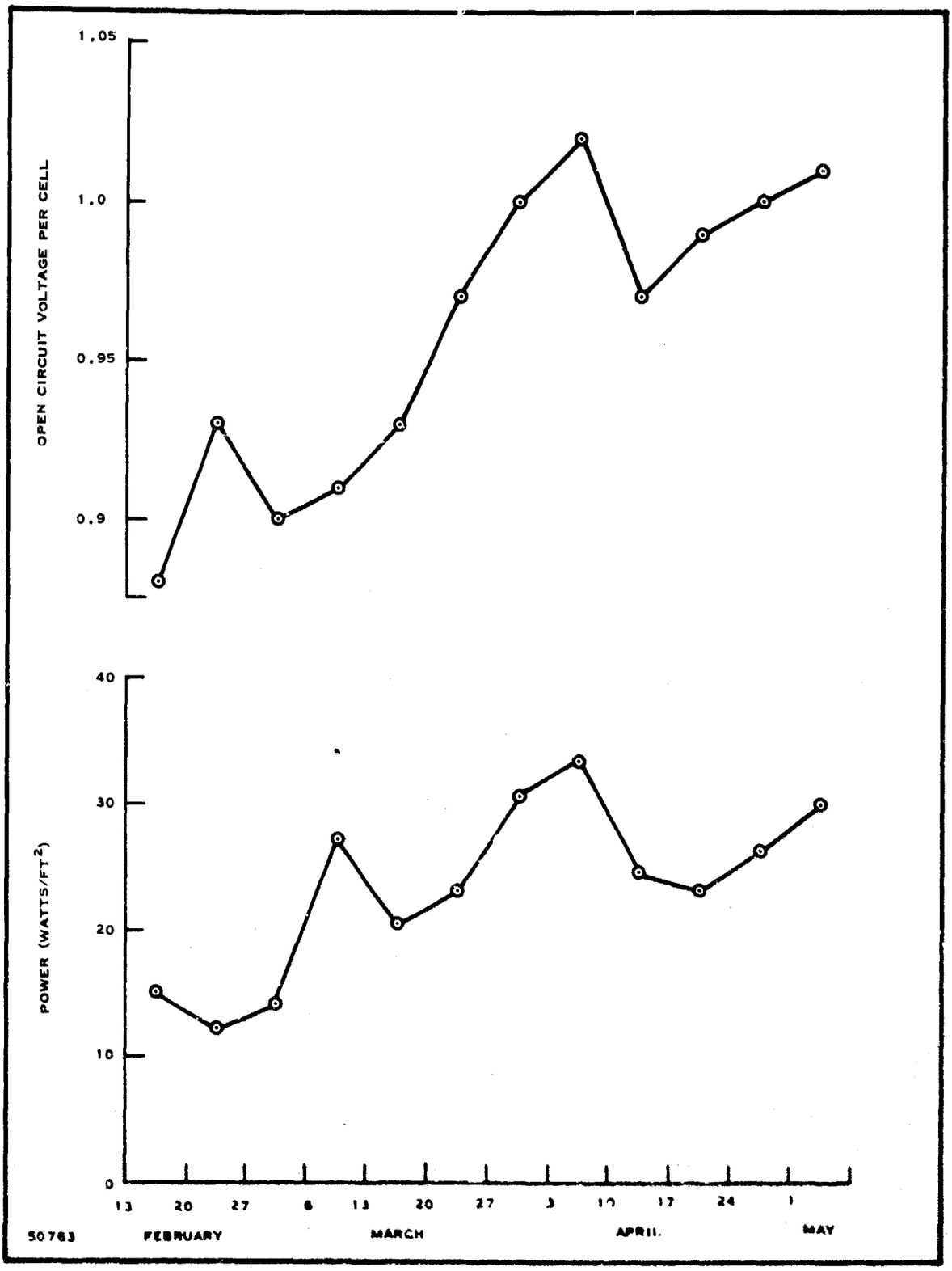

Figure 2-19. Cell Performance with Time

(1) Influence of Structure

In general, it can be stated that structural details have no apparent effect on cell performance, provided the structure meets the engineering requirements of the cell.

The material separating the anode and cathode is called the matrix and must perform a variety of functions. Ideally, it must be (a) an electronic insulator, (b) a porous structure capable of absorbing an optimum amount of electrolyte, (c) transparent to electrolyte ions, (d) opaque to fuel side and air side gases, (e) invariant with time of operation, and (f) easily and economically applied to the anode. Small changes in specific matrix materials do not seem to change measurably the performance, but may have a marked effect on ease of application.

In the Texas Instruments fuel cell concept, the electrodes also must perform several functions. Primarily, of course, the electrodes contain the active sites where the electrochemical reactions proceed. In addition, the electrodes are designed to provide structural strength to the modules, support for the matrix, and a low resistance path for the current generated.

The electrode configurations represent a reasonable compromise in optimizing the above functions. Both anodes and cathodes consist of two primary electrodes, separated by a secondary electrode, as in Figures 2-1 and 2-10. For the anode, the electrode material is nickel screen (80 mesh) for both primaries and secondaries. The cathode is built in dual form (two cathodes) of stainless steel screen (also 80 mesh) and then silver-plated to a thickness of about 0.0005 inch.

It is apparent that active materials are required for both anodes and cathodes. At present, the nickel anodes and silver cathodes seem to supply the most performance at the least cost.

A recent change in the configuration of the anode has resulted in a dramatic improvement in performance. Further confirming tests of this configuration may result in a new concept of the actual anode mechanism, which, in turn, may allow improved cell designs.

The electrolyte applied to the fuel cell is an eutectic mixture of sodium and lithium carbonates that melts at about 520°C. Some potassium is also present, which results in a small amount of a ternary eutectic having a melting point of 375°C.

The quantity of electrolyte in and on the cell or module is quite critical. Too little electrolyte in the matrix allows gas communication between anode and cathode. A minor amount of gas communication results in lowering the cell potential. Excessive gas communication

results in fires (either internal or external) which are destructive to cell structure. Conversely, too much electrolyte may tend to obscure the active sites on the anode, resulting in excessive anode polarization. This condition is called "flooding" and may at times be corrected by raising the cell temperature for a short while.

In the laboratory it has been noticed that cell operation can be improved sometimes by the addition of electrolyte. In the case of long-term operation, there is evidently a slight continuing loss due to evaporation or absorption on oxidized structural parts. In addition, there is evidence that the process of activation either destroys or redistributes the electrolyte in such a manner that additional electrolyte is needed.

The above problems (too much or too little electrolyte) are annoying, but not critical. It is apparent that the cell can be designed to minimize the cell sensitivity to electrolyte quantity. In addition, small electrolyte reservoirs for each cell can be used to establish an optimum electrolyte level.

From an economic standpoint, it is obvious that individual cell size should be as large as possible. Increasing the cell size increases the ratio of active area to total area and reduces the number of piece parts per square foot (or per kilowatt). However, there are certain limitations. The height of the cell may be limited by electrolyte distribution and is certainly limited by the difficulties involved in welding tall cells in series. The length of the cell is not limited by the electrolyte or by assembly processes; however, increasing the length increases the cell current without a proportional increase in current carrying structure, thus leading to increasing ohmic losses in the cell.

The present test cells are 5 inches high by 1.46 inches long, for an effective area of about 7.3 square inches. A few cells have been tried that are 8 by 3 inches, for a total of 24 square inches of effective area. No unusual problems have been encountered in operating the larger cells.

For the purpose of minimizing costs, both in money and in time, most test fuel cells are single cells. It is recognized, however, that a module consisting of several cells in series may have different performance characteristics than single cells. Since the Texas Instruments module is in series, both flow-wise and electrically, it is obvious that under load the last cell will "see" a different fuel mix than the first cell and, hence, will perform differently. Even under open circuit condition the last cell may experience a slightly different fuel mix because of additional shifting within the cells. In addition to the above differences, the degree of activation (or passivation) of any single cell in a series is much more nearly random than in the case of a single test cell. This means that the series

module is much more sensitive to its time-power operating history than the single test cell.

(2) Influence of Operation

It has become obvious that the degree of activation (or passivation) results in such gross changes in performance that other differences in structure and operation cannot be clearly defined. For single test cells, activation (in some degree) can be attained by shorting the cell without fuel for a short period. After recovery (a "rest" at open circuit voltage with fuel flow) the performance may be found to have increased by a factor of 2 to 4. This active state tends to disappear with time but may be regained by another activation process. In series modules the process of activation does not act on each cell in the same way. Some cells may be overdriven to the damage point while others may not be driven sufficiently to induce activation. In addition, the recovery period does not always result in recovery of all the cells. Although further experience with series modules will improve the understanding of the activation process for these modules, it is not likely that the specific performance will ever reach that of single cells.

Laboratory experience has indicated that continuous operation at no load (open circuit) or design load conditions has a deleterious effect on the cell or module. Fortunately, in an actual system these conditions would occur only rarely. The system auxiliaries would provide a small continuous load and the actual load would probably vary randomly up to design load (or some overload).

The temperature sensitivity of the fuel cell depends upon the controlling mechanism of the cell. In general, the performance seems to increase almost linearly up to about 700°C. Above 700°C, the gains in performance with increases in temperature become progressively smaller (one reason for operating at the700°C limit). This characteristic points toward the desirability of temperature control programmed to load. Ideally, the operating temperature could be kept at some minimum figure, say 600°C, for no load conditions and would approach 700°C only as the actual load approached the design load. This should reduce corrosion and extend the cell life.

Because of convenience, the laboratory test cells have been operated on synthetic mixtures of gases. At present, the fuel side is composed of 38 percent H_2, 12 percent CO_2, and 50 percent N_2, which is passed through a shift reactor before reaching the fuel cell. This mixture is expected to give very nearly the same open circuit voltage as the actual partial-oxidation fuel. There is a small possibility, however, that the actual fuel will perform slightly better than the synthetic fuel because of the lower CO_2 content.

The air side gas mixture is controlled to approximately 5 percent O_2, 10 percent CO_2, 10 percent H_2O, and 75 percent N_2. This is an accurate representation for a molten carbonate system using liquid hydrocarbons and air. Improved performance can be obtained by increasing the CO_2 content on the air side (while maintaining a 2:1 CO_2 to O_2 ratio), but this is possible only in the laboratory and requires a source of CO_2 in addition to that available from fuel oxidation.

b. Analysis of Control Factors

The technological goal of molten carbonate fuel cell research and development is to ensure a reproducible and time-invariant (or reproducible with known time-variancy) fuel cell system operating at optimal power. At constant current the fuel and air side compositions in a molten carbonate fuel cell are time-invariant. The system is amenable to either isothermal or temperature-programmed operation. To secure reproducibility of performance and long life, the mechanical components of the fuel cell (electrodes, matrix, electrolyte, and electrical connections) are of paramount importance. The physio-chemical phenomena at the 3-phase interfaces is perhaps the controlling factor in overall performance of these cells.

The composition of the fuel available for fuel cell operation is dependent primarily on four factors: (1) inlet fuel composition, (2) fuel utilization, (3) shift equilibrium, and (4) electrode mechanism. Inlet fuel composition is dependent on the hydrocarbon mixture (C_nH_m) used, air/C_nH_m ratio, recycle ratio, and degree of completion of the partial-oxidation reactions. Fuel utilization, excepting fuel losses due to leakage, is a function of current density and the fuel flow rate. Temperature of fuel cell operation, together with other variables mentioned before, determines the shift equilibrium. Furthermore, fuel composition is dependent on the electrode mechanism and side reactions, if any.

The air side composition is determined by two factors, the composition of the hydrocarbon mixture and the CO_2/O_2 ratio desired for the cathode reactions. Thus, for a particular fuel and a fixed CO_2/O_2 ratio, the air/fuel ratio is fixed over the operating range of the system.

(1) Optimal Current Density (amperes per square foot)

Optimal current density in series connected cells, notwithstanding constructional defects in module structure, is controlled by the cells performing on the leanest fuel. However, performance of cells

with nickel anodes is subject to another important variable, the pH_2/pH_2O ratio. This ratio determines the position of the equilibrium.

$$Ni + H_2O \rightleftharpoons NiO + H_2 \qquad (1)$$

and thereby limits the percentage fuel utilization. This short-coming may, however, be offset by supporting the anode material on a conductive, non-oxidizable substrate, or by permitting formation of a passive oxide layer on the nickel surface.

(2) Optimal Power Density (watts per square foot)

The optimal power density for Texas Instruments module arrangement is given by

$$\text{watts per square foot} = \sum_{n=1}^{P} (V_n)\ (\text{optimal current density})$$

where

V_n = cell voltage at optimal current density

P = number of cells in series.

By area programming, current density can be made to vary from one group of cells to another, to optimize cell polarization. In such case,

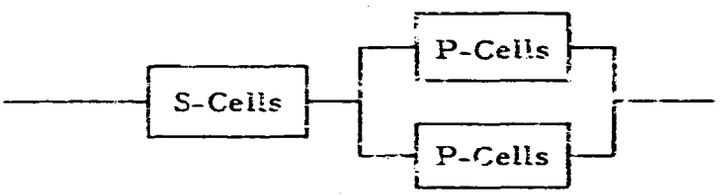

$$\text{watts per square foot} = \sum_{n=1}^{S} (V_n)\ (\text{optimal current density})S$$

$$\div \sum_{m=1}^{P} (V_m)\ (\text{optimal current density})P$$

V_n = cell voltage at optimal current density of S cells in series

V_{rn} = cell voltage at optimal current density of P cells in series.

Figure 2-20 gives plots of fuel composition and open circuit voltages of series connected cells as functions of fuel utilization. The inlet fuel composition is based on CITE military fuel, partial oxidation with 20.4-percent excess air, 80-percent fuel utilization and 10-percent recycle. The gas is in equilibrium at 700°C. Figure 2-21 is a plot of the reaction where pH_2 is plotted against pH_2O. From these figures it is inferred that with less than 9-percent hydrogen in the fuel stream (i.e., above 51 percent fuel utilization per pass based on partial-oxidation fuel) continuous corrosion of nickel will set in. If corrosion of nickel cannot be prevented by passivation in molten carbonate environment, higher fuel utilization can be obtained by sacrificing lifetime of the cells or by resorting to supporting nickel on a substrate material, as mentioned before, in which case we must depend on oxide catalytic activity.

There exists the possibility of diffusion of carbon dioxide from the anode to the cathode because of carbon dioxide solubility in the melt and the higher partial pressure of carbon dioxide at the anode after a certain percentage utilization of the fuel. This tends to decrease the partial pressure of water vapor in the anode gas because, by shift reaction, more water reacts to form hydrogen. Thus, much higher fuel utilization can theoretically be obtained without corroding nickel anodes. Figure 2-22 gives a plot of moles of carbon dioxide diffusing from anode to the cathode against fuel utilization. Experimental testing of this hypothesis shall be done on 10 by 10 modules.

Flux of carbon dioxide across the electrolyte-matrix,

$$N_{CO_2} = \frac{D_{CO_2(l)}}{\delta_l} C_{CO_2(ii)}$$

and

$$C_{CO_2(ii)} = \frac{\left[K_{CO_2(g)}\right]\left[C_{CO_2(g)}\right]}{\left[H_{CO_2(ii)}\right]\left[K_{CO_2(g)}\right] + \left[K_{CO_2(l)}\right]}$$

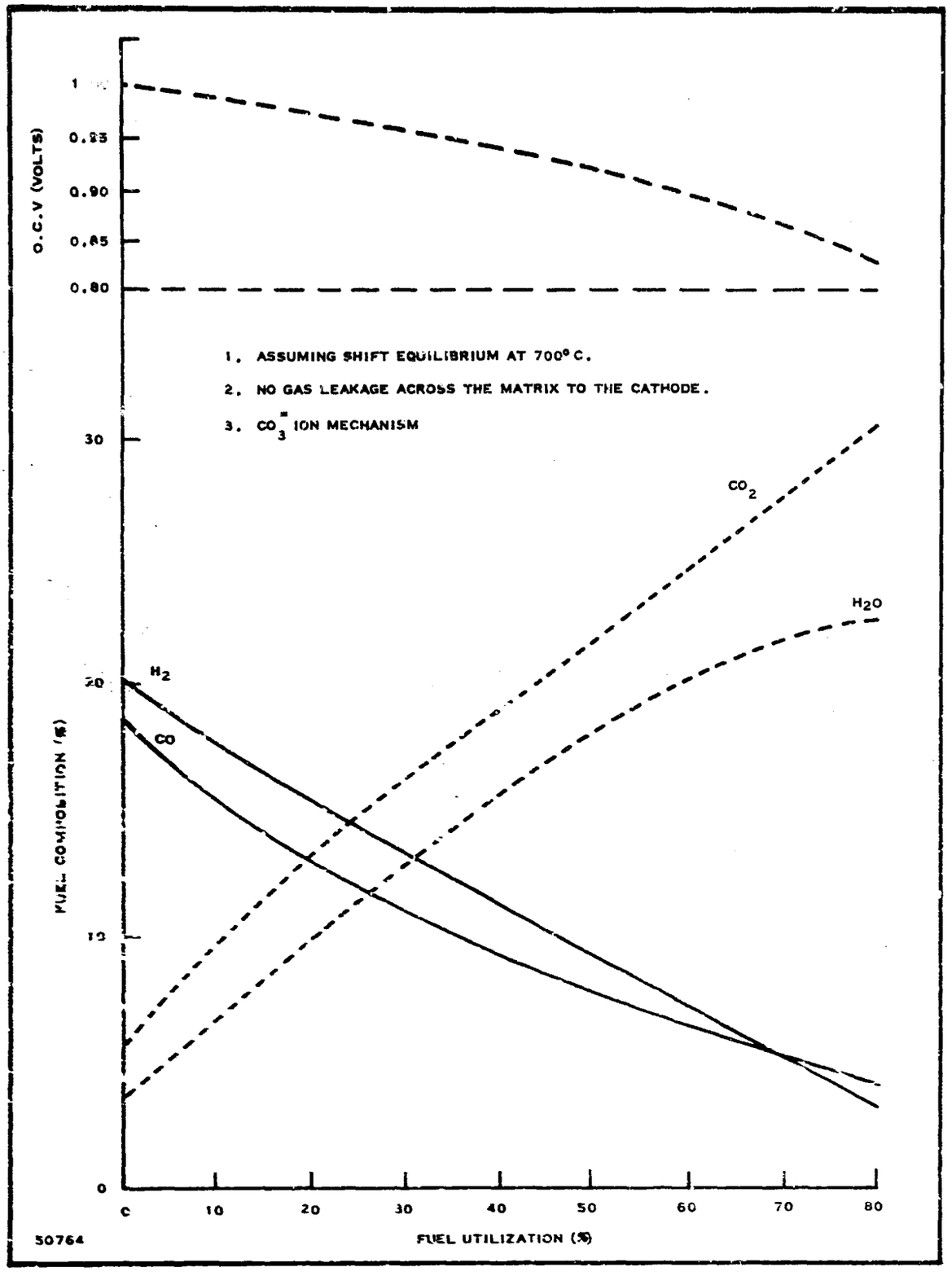

Figure 2-20. Fuel Composition in Series Connected Cells

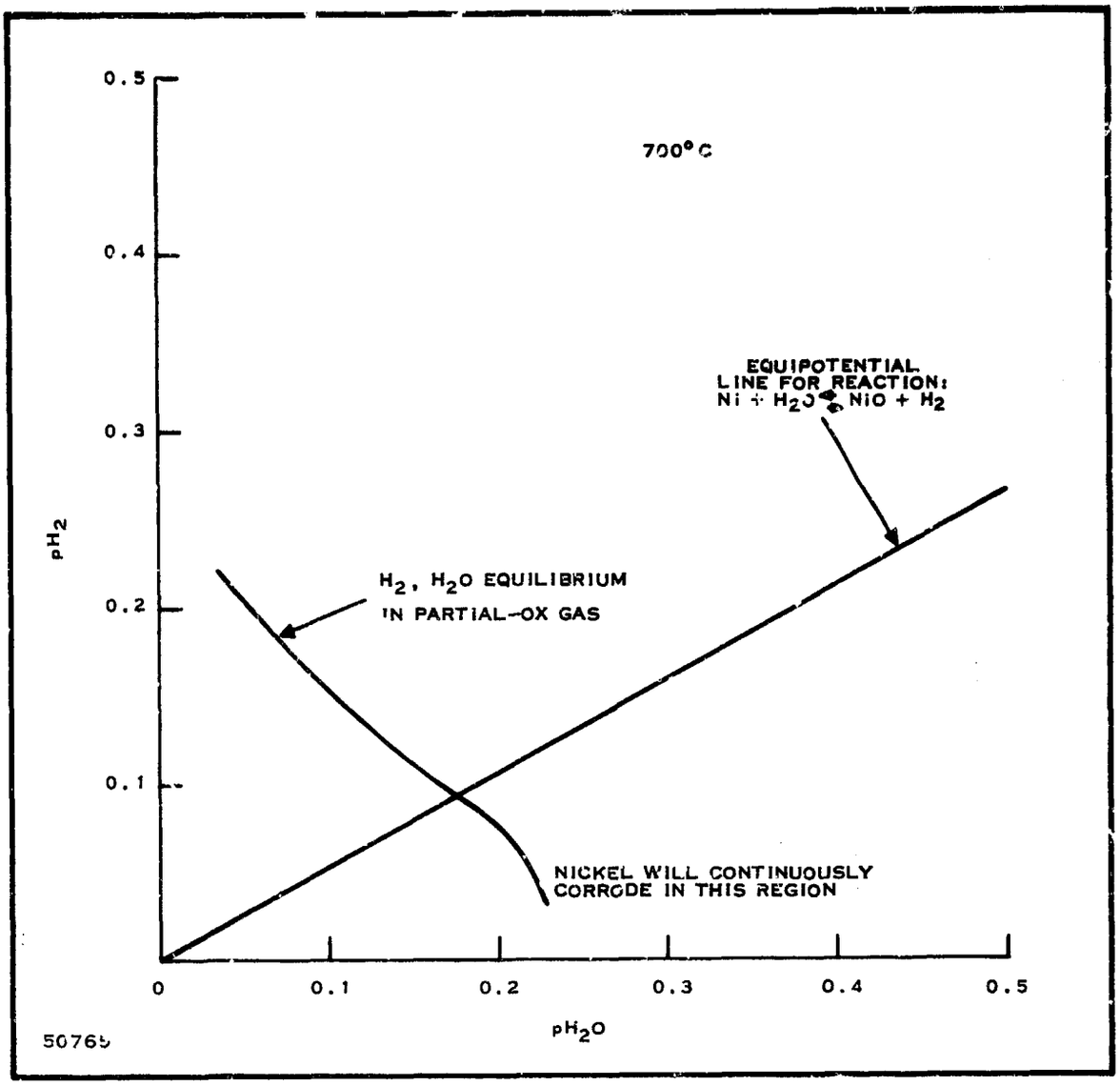

Figure 2-21. Corrosion of Nickel in Hydrogen Steam Mixtures

where

$K_{CO_2(g)}$ = mass transfer coefficient of CO_2 in gas phase ≈ 100 cm/sec

$K_{CO_2(l)}$ = mass transfer of CO_2 in electrolyte phase $\approx 2 \times 10^{-2}$ cm/sec

$C_{CO_2(g)}$ = concentration of CO_2 in gas phase, grams mole/cm^3

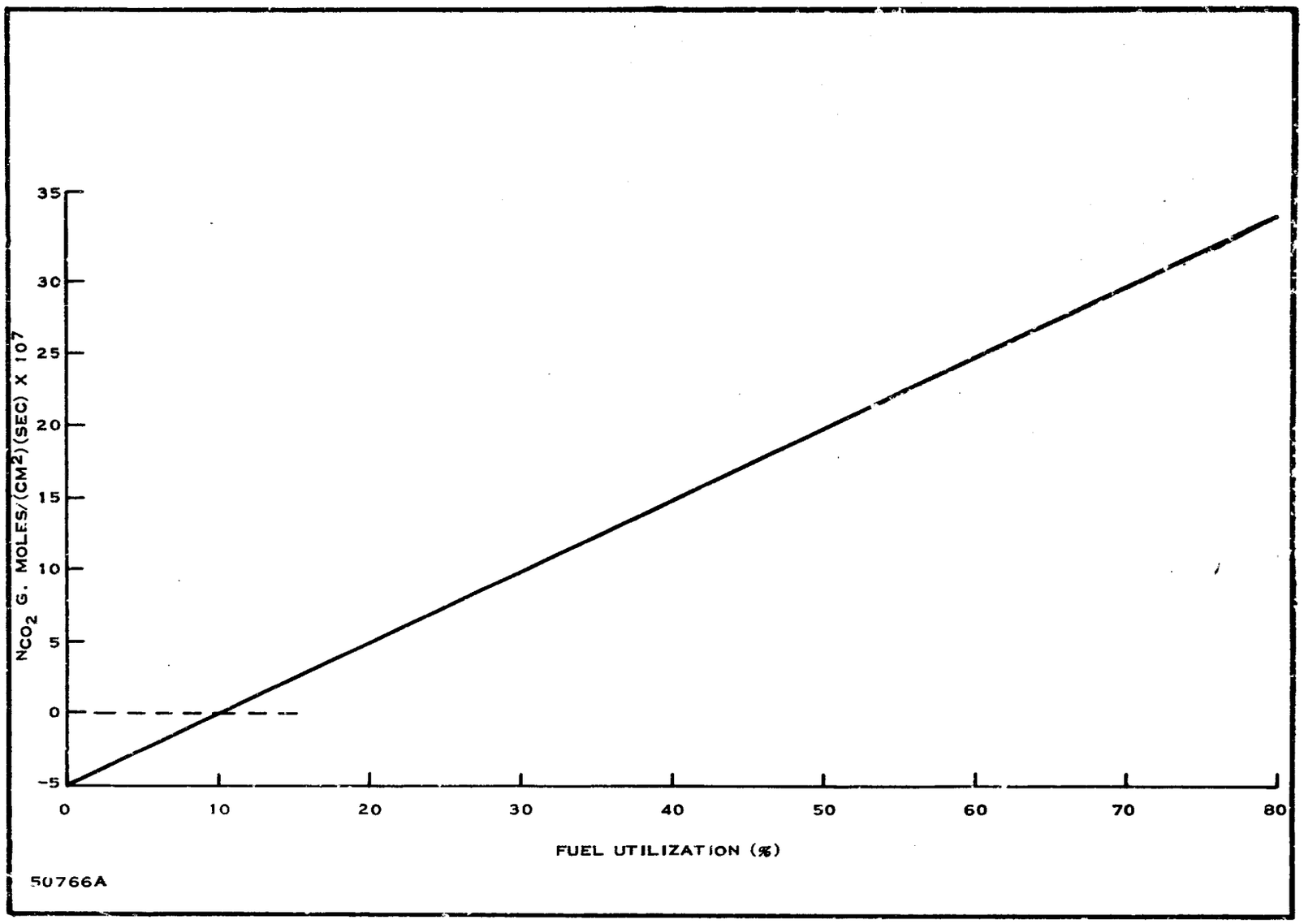

Figure 2-22. Moles of Carbon Dioxide Diffusion Across Electrolyte Matrix

$C_{CO_2(ig)}$ = concentration of CO_2 (gas) at the gas-electrolyte interface, grams mole/cm^3

$C_{CO_2(il)}$ = concentration of CO_2 (dissolved) at the gas-electrolyte interface, grams mole/cm^3

$H_{CO_2(i)}$ = Henry's constant (dimensionless) ≈ 8

$D_{CO_2(g)}$ = diffusion coefficient of CO_2 in gas-phase ≈ 1 cm^2/sec

$D_{CO_2(l)}$ = diffusion coefficient of CO_2 in electrolyte phase $\approx 10^{-5}$ cm^2/sec

δ_g = gas side diffusion film ≈ 0.01 cm

δ_l = electrolyte matrix thickness ≈ 0.05 cm.

On the basis of best instantaneous performance so far obtained, it can be theorized that it should be possible to obtain an optimal current density of 160 amperes per square foot at 0.60 volt, e.g.,

Internal resistance (R) of 0.05-square-foot cell = 0.010 ohm

$$\frac{\text{IR-free polarization}}{\text{IR drop}} = 3$$

Operating voltage of the cell = 0.60 volt

At 50-percent fuel utilization, open circuit voltage = 0.92

Solving for I,

$$I = 8 \text{ amperes} \equiv 160 \text{ amperes/ft}^2.$$

In the above analysis it is assumed that it would be possible to generate 160 amperes per square foot at 0.60 volt continuously. Most of the data so far obtained does not so indicate. The stable current density is found to lie between 20 and 40 amperes per square foot, at 0.75 to 0.85 volt, at 2 to 5 percent fuel utilization. Theoretically, based on the

above reasoning, we should have the following current densities at the indicated voltages.

At 5-percent fuel utilization,

Cell Voltage (volts)	Current Density (amperes/ft^2)
0.85	75
0.75	125
0.65	175

The above values can be improved by reducing the matrix thickness and by diminishing the η/IR ratio, where η is defined as IR-free polarization. In certain instances, the performances of molten carbonate fuel cells have met the above-mentioned values half-way. However, these could not be sustained over long periods of time. The causes of unsteady performance therefore need to be examined in light of transport processes that take place in fuel cell operation, and the electrode reaction mechanisms.

(3) Transport Process in Molten Carbonate Fuel Cells

Figure 2-23 is a summary of the transport processes involved in the operation of molten carbonate fuel cells. Unfortunately, few data are available to evaluate the mass transport limitations on steady-state performance. Probably greater obstruction to theoretical understanding is the dependence of transport processes on electrolyte-matrix environment. Any model based on gross assumptions and indifferent to random changes leads to poor correlations.

(4) Cathode Reaction Mechanism

The overall cathode reaction is given by:

$$CO_2 + 1/2\ O_2 + 2\bar{e} \rightleftharpoons CO_3^{--} \qquad (2)$$

Case I—Both CO_2 and O_2 diffuse through the electrolyte film present on the cathode.

This would seriously limit the cathode performance as the activity of CO_2 and O_2 will be controlled by their solubility equilibrium in the electrolyte. Solubility of CO_2 in the electrolyte at 700°C is about 1000 times that of oxygen, while

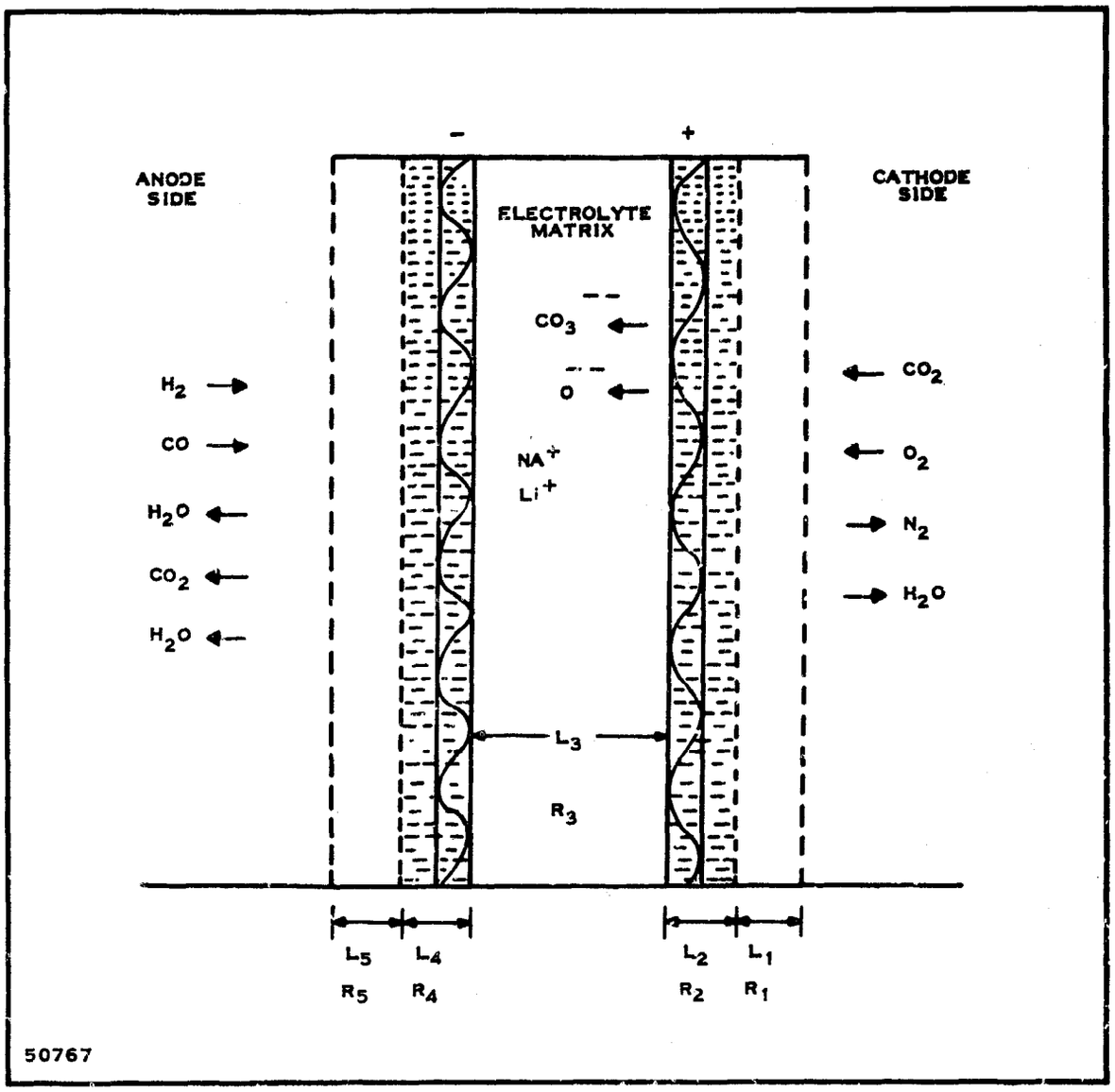

Figure 2-23. Transport Processes in Molten Carbonate Fuel Cells

their diffusion coefficients are about the same. A factor of 2 in the stoichiometry in favor of CO_2 will still limit the O_2 supply.

Case II—O_2 diffuses through the nonwetted silver and reacts with the CO_2 at the triple interface.

$$1/2\ O_2 + 2Ag \rightleftharpoons Ag_2O \quad (3)$$

$$Ag_2O \rightleftharpoons 2Ag^+ + O^{--} \quad (4)$$

$$2Ag^+ + 2\bar{e} \rightleftharpoons 2Ag \quad (5)$$

$$CO_2 + O^{--} \rightleftharpoons CO_3^{--} \quad (6)$$

The cathode potential is given by:

$$E_{cathode} = E^{\circ}_{cathode} - \frac{RT}{nF} \log_e \frac{\left(A_{CO_3^{--}}\right)}{\left(A_{CO_2}\right)\left(A_{O_2}\right)^{1/2}} \quad (7)$$

CO_2 and O^{--} in reaction (6) are probably chemisorbed species. Either of the reactions (3) or (4) can be slow, depending upon the wetting of the cathode and the proximity of oxygen dissolution and reaction sites.

(5) Anode Reaction Mechanism

The anode reactions may be postulated as follows:

Shift equilibrium $H_2 + CO_2 \rightleftharpoons H_2O + CO$ (8)

Dissociation equilibrium $CO_3^{--} \rightleftharpoons CO_2 + O^{--}$ (9)

Electron transfer $M + O^{--} \rightleftharpoons MO + 2\bar{e}$ (10)

Oxide reduction $MO + H_2 \rightleftharpoons M + H_2O$ (11)

If reaction (10) is also assumed at equilibrium, the anode potential may be represented as:

$$E_{anode} = E^{\circ}_{anode} - \frac{RT}{nF} \log_e \frac{\left(A_{H_2O}\right)\left(A_{CO_2}\right)}{\left(A_{H_2}\right)\left(A_{CO_3^{--}}\right)} \quad (12)$$

According to the preceding postulate, the anode reaction is slowed down due to either decreasing ionic population or by buildup of the partial pressure of carbon dioxide at the interface.

Excessive electrode wetting by the electrolyte can also limit anode performance by providing a barrier against elimination of the reaction products CO_2 and H_2O.

Alternatively, it may be postulated that the nickel surface provides catalytic sites and means for carrying electrons. In the examination of the controlling factor in this anode mechanism, the following reaction scheme may be examined:

$$H_2 \rightleftharpoons H_2(ads) \qquad (13)$$

$$CO_3^{--} \rightleftharpoons CO_3^{--}(ads) \qquad (14)$$

$$H_2(ads) + CO_3^{--}(ads) \rightleftharpoons H_2O(ads) + CO_2(ads) + 2\bar{e} \qquad (15)$$

$$H_2O(ads) + CO_2(ads) \rightleftharpoons H_2O + CO_2 \qquad (16)$$

In this case, at fixed total pressure, increasing the partial pressure of hydrogen at any voltage setting under load should have the following effects:

(a) Increase the current density if the adsorption of hydrogen is the controlling factor, i.e., reaction (13) controls

(b) Decrease the current density if the adsorption of CO_3^{--} ions is the controlling factor, i.e., reaction (14) controls

(c) Increase the current density to an optimum and then decrease if reaction (15) is controlling

(d) Result in no change in current density if the desorption of the products, i.e., reaction (16) is controlling.

Although the increase in performance with increase in temperature over a range of 600°C to 800°C, appears to parallel the permeation of hydrogen through nickel (Figure 2-24), and also the current density invariably increases with increase in partial pressure of hydrogen, the elucidation of the anode mechanism is made difficult due to uncontrolled wetting of the anode and by gas leakage.

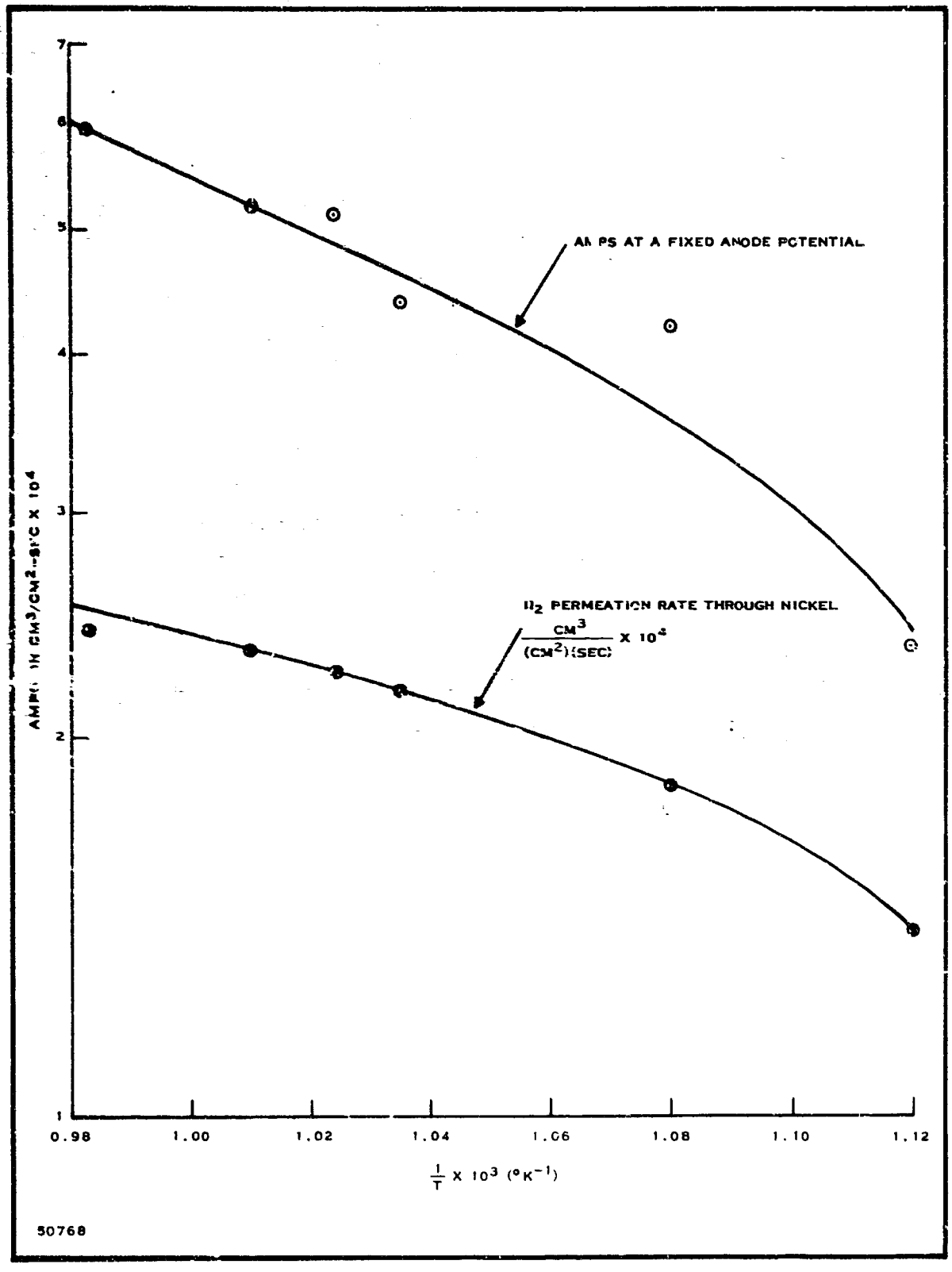

Figure 2-24. Effect of Temperature

By combining Equations (7) and (12), one obtains the equation for theoretical cell potential:

$$E_{cell} = E^{\circ}_{cell} + \frac{RT}{nF} \log_e \frac{\left(A_{H_2}\right)_a \left(A_{CO_2}\right)_c \left(A_{O_2}\right)_c^{1/2}}{\left(A_{H_2O}\right)_a \left(A_{CO_2}\right)_a} \qquad (17)$$

Subscripts a and c designate anode and cathode.

4. Exploratory Testing

The exploratory testing of thin matrix modules comprised the following constructional and operational changes:

Constructional Changes

- Module design
- Size of the module
- Electrode size
- Electrode materials (including special coatings on the electrodes)
- Matrix composition

Operational Variables

- Temperature and temperature cycling
- CO_2/O_2 ratio on air side, and air side composition
- Fuel composition and fuel flow rate
- Load characteristics
- Activation and deactivation.

a. Module Design

Two designs of thin matrix modules were investigated, the development type shown in Figures 2-25 and 2-26, and the production type shown in Figure 2-27 (see Figures 2-1, 2-10, 2-13, and 2-16). Pertinent data on these types are given in Tables 2-1 and 2-2, respectively.

b. Size of the Module

Module size varied from one cell to 20 cells for development type and from two cells to 100 cells for the production type.

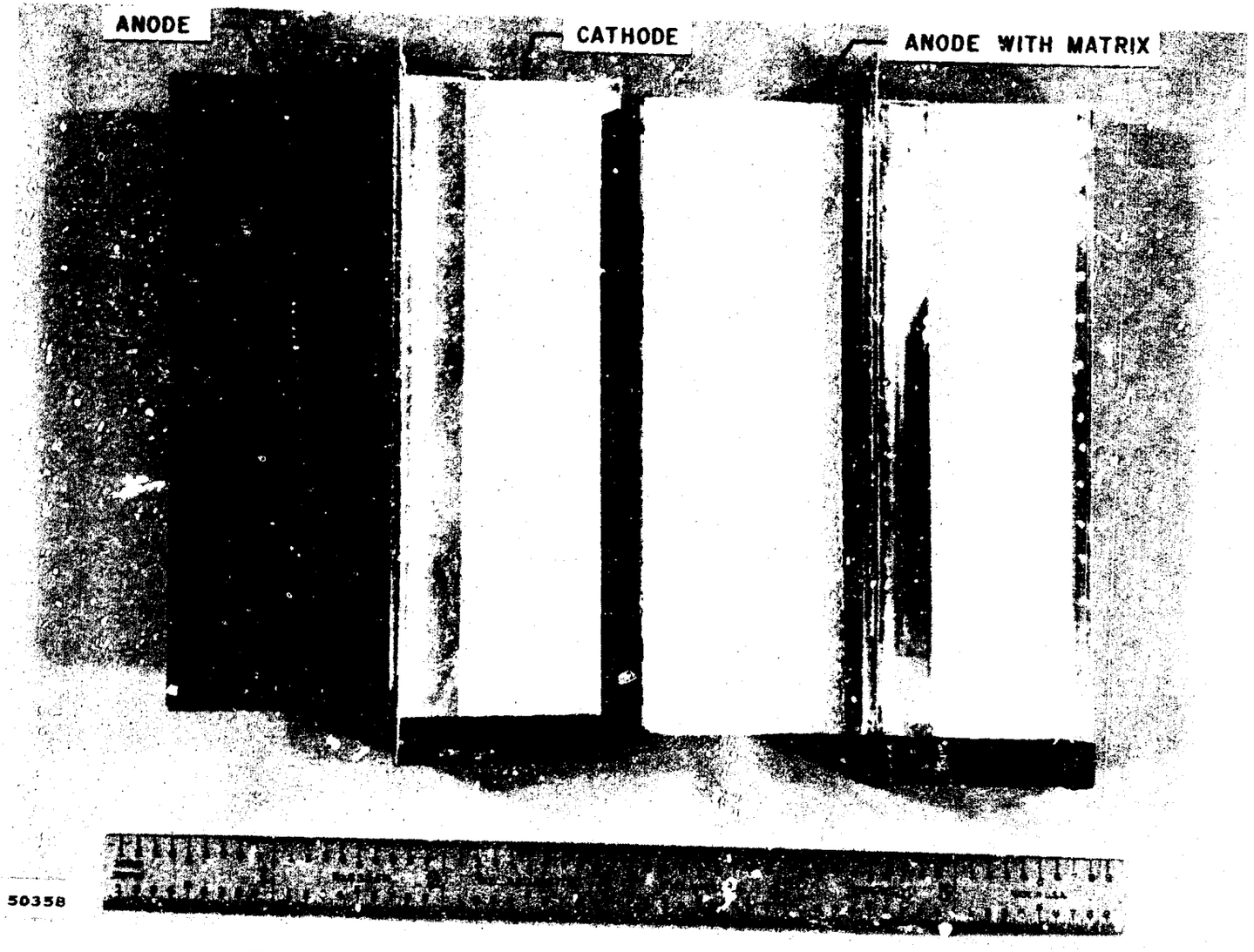

Figure 2-25. Development Type Thin Matrix Electrodes

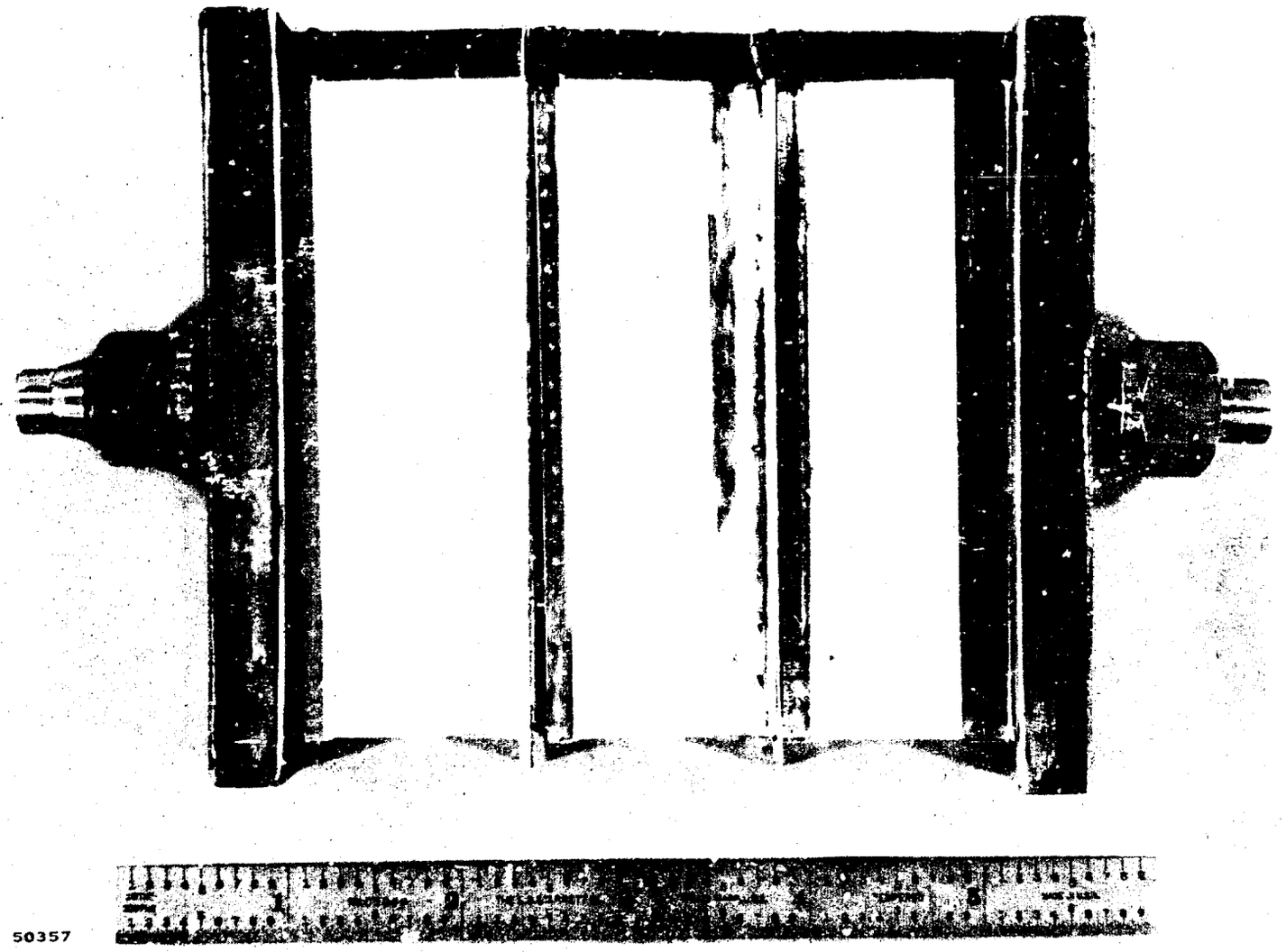

Figure 2-26. A Six-Cell Development Type Module

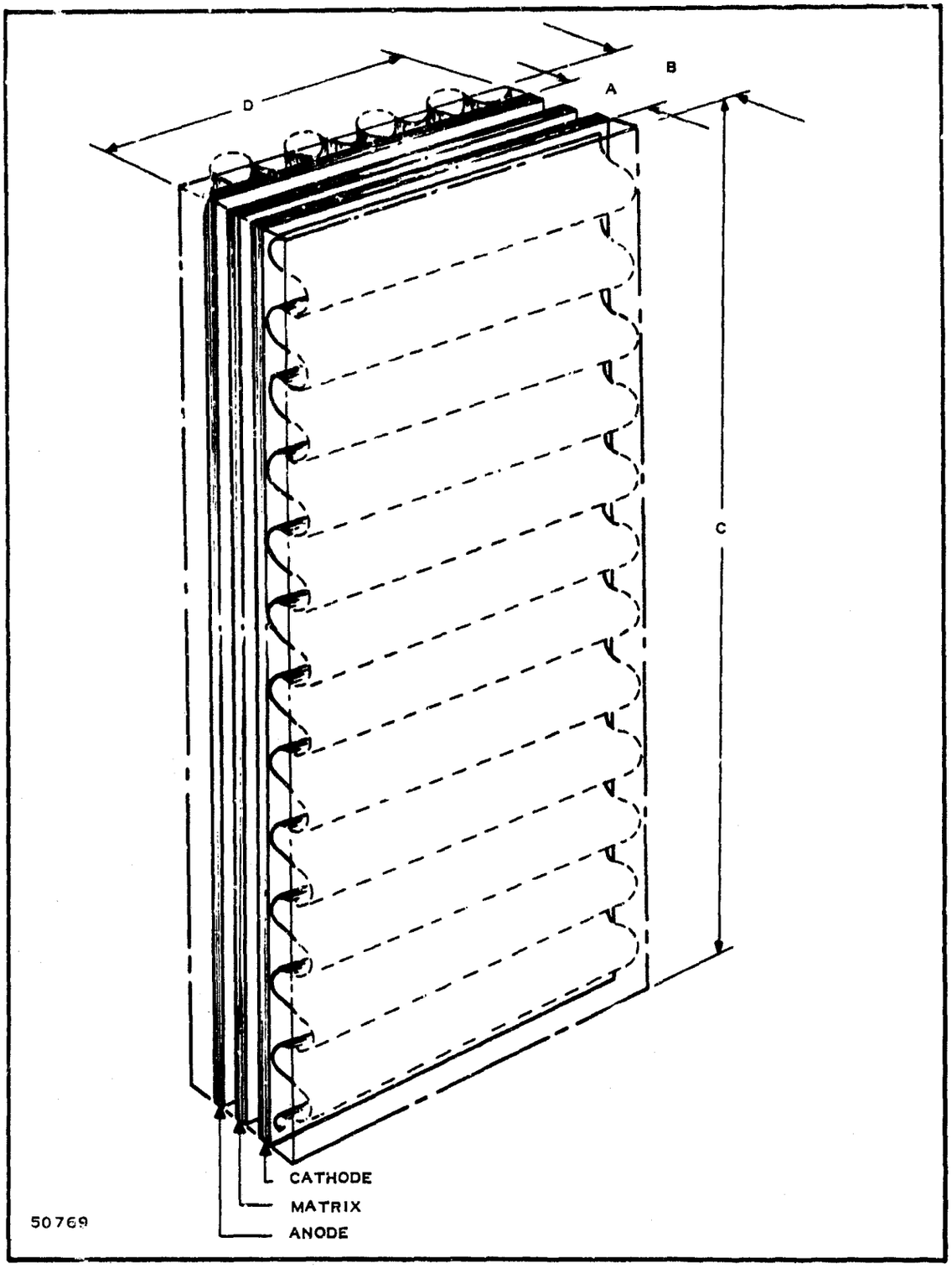

Figure 2-27. Thin Matrix Module Cell Design

Table 2-1. Performance of Development-Type Modules

Module TMM No.	Construction	Factor	Open Circuit Voltage on P. Ox. Fuel	η/IR Ratio	Best Performance amps/ft^2 at 0.7 volt	Lifetime (hours)	Reasons for Shutdown
				June 1966			
30-A	1 × 2	18	0.98	8.3	50.6	142.7	Decline in performance
30-B	1 × 2	18	0.99	13.7	46.0	7.3	Cathodes split open
30-D	1 × 2	18	1.02	6.2	42.2	30.6	Mechanical shorts
				July 1966			
30-E	1 × 2	18	0.76	—	—	7.5	Cathodes split open
30-F	1 × 2	18	0.93	6.2	37.1	52.9	Poor performance
30-G	1 × 2	18	—	—	—	0.9	Shorted
30-H	1 × 2	18	0.96	13.3	32.0	18.2	Unstable
31	1 × 2	24	0.98	11.5	29.2	119.0	Mechanical shorts
32	10 × 2	2.4	9.40	15.8	70.0	20.1	Mechanical shorts
33	1 × 6	18	1.04	4.8	63.8	47.0	Mechanical shorts
34	1 × 2	18	1.02	15.4	37.4	35.5	Mechanical shorts

Table 2-1. Performance of Development-Type Modules (Continued)

Module TMM No.	Construction	Factor	Open Circuit Voltage on P. Ox. Fuel	η/IR Ratio	Best Performance amps/ft^2 at 0.7 volt	Lifetime (hours)	Reasons for Shutdown
			July 1966 (Continued)				
36	1 × 2	18	1.02	7.7	34.0	23.7	Short-term test
37	1 × 2	18	1.04	10.0	51.0	30.1	Shorted
38	1 × 2	18	0.97	7.7	31.6	93.6	Decline in performance
39	1 × 2	18	0.98	12.8	14.0	41.2	Poor performance
40	1 × 2	18	0.97	6.3	28.6	77.0	Decline in performance
41	1 × 2	18	0.95	8.4	28.2	51.5	Decline in performance
			August 1966				
42	3 × 2	6	—	—	—	1.0	Mechanical shorts
43	1 × 2	18	—	—	—	3.8	Mechanical shorts
45	1 × 2	18	0.95	7.1	27.5	74.0	Unstable
46	1 × 2	18	0.98	8.1	34.6	70.7	Unstable
47	1 × 2	18	0.93	10.5	11.3	41.1	Poor performance

Table 2-1. Performance of Development-Type Modules (Continued)

Module TMM No.	Construction	Factor	Open Circuit Voltage on P. Ox. Fuel	η/IR Ratio	Best Performance amps/ft^2 at 0.7 volt	Lifetime (hours)	Reasons for Shutdown
			August 1966 (Continued)				
48	1 × 2	18	0.95	5.6	15.4	7.0	Fires
49	1 × 2	18	0.95	6.7	51.7	46.2	Shorted
50	1 × 2	18	—	—	—	1.3	Shorted
51	1 × 2	18	1.05	4.7	66.8	74.5	Shorted
52	1 × 2	18	1.07	8.9	41.5	162.0	Decline in performance
53	3 × 2	6	3.10	12.0	42.7	55.8	Unstable
54	1 × 2	18	0.95	5.7	22.5	3.5	Poor performance
55	1 × 2	18	0.45	—	—	24.0	Low open circuit voltage
56	1 × 2	18	0.95	10.0	18.0	2.3	Fires
			September 1966				
35	8 × 2	1.5	7.70	13.8	40.0	55.0	Unstable
57	1 × 2	18	1.07	7.3	20.7	80.3	Unstable

Table 2-1. Performance of Development-Type Modules (Continued)

Module TMM No.	Construction	Factor	Open Circuit Voltage on P. Ox. Fuel	η/IR Ratio	Best Performance amps/ft^2 at 0.7 volt	Lifetime (hours)	Reasons for Shutdown
			September 1966 (Continued)				
58	1 × 2	18	1.03	5.4	22.9	59.0	Unstable
59	1 × 2	18	1.03	7.7	38.6	23.7	Unstable
60	1 × 2	18	1.07	4.3	55.3	418.7	Decline in performance below 10 W/ft^2
61	1 × 2	18	0.95	9.0	24.8	144.5	Decline in performance below 10 W/ft^2
62	1 × 2	18	0.99	8.9	29.2	196.2	Decline in performance below 10 W/ft^2
63	1 × 2	18	0.98	3.6	63.7	96.3	Decline in performance below 10 W/ft^2
64	1 × 2	18	0.99	13.3	21.8	262.8	Decline in performance below 10 W/ft^2
65	1 × 2	18	1.02	6.2	58.0	318.0	Decline in performance below 10 W/ft^2

Table 2-1. Performance of Development-Type Modules (Continued)

Module TMM No.	Construction	Factor	Open Circuit Voltage on P. Ox. Fuel	η/IR Ratio	Best Performance amps/ft^2 at 0.7 volt	Lifetime (hours)	Reasons for Shutdown
			September 1966 (Continued)				
66-A	1 × 2	18	1.04	13.3	25.6	366.4	Decline in open circuit voltage
			October 1966				
66-B	1 × 2	18	1.00	—	—	28.8	Unstable
66-O	1 × 2	18	0.96	—	—	6.9	Unstable
68	1 × 2	18	0.93	24.5	7.3	22.2	Poor performance
70	1 × 2	18	0.91	—	—	18.8	Unstable
			November 1966				
66-M	1 × 2	18	0.98	13.0	16.8	73.6	Poor performance
66-H	1 × 2	18	1.06	10.7	15.5	51.3	Poor performance
71-C	1 × 2	18	0.90	—	—	2.8	Shorted
71-D	1 × 2	18	0.92	—	—	29.6	Unstable

Table 2-1. Performance of Development-Type Modules (Continued)

Module TMM No.	Construction	Factor	Open Circuit Voltage on P. Ox. Fuel	η/IR Ratio	Best Performance amps/ft^2 at 0.7 volt	Lifetime (hours)	Reasons for Shutdown
			December 1966				
66-C	1 × 2	18	0.97	15.0	22.3	213.5	Decline in performance
66-D	1 × 2	18	0.94	20.0	10.6	5.8	Poor performance
66-K	1 × 2	18	0.97	38.6	5.4	27.5	Poor performance
66-I	1 × 2	18	0.90	12.5	14.4	85.2	Poor performance
66-N	1 × 2	18	0.98	26.6	12.6	235.9	Unstable and poor performance
71-E	1 × 2	18	0.96	22.5	12.4	24.7	Unstable and poor performance
71-F	1 × 2	18	0.96	24.0	24.4	22.7	Unstable
72-A	1 × 2	18	0.97	13.6	39.6	21.5	Unstable
73-A	1 × 2	18	0.99	10.0	43.5	298.8	Decline in performance
73-B	1 × 2	18	1.00	6.0	60.0	353.0	Decline in performance

Table 2-1. Performance of Development-Type Modules (Continued)

Module TMM No.	Construction	Factor	Open Circuit Voltage on P. Ox. Fuel	η/IR Ratio	Best Performance amps/ft^2 at 0.7 volt	Lifetime (hours)	Reasons for Shutdown
				January 1967			
73-C	1 × 2	18	1.04	6.5	58.8	3.7	Unstable
73-D	1 × 2	18	1.00	21.5	16.5	24.8	Poor performance
74	1 × 2	18	0.98	16.5	30.6	98.3	Decline in performance
74-A	1 × 2	18	0.99	10.8	28.4	25.4	Shorted
75-A	1 × 2	18	1.02	8.3	43.2	70.3	Decline in performance
76-A	1 × 2	18	1.01	7.2	38.7	150.4	Decline in performance
D-1	1 × 2	18	—	—	—	16.0	Fires
D-2	1 × 2	18	0.98	5.7	42.2	26.3	Unstable
D-3	1 × 2	18	1.00	15.0	27.0	22.0	Unstable
D-4	1 × 2	18	1.05	7.5	18.0	23.9	Poor performance
[illegible]	1 × 2	18	1.00	4.0	36.0	45.0	Decline in performance
D-6	1 × 2	18	0.95	2.3	88.7	40.0	Low open circuit voltage and anode flooded

Table 2-1. Performance of Development-Type Modules (Continued)

Module TMM No.	Construction	Factor	Open Circuit Voltage on P. Ox. Fuel	η/IR Ratio	Best Performance amps/ft² at 0.7 volt	Lifetime (hours)	Reasons for Shutdown
				January 1967			
D-8	1 × 2	18	0.99	—	—	29.7	Unstable
D-9	1 × 2	18	—	—	—	1.4	Shorted
D-10	1 × 2	18	1.04	10.8	33.4	71.4	Drop in open circuit voltage
D-11	1 × 2	18	0.95	2.2	44.5	24.0	Unstable
D-12	1 × 2	18	1.03	3.8	33.3	102.1	Decline in performance
D-13	1 × 2	18	0.92	1.0	82.3	65.7	Low open circuit voltage and unstable
D-14	1 × 2	18	0.94	14.6	22.8	47.5	Poor performance
D-15	1 × 2	18	0.83	—	—	2.0	Fire
D-16	1 × 2	18	1.06	7.1	54.0	47.7	Decline in performance
D-17	1 × 2	18	0.98	7.3	28.8	117.7	Unstable

Table 2-1. Performance of Development-Type Module (Continued)

Module TMM No.	Construction	Factor	Open Circuit Voltage on P. Ox. Fuel	η/IR Ratio	Best Performance amps/ft at 0.7 volt	Lifetime (hours)	Reasons for Shutdown
				February 1967			
D-18	1 × 2	18	0.98	22.0	16.4	47.0	Poor performance
D-19	2 × 4	9	—	—	—	1.3	Shorted
D-20	1 × 2	18	—	—	—	2.1	Fire

Explanation

Construction: First number designates cells in series, and second number designates cells in parallel.

Factor: It is computed by (1 ft^2)/area of test cells—ft^2

P. Ox. Fuel: Partial-oxidation fuel containing 20- to 40-percent combustibles.

η/IR Ratio = $\frac{\text{total polarization}}{\text{IR drop}}$

Best Performance at 0.7 volt: It is computed from performance at a given time, corrected to 0.7 volt by η/IR ratio.

Lifetime: The total time cell was in operation or under test.

Table 2-2. Performance of Production-Type Modules

Module No.	Arrangement[1]	Starting Date	Operating Hours[2]	Maximum Open Circuit Voltage[3]	Maximum Performance[4] (watts/square foot)	Reason for Shutdown[5]
		1966				
1	2 × 4	7-14	19.4	1.32	—	Fires—probable short
2	3 × 4	7-22	9.2	2.60	6.1	—
3	1 × 2	8-11	26.0	0.95	26.0	Probable short
4	1 × 4	8-17	—	—	—	Probable short
5	1 × 2	8-22	22.5	0.96	42.0	Probable short
6	1 × 2	8-25	186.2	0.89	17.5	Probable short
7	1 × 4	8-31	10.6	1.00	10.7	Probable short
8	1 × 4	9-12	12.0	1.03	28.5	Probable short
9	1 × 4	9-20	54.8	0.86	10.0	
10	1 × 4	9-28	217.6	0.96	19.0	Fire at anode plenum
11	2 × 4	9-30	57.7	1.83	9.3	Fires
12	1 × 4	10-5	2.1	0.97	—	—
13	1 × 4	10-11	17.7	0.94	19.0	Suspected gas communication
14	1 × 4	10-18	47.8	0.92	12.5	—
15	1 × 4	10-26	21.9	0.94	13.3	Inadequate performance
16	1 × 4	11-25	23.0	0.92	19.7	Inadequate performance
17	1 × 4	11-28	193.1	0.98	15.7	Inadequate performance
18	1 × 10	12-8	42.8	1.04	20.5	Inadequate performance
		1967				
19	1 × 4	1-9	24.2	1.00	7.7	—

Table 2-2. Performance of Production-Type Modules (Continued)

Module No.	Arrangement[1]	Starting Date	Operating Hours[2]	Maximum Open Circuit Voltage[3]	Maximum Performance[4] (watts/square foot)	Reason for Shutdown[5]
		1967				
20	1 X 4	2-1	23.0	0.92	—	Inadequate performance
21	2 X 10	2-3	35.8	1.74	11.3	Inadequate performance
22	2 X 10	2-4	85.7	1.80	10.5	Inadequate performance
23	1 X 4	2-10	232.0	0.98	24.8	Inadequate performance
24	1 X 4	2-14	23.7	0.85	14.0	Inadequate performance
25	1 X 4	2-14	23.3	0.87	7.0	
26	1 X 4	2-15	114.2	0.93	24.4	Inadequate performance
27	1 X 4	2-20	0.5	1.00	—	Fire at anode plenum
28	1 X 4	2-20	49.7	0.92	22.8	Fire at cathode plenum
29	1 X 4	2-21	70.3	0.96	12.4	Fire on center cathode
30	1 X 4	2-24	19.2	0.97	8.0	Inadequate performance
31	1 X 4	2-28	10.2	0.92	10.0	Inadequate performance
32	2 X 10	2-24	113.8	1.71	5.4	Inadequate performance
33	3 X 4	3-1	145.5	2.43	8.4	Inadequate performance
34	3 X 4	3-1	171.8	2.83	7.2	Inadequate performance
35	1 X 2	3-2	229.0	1.05	31.0	Inadequate performance
36	1 X 2	3-7	19.3	0.94	17.2	Inadequate performance
37	1 X 2	3-8	150.3	0.90	58.8	Experiment complete
38	1 X 2	3-8	18.2	0.80	—	Experiment complete
39	1 X 2	3-9	91.7	0.94	11.2	Shorted

Table 2-2. Performance of Production-Type Modules (Continued)

Module No.	Arrangement[1]	Starting Date	Operating Hours[2]	Maximum Open Circuit Voltage[3]	Maximum Performance[4] (watts/square foot)	Reason for Shutdown[5]
		1967				
40	1 X 4	3-10	85.6	0.98	21.3	Inadequate performance
41	1 X 2	3-13	6.2	0.97	15.0	Shorted
42	1 X 2	3-14	2.9	—	25.2	Experiment complete
43	1 X 2	3-15	3.4	—	—	Experiment complete
44	1 X 4	3-15	491.0	1.0	34.5	Inadequate performance
45	3 X 10	3-16	250.0	2.74	16.8	Fire on center cell
46	1 X 4	3-16	71.5	1.0	11.4	Inadequate performance
47	1 X 2	3-16	29.8	—	22.5	Experiment complete
48	1 X 2	3-17	69.2	—	—	Experiment complete
49	3 X 10	3-17	189.0	2.65	18.2	Inadequate performance
50	1 X 4	3-20	712.0	0.99	24.5	Inadequate performance
51	1 X 2	3-20	68.0	0.97	18.7	Inadequate performance
52	3 X 4	3-21	380.0	2.92	24.6	Inadequate performance
53	1 X 2	3-21	151.0	0.94	20.0	Inadequate performance
54	1 X 2	3-22	143.0	1.03	26.7	Inadequate performance
55	3 X 4	3-22	504.0	2.87	22.6	Inadequate performance
56	1 X 2	3-23	311.0	0.96	29.2	Inadequate performance
57	1 X 4	3-27	47.0	0.96	28.1	Shorted
58	1 X 2	3-28	221.0	1.03	24.0	Inadequate performance
59	1 X 4	3-29	4.0	0.1	—	Massive gas communication

Table 2-2. Performance of Production-Type Modules (Continued)

Module No.	Arrangement[1]	Starting Date	Operating Hours[2]	Maximum Open Circuit Voltage[3]	Maximum Performance[4] (watts/square foot)	Reason for Shutdown[5]
		1967				
60	1 X 2	3-30	411.0	1.00	45.3	Inadequate performance
61	1 X 2	3-30	176.0	1.02	25.2	Fire at anode plenum
62	1 X 2	4-3	146.0	1.05	32.0	Inadequate performance
63	3 X 10	4-4	312.0	3.00	40.3	Fires at anode plenum
64	1 X 6	4-5	54.0	1.03	15.0	Massive fires
65	1 X 2	4-5	427.0	1.03	42.0	Fire at anode plenum
66	1 X 4	4-5	164.0	1.02	37.0	Inadequate performance
67	3 X 10	4-10	50.0	2.90	23.7	Inadequate performance
68	1 X 4	4-10	15.0	0.93	17.5	Faulty test station
69	1 X 2	4-11	123.0	0.99	31.0	Shorted
70	1 X 4	4-12	50.0	0.99	35.0	Test completed
71	3 X 10	4-13	26.0	2.92	18.5	
72	1 X 4	4-13	58.0	1.02	21.3	Test station failure
73	1 X 4	4-18	6.0	0.97	24.5	Internal fires
74	1 X 4	4-18	146.0	0.96	33.5	Test completed
75	1 X 4	4-19	22.0	—	16.5	Test completed
76	1 X 4	4-19	26.0	1.01	38.5	Faulty weld
77	1 X 4	4-20	5.0	—	—	Faulty weld
78	1 X 4	4-21	70.0	1.02	16.5	Shorted
79	1 X 2	4-22	102.0	0.97	9.8	Test completed
80	1 X 4	4-24	209.0	1.05	26.8	Inadequate performance

Table 2-2. Performance of Production-Type Modules (Continued)

Module No.	Arrangement[1]	Starting Date	Operating Hours[2]	Maximum Open Circuit Voltage[3]	Maximum Performance[4] (watts/square foot)	Reason for Shutdown[5]
		1967				
81	1 X 4	4-24	212.0	1.04	22.8	Test completed
82	1 X 4	4-24	248.0	0.99	27.0	Test completed
83	1 X 4	4-25	36.0	1.00	43.0	Faulty weld
84	3 X 10	4-25	150.0	2.94	31.3	Plenum leakage
85	1 X 2	4-25	37.0	1.01	22.5	Inadequate performance
86	1 X 2	4-27	113.0	0.99	12.6	Shorted
87	1 X 10	4-28	186.0	1.02	24.1	Fires
88	1 X 4	5-2	12.0	1.03	28.0	Plenum separation
89	1 X 4	5-2	114.0	0.99	24.8	Shorted
90	3 X 10	5-2	60.0	2.98	33.8	Plenum leakage
91	1 X 2	5-2	120.0	1.01	30.0	Shorted
92	1 X 2	5-3	147.0	1.05	24.6	Faulty welding
93	1 X 4	5-3	154.0	1.02	33.5	Shorted
94	1 X 2	5-4	145.0	1.03	35.0	Inadequate performance
95	1 X 4	5-8	220.0	1.00	20.3	In operation
96	3 X 10	5-9	72.0	2.83	16.1	In operation
97	1 X 2	5-11	8.4	1.02	14.8	Shorted
98	1 X 2	5-11	—	—	—	Inadequate performance
99	3 X 2	5-15	—	2.60	—	In operation
100	1 X 10	5-16	—	—	—	In operation

Table 2-2. Performance of Production-Type Modules (Continued)

Module No.	Arrangement[1]	Starting Date	Operating Hours[2]	Maximum Open Circuit Voltage[3]	Maximum Performance[4] (watts/square foot)	Reason for Shutdown[5]
		1967				
101	1 × 2	5-17	—	—	—	In operation
102	1 × 4	5-17	—	—	—	In operation

****

35 Operated above 25 W/ft^2 for 61 hours

44 Operated above 25 W/ft^2 for 86 hours

60 Operated above 25 W/ft^2 for 110 hours

60 Operated above 30 W/ft^2 for 66 hours

63 Operated above 30 W/ft^2 for 41 hours

66 Operated above 30 W/ft^2 for 94 hours

76 Operated above 30 W/ft^2 for 18 hours

83 Operated above 30 W/ft^2 for 21 hours

83 Operated above 35 W/ft^2 for 16 hours

83 Operated above 40 W/ft^2 for 7 hours

DESCRIPTION OF SUPERSCRIPTS FOR TABLE 2-2

1. In the Texas Instruments designate of fuel cell arrangement, the first number is the number of cells in series, and the second number is the number of cells in parallel. For example, a 12 by 10 module consists of 12 cell blocks in series, each block containing 10 cells in parallel.

2. Operating hours is the time the fuel cell module has spent above approximately 500°C.

3. The maximum open circuit voltage is listed for the entire module. For example, the module open circuit potential of No. 2 is 2.6 volts, and the average cell open circuit is 0.86 volt. The maximum open circuit potential usually (but not always) occurs early in life.

4. Data on maximum performance is short time data but is <u>not</u> taken from E-I plots.

5. The reason for shutdown does not necessarily reflect the ability of the unit to continue. Many were shut down for specific post-operation examination. "Inadequate performance," as a reason for shutdown, merely means that power output was below 20 watts/ft^2 at the time of shutdown.

c. Electrode Size

Electrode size was varied widely in both types of modules. The single cell area of the development module was varied from 3 square inches (3/4 by 4 inches) to 8 square inches (1 by 8 inches). For the production type modules the single cell area was varied from 4 square inches (1 by 4 inches) to 24 square inches (3 by 8 inches).

d. Electrode Materials

Anode and cathode materials normally employed were nickel 200 and S. S. 316 wire screen mesh, size 80. The wire thickness varied from 5 to 10 mils. For production-type modules the electrodes were cleaned in an ultrasonic cleaner. The cathodes were silver-plated and/or painted with Englehard silver 321. For some tests S. S. 446, S. S. 430, and S. S. 304 wire screen, or expanded or perforated metal of various mesh sizes, were tested as anodes and cathodes. A summary of the materials tested is given below:

Anodes

- Nickel wire mesh, with or without coatings
- Nickel expanded metal, with or without coatings
- S. S. 446 wire mesh, with or without coatings
- S. S. 446 expanded metal, with or without coatings
- S. S. 430 expanded metal, with coatings
- S. S. 304 perforated metal, with coatings
- Nickel plaque, activated or nonactivated

Cathodes

- S. S. 316 wire mesh, silver-plated and/or silver-painted
- S. S. 446 wire mesh, silver-plated and/or silver-painted
- S. S. 446 expanded metal, with or without silver paint
- S. S. 316, copper-plated
- S. S. 316, silver-plated with specific coatings

The thickness of silver plate or paint varied from 0.1 to 1.0 mil.

The coatings on the anode screen included silver, cobalt, graphite, iron, chromium, copper, molybdenum, nickel aluminite, lithium aluminate, lithium manganite, lithium borate, lithium ferrite, lithium silicate, lithium cobaltite, and lithium nickelite. No correlation between anode coating and anode performance could be established. The presence of graphite and/or silver seemed to preserve the anode from becoming over-oxidized and flooded. Electrodes without nickel (S. S. 446) did not function as anodes. Nickel plaque anodes were flooded and showed low voltages and severe polarization characteristics. The performance of two of these cells is described below.

Two 1 by 2 modules were constructed with activated nickel plaque as the anodes. The anodes were supported with S. S. 446–80 mesh secondaries. The cathode in one module (D5) consisted of S. S. 446–80 mesh screen, painted with Englehard No. 321 silver paint. The cathode of the second module (D6) had Englehard No. 321 paint containing CdO—20 percent by weight—on S. S. 446–80 mesh screen. The cathodes had corrugated stiffeners of material similar to cathodes, simulating construction pattern of the production-type modules.

Both modules were normally operated at 700°C with simulated partial-oxidizer fuel containing about 40 percent combustibles. The air side composition was CO_2 — 10 percent, O_2 — 5 percent, H_2O — 10 percent, N_2 — 75 percent. Their performance characteristics were similar. Some notable features are as follows:

Internal resistance of the cells was higher by factor of about three, compared to other thin matrix cells

The open circuit voltages were equal to theoretical. The open circuit voltage using H_2 (100 percent) stream was 1.23 volts, signifying good sealing.

The IR-free cell polarization was three to six times the IR drop.

On depolarization at constant speeds, there was severe hysterisis effect.

The modules could not be activated by normal procedure of short—circuiting, or by attempts to reduce activated nickel to elemental form by using hydrogen (100 percent) in the fuel stream.

Examination after discontinuation of the experiments revealed flooding of the anodes.

The cathode of the module (D6) had black shiny crystalloids on the matrix side.

Cathodes made of S. S. 446 without silver showed low voltages and severe polarization. Some examples of coatings on cathodes of development-type modules are given below.

TMM No. 18

This cell, after 171 hours of operation, was cooled and its cathodes were repainted with silver containing 20-percent Cu_2O by weight. The cell improved 220 percent, from 10.8 watts/square foot at 0.7 volt to 23.8 watts/square foot at 0.7 volt; and after 75 hours of operation, it was operating at 126 percent improvement.

TMM No. 20

This cell operated for 126 hours using silver-painted (without any additives) cathodes. The cell was cooled and repainted with silver paint (without any additives). Its performance improved by 47 percent, from 6.8 watts/square foot at 0.7 volt. The cell was cooled and heated up again. The performance improved by 12 percent, from 10.0 watts/square foot at 0.7 volt. The cell was cooled again and the cathodes were painted with silver containing Cu_2O (20 percent by weight). The cell improved 240 percent, from 11.2 watts/square foot to 26.9 watts/square foot at 0.7 volt.

TMM No. 22

After 48 hours of operation the cell was cooled and its cathodes painted with silver containing Cu_2O (20 percent by weight). The performance of the cell improved 320 percent, from 11.2 watts/square foot to 36 watts/square foot at 0.7 volt. It operated for 70 hours more at average improvement of 150 percent

TMM No. 23

After 43 hours of operation the cell was cooled and its cathodes painted with silver containing aluminum powder (5 percent by weight). The performance of the cell improved 100 percent, from 19.8 watts/square foot to 39.6 watts/square foot at 0.7 volt; and it operated for 60 hours more at an average improvement of 80 percent.

TMM No. 21

After 160 hours of operation the cell was cooled and its cathodes were painted with silver containing aluminum powder (5 percent by weight). The performance of the cell improved 100 percent, from 15.7 watts/square foot to 31.4 watts/square foot; and for 40 hours more it operated at an average improvement of 80 percent. The cell was again cooled and its cathodes painted with silver containing SnO_2 (20 percent by weight). The cell improved 56 percent, from 19.2 watts/square foot to 30 watts/square foot at 0.7 volt.

TMM No. 52

The cell operated for 69 hours, after which it was cooled and its cathodes painted with silver containing coloidal alumina (10 percent by weight). The performance of the cell improved 45 percent, from 19.4 watts/square foot to 28.1 watts/square foot at 0.7 volt; and it operated for 80 hours more at an average improvement of 35 percent.

e. Matrix Composition

The matrix for use in molten carbonate fuel cells should have the following properties.

Basic Properties

Porous enough to hold electrolyte

Gas tight

Electrically insulating

Some Desirable Properties

Composition invariance

Able to withstand thermal shock

Able to withstand mechanical stresses, strengthen the modules

Able to prevent silver migration

Able to prevent electrolyte decomposition

Easy application on the electrodes

The matrix materials tested consisted of:

Materials easily assembled, which on partial reaction with the electrolyte inside of the molten carbonate cells, yield a suitable matrix

Those materials which can be prereacted with the electrolyte or used as additives to form a viscous jelly type electrolyte matrix. This matrix can be used alone or in conjunction with a granular material like MgO, $LiAlO_2$, etc., to form a gas-tight matrix.

A suitable combination of the above concepts.

Materials tested have been found to meet the basic requirements of the matrix. However, none of the substances tested so far have shown all of the desirable properties listed above.

f. Matrix Thickness

Matrix thickness for development-type modules was varied from about 3 to 50 mils. For production-type modules, matrix thickness was 20 to 40 mils.

g. Temperature of Operation

Normal temperature of fuel cell operation was 700°C. Some tests were done at about 650°C, 720°C, 750°C, 780°C, and 800°C. The increase in performance with increase in temperature appears to depend on the enhanced activity of the electrodes, wetting characteristics

and cell sealing. No quantitative attempts are possible at this stage to optimize operating temperature. The influence of temperature on anode and cathode polarization of module D-69 is given in Table 2-3.

Table 2-3. Effect of Temperature of Operation on Anode and Cathode Polarization of D-69

Current Density amps/ft^2	IR-Free Polarization (millivolts (η))	
	Anode	Cathode
740°C		
10	12	40
20	40	60
30	60	80
40	90	100
714°C		
10	25	40
20	55	60
30	82	80
40	128	100
700°C		
10	30	40
20	65	60
30	95	80
40	147	100
690°C		
10	47	40
20	84	60
30	117	80
40	180	100

Table 2-3. Effect of Temperature of Operation on Anode and Cathode Polarization of D-69 (Continued)

Current Density amps/ft^2	IR-Free Polarization [millivolts (η)]	
	Anode	Cathode
652°C		
10	50	70
20	90	95
30	129	135
40	196	170
613°C		
10	70	150
20	230	220
30	380	305

The effect of temperature (given in Table 2-3) on anode and cathode polarization is by no means typical. In several instances cathode polarization, like the anode, continues to decrease with increase in temperature. There is no simple explanation for this discrepancy between behavior of two cathodes. Furthermore, the slope of polarization with temperature ($d\eta/dT$) at fixed current density varies from module to module.

h. CO_2/O_2 Ratio

Before September of 1966, air side composition was not monitored. Consequently, due to furnace leakage, etc., the air side composition before this date is questionable. However, subsequent to this date air side composition was fixed at CO_2/O_2 ratio of two and close to what would be obtainable under realistic conditions of fuel cell operation.

CO_2	10 percent
O_2	5 percent

H_2O	10 percent
N_2	75 percent

i. Fuel Composition and Flow Rate

Inlet fuel composition obtainable from the fuel preparation device is stated elsewhere. For operation on synthetic mixture the following mixture of gases shifted at 700°C was chosen as a standard.

Component	Feed Composition (percent by volume)	Shifted Composition (700°C) (percent by volume)
H_2	38.0	29.6
CO	—	8.4
CO_2	12.0	3.6
H_2O	—	8.4
N_2	50.0	50.0

This gas, after shift reaction, gives an open circuit voltage of 1.045 volt, similar to that obtainable from the gas (of the following composition) produced by the fuel preparation device. The following table gives the partial oxidation gas composition (700°C) based on CITE fuel, 20.4 percent excess air, and enough recycle to suppress carbon deposition.

Component	Partial Oxidation Gas Composition (700°C) (percent by volume)
H_2	20.0
CO	19.0
CO_2	5.4
H_2O	3.7
N_2	51.9

The standard fuel flow rate is 5 cfh at room temperature per fuel channel. Some testing was done with simulated partial oxidation fuel containing 20 to 40 percent combustibles at flow rates of 2 to 20 cfh per anode channel. A summary of results obtained is shown in Figure 2-28.

j. Load Characteristics

The normal loading of the fuel cells was to 0.7 volt. However, for several tests the cells were loaded from 0.6 to 0.9 volt.

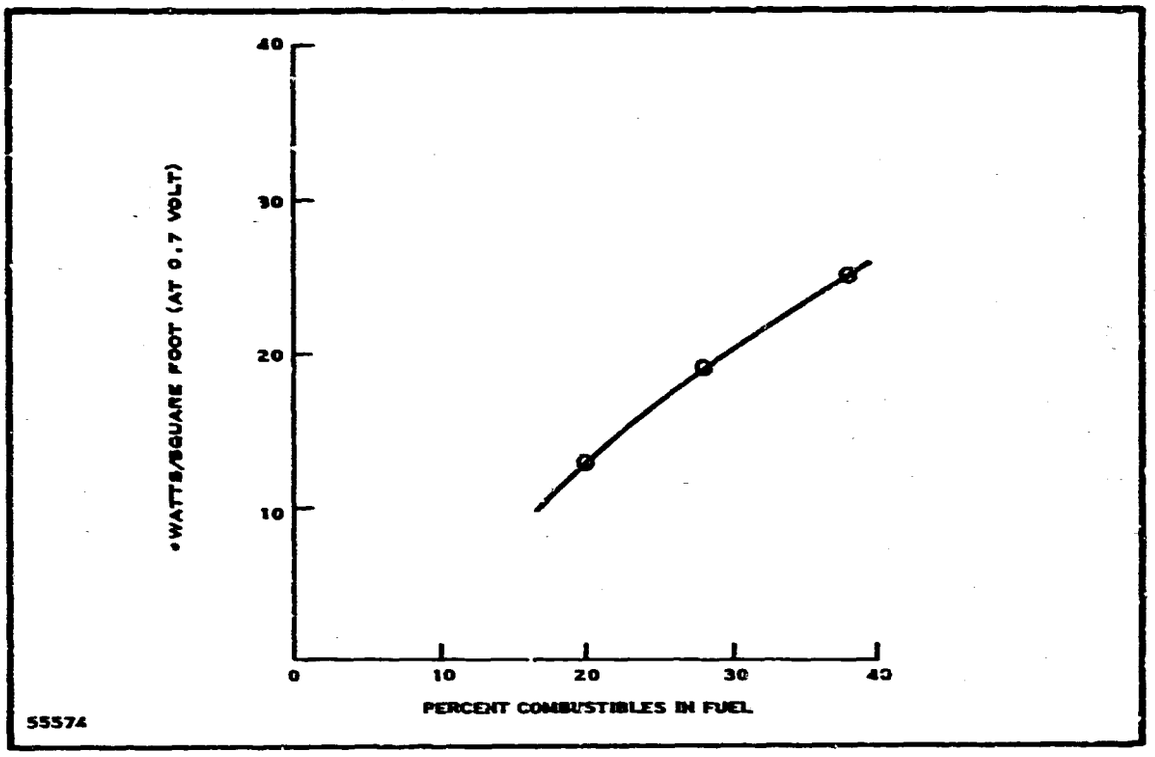

Figure 2-28. Effect of Fuel Composition on Module Performance

k. Activation and Deactivation

Little is known of the mechanism of activation. Some of the procedures followed for activation were as follows:

Short-circuiting the cell after cutting off hydrogen in the fuel

Passing a heavy current (100 to 150 amps/ft^2) after cutting off hydrogen in the fuel

Charging the cell with a heavy current (100 to 150 amps/ft^2), with or without fuel.

Some results of the activation in a typical cell are given below.

EFFECT OF ACTIVATION PROCEDURES ON D-59

Anodes: Nickel wire screen, 80 mesh, silver and Ni, Ni_2O (1:1) in Krylon painted

Cathodes: S. S. 316 80 mesh, silver-painted

Operation: Standard air side, partial-oxidation (10 cfh), 700°C.

Time	Performance at 0.7 Volt (amps/ft^2) From E-I Plots: Increasing Current*	Decreasing Current*
1. Initial performance	22.5	11.3
Five to Ten Hours		
2. After 15-minute drive at 100 amps/ft^2 without H_2	24.0	20.3
3. After another 15-minute drive at 100 amps/ft^2 without H_2	18.0	14.7
4. After 3-minute charging at 100 amps/ft^2 without H_2	25.7	22.9
5. After another 12-minute charging at 100 amps/ft^2 without H_2	45.5	43.2
6. After 3-minute ac supply 75 amps/ft^2 without H_2	31.0	29.5
7. After another 12-minute ac supply 100 amps/ft^2 without H_2	13.5	9.5
8. After 12-minute charging at 100 amps/ft^2 without H_2	44.0	41.0
Twenty-Five to Thirty Hours		
9. After 15-minute ac supply 40 amps/ft^2 through 0.6-ohm resistance without H_2	12.7	8.8
10. After 15-minute charging at 100 amps/ft^2 without H_2	41.5	41.5 (jiggles appear)
11. After 6-minute drive followed by 6 minutes of charging at 100 amps/ft^2 without H_2	34.0	28.0 (jiggles persist)
12. After 6-minute ac supply 20 amps/ft^2 through 1-ohm resistance without H_2	25.0	19.5 (jiggles disappear)
13. After charging for 3 minutes at 100 amps/ft^2 without H_2	37.0	30.3 (slight jiggles reappear)

	Time	Performance at 0.7 Volt (amps/ft^2) From E-I Plots: Increasing Current*	Performance at 0.7 Volt (amps/ft^2) From E-I Plots: Decreasing Current*
14.	After 3 minutes of ac supply at 20 amps/ft^2 through 0.3-ohm resistance with H_2	26.0	20.0 (jiggles disappear)
15.	After 15-minute short-circuit without H_2	14.5	11.0 (no jiggles)
16.	After 9 minutes of drive followed by 6 minutes of charging both at 100 amps/ft^2 without H_2	25.0	18.0 (slight jiggles appear)
17.	After 9 minutes of charging at 50 amps/ft^2 with H_2 on	25.5	17.5 (jiggles persist)

*At constant speeds.

A summary of some of the problems and probable reasons for these is given below.

Problem	Probable Reasons
Low open circuit voltage	Fuel composition Air side composition Lack of sealing Flooded anode Side reactions
Gas communication	Nonuniform matrix Lack of electrolyte in matrix Nonwetted anode Faulty welds
Jiggles	Gas communication Mixed potentials Side reactions Nonuniform wetting
Inadequate performance	Fires Shorts

Problem	Probable Reasons
Inadequate performance (continued)	Gas communication Low activity of the electrodes Poor contact between electrodes and matrix
Fires	Faulty welds Poor sealing Leaks through matrix-electrolyte
Shorts	Mechanical shorts due to poor assembly Nonrigid matrix—shear between electrodes and matrix Silver dendrite shorts Lack of adequate CO_2 on cathode side Lack of electrolyte in matrix
Failure of anode plenums	Electrochemical corrosion

Electrolyte control, sealing, and electrode activation remain the major problems in molten carbonate fuel cell development. Without positive control of these, the impact of configurational and operational changes more often than not becomes questionable. Operational curves of some typical modules are given in Figures 2-29 through 2-33. *

5. 1-Kilowatt Stack Breadboard, Design

a. General

The test of the 1-kilowatt fuel cell stack was designed to simulate conditions that are expected in an actual 1-kilowatt system. Thus, in certain respects, the features of the breadboard are identical to those of a complete unit:

Module supports

Headers and manifolds

Insulating enclosure

*Additional performance results are graphically presented in Appendix B.

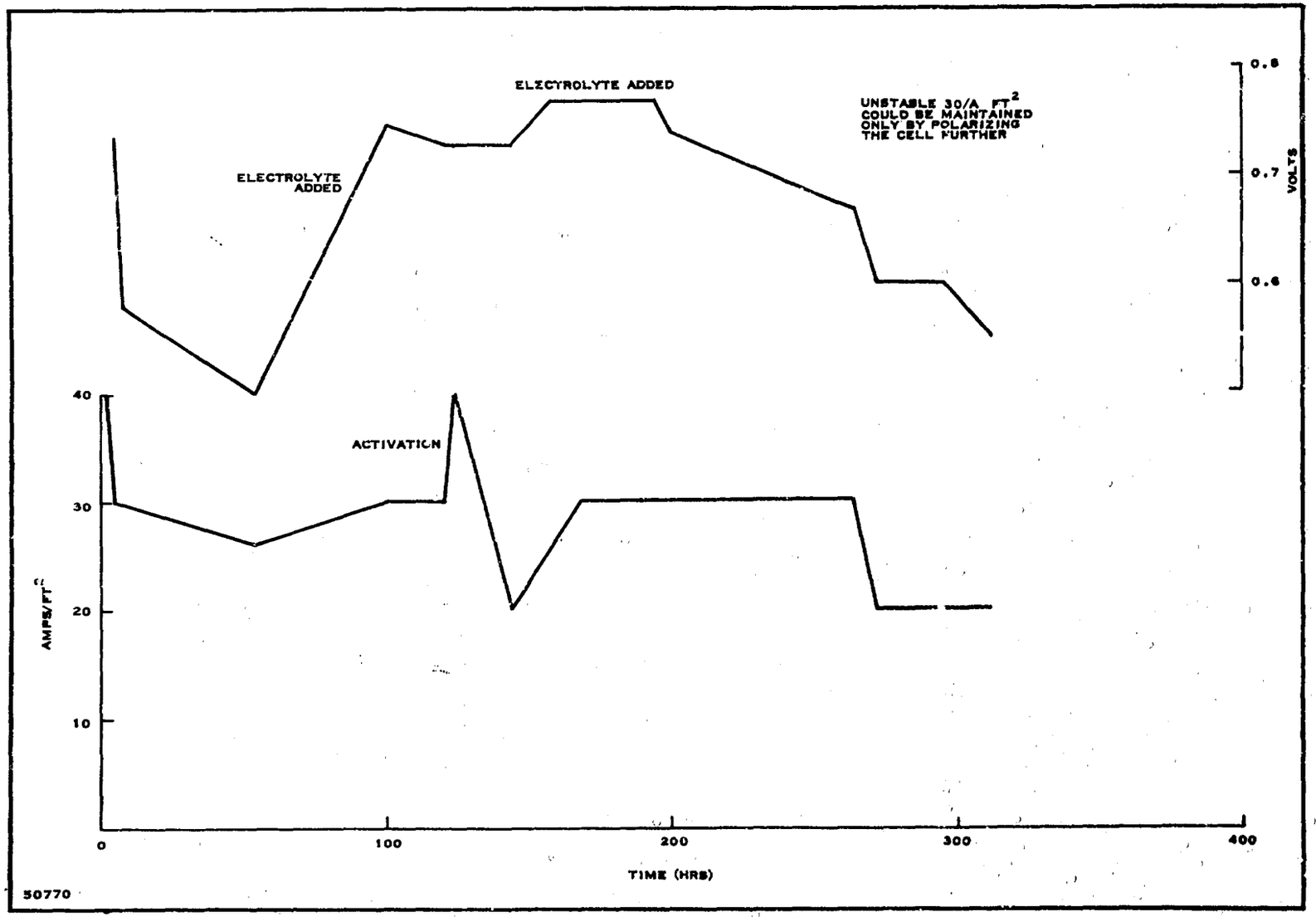

Figure 2-29. Operational Curve of TMM D-50

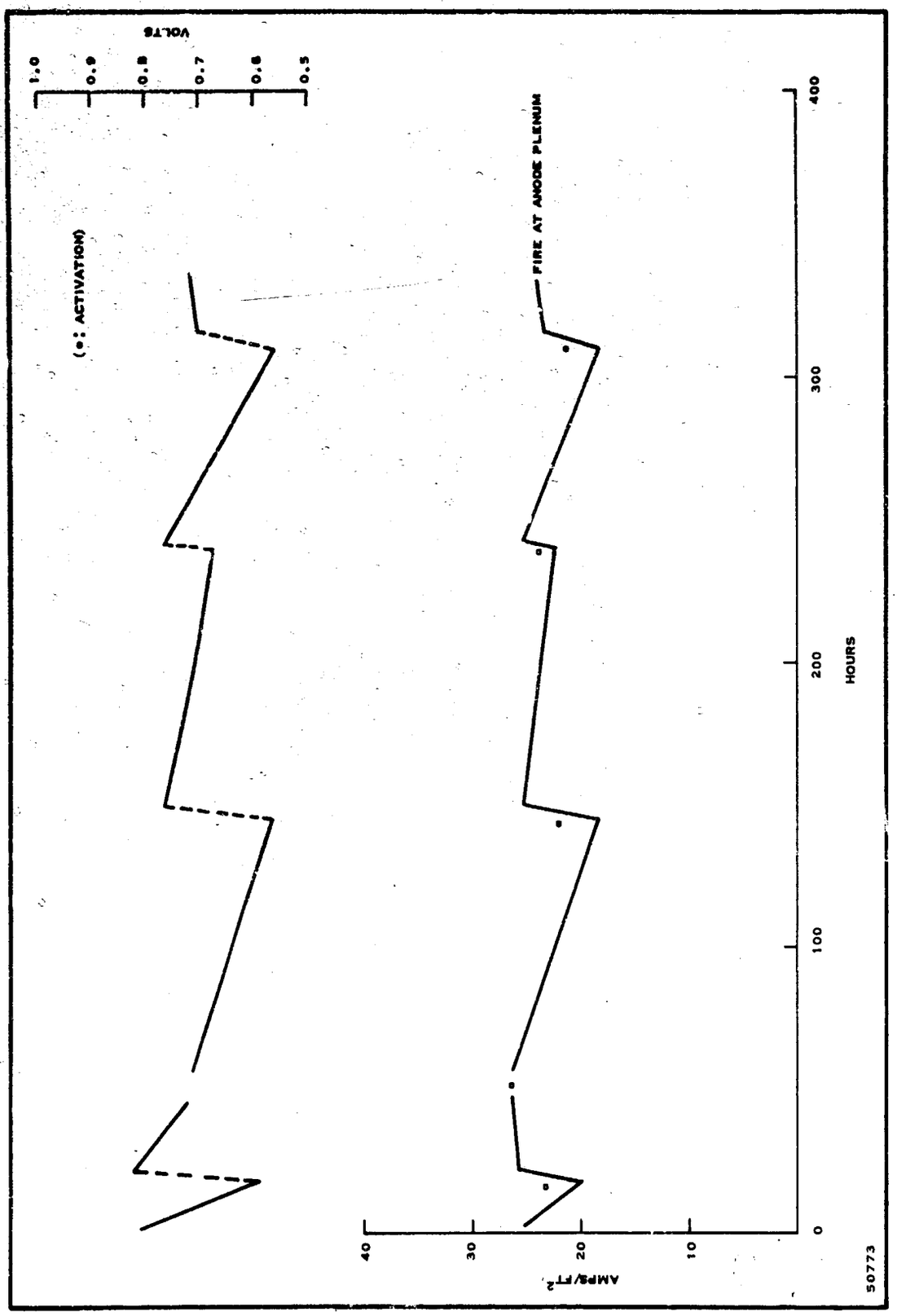

Figure 2-30. Operational Curve of TMM D-54

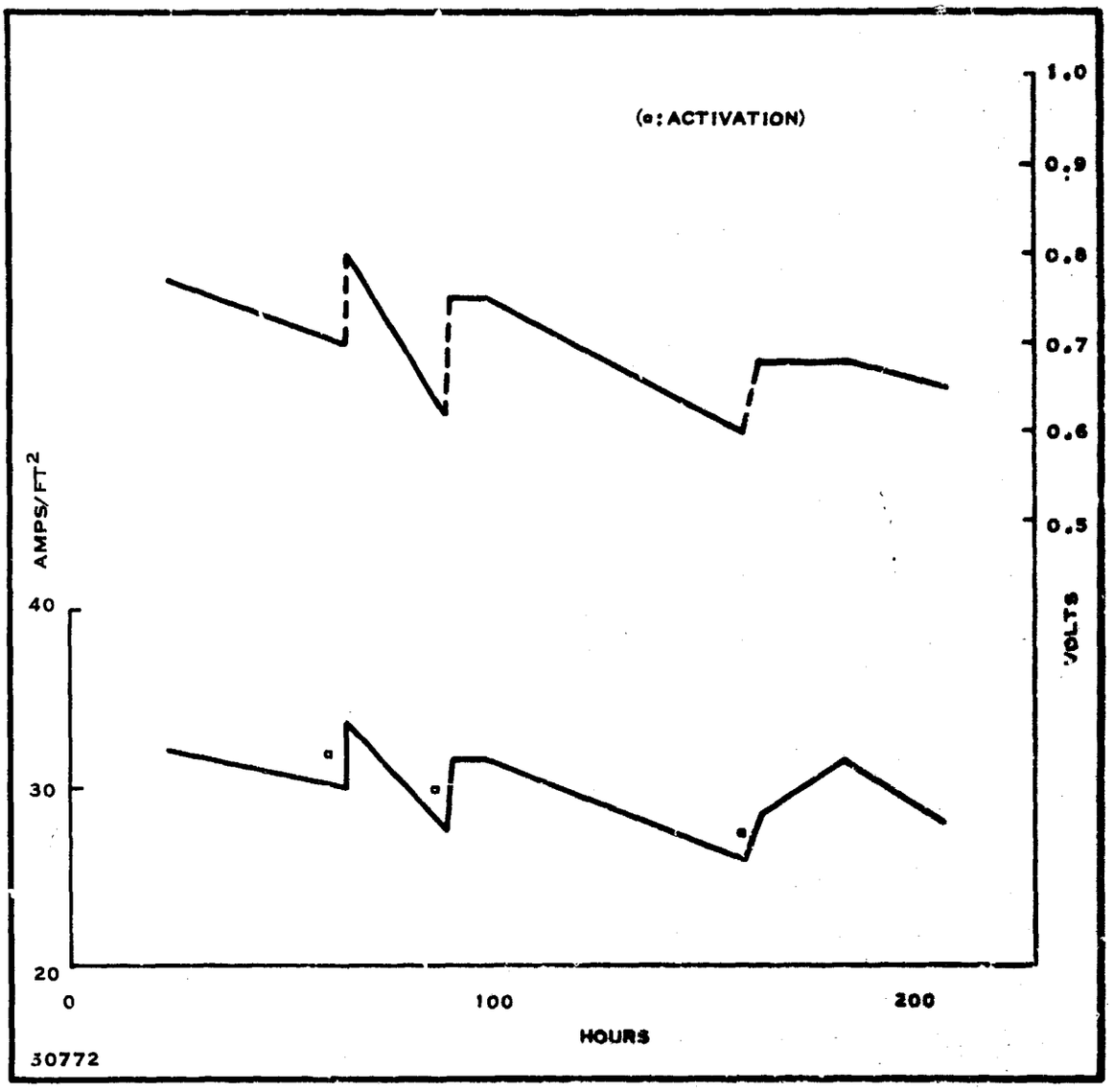

Figure 2-31. Operational Curve of TMM D-58

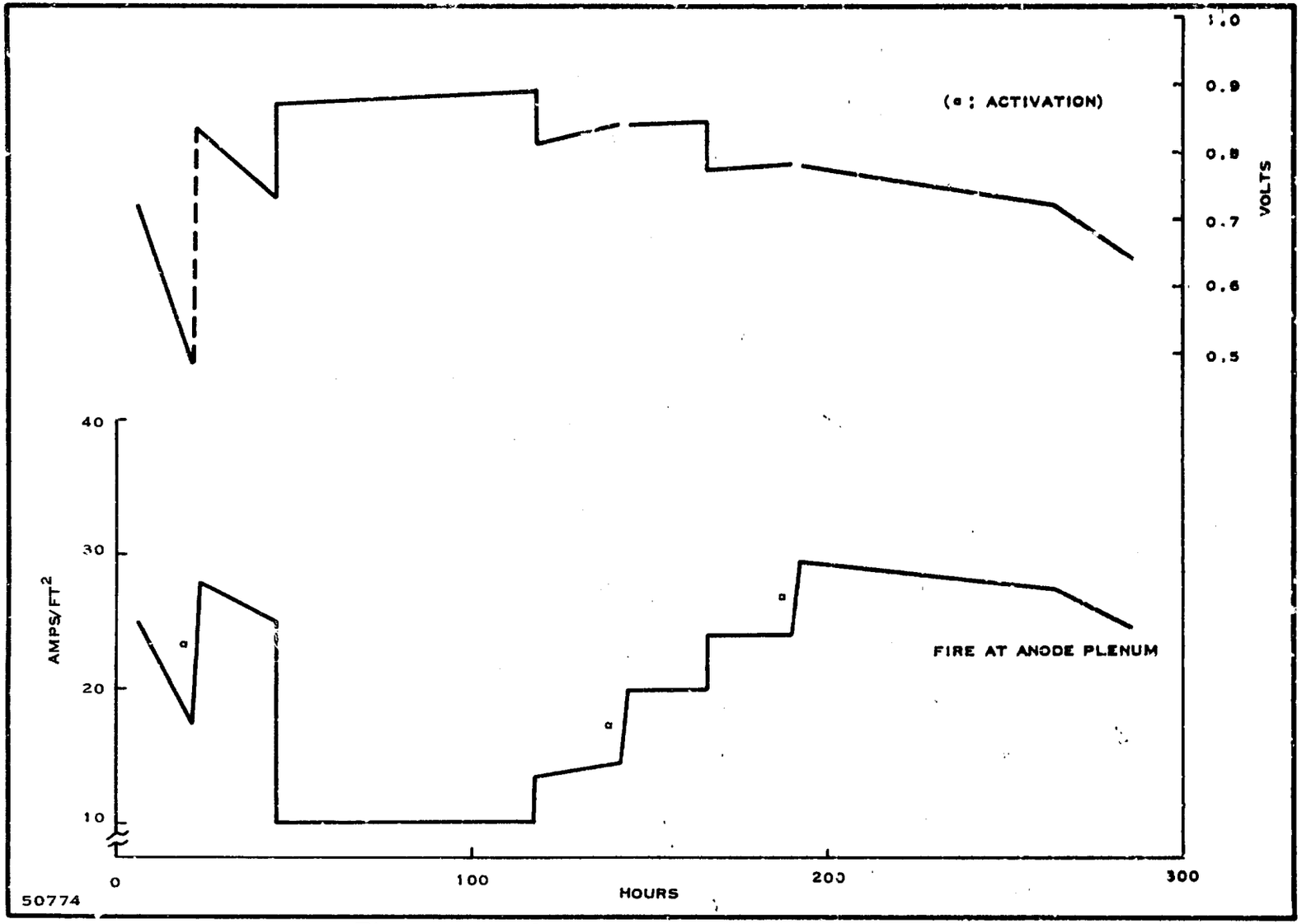

Figure 2-32. Operational Curve of TMM D-62

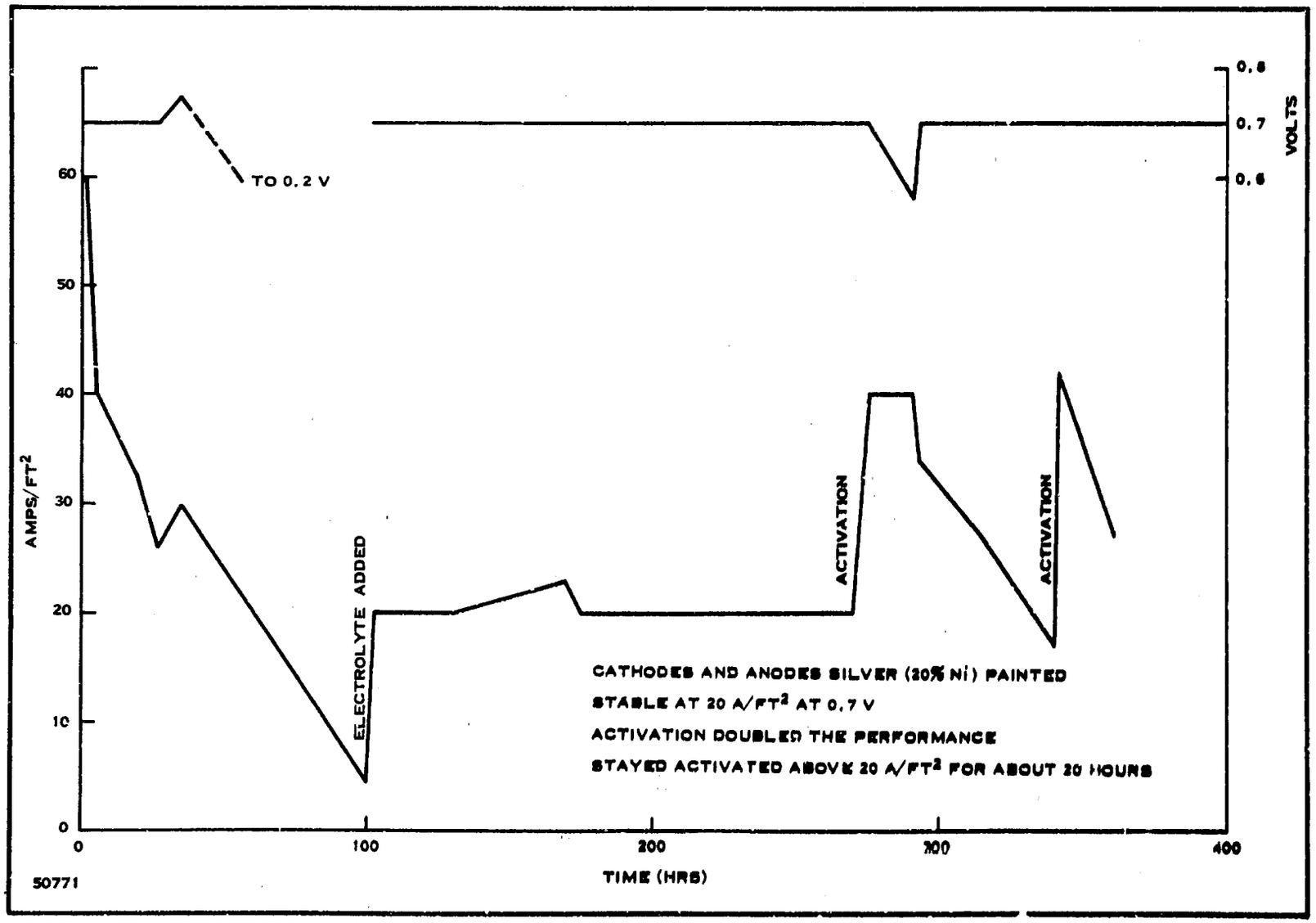

Figure 2-33. Operational Curve of TMM D-65

Cathode gas system

Circulating fans

Baffles

Exhaust.

In some matters it was necessary to simulate the expected conditions:

Fuel composition

Heating (electrical rather than with a startup burner).

No attempt was made to incorporate any of the control functions (except for temperature) which would be required in a system.

b. Description of Breadboard

The physical arrangement of the breadboard is shown in Figure 2-34. The stack consisted of twelve 10 by 10 modules. These were arranged and connected in four groups (in series) of three modules (in parallel). The complete stack was thus 30 cells in parallel by 40 cells in series.

Fuel was introduced to the center of the series and conducted to either end (Figure 2-35). This arrangement was selected because other components of a system fit into it well, and because it aids greatly in obtaining good cathode flow and uniform temperature. In order to have an output voltage of approximately 28 volts, it was decided to employ a center ground, with the two sides of the stack operating plus and minus. This is a matter of convenience. Other choices are possible.

The details of the module supports are shown in Figure 2-36. Each group of three modules was suspended in a series of U-bolts with two intermediate members. These were fastened to, but electrically insulated from, a beam. The beams were bolted to the vertical supports.

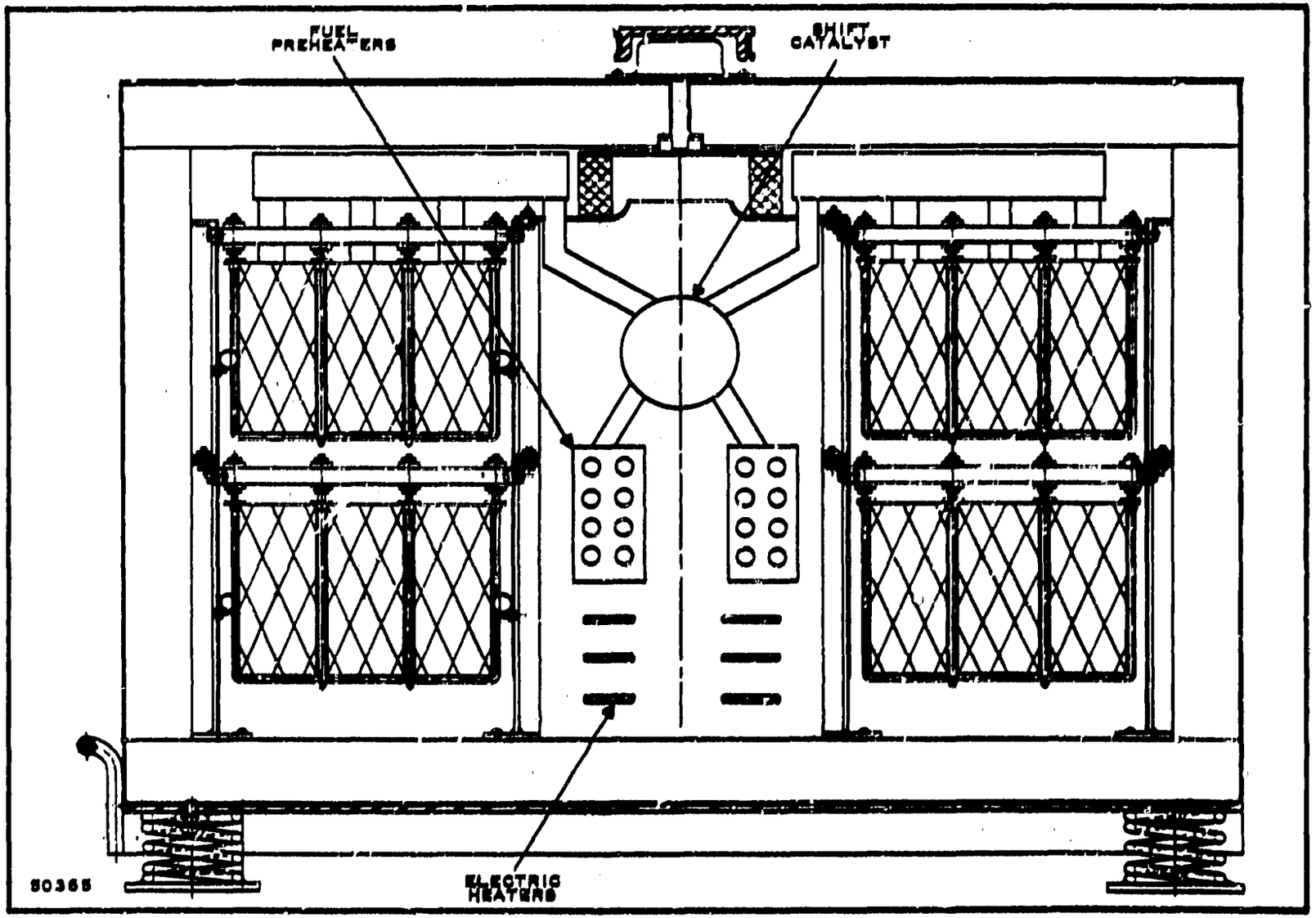

Figure 2-34. 1-Kilowatt Fuel Cell Breadboard

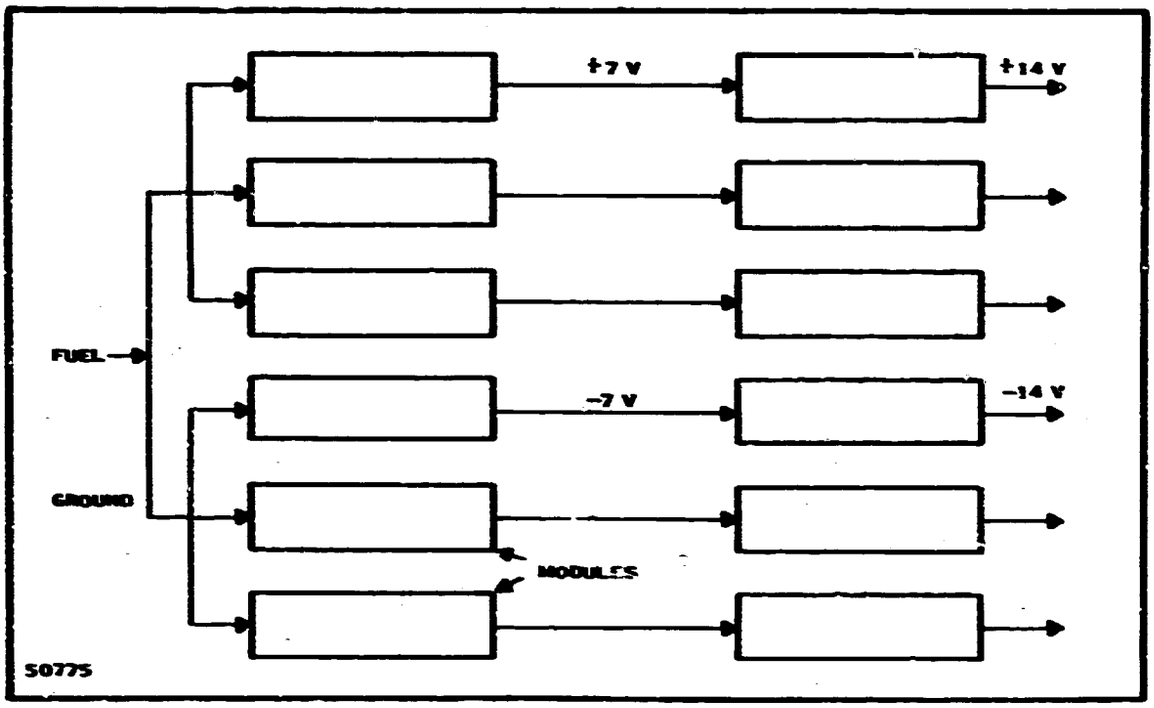

Figure 2-35. Fuel Flow Diagram

The headers for these modules (Figure 2-37) were designed so that all modules would be identical. As the module is to be a replaceable unit, the desirability of having them all alike is obvious. The design shown here permits a module to be turned upside-down or end-for-end.

Manifolds were designed for the fuel inlet end. One of these may be seen in the photograph of the stack, Figure 2-38. At the outlet end, burnoff pipes carried the stream away from the stack to the center of the enclosure. Manifold and header connections were made with Marmon-type clamps. These provide a good seal, yet disassemble readily after having been heated to 700°C. However, they were not deemed reliable for electrical connection, so this function was provided separately. Fittings were welded to the headers. Stainless-clad copper rods were inserted; a silver-bearing compound was used to obtain good contact.

The cathode circulation system is evident from Figure 2-34. Centrifugal fans impart a flow upward through the center of the enclosure and downward through the modules. The fans were designed for a circulation rate of ten times the throughput. It is not possible to measure the circulation rate. Tests on the fans, however, indicated that they were adequate.

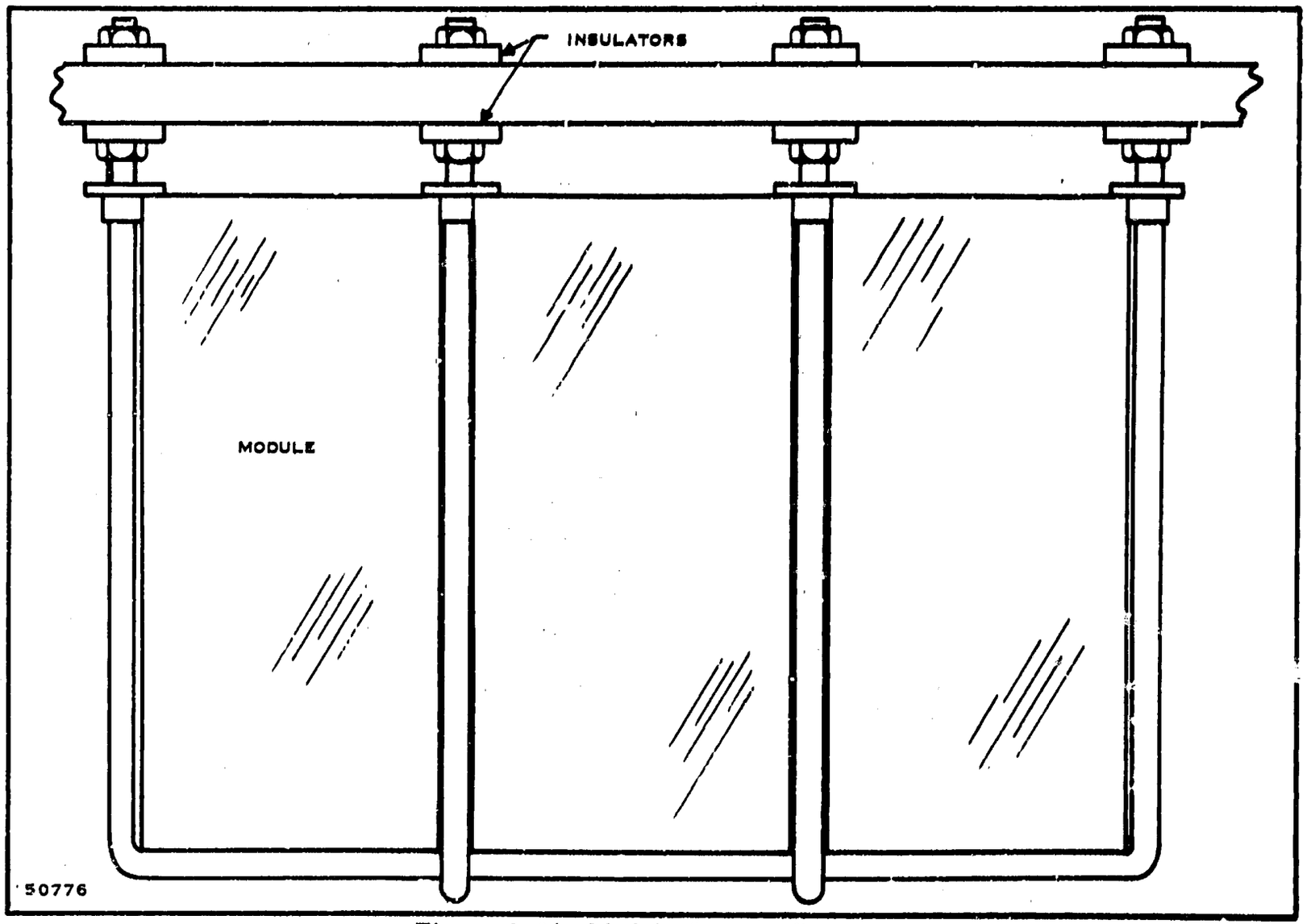

Figure 2-36. Module Support Detail

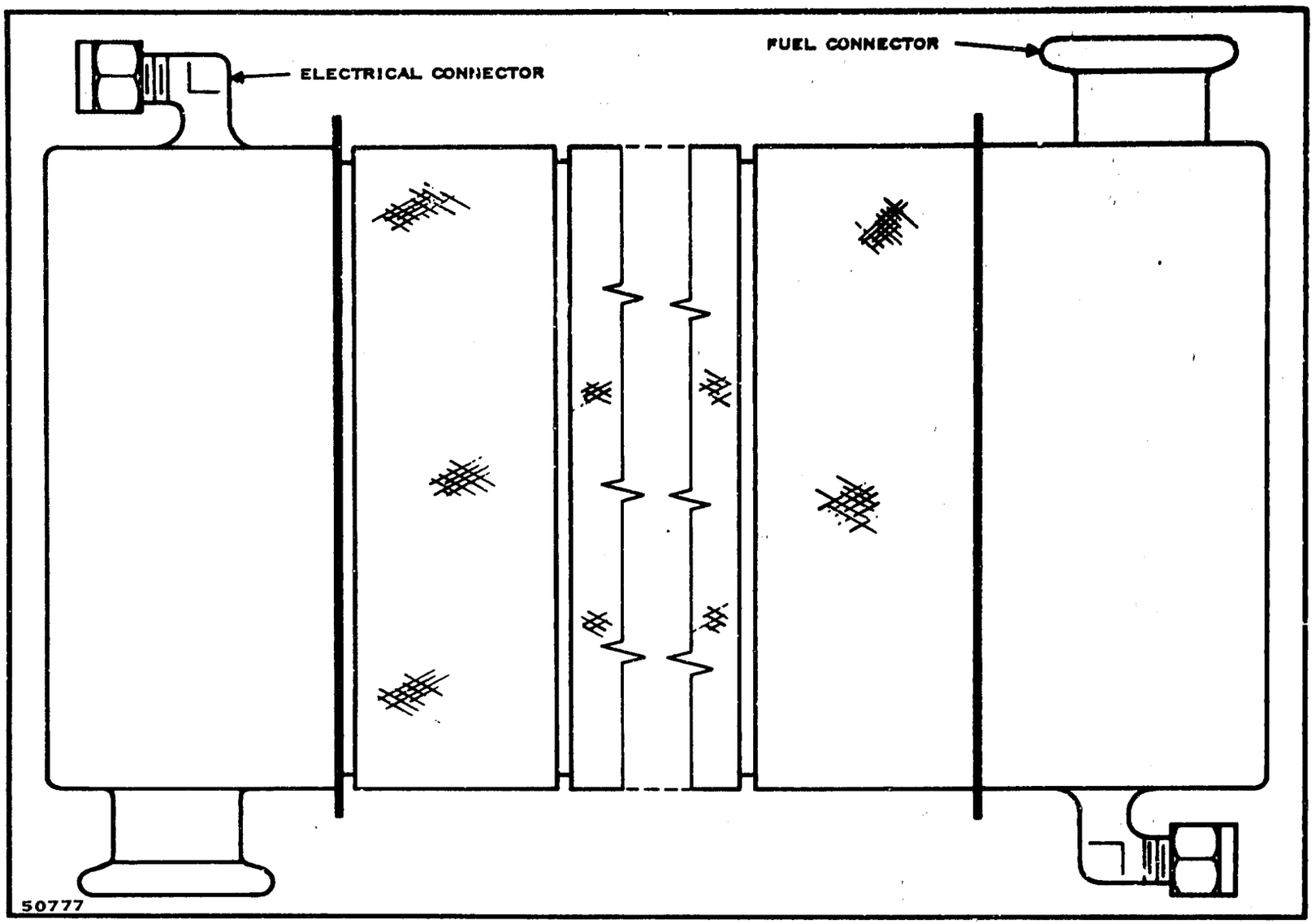

Figure 2-37. Fuel Cell Module

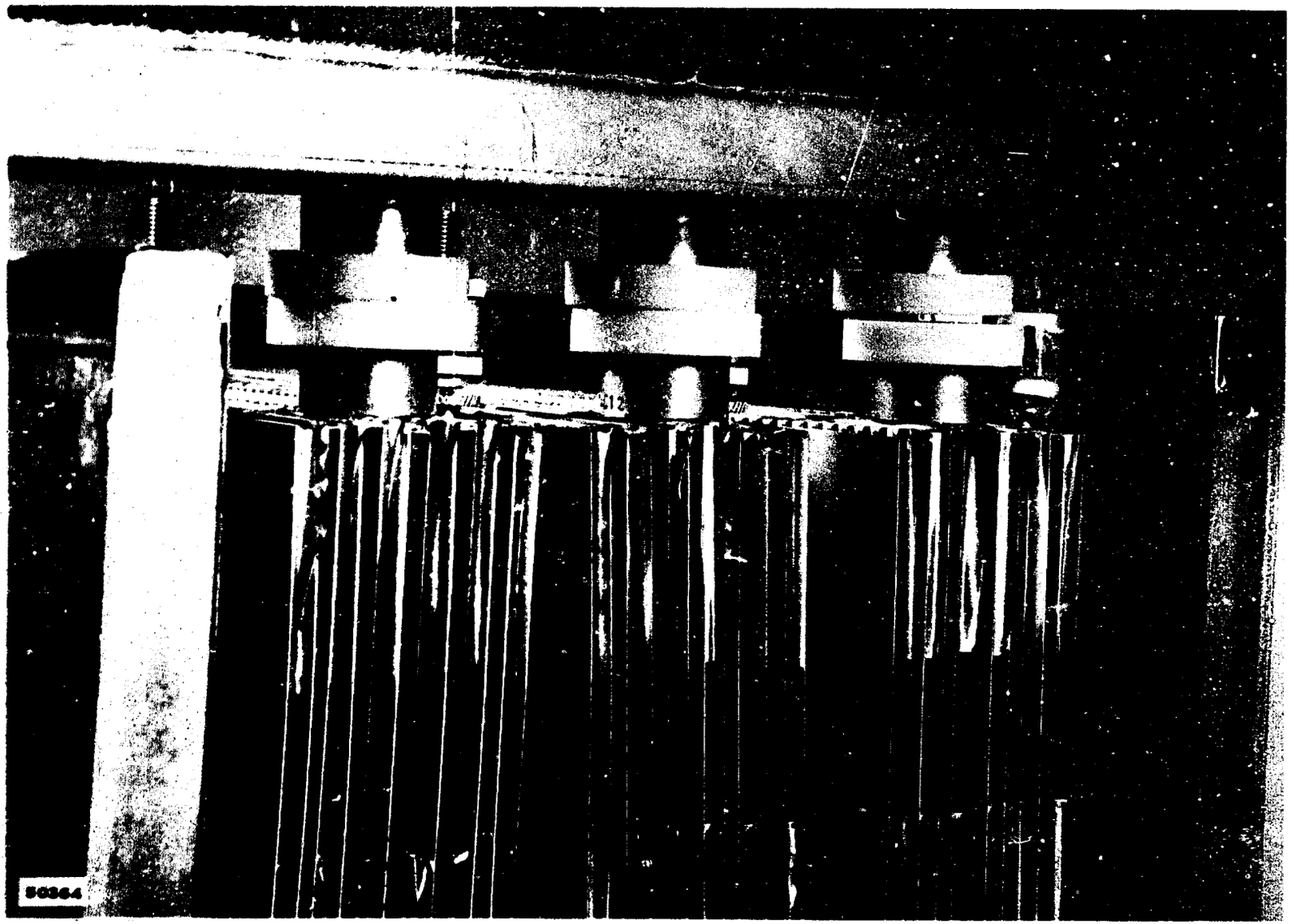

Figure 2-38. Modules and Manifold

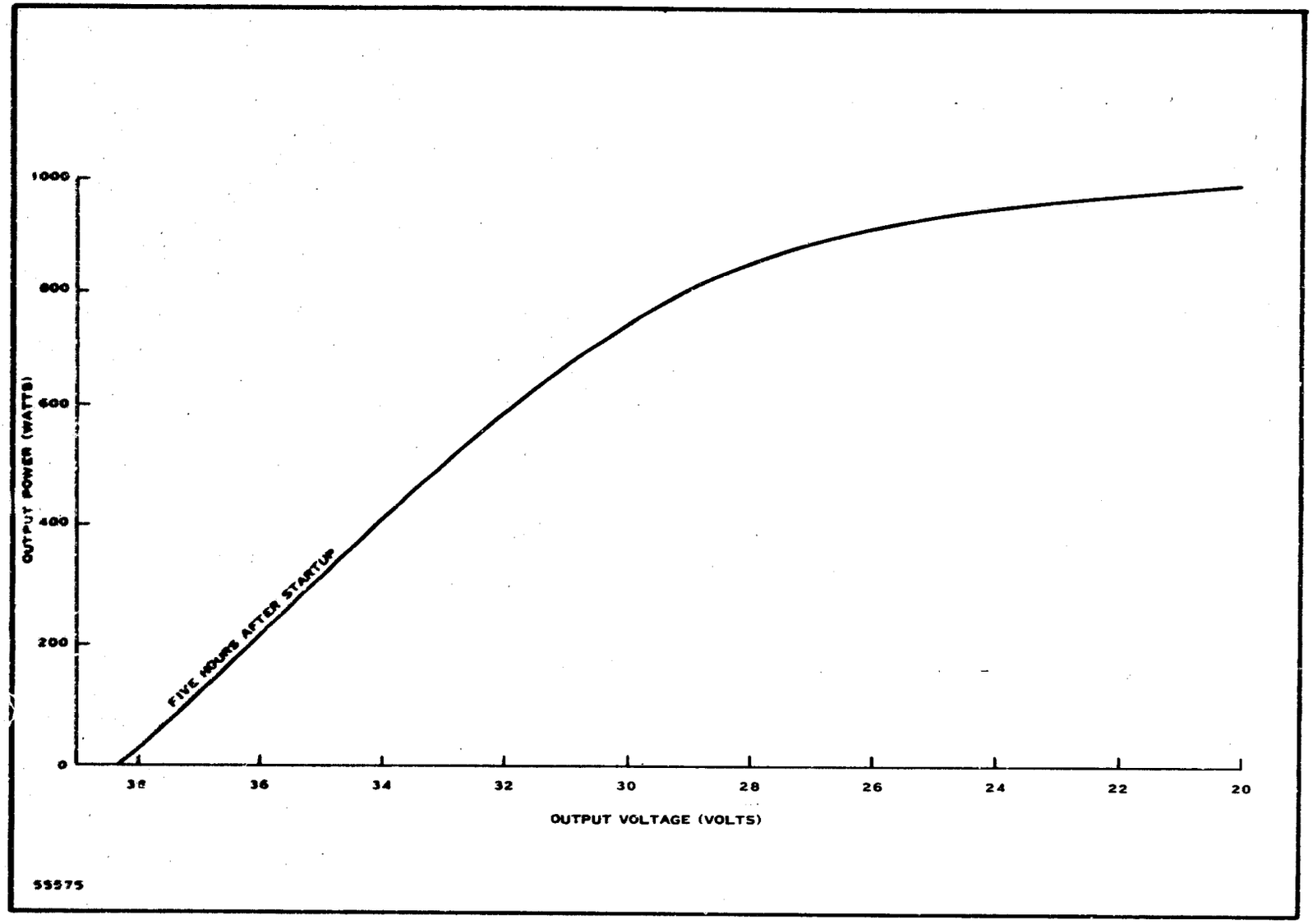

Figure 2-39. Performance of the 1-Kilowatt Fuel Cell Breadboard

c. Performance

Performance of the 1-kilowatt breadboard test of the fuel cell stacks is summarized in Figure 2-39, where output power in watts is plotted as a function of voltage. At 28 volts, the power output was 865 watts. However, a power output of 1 kilowatt was achieved at 20 volts. The open circuit voltage was 38.3 volts—essentially, the expected value based on module test data. At power output of 608 watts, the top stacks of three modules in parallel operated at 8.5 and 8.7 volts while the lower stacks were at 7.3 and 7.5 volts. Apparently, the less-than-desired 1-kilowatt power output at 28 volts was caused by an oxygen deficiency on the cathode side of the lower banks of modules. An oxygen deficiency in the lower modules appears to have been aggravated by the cathode air flow area outside the cell cathode channels and the poor mixing due to laminar flow between the upper and lower banks of modules. Although stack off-gas analyses showed a more than adequate oxygen concentration in the bulk stream, flow into the cathode channels of the lower bank apparently consisted of primarily the exhaust from the upper bank cathode channels which would be low in oxygen concentration. A contributing factor to low power output could be fuel leakage from the anode side to the cathode. Subsequent testing of individual modules did indicate leakage.

The 1-kilowatt breadboard test unit was operated continuously for 24 hours. During the first six hours, extensive testing was done at various power loads. After 12 hours of overnight operation at 400 to 430 watts, power output was 400 watts at 31 volts. Additional testing during the following six hours showed that performance was gradually deteriorating; therefore, the test was terminated.

Visual examination of the modules showed that only one was cracked. Otherwise, there was very little evidence of corrosion or other physical damage to the modules. Retesting of individual modules showed no significant performance decay. However, cell resistance had increased and there was an increase in obvious leakage as evidenced by numerous small fires. General operation of the 1-kilowatt breadboard test facility was excellent. There was no indication of electrical shorting, which had been expected to be a problem area. Operation of the cathode circulation blower also appeared to be entirely satisfactory even at significantly less than design speeds.

As stated previously, a fuel stream simulating the product of a partial oxidizer was fed to the cell stack. This simulation was based on a tentative design for a 1-kilowatt system which calls for a fuel rate of 1.25 pounds per hour of gasoline. This design also calls for the partial oxidizer air rate to provide an oxygen-to-carbon ratio of 1.25. Assuming that gasoline may be represented as $(CH_2)_n$, and assuming the partial-oxidizer product to be a thermodynamic equilibrium at 700°C, the composition will be:

H_2	19.7 percent
CO	19.0 percent
CO_2	3.8 percent
H_2O	2.5 percent
N_2	54.5 percent
CH_4	0.5 percent.

To simulate the above, the following fuel was used:

H_2	23.0 percent
CO	17.2 percent
CO_2	5.8 percent
N_2	54.0 percent.

This was preheated to 700°C and passed through a bed of shift catalyst before entering the stack. At equilibrium, the composition of this stream is identical to the equilibrium composition from air partial-oxidation of $(CH_2)_n$. The shift catalyst used was Girdler G-56 nickel reforming catalyst (1/4- by 1/4-inch tablets).

6. Design and Performance Projection to Engineering Development Units

The present fuel cell design concept (Thin Matrix Module) represents a near-maximum packing density of electrode area which can be assembled. Referring to Figure 2-27, a single cell consists of a cathode screen (0.011 inch thick), the matrix (0.024 inch), the anode screen (0.011 inch) and one-half of the anode and cathode secondaries (0.160 inch total). The volume occupied by the active cell is then 8 by 3 by 0.206 = 4.95 cubic inches or 0.00286 cubic foot. Translated to packing density this means a maximum of about 350 cells or 58 square feet of cell area per cubic foot of module. Several factors prevent reaching this maximum: (a) some structure is necessary to bind together the parallel cells and to assemble the cells in series; (b) added cathode structure occurs on the outside surfaces of every parallel stack; and (c) in a fuel cell system some volume must be allowed for maintenance access, air and fuel flow, and power connections. It is estimated that, based on the existing design, the overall cell packing density for a 15-kilowatt system would be about 35 square feet per cubic foot of cell stack. It is unlikely that this figure can be increased appreciably.

The packing density may also be specified in terms of performance, i.e., assuming 20 watts per square foot, the volume specific performance would be 0.7 kilowatt per cubic foot. Obviously, any increase in cell performance would decrease proportionally the required cell stack volume.

The figure of 20 watts per square foot is validated by the performance of a number of single test cells which have exceeded this figure for reasonable time periods. A recent change in the anode configuration indicates a good possibility of doubling this figure (to 40 watts per square foot). However, the performance of single cells is not related to cell stack on a one-to-one basis. Where cells are connected in series, both electrically and flow-wise, the module current density cannot exceed that of the poorest cell. In any random selection of parallel cell stacks for a series module there is bound to be a spread in performance. Hopefully, this spread is negligibly small. In addition, even though all cells are physically identical, the last cell will "see" a much different fuel than the first cell. The last cell probably will tend to limit the performance of a series module. Due to the above it is not expected that the average performance of a series cell stack will exceed about 30 watts per square foot. This is equivalent to about 1.0 kilowatt per cubic foot of stack volume.

C. FUEL PREPARATION

1. Ultrasonic Atomizer

As part of the work on methods of fuel dispersion, a subcontract was let to Battelle Memorial Institute for the development of an ultrasonic atomizer for use with a partial-oxidizer. This subcontract was terminated by Texas Instruments on 10 February 1967, with the approval of USAERDL. Battelle's Summary Report is included in this document as Appendix A.

Their progress up to termination is summarized here. The objectives of the subcontract were:

Design and fabrication of an atomizer

Design and fabrication of a driver

Design of mount for the atomizer, to ensure that the piezo-electric crystals remain cool

Operation with a partial-oxidizer supplied by Texas Instruments.

The first two items, an atomizer and driver, were built and operated briefly. Performance appeared entirely satisfactory. The third item was partially completed. The mount was designed, and analysis indicated it would meet the requirements. However, it was not fabricated.

Although the early results were very encouraging, the subcontract was terminated before operation with a partial-oxidizer could be attempted. The decision to terminate was based entirely on budgetary considerations, and in no way reflected dissatisfaction with any technical aspect of the contract. It was deemed essential to put the effort on other problems.

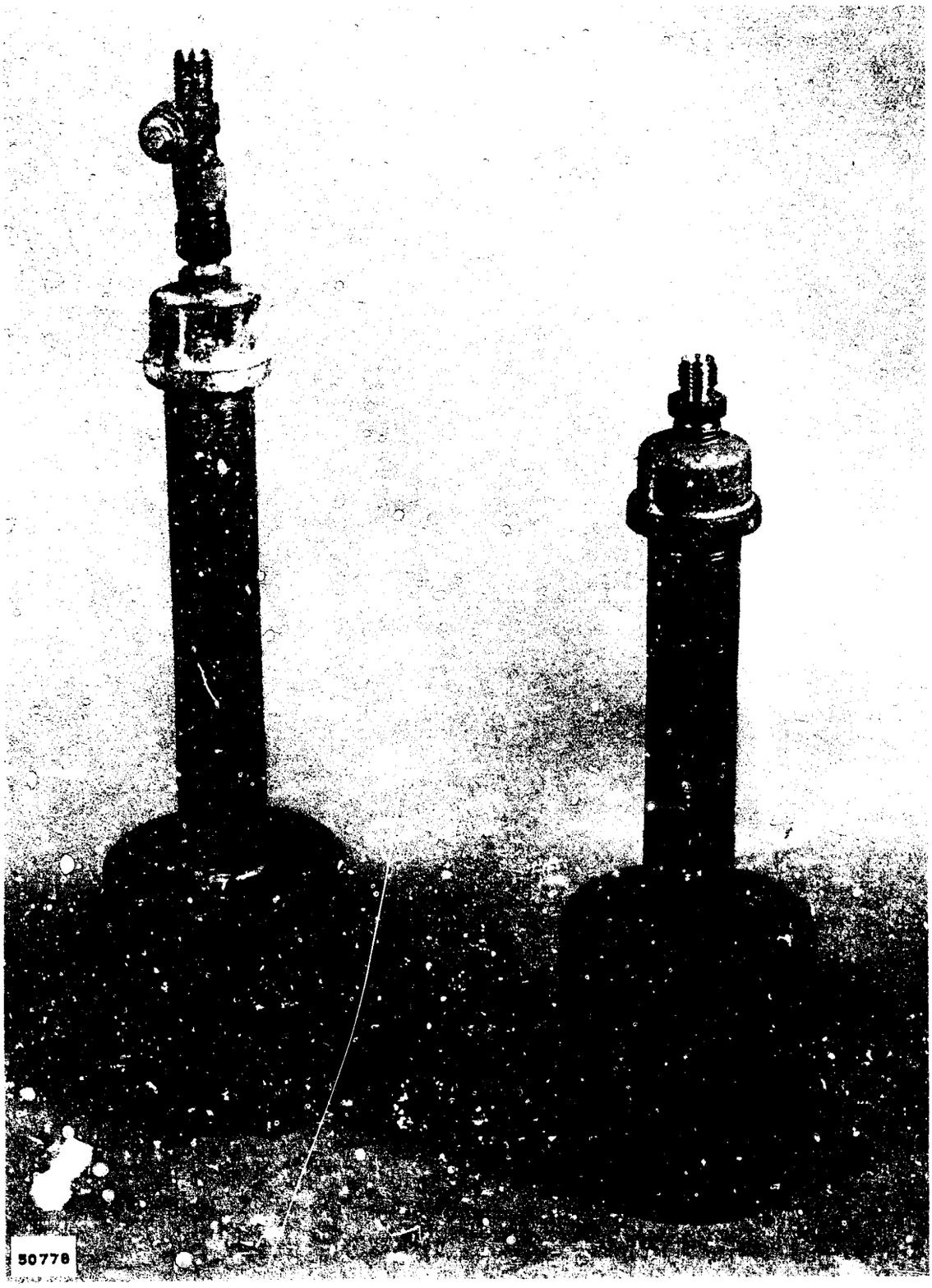

Figure 2-40. Liquid Fuel Vaporizer (Film Boiling)

2. Film Boiler

The film boiling technique developed under API sponsorship for vaporization of No. 2 Heating Oil* was investigated for vaporization of gasoline and CITE fuel. Film boiling results in fewer deposits than nucleate boiling since a vapor film separates the hot surfaces from the liquid. Film boiling of No. 2 Heating Oil occurred at 750°F or higher.

The initial film boiler design for vaporization of gasoline is shown in Figure 2-40. This vessel was a 3-inch diameter by 3-inch-long cylinder of 316 stainless stell, with a 1-inch diameter by 2-inch-long inner cavity for vaporization. This vessel was mounted in the 700°C furnace and gasoline entered through the top. Air also entered through the top and/or the side, with vapor exiting from the side. This vaporizer was unsatisfactory for use with combat gasoline due to:

Lead oxide deposits in the vaporizer and its exit line

Preignition of the fuel-air mixture in the vaporizer or its exit line

Unstable fuel flow.

Calculations indicated that heat transfer from the furnace to the vaporizer base could be insufficient to maintain the inner surfaces at film boiling temperatures. Therefore, the vaporizer base was machined to fit directly on the reactor, with heat transfer by close radiation coupling with the 1000°C to 1200°C reactor wall. This technique increased vaporization temperature and improved fuel flow stability; however, preignition and lead deposit problems remained. A high temperature vaporizer was constructed using the reactor wall as the base. This vaporizer exhibited severe preignition and carbon deposit problems.

From this work we concluded that satisfactory fuel vaporization by film boiling of gasoline in a vessel inside the 700°C furnace would be very difficult, due to hot surfaces causing preignition at high air rates and unsteady fuel flow at the low air rates required to prevent preignition. Lead deposits were also a problem.

3. Premixing Technique

Steady vaporized fuel flow without carbon deposition, lead deposits, or preignition was obtained by cool air entrainment of liquid fuel into a preheated air stream. Proper line sizing and control of the preheated-to-cool air ratio was successful in preventing preignition. With larger scale units, a spray nozzle will probably improve dispersion of the fuel into the air stream.

*Proceedings: API Research Conference on Distillate Fuel Combustion, 1961-5.

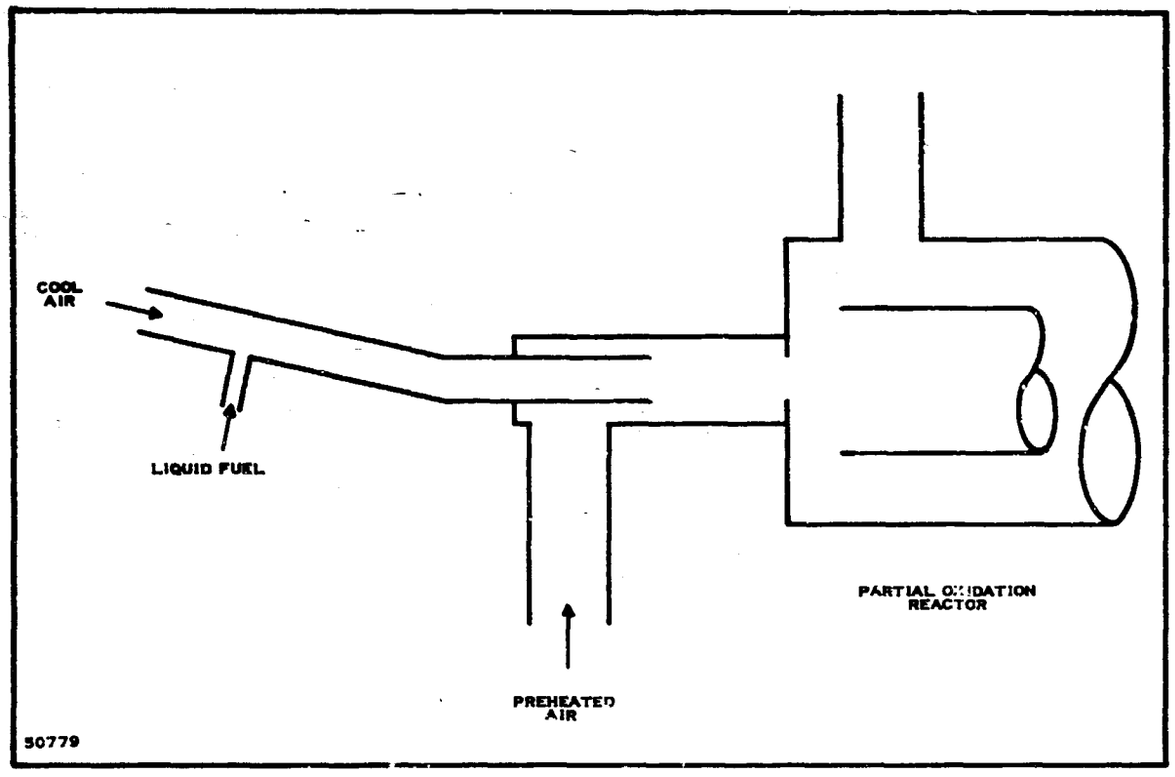

Figure 2-41. Liquid Fuel Vaporization and Air Premixing

Figure 2-41 shows additional details regarding this fuel vaporization system. Liquid fuel enters the inclined cool air line and is partially vaporized by the cool air. The bulk of the liquid fuel is blown down the inclined air line into the hot air stream. The 1.25-pound-per-hour gasoline vaporizer utilized a fuel-cooled air line extending into the hot air stream. A smaller vaporizer (0.3 – 0.7 pound per hour) gave satisfactory performance with perpendicular entry of the cool air-fuel mixture into the hot air stream.

4. Reactor Geometry Evolution

The three basic types of partial oxidation reactors investigated were of swirl stabilized, tangential entry, and recirculation designs. Various techniques were investigated for fuel and air entry into each type reactor. In general, premixing of fuel and air was the only technique which resulted in clean, satisfactory operation.

a. Swirl Stabilized Reactor

As shown in Figure 2-42, the swirl stabilized vortex reactor consisted of two tubes with air flowing into the annulus where it

Figure 2-42. Swirl Stabilizer Vortex Reactor

Figure 2-43. Tangential Entry of Fuel and Air into Partial Oxidation Reactor

was preheated, then through multiple tangential slots into the inner tube which was the reaction zone. Initially, axial fuel entry was investigated; however, clean reaction could not be obtained with either propane or liquid fuels without use of water or a large excess of air.

Premixing of fuel and air at low temperatures resulted in clean, stable reaction with the swirl type reactor. A reactor was operated with premixed propane and air for 41 hours continuously and produced a fuel containing, by volume, 20- to 21-percent hydrogen and 16- to 18-percent carbon monoxide. Shutdown was due to preburning in the preheater coil. Operations with premixed CITE fuel and air were plagued with preignition and carbon deposition in the annular space.

A modified premixing technique involving injection of vaporized fuel near the annular slots showed limited promise. The major problems with vaporized gasoline or CITE fuel were carbon deposition and locally excessive temperatures near the fuel inlet. Preignition in the annulus and inadequate mixing of fuel and air prior to ignition were the probable causes for these problems.

b. Tangential Entry

Tangential entry of fuel and air into a single tube reactor was successful in eliminating preignition and carbon deposition problems in the fuel inlet to the reactor. A typical reactor, as shown in Figure 2-43, used premixed fuel and air flow through the tangential entry. A modification of this design utilized an inner tube in the tangential entry line for vaporized fuel flow with air flow through the annular space. All tangential entry reactors were plagued with dirty luminous combustion, carbon deposition inside the reactor, and a high noise level. Attempts to alleviate this problem with mixing rings and baffles were unsuccessful. Apparently, impingement of fuel and air on the hot reactor walls resulted in ignition without establishment of a stable flame.

c. Internal Recirculation

Internal recirculation of reaction products to the fuel-air entry point resulted in clean, nonluminous combustion of combat gasoline and air without carbon deposition in the reactor, its inlet, or outlet piping. Presented in Figure 2-44 are the basic reactor designs for annular and baffled recirculation within the reactor. Both designs utilized premixed fuel and air with an inlet orifice to establish jet pumping for recirculation of a portion of the reaction products. In general, performance of the annular reactor was superior to the baffled reactor; however, the annular reactor received more extensive development study. Both types of reactors were operated at 1-kilowatt system design rates of 1.25 pounds per hour of

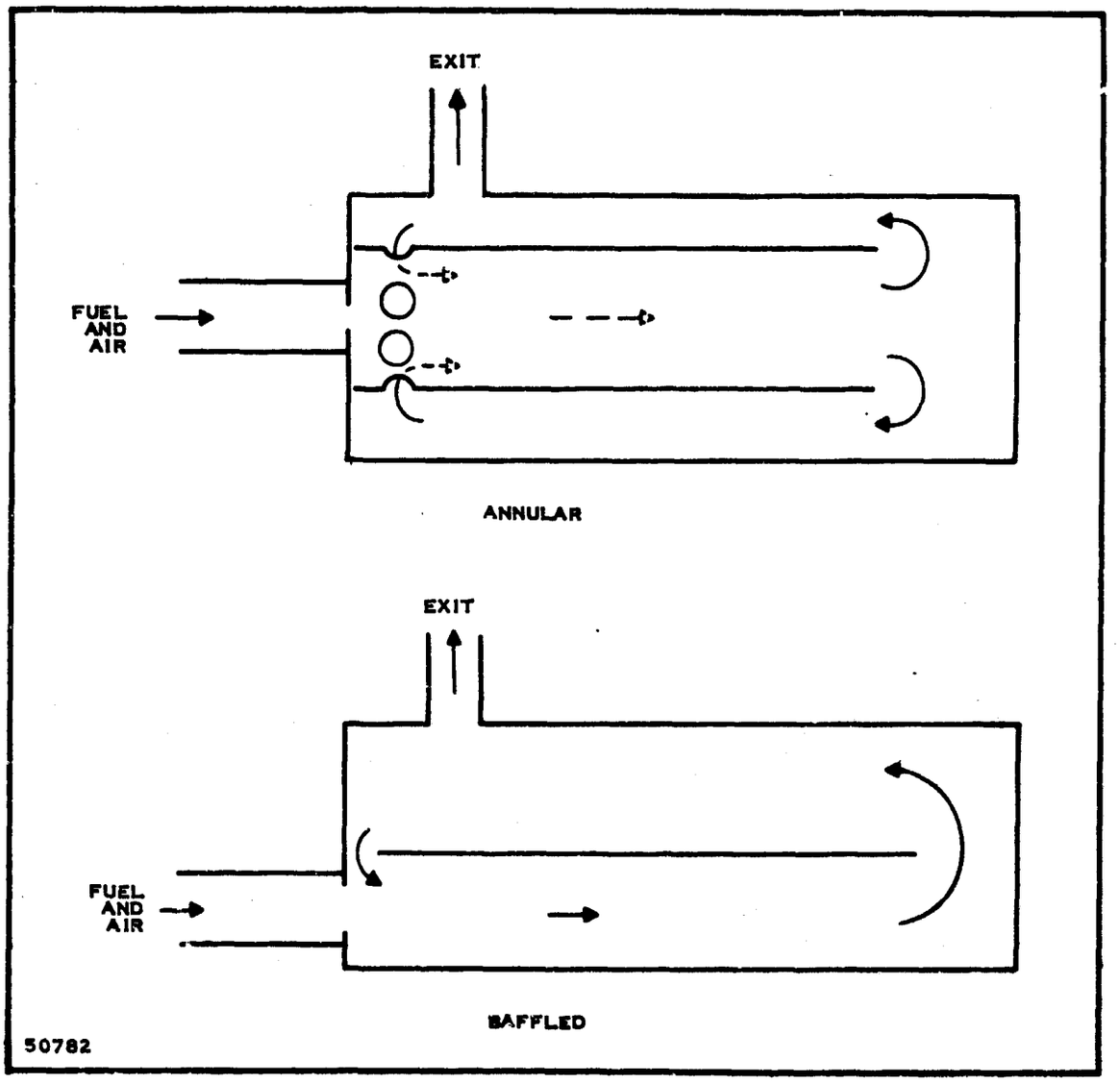

Figure 2-44. Recirculation Reactor Designs

combat gasoline and 100 cfh of air. The annular recirculation reactor was used for the 1-kilowatt partial-oxidation breadboard test.

d. Ignitor

A conventional Janitrol aircraft heater spark plug was modified for startup of the partial-oxidizer by machining the spark plug to a 0.61-inch outside diameter and extending its insulated length. This ignitor was usually inserted at the observation port (3/4-inch tubing); however, a smoother startup was obtained with the ignitor near the fuel-air entry orifice. With the partial-oxidizer near 700°C, minor pressure fluctuations were experienced during startup. At lower temperatures considerable pressure variations and noise persisted until the unit was sufficiently hot for flame stabilization. This type of ignitor should be satisfactory for use on larger scale fuel preparation units.

5. The 1-Kilowatt Breadboard

a. Design

The 1-kilowatt breadboard fuel preparation unit was designed to partially oxidize combat gasoline with air to produce a hydrogen and carbon monoxide rich fuel for the fuel cell stack. Sufficient air was used to prevent carbon deposition down to 700°C. Assuming the liquid fuel was $(CH_2)_n$, the required oxygen to carbon atomic ratio was 1.25. Thermodynamic calculation showed that the equilibrium fuel composition at 700°C should be:

	Volume (percent)
H_2	19.7
CO	19.0
CO_2	3.8
H_2O	2.5
CH_4	0.5
N_2	54.5

Assuming that methane is reformed in the fuel cell, this corresponds to 40.2-percent fuel, by volume, in the partial-oxidizer product.

The 1-kilowatt demonstration test used premixed combat gasoline and air, with air vaporization as previously discussed. The reactors were of the annular recirculation type. Two reactors were operated continuously at 1-kilowatt design rates of 1.25 pounds per hour combat gasoline

and 100 cfh air. A smaller reactor was run to obtain additional data for design of a 15-kilowatt system. The general design of annular recirculation reactors was discussed earlier. Specific size data are:

Test Station	3	4	1
Capacity, pounds of fuel per hour	1.25	1.25	0.3—0.7
Dimensions, inches			
Overall length	10	10	10
Recirculation tube internal diameter	1.278	1.380	0.824
Outer tube internal diameter	2.067	3.38	1.500
Reaction volume, cubic inches	30	83	20

b. Performance

The demonstration tests of the 1-kilowatt partial-oxidation reactors showed that the reactor design was satisfactory for use with the 1-kilowatt system. The two reactors operated 97 and 102 hours on combat gasoline and air. The 102-hour run was voluntarily terminated at the end of the work week; however, the 97-hour run was terminated due to failure of a 316 stainless steel observation port. The only problem requiring operator attention during the test was a buildup of deposits on the premixed fuel-air orifice at the reactor inlet. These orifice deposits were removed by passing a rod through the orifice, after shutting off the fuel and air flows, and purging with nitrogen. This orifice cleaning operation required about two minutes. Specific operational performance of each partial-oxidation unit is summarized below.

(1) Test Station 3

This smaller volume 1-kilowatt partial oxidizer was operated for 97 hours before failure of a 316 stainless steel observation port forced termination of the run. This reactor had 23 hours of intermittent operation prior to the 97-hour test run. Gradual buildup of deposits on the fuel-air inlet orifice required that the orifice be cleaned five times during the test. At 12.5 hours of operation, the fuel was accidentally shut off with no adverse effects. Reactor inlet pressure was normally 5 to 7 inches of water and increased to 15 to 20 inches of water before cleaning the orifice.

(2) Test Station 4

This larger 1-kilowatt partial-oxidation reactor was operated continuously for 102 hours on combat gasoline. The run was voluntarily terminated at that time due to ending of the work week. Deposits also built up at the inlet orifice of this reactor and had to be removed three times. However, we found that the deposits were removed during the nitrogen purge after shutoff of fuel and air. The reason for this is unknown. Normal reactor inlet pressures were 8 to 10 inches of water.

(3) Test Station 1

This small partial oxidizer was designed for reduced flows of about 1/4 to 1/3 of 1-kilowatt rates for module development studies. However, this reactor was operated during the test to obtain additional data for design of the 15-kilowatt system and a better understanding of the partial-oxidation process. A range of flow rates and the addition of carbon dioxide at reduced air rates was investigated. The results of these tests are summarized later in the report.

Visual observations of the partial-oxidizer product gas burnoff flame indicated that a "cleaner" product was obtained from this small unit at all flow rates tested. The product gases burned with a clear blue flame, compared with the slightly yellow tinted flame from the 1-kilowatt units. The yellow tint is apparently due to traces of free carbon. The reasons for this difference in reactors are not fully defined; however, design modification of the 1-kilowatt reactor is being investigated.

Partial-oxidation product analyses obtained by gas chromatography and process conditions are tabulated in Table 2-4. An analysis of this data shows that:

At 1200°C reactor temperature, equilibrium product compositions are closely approached, except for high methane concentrations (2.5 — 3.5 versus 0.5 percent) and correspondingly lower hydrogen and CO levels.

At lower temperatures of 1000 to 1100°C, the methane concentration increases to about 5 to 6 percent and ethylene begins to increase to about 2 percent.

Partial oxidation at about 1200°C with 1.0 atom of oxygen from air per atom of carbon from gasoline and sufficient CO_2 to

Table 2-4. Partial-Oxidizer Demonstration Test

Test Station	3			4					1								
Hours on Test	5	6	97	7	8	98	100	-- (1)	12 (2)	14	26	28 (2)	31	49	53	54 (2)	55 (2)
Partial Oxidizer																	
Temperature, °C	1180	1180	1150	1100	1100	1110	1100	1100	975	1060	1000	1130	1185	1170	1170	1170	980
Fuel Rate, lbs/hr	1.25	1.25	1.25	1.25	1.25	1.25	1.25	0.98	0.35	0.35	0.35	0.35	0.68	0.68	0.68	0.68	0.68
Quenched Product Analyses, Vol%																	
H_2	13.6	14.0	12.4	10.7	10.9	8.4	9.1	12.4	5.8	12.3	6.7	18.5	15.5	14.9	15.6	18.0	5.0
CO	19.3	19.3	18.0	19.2	19.1	17.3	18.6	16.9	13.6	20.7	16.7	29.0	20.1	21.6	21.4	26.9	12.6
CO_2	2.6	2.4	3.2	2.6	2.6	3.3	2.9	2.9	13.4	2.1	4.0	3.9	3.1	2.5	2.1	6.6	16.1
N_2	60.7	60.7	63.3	62.2	62.2	66.7	65.2	64.4	59.2	59.5	64.8	43.5	58.4	57.7	57.7	42.9	57.9
Methane	3.8	3.6	2.8	5.2	5.1	3.9	3.9	3.4	5.9	4.9	5.7	4.8	2.8	3.2	3.2	5.2	5.5
Ethylene	0.0	0.0	0.3	0.1	0.1	0.4	0.3	0.0	2.1	0.5	2.1	0.3	0.1	0.1	0.0	0.4	2.9

Fuel: Combat Gasoline
Oxidant: Air
Oxygen/Carbon Atomic Ratio: 1.25
Furnace Temperature: 700°C

(1) CITE fuel test
(2) 1.0 oxygen/carbon atomic ratio from air with CO_2 addition for 1.25 oxygen/carbon total

increase the overall oxygen to carbon ratio to 1.25 showed that CO_2 did react to give the expected product composition. At lower temperatures near 1000°C, very little CO_2 reacted.

Reactor temperature was the major process variable affecting partial-oxidizer product composition. Doubling reactor size (Station 3 versus 4) or doubling the fuel-air rates (Station 1) had no detectable effect on partial-oxidizer product composition.

The methane content of partial-oxidizer product gases decreased by about 1.0 percent, by volume, between 5-10 and 100 hours of continuous operation. This is apparently due to a change of catalytic reactor surface effects during the extended period of continuous operation.

(4) CITE Fuel Test

After completion of 102 hours of continuous operation, the Test Station 4 partial-oxidizer was operated for two 6-hour periods on CITE fuel. Performance of the vaporizer-mixer was satisfactory and essentially equivalent to gasoline operations. The partial-oxidation reactor also gave satisfactory performance at 0.8 to 1.0 pounds per hour of CITE fuel. Visual observations indicated less free carbon in the exhaust flame than was obtained with combat gasoline. However, increasing rates to 1.25 pounds per hour resulted in a luminous exhaust flame and carbon deposition in the reactor and its exit lines. This superior performance at lower rates was surprising in view of combat gasoline experience showing improved performance at higher rates. Additional development work is required to resolve these differences in behaviour of gasoline and CITE fuel during partial oxidation.

(5) Post-Test Equipment Examination

Examination of the fuel preparation units after the breadboard test showed that the Incoloy 800 reactor walls and end plates were in good condition, although coated with a hard glossy scale in areas where temperatures were about 1200°C. Photographs taken of the two 1-kilowatt test reactors during disassembly are presented in Figures 2-45

through 2-49. The Station 4 reactor was constructed from Inconel or Incoloy except for the 316 stainless steel fuel-air inlet tube, which showed minor evidence of heat damage at its relatively low operating temperature. The Station 3 reactor was also of Inconel or Incoloy except for the fuel-air inlet line and orifice, and the observation port line which were of 316 stainless steel. In summary, Inconel 600 or Incoloy 800 appear satisfactory for construction of partial oxidizers to operate around 1200°C.

Inspection of the vaporizer lines showed only trace deposits which appeared carbonaceous. However, the fuel-air inlet line, exposed to the 700°C furnace temperature in addition to radiated and conducted reactor heat, showed a thin coating of loosely attached gray-yellow deposits which are apparently lead oxides. These deposits should not interfere with extended operations.

The interior of the reactors contained minor quantities o scale and dust-like magnetic particles The reactor exhaust lines also contained a limited quantity of scale and showed a slight buildup of tightly adhering deposits which are probably carbon and lead compounds.

6. Design Projection to 15 Kilowatts

a. General

The proposed 15-kilowatt fuel preparation system is designed to operate at a 1.0 oxygen/carbon atomic ratio from air, with 30 percent of the anode exhaust stream recycled to the partial-oxidizer inlet. The thermodynamic equilibrium (at 700°C) of the partial-oxidizer product and the recycle stream are shown below, assuming zero methane. The partial-oxidizer product should actually contain about 0.5 volume-percent methane and the anode exhaust <0.1 volume-percent methane.

Component	Partial-Oxidizer Product (percent by volume)	Anode Exhaust (percent by volume)
H_2	2 . 4	9.2
CO	19.3	8.2
CO_2	5.1	12.8
H_2O	3.8	18.2
N_2	49.4	51.6

Figure 2-45. Test Station 4 Partial Oxidizer—Reactor, Air Preheater and Fuel-Air Mixer

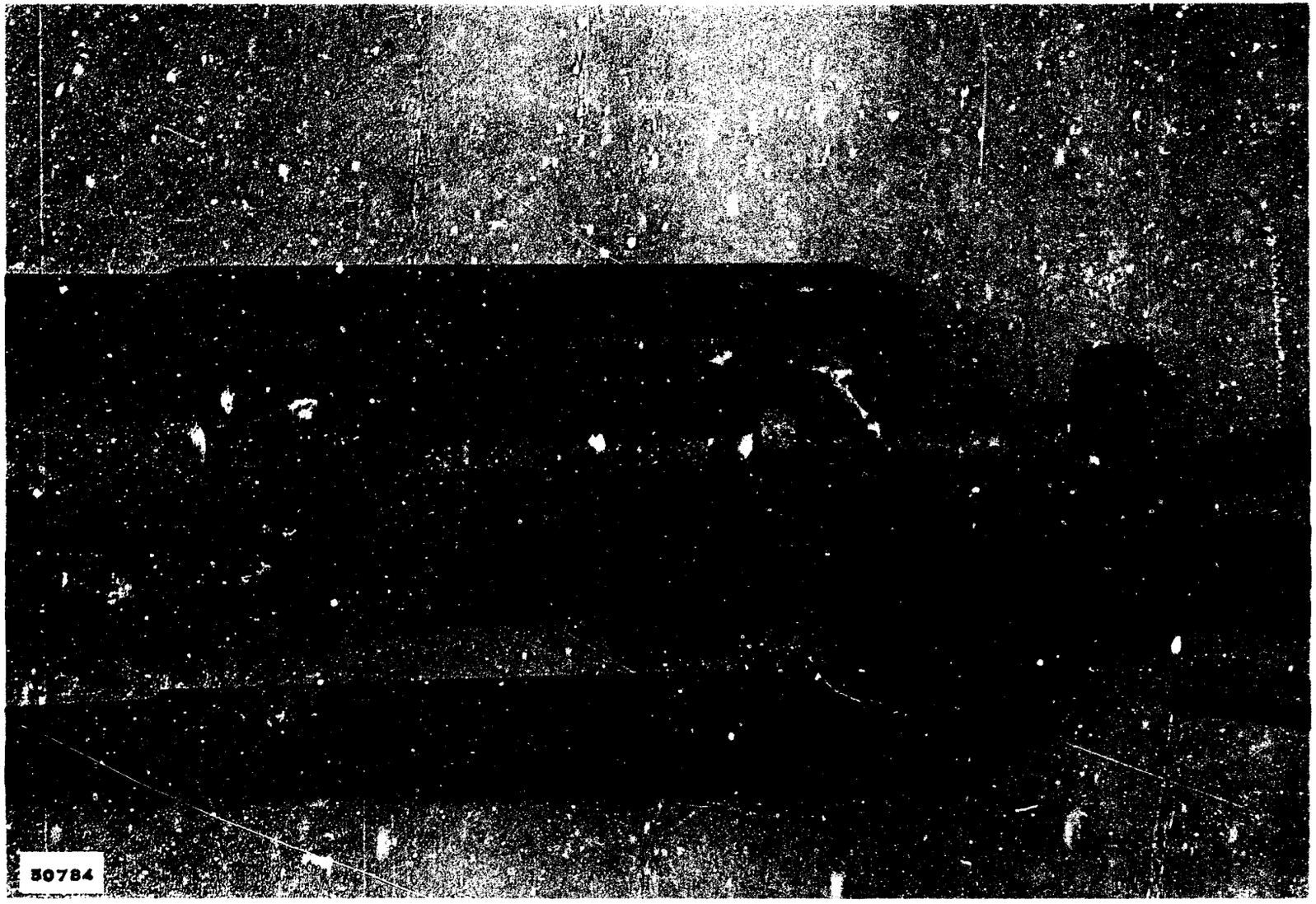

Figure 2-46. Test Station 3 Partial Oxidizer—Disassembly View Showing Observation Port Line Failure and Ignitor

Figure 2-47. Test Station 3 Partial Oxidizer—Deposits Inside Reactor

Figure 2-48. Test Station 3 Partial Oxidizer—Deposits Removed From Inside Reactor

Figure 2-47. Test Station 3 Partial Oxidizer—Deposits Inside Reactor

Figure 2-48. Test Station 3 Partial Oxidizer—Deposits Removed From Inside Reactor

50787

Figure 2-49. Test Station 3 Partial Oxidizer—Reactor, Recirculation Tube, and End Plate with Fuel-Air Orifice and Ignitor Inlet

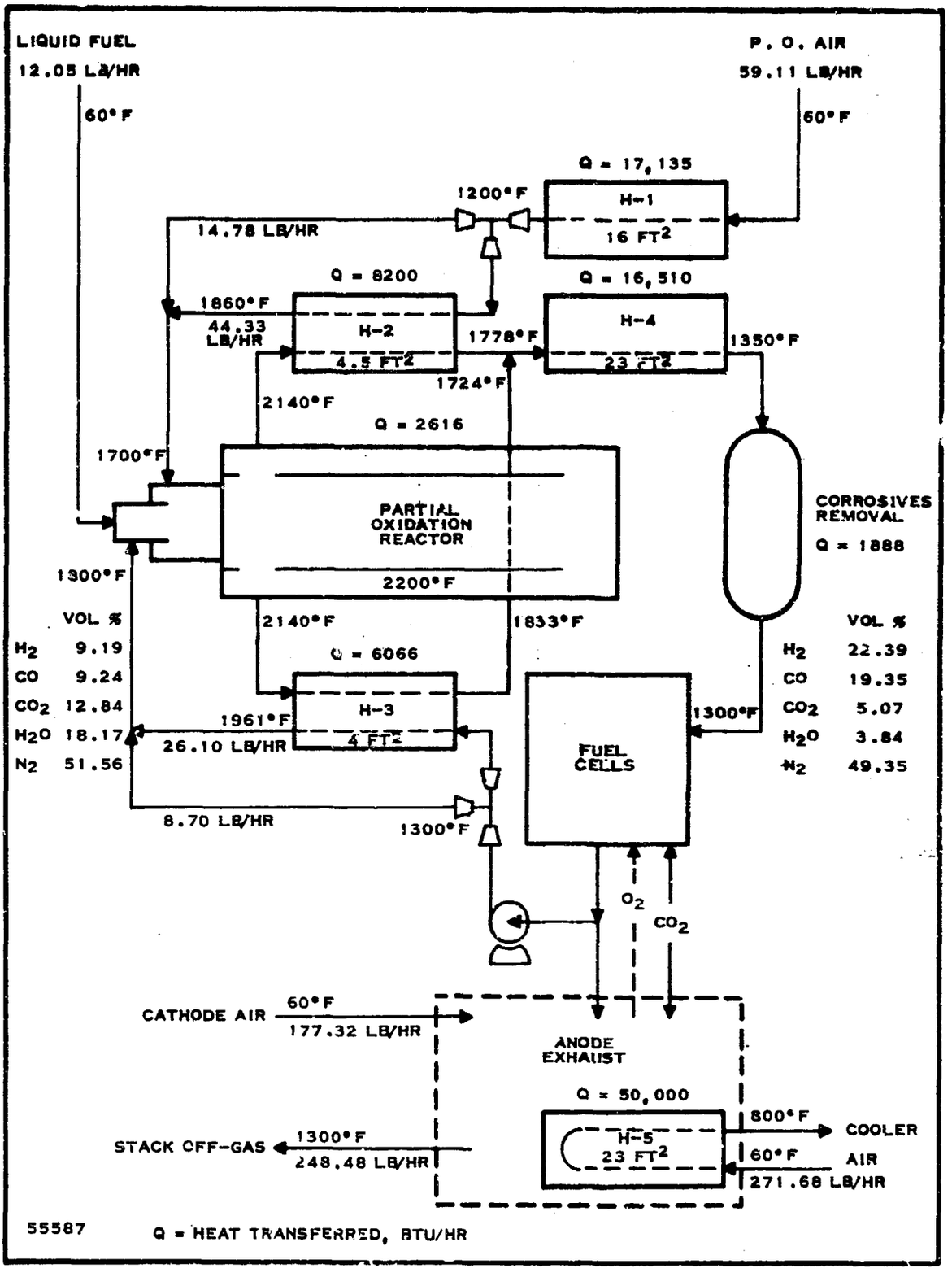

Figure 2-50. 15-Kilowatt Fuel Preparation Unit, Process Flow Schematic

These compositions were calculated at an overall fuel utilization of 68.2 percent which corresponds to a H_2O/H_2 ratio of 1.98 (2.0 is maximum considering nickel corrosion). The effects of CO_2 diffusion from the anode was accounted for in these calculations. The carbon deposition temperature of the partial-oxidizer product is 1265°F, well under the 1300°F system temperature.

Presented in Figure 2-50 is a process flow schematic of the 15-kilowatt system showing stream compositions, temperatures, and flow rates plus heat exchanger duties and surface area requirements at the design 15-kilowatt load. Detailed design calculations are presented in Appendix C. Basically, air preheated and mixed with fuel vaporized by the recycle gases enters the reactor through an inlet orifice to obtain recirculation by jet pump action. After reaction at 2200°F, the partial-oxidizer product gases are cooled to 1350°F prior to entering the corrosives removal unit. Gases from this unit enter the fuel cell stack for electrochemical reaction and a portion of the anode exhaust is recycled to the partial-oxidizer for control of carbon deposition.

b. Air and Anode Exhaust Recycle Heaters

To obtain the desired adiabatic reaction temperature of 2200°F, it will be necessary to heat the partial-oxidizer air and anode exhaust recycle streams to 1700°F and 1800°F, respectively. Control of these temperatures is accomplished by splitter valves which adjust the fraction bypassing the heat exchanger

Partial-oxidizer air is preheated to about 1200°F in a 16-square-foot heat exchanger by the 1300°F furnace gases. The air stream is then split (for temperature control) and 75 percent is heated to about 1860°F by partial-oxidizer product gas in a 4.5-square-foot heat exchanger. Recombining the air streams gives the desired 1700°F preheat temperature.

The anode exhaust recycle stream is split in a similar manner and 75 percent is heated to 1960°F by partial-oxidizer product gas, then recombined with the preheater bypass stream to give a temperature of 1800°F entering the partial oxidizer. About 4 square feet of heat exchanger surface will be required in this preheater.

c. Vaporizer-Mixer

Fuel vaporization and mixing of fuel with air and anodes exhaust recycle may be a major problem due to preignition at the high preheat temperatures required on the 15-kilowatt system. The preignition temperature of fuel-air mixtures is also lowered as line size is increased; however, this effect can be counteracted to some extent by baffling to reduce the effective cross-sectional area of the inlet piping.

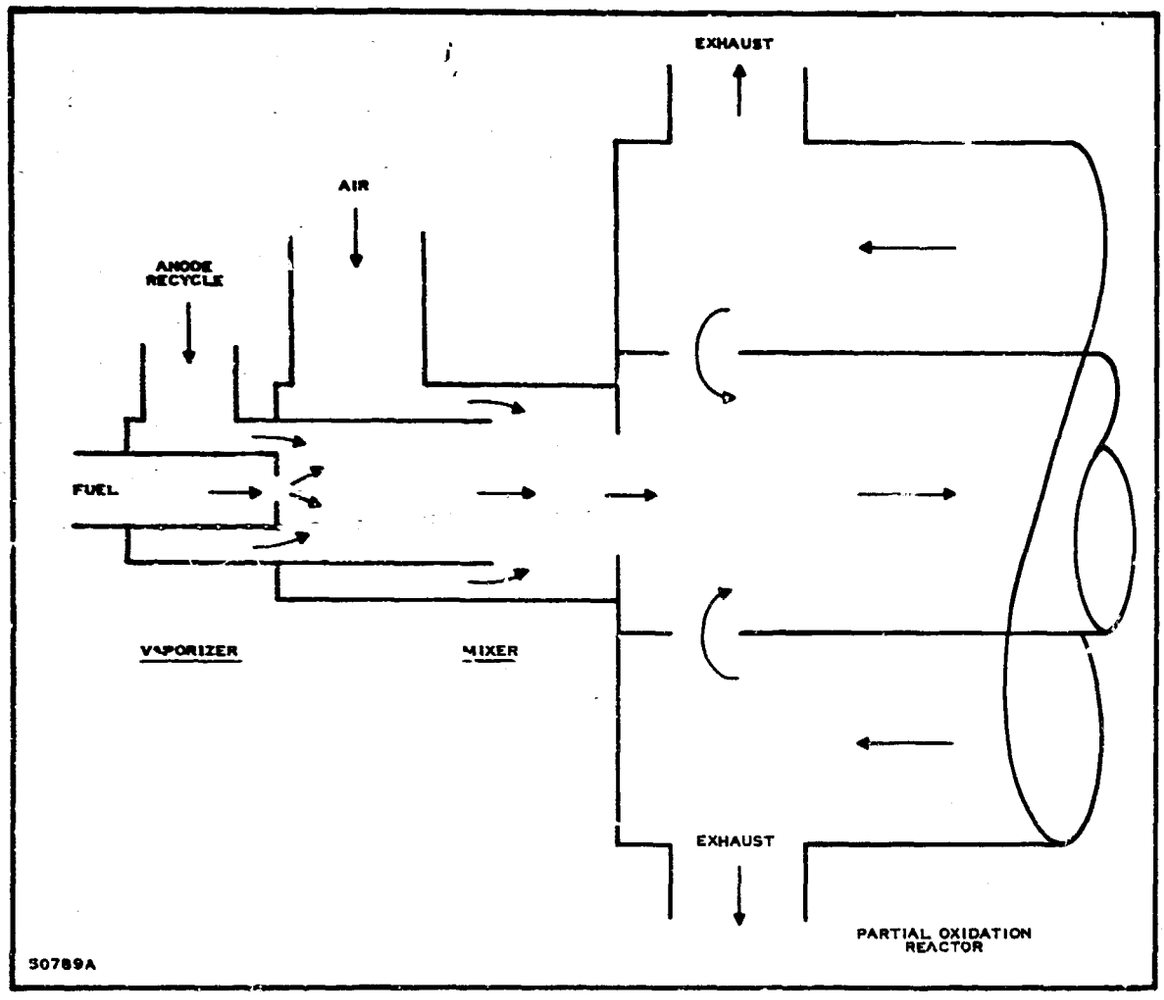

Figure 2-51. 15-Kilowatt Partial Oxidizer, Vaporizer-Mixer-Reactor

The initial mixing of preheated air with fuel vapors is expected to be the most critical area in this system since intermediate mixtures of high fuel-air ratio which favor preignition can be formed. In order to minimize preignition problems, the liquid fuel will be dispersed into the anode exhaust recycle gas stream using a spray nozzle. The fuel vapors, diluted with recycle anode exhaust gases, is then mixed with air preheated to 1700°F. This mixture enters the partial-oxidation reactor at about 1225°F, which should result in an adiabatic reaction temperature of 2200°F. This fuel vaporization technique and the partial-oxidation reactor are shown in Figure 2-51.

d. Reactor

The reactor design proposed for the 15-kilowatt system is shown in Figure 2-51. This reactor is 5 inches in diameter, 24 inches long, and has an internal volume of 470 cubic inches. Internal recirculation will be provided by a 2-inch diameter recirculation pipe. Inconel 600 or Incoloy 800 will be satisfactory materials of construction.

e. Fuel Cooler

Partial-oxidizer exhaust gases are cooled from 2140°F to 1780°F by heat exchange with partial-oxidizer air and anodes exhaust recycle as previously discussed. Cooling to 1350°F is accomplished with 1300°F furnace gases in a heat exchanger with 23 square feet of heat transfer surface. Further cooling to 1300°F will occur in the corrosives removal unit and the plumbing to the fuel cell stacks.

f. Development Work Required

Considerable development work will be required on the fuel preparation unit for the 15-kilowatt system. The major effort will probably involve the vaporizer-mixer-reactor equipment. Preignition, mixing efficiency, reaction stability, carbon formation, and approach to thermodynamic equilibrium are some of the major problems to be solved with the 15-kilowatt unit. Lead and sulphur removal also require additional study.

Throttling of the 15-kilowatt fuel preparation unit requires development work in view of the problems mentioned previously. Throttling also affects the internal recirculation rate, which appears to be a pertinent variable in obtaining clean reaction without carbon formation.

D. STARTUP BURNER SYSTEM

1. Design Approach

In the design of a liquid-fueled startup burner for fuel cell power plants, there are four important aspects to be taken into consideration. These are listed below.

The burner must start and run clean; it must not develop soot or smoke.

It must have high heat output and minimum size and weight.

It must have uniform heat distribution along the length of the furnace.

It must operate equally well on either combat gasoline or CITE fuel, with a minimum of readjustment.

In our first approach to the startup burner problem we investigated several commercially available boiler burners. It became immediately obvious that these units were too large and too heavy. In addition, they required 60-hertz ac power to operate. It was then decided to investigate the burner used in aircraft cabin heaters. Such burners have the advantages of being light in weight and relatively small, and they operate on 24 volts dc. Several sizes were purchased and tested. They seemed to be very promising even though they did not burn as cleanly as desired.

Next, the problem of uniform heat distribution was approached. Several cold flow models of plywood and cardboard were constructed to verify ideas. The most promising model (also one of the easiest to build) was a simple box, 8 inches square and 24 inches long (inside length of 1-kilowatt furnace). The top surface (8 by 24 inches) had two rows of eight 9/16-inch holes. The only part of the aircraft cabin heater used was the inner combustion tube and cone assembly. This combustion tube (with an extension added) ran down the center of the box to within about 2 inches from the end. The box served as a plenum and the 16 holes were sized to get uniform distribution.

2. The 1-Kilowatt Breadboard Startup Burner

For the 1-kilowatt breadboard startup burner the inner combustion tube and cone from a Janitrol Aircraft heater, Type S200, was used. This heater carries a 200,000 BTU per hour input rating. To make it suitable for use, an extension was welded to the combustion tube and an air supply box for the nozzle end was built. This tube was mounted centrally in an 8- by 8- by 24-inch metal box with two rows of eight 9/16-inch holes in the top face. The box was mounted in a simple open top furnace.

First, operation of the burner in this configuration resulted in unclean startup and burning. The original nozzle operated on only 15 psi pressure (supplied by two Bendix pulse-type fuel pumps in tandem). To get better atomization, a smaller nozzle was used, and fuel pressure increased to 34 psi. At this pressure, 5 pounds of combat gasoline per hour was being burned, representing an input of 94,000 BTU per hour. Startup and burning still were not clean enough so experiments were tried with the air supply. The original burner injected a small amount of air from an annular orifice surrounding the fuel nozzle. Using shop air supply it was found that if 4-inch H_2O pressure in the nozzle box was maintained, the desired type of

startup and burning could be accomplished. A new nozzle box with a 1-inch inlet was built, with air supplied from a tee at the combustion blower output. To obtain the 4-inch H_2O pressure, an orifice was installed down stream from the tee.

a. Performance of Combat Gasoline

Setup was upgraded to accurately measure total air supply, using a venturi meter. At 34 pounds per square inch gage fuel pressure (5 pounds of fuel per hour) and sufficient air to give a 2:1 ratio of CO_2 to O_2, burner performance was excellent.

b. Performance of CITE Fuel

The only change necessary from the above to burn CITE fuel was to reduce the fuel pressure to 20 pounds per square inch gage pressure to obtain the 5 pounds per hour flow rate. Performance was excellent on CITE fuel.

3. Design Extension to 15-Kilowatt Size

Texas Instruments is convinced that the technique used in the 1-kilowatt breadboard startup burner can be fairly easily scaled-up for use in the 15-kilowatt power plant. Fortunately, Janitrol Aero makes a large liquid heater package that has an output rating of 1,000,000 BTU per hour. Plans call for the use of the combustion head and tube from this heater. Calculations indicate that an output of approximately 750,000 BTU per hour for the 15-kilowatt plant is needed. This will require a fuel flow of 40 pounds per hour. As designed, the blower for the combustion air requires 1.5 horsepower. This will require 40 amperes at 28 volts. A considerable reduction in this power requirement may be realized by burner redesign to incorporate induced draft.

There is no way of knowing at this time whether this burner, as is, will start and burn clean. In the event that it does not, Texas Instruments is prepared to perform whatever modifications are necessary.

E. CORROSIVE MATERIALS REMOVAL

The Texas Instruments fuel cell employs a nickel anode, the electrochemical and structural functions both being served by the single material. As a catalyst, nickel is a candidate for poisoning. In practice, this is found not to be a problem. As a structure, however, nickel is a target for corrosion, and this threat turns out to be very real.

One source of nickel corrosion is the water (or CO_2) which is formed at the anode. That is a matter of operation and electrode polarization and is not the subject of this section. Here we are concerned with the sulphur, lead, and halogens present in common hydrocarbon fuels. After the reaction in the partial oxidizer, these are found in the fuel stream as H_2S, PbO or $PbBr_2$, and HBr.

The effect of H_2S on the Texas Instruments fuel cell has been examined experimentally. In one test, for example, a module was fed a stream containing 700 parts per million of H_2S. This module previously had been operated for 95 hours without H_2S, and was performing well. In 30 hours of exposure to sulphur, the anodes were severely damaged by corrosion. On the other hand, the electrochemical properties do not appear to be greatly affected. In the test above, and others, the module continued to produce power until its physical structure was ruined.

The experiments described here were performed on an earlier model (LCM) fuel cell. The anode structure was nearly identical to that of the present cell, however.

The effect of lead salts or HBr is not known. Lead is a very corrosive material at high temperature in an oxidizing atmosphere, but no data have been found for a reducing environment.

The two general approaches for dealing with these corrosive constituents are: remove them, or employ a resistant material for the structural features of the anode. The second possibility is being studied, but attempts thus far have not been successful. This report will be concerned with methods of removal.

1. CITE Fuel

The maximum permitted sulphur content of CITE fuel is 0.4 percent by weight. If this is fed to a partial oxidizer, the product will contain about 500 parts per million H_2S by volume. The Texas Instruments fuel cell in its present form cannot tolerate that.

2. Gasoline

The specifications for combat gasoline permit a maximum of 0.15 percent sulphur. This would give about 200 parts per million H_2S in the partial oxidizer exit stream—less than for CITE, but probably still enough to cause rapid deterioration of the cell. On the other hand, most gasoline actually has much less sulphur than that. For example, the gasoline used in the demonstration tests of the partial oxidizer had only 0.002 percent sulphur. In the cell this would be only 2 parts per million. If the concentration were much less than this, the formation of nickel sulfide would not be thermodynamically favored, so the cell probably would not be affected by this level of H_2S.

If gasoline typically available in the field is found to have a sulphur content this low, it may not be necessary to remove it at all. In any case, a process that will remove sulphur from CITE fuel will work for gasoline.

3. Sulphur Removal

Preliminary experiments were conducted to examine potential sulphur-removing agents. A simulated fuel stream containing 400 parts per million H_2S was passed through a tubular bed containing the candidate material. The flow rate was equivalent to that of a 100-watt system; the duration of each of the tests was 50 hours. All tests were performed at 700°C. After the run, samples of the material were analyzed for sulphur.

Several materials were checked in this way, among them, nickel screen, steel wool, the lithium-sodium carbonate used in the cell, and a number of commercial catalysts. Of these, two gave encouraging results: the molten carbonate and a Girdler catalyst, G-49A. These are summarized below:

	G-49A	Carbonate
Total sulphur passed	11.65 grams	10.46 grams
Sulphur retained	5.41 grams	7.17 grams
Percent retained	46.4 percent	68.5 percent
Amount of material	410.0 grams	210.0 grams
Gram Sulphur/Gram Material	0.013	0.06

In two respects, improvements over these results are desired. A greater proportion of the sulphur must be removed, and the amount of material required to do it should be reduced. Additional work is needed to determine whether either of the above agents can be developed into a practical process, and also to investigate other possibilities.

The importance of this project is recognized, and it is being continued.

4. Lead and Halogens

No work has been done directly on the matter of lead salts, either to determine the effects on the Texas Instruments cell or to investigate methods of removal. Partial-oxidation reactors have been operated extensively on combat gasoline. Some lead deposits have been found, but no evidence of corrosion. During the 100-hour demonstration runs, a piece of nickel screen was inserted in the outlet pipe of one of the reactors. After the test it was coated with carbon but the metal itself was bright and ductile. These observations suggest that the lead salts may pass through the fuel cell without producing any effect.

There appears to be no satisfactory way to simulate a fuel stream containing lead salts, as with H_2S. It will be necessary to operate fuel cells on actual gasoline product gas to determine whether their operation will be affected.

5. The 15-Kilowatt Design

In 50 hours of operation, the power plant might consume 500 pounds of fuel. If CITE fuel with 0.4-percent sulphur is used, approximately 2 pounds of sulphur (essentially all of it) must be removed. The experiment on molten carbonate suggests that 40 pounds of carbonate might suffice.

Although the nickel-containing catalysts tested to date have not shown as much promise, they will be studied further, because nickel is theoretically a good removal agent. To remove 2 pounds of sulphur would take about 4 pounds of nickel. A catalyst loading of 40-percent nickel is reasonable, so 40 pounds of catalyst might well carry four times the amount of nickel required stoichiometrically.

Concerning lead, the information at hand is not sufficient to warrant an estimate of requirements for the 15-kilowatt design.

Texas Instruments fully appreciates the importance of this aspect of system performance. Exploratory and developmental work are both being continued.

F. SPENT FUEL RECYCLE BLOWER

1. The 1-Kilowatt Size

a. Design

During the early design phase, it was determined that the spent fuel recycle blower for a 1-kilowatt fuel cell power plant should have a pumping capacity of 1 cubic foot per minute against a head of 5 inches H_2O when pumping hot gas (700°C) having a density of 0.026 pound per cubic foot. Ten manufacturers of small blowers were contacted in an attempt to have someone design and construct this blower. None of the manufacturers contacted were willing to undertake the design and construction of the entire blower (the blower itself plus mounting and spindle). Torrington Manufacturing Company agreed to design and construct two impellers and scroll cases and Texas Instruments would design and construct the mount and spindle.

The Torrington design is shown in Figure 2-52. The impeller is 3-1/4 inches diameter and must run at 19,000 revolutions per minute.

The mounting and spindle designed by Texas Instruments is shown in Figure 2-53. The entire blower and spindle is mounted on a "plug" which is inserted in a hole in the furnace wall. This is to facilitate inspection and maintenance of the blower. The furnace side of this plug is shown in Figure 2-54. The insulation between the inner and outer mounting plates and the blower scroll case is evident.

Figure 2-55 shows the exterior side of the blower plug. The spindle is hollow (in the hot zone) and is made of 316 stainless steel. Three copper pin fin heat dissipators are silver soldered to the hollow shaft just outside the outer furnace wall to provide a heat dam between the hot part of the shaft and the bearings. Since the shaft has a rather large overhang, precision ABEC 7 bearings are used in a preloaded quill. We believe that this technique will hold the bearings to a satisfactory operating temperature. There may be a problem when the system is shut down. The pin fins cannot be made large since they would absorb too much power at this speed. Therefore, they may not be large enough to dissipate sufficient heat when not rotating. There are three possible solutions that may be used singly or in combination. One is to operate the blower at reduced speed (1/3 to 1/4) for some time after shutdown. The second possibility is to use a small fan to blow some air across the pin fins after shutdown. The third is to mount the pin fins in a duct to obtain natural convective cooling. The inlet and discharge of the blower will be coupled to the system "plumbing" with MARMON type flanges and clamps.

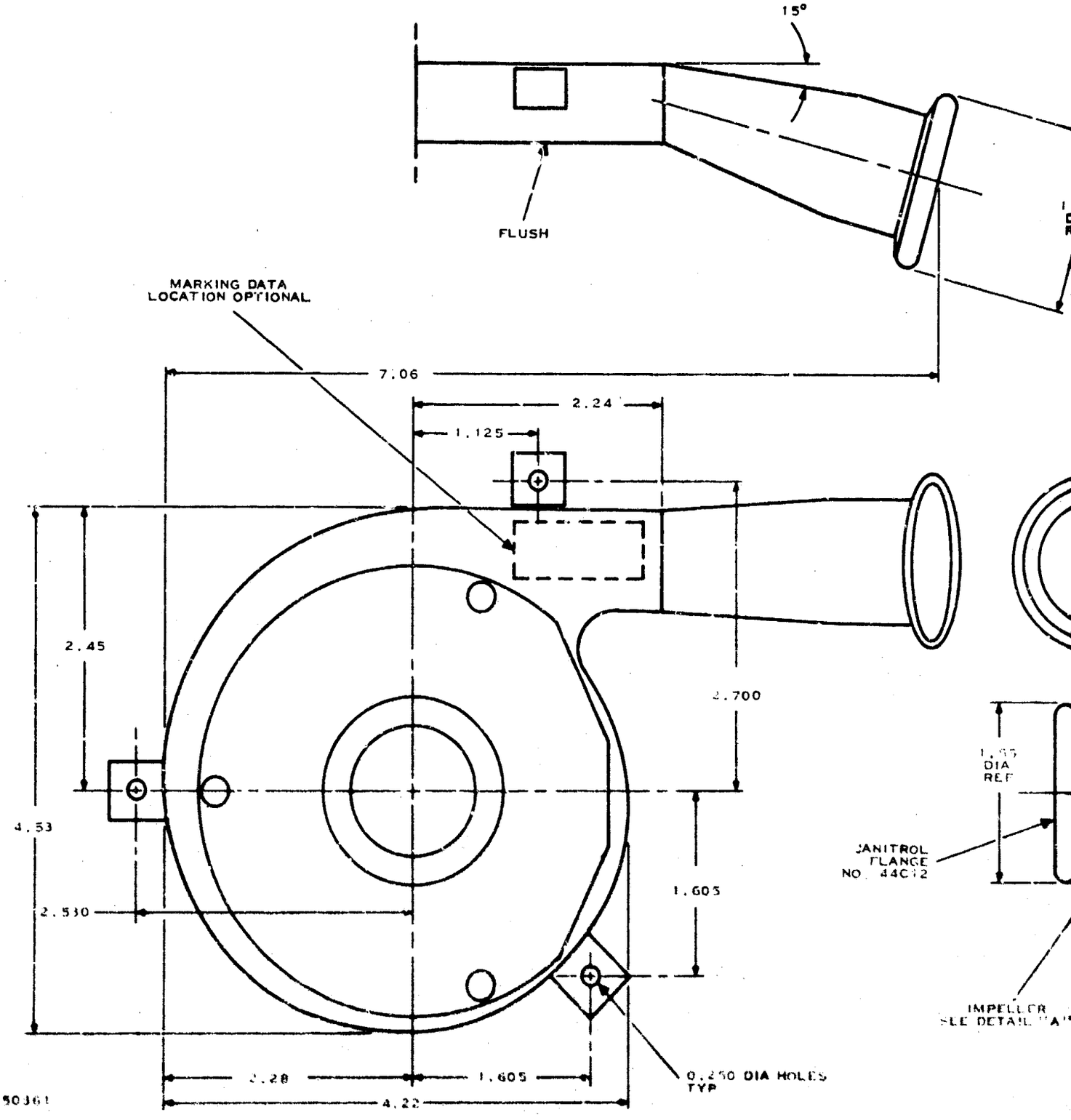
15°
FLUSH
MARKING DATA
LOCATION OPTIONAL
7.06
2.24
1.125
2.45
2.700
4.53
2.530
1.605
2.28
1.605
4.22
0.250 DIA HOLES
TYP
JANITROL
FLANGE
NO. 44C12
IMPELLER
SEE DETAIL "A"
50361

A.

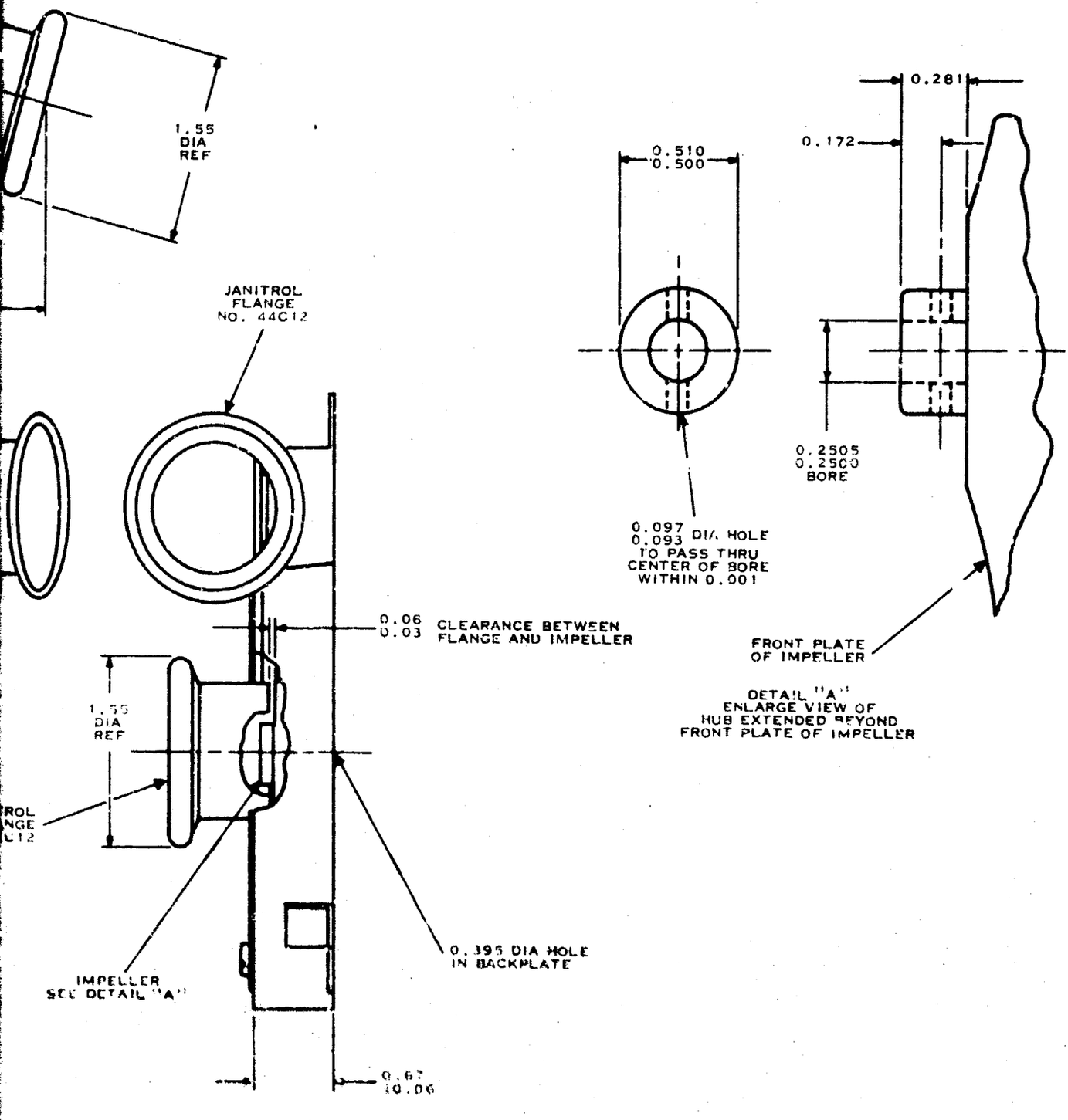

Figure 2-52. Recycle Blower

B.

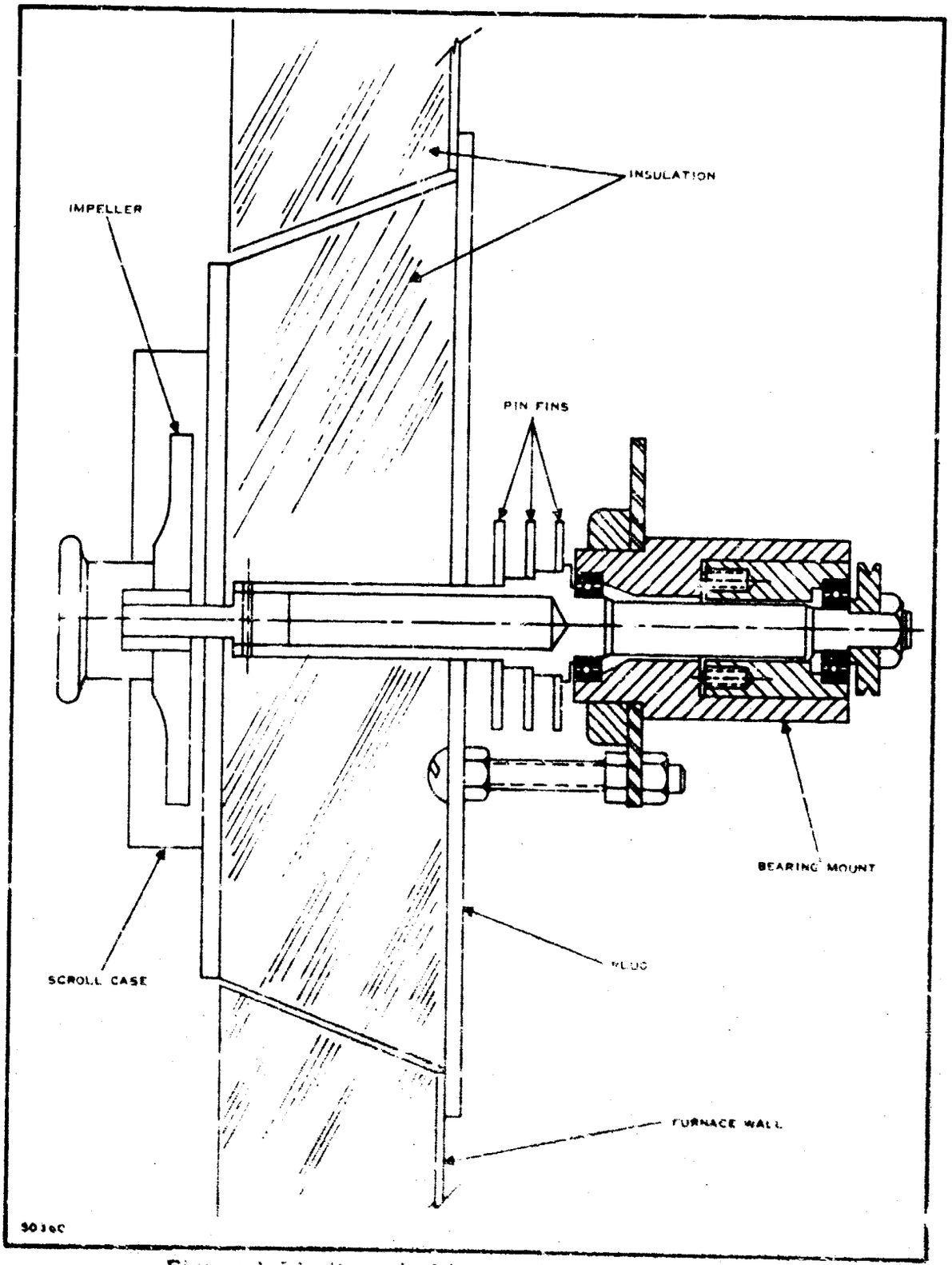

Figure 2-56. Recycle Blower Mounting and Spindle

30790

Figure 2-54. Furnace Side of Blower Plug

b. Test Program

In order to test the performance of this design, the blower "plug", as shown in Figure 2-53, was mounted in the wall of a small electrically heated furnace. A closed loop of tubing couples from blower discharge to inlet. This loop has provision for the insertion of various orifices and has four pressure taps, one on each side of the orifice and one at the blower inlet and discharge. The circulation loop is shown in place in the furnace in Figure 2-56. The spindle is driven by a miniature Vee belt from a 3450-revolutions per minute AC motor. This setup is shown in Figure 2-57. Two differential manometers are used to measure the pressure drop across the orifice and the pressure boost across the blower.

c. Performance

Figure 2-58 is a performance curve run by Torrington, obtained by operating the blower at room ambient temperature and scaling the speed down to 6000 revolutions per minute.

The blower was tested at 700°C at four different flow rates. A solid orifice plate and three orifices, 0.250 inch, 0.375 inch, and 0.5625 inch in diameter, were used. The data obtained is given below in tabular form.

Orifice Size (inch)	Pressure (Inches H_2O)	Flow (CFM)
0.000	5.9	0.00
0.250	5.2	3.76
0.375	4.8	8.59
0.562	3.1	13.42

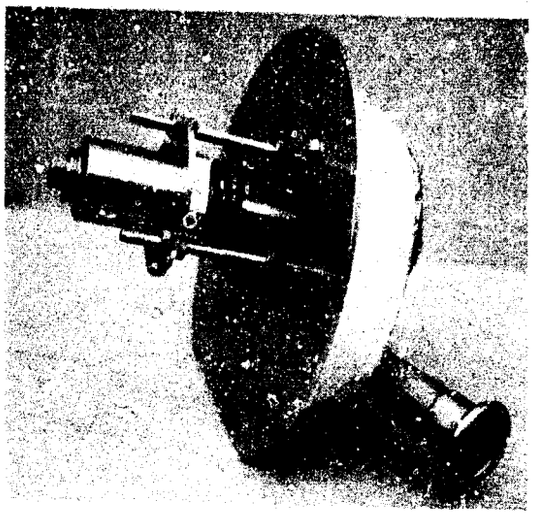

50791

Figure 2-55. Outer Side of Blower Plug

Flows were calculated using a density of 0.0221 pounds per cubic foot (700°C). The experimental points obtained are plotted as circles on Figure 2-58 and show good agreement with the Torrington curve.

The blower spindle and drive worked very well. The hollow spindle and pin fins were very effective in isolating the furnace heat from the bearings. In fact, the bearing temperature rise was the same with the furnace hot or cold, thus indicating that the only temperature rise was from the bearings' own grease-churning action.

Further tests will be made to determine the bearing temperature rise with the furnace hot and the blower not rotating, to simulate shutdown conditions. A number of furnace cycles with the blower not turning will be run to see if any sag and resulting unbalance occurs. We also will run hot life test to failure.

Texas Instruments believes that the hot recycle blower has been demonstrated to be feasible and practical. The major problems have been solved and only some refinement may be necessary.

2. Design Projection to 15-Kilowatts

The spent fuel recycle blower for the 15-kilowatt system is required to pump approximately 30 cubic feet per minute against a head of 5 inches H_2O at 700°C.

For a given flow, speed and impeller diameter can be traded directly. An impeller diameter of 8 to 9 inches would permit a more reasonable speed of 7000 to 8000 revolutions per minute. Having successfully designed and constructed some furnace circulation blowers for the 1-kilowatt breadboard unit, Texas Instruments now feels competent to design and construct recycle blowers.

50792

Figure 2-56. Circulation Loop in Furnace

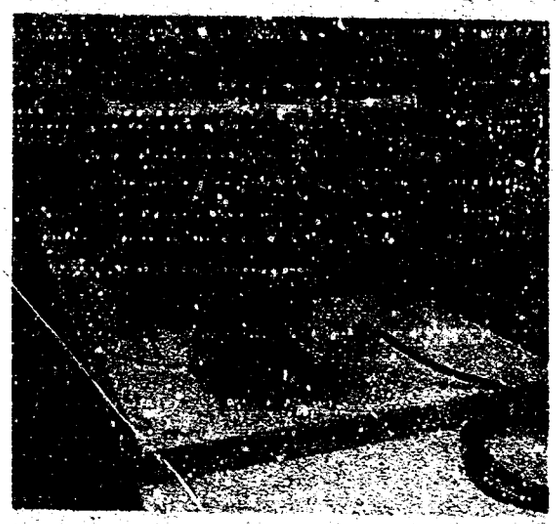

50793

Figure 2-57. Blower Drive and Test Furnace

G. CONTROL SYSTEM DESCRIPTION

A control system designed to make a fuel cell power plant completely automatic has been designed by Texas Instruments. The various control functions are based on the best available knowledge.

A detailed description of the control system, describing a typical startup, run, and shutdown sequence follows. For convenience, the total system has been divided into various subsystems.

The auxiliary power verification and switchover subsystem, shown in Figure 2-59, contains the master start and stop controls. When the "start" push botton is pressed, relay K1 is energized. It seals itself in through its own holding contacts. In addition, it closes the circuit of the voltage sensor, closes the fuel cell output circuit and supplies battery power for the control power line and the auxiliaries. The negative side of the startup battery, and the fuel cell are common. For simplicity of shutdown, battery power is used in several hold-in circuits throughout the total system. Intentional shutdown is accomplished by pushing the master "stop" botton. This breaks the hold-in circuit of K1 and removes power from the control power line. It also applies

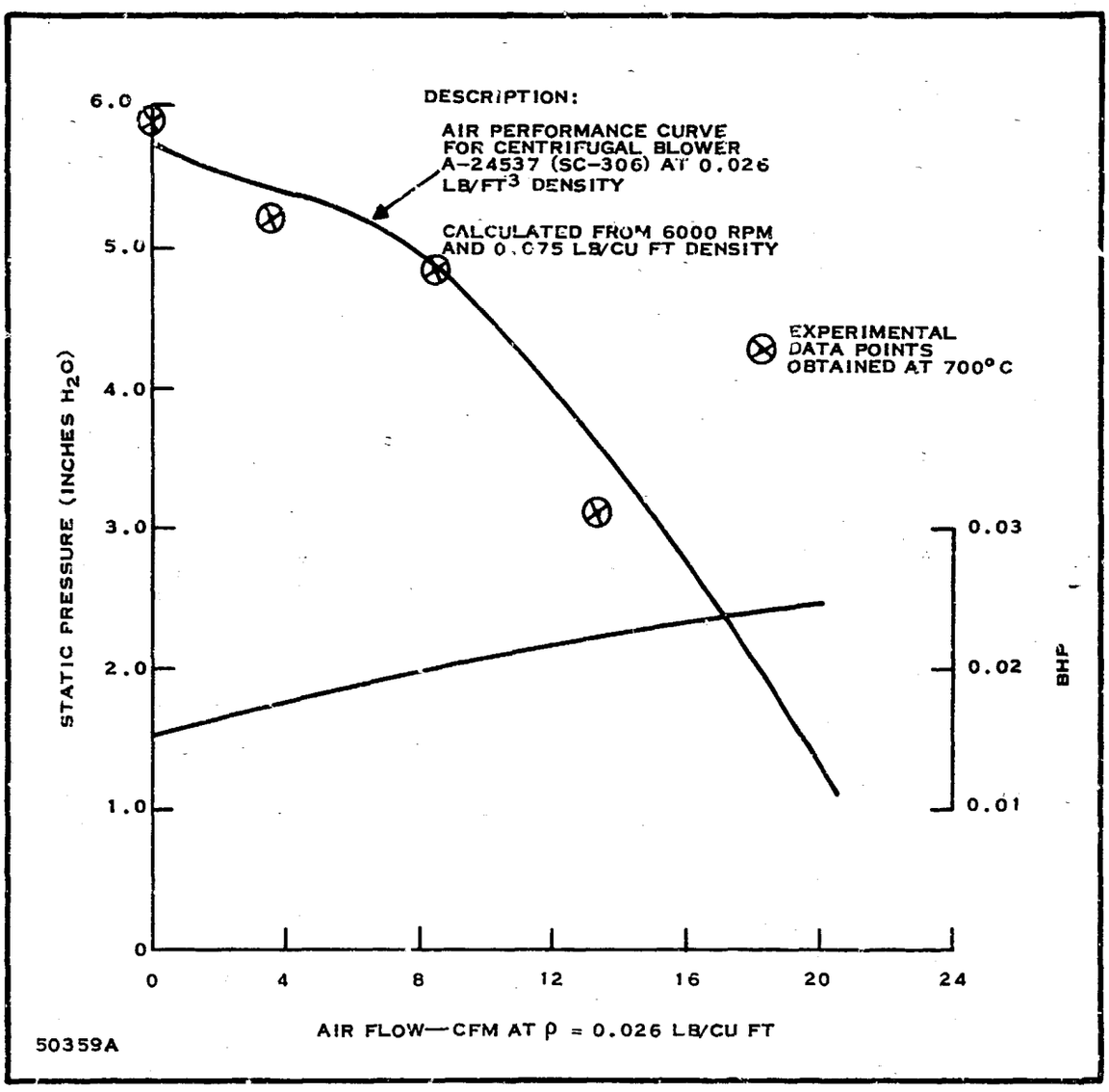

Figure 2-58. Performance of Recycle Blower

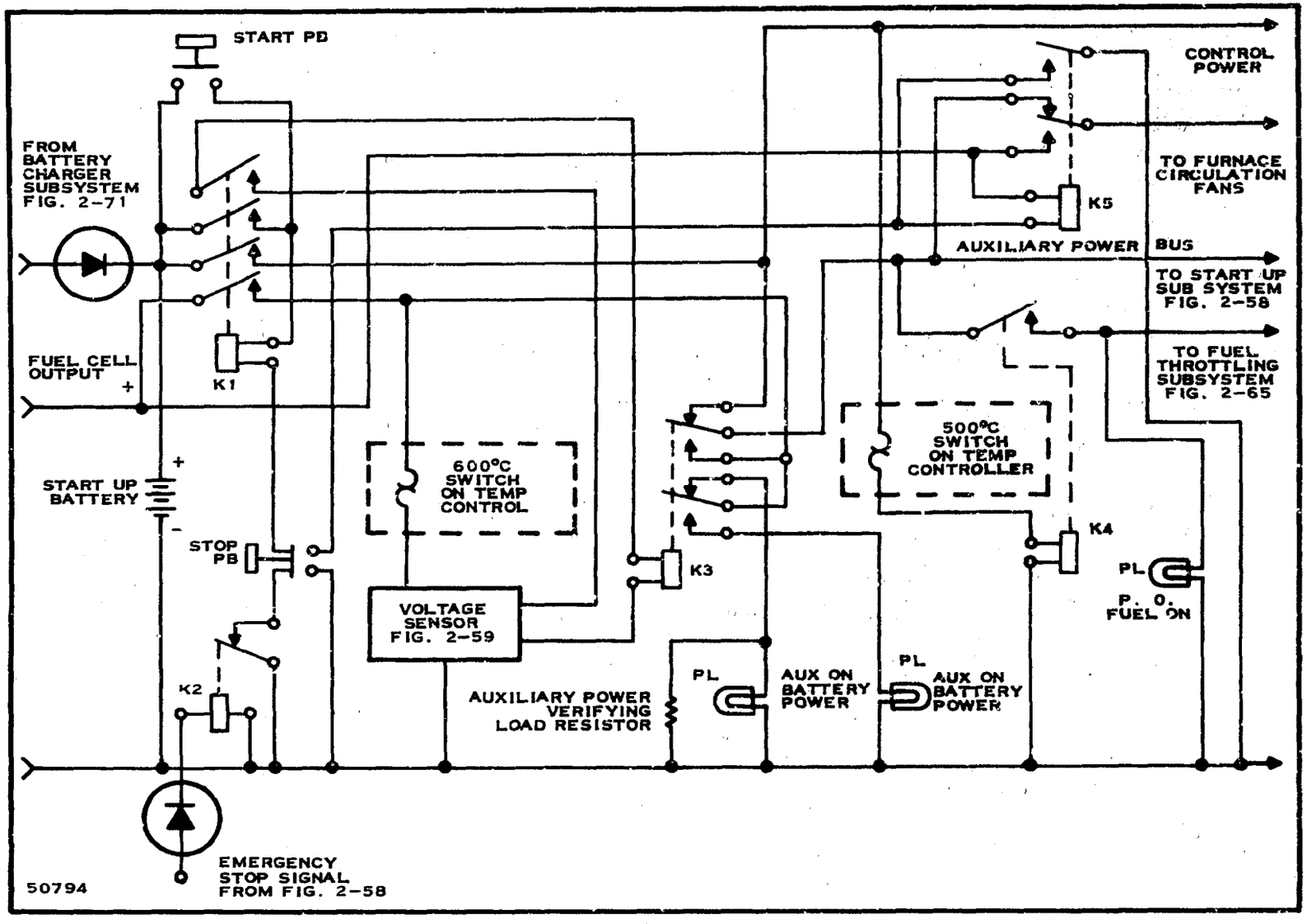

Figure 2-59. Auxiliary Power Verification and Switchover System

power to relay K5 which seals itself in. This relay switches the furnace circulation fans from the auxiliary power bus to fuel cell power. This serves to keep the circulation fans running for some time after shutdown to avoid furnace hot spots. Relay K5 is margined so that it will drop out at about 20 volts. In addition, an emergency shutdown can be accomplished by energizing relay K2.

When the "start" push botton is pressed, battery power passes through the contacts of relay K3 (normally closed) and is applied to the startup subsystem shown in Figure 2-60.

In Figure 2-60, this voltage causes relay K6 to close, applying power to the combustion blower, startup fuel pump, the ignitor and to the air pressure sensor. The bottom of the coil of relay K6 is tied to the negative side of the line through normally closed contacts on relay K7. This relay is used to stop the startup system. When the combustion air pressure and the startup fuel pressure have reached satisfactory levels, the two contacts close, applying power to the startup fuel solenoid valve. Power is also applied to the flame verification safety cutoff consisting of the thermal time delay relay, the Cds photoconductive cell, the transistor and relay K8. The thermal time-delay relay has normally closed contacts that will open 2 seconds after power is applied to the heater. If the fuel ignites and produces a flame, the photoconductive cells' resistance drops, thus turning on the transistor. The transistor collector current pulls in relay K8. This relay shorts across the contacts of the thermal time delay relay, forestalling its opening of the fuel solenoid valve circuit and operating a pilot light indicating that the burner has ignited. If the fuel fails to ignite, the delay relay will turn off the fuel flow after 2 seconds. The operator should let the unit operate for five minutes so the combustion air can sweep the unburned fuel from the furnace. He then pushes the "stop" botton, waits 1 minute, and presses the "start" botton to recycle the startup. The photoconductive cell will be mounted in a heat dam tube protruding several inches from the furnace in the accepted photoflame sensor manner.

Referring again to Figure 2-59, at 500°C, a switch on the temperature controller closes. This applies control power to relay K4 which switches power from the auxiliary power bus to the fuel throttling sybsystem. The fuel subsystem starts furnishing fuel to the partial-oxidization reactor. Thus, as the furnace continues to heat up, we have the increasing possibility of drawing some power from the fuel cell. In order to conserve the startup battery, it is highly desirable to switch the auxiliaries over to fuel cell output at the earliest moment. We believe that his should not be attempted before the furnace reaches 600°C. Therefore, at 600°C, a switch on the temperature controller closes, applying fuel cell voltage to the voltage sensor (Figure 2-61). In order to be certain that the fuel cell output can sustain the auxiliary power draw, an output verifying technique has been incorporated. During startup the fuel cell output is connected through normally closed contacts on relay K3 to the auxiliary power

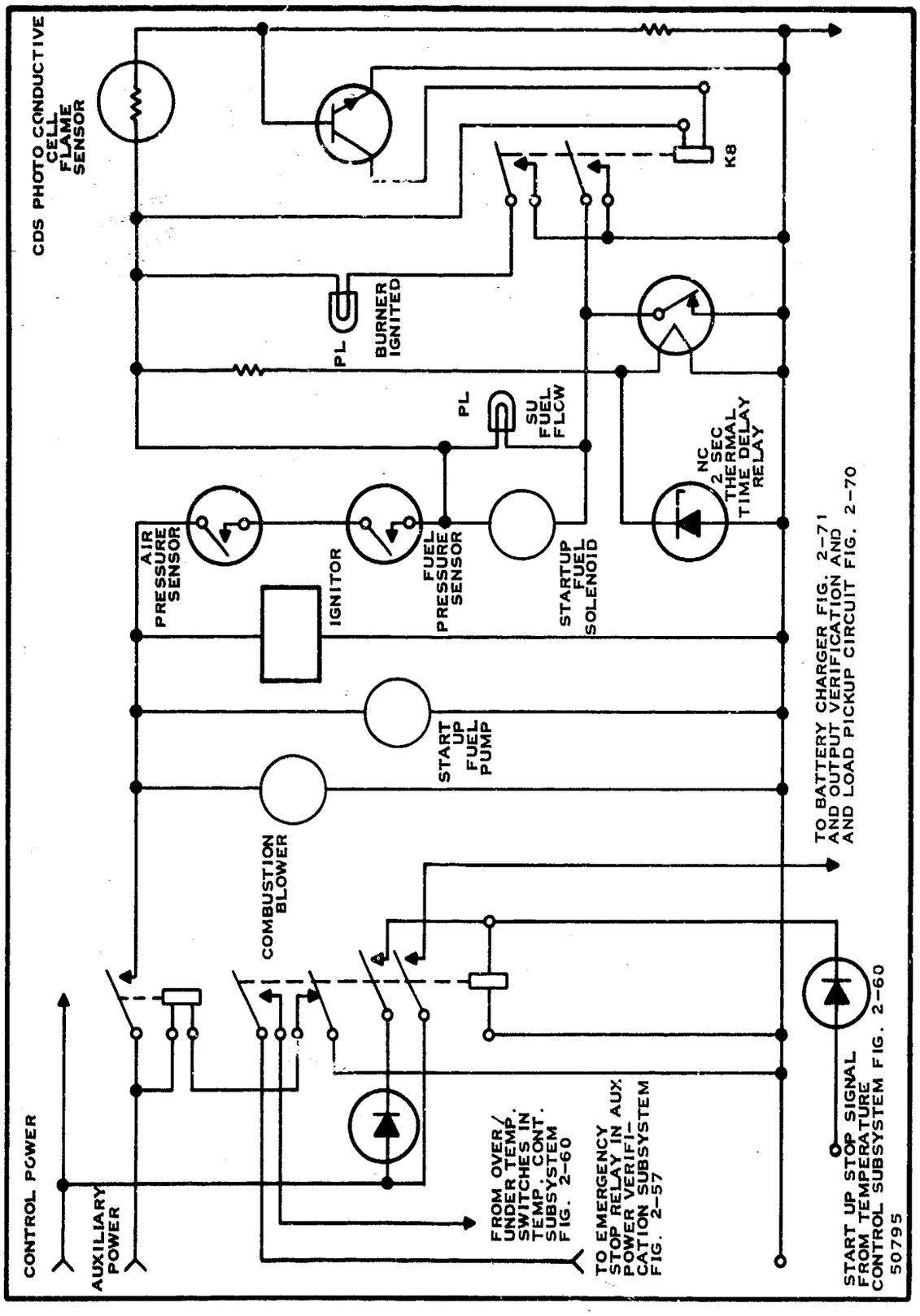

Figure 2-60. Startup Subsystem

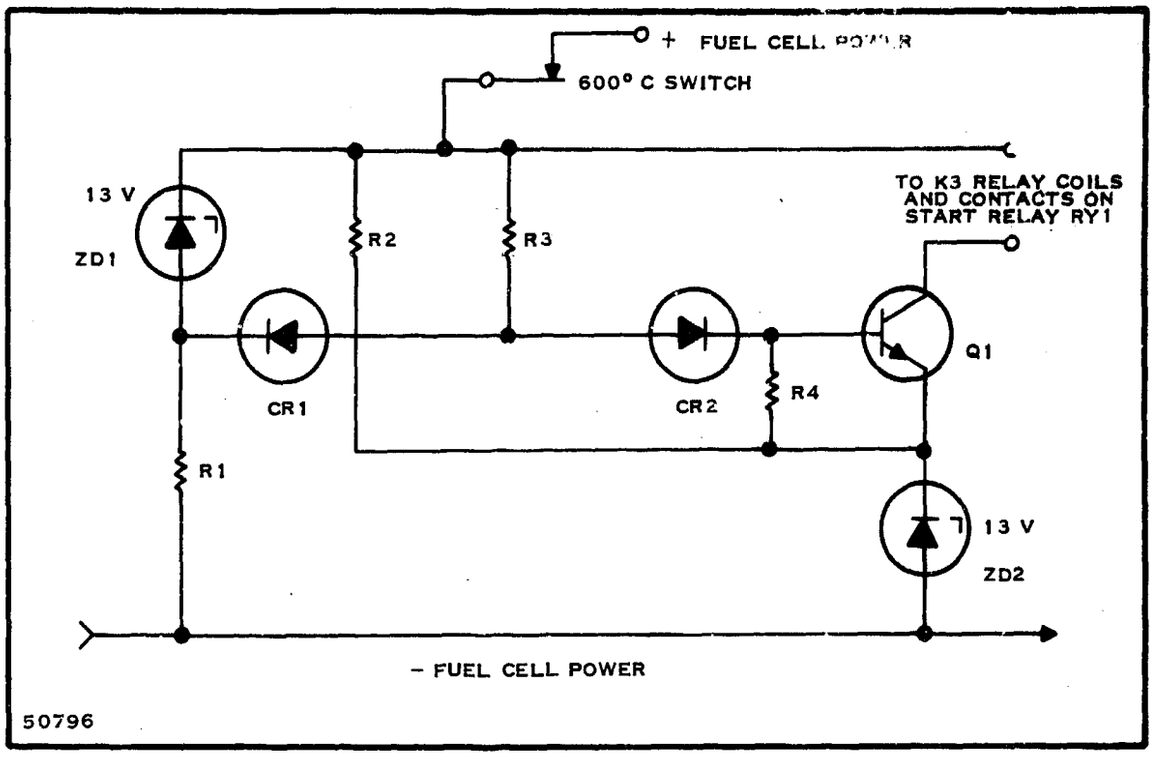

Figure 2-61. Voltage Sensor

load verifying resistor. This resistor is of such a resistance and wattage rating that at the lowest voltage at which the auxiliaries will operate satisfactorily, it will draw slightly more power than the auxiliaries. The voltage sensor, Figure 2-61, is so designed that it will actuate the relay K3 when the minimum operating voltage of the auxiliaries is reached. When K3 operates, it does the following things: (1) switches the auxiliaries from battery power to fuel cell power, (2) disconnects the power verifying resistor, and (3) lights a pilot light indicating that the auxiliaries are now operating on fuel cell power. The power verifying resistor will consist of heater elements inside the furnace to utilize the approximate 2 kilowatts of power that it will dissipate. This will help bring the furnace up to temperature a little faster.

The next step in the startup sequence is for the furnace to reach the operating temperature of 700°C. The Temperature Sensor, Figure 2-62, will be modified from a standard Burling Instrument Rod and Tube Controller. This controller consists of a plugged inconel tube protruding into the furnace about 1 foot. Inside this tube, there is an alumina ceramic rod which extends back to the furnace wall. There is an inconel rod extending from the end of the alumina rod to the sensing head. The end of this rod pushes on a spring-loaded lever which provides motion multiplication. This lever operates four snap action switches. The switches closed above 500°C, and closed above 600°C

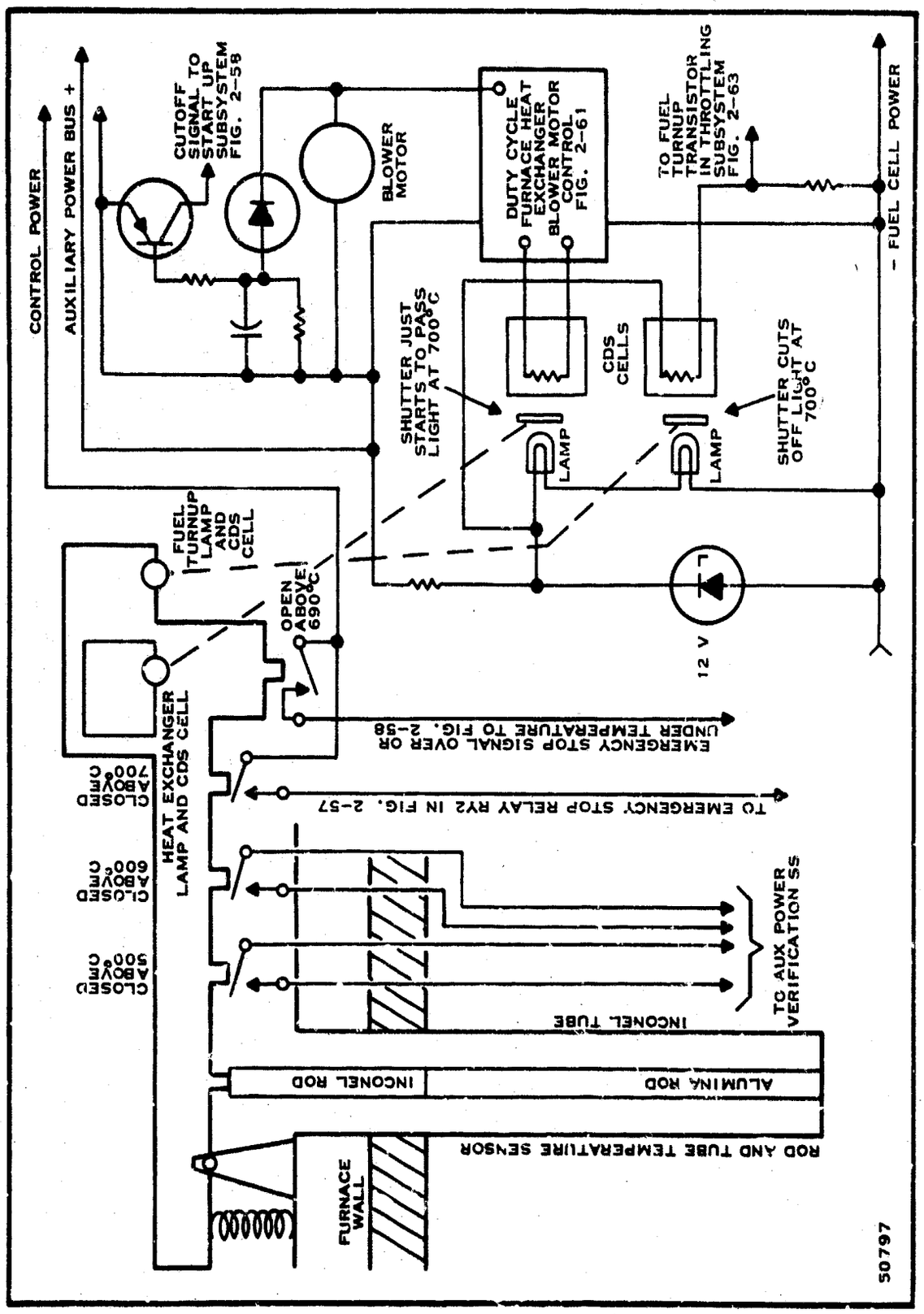

Figure 2-62. Temperature Control Subsystem

have had their functions covered in the description of Figure 2-59. The remaining two, one closed above 715°C and one open above 690°C, provide emergency over- and under-temperature shutoff. Since the 690°C constacts are closed below 690°C, they would attempt to shut the system down. To avoid this, the wire from this switch is routed through normally open contacts on the startup-shutoff relay K7 on Figure 2-60, before going to the emergency stop relay K2 in Figure 2-59. The wire from the over-temperature switch goes directly to relay K2.

At the end of the lever, where the motion multiplication is greatest, there are two vanes or shutters. These are used to interrupt light beams to achieve proportional temperature control. In Figure 2-62, the light beams are perpendicular to the paper. At the center of this figure, the sensors are shown in schematic form with the light beams into the plane of the paper. For the purposes in this discussion, it is sufficient to say that the fuel supplied to the partial oxidizer reactor is programmed as a function of fuel cell output current so that it should supply the fuel cell's needs and maintain the furnace temperature at 700°C. Due to error in the fuel program, changing loads, and ambient conditions, the furnace either will not receive enough heat or will try to overheat. The fuel rate will never be turned down from the programmed value. If the furnace tries to overheat, the upper shutter (Figure 2-62) will start to move out of the light beam. This will allow light to enter the Cds photoconductive cell, thus lowering its resistance. This cell provides the control signal for the duty cycle motor control shown in Figure 2-63. As more light strikes the Cds cell, the blower motor runs faster, blowing more air through the furnace heat exchanger, thus keeping the temperature down.

If the furnace tends to cool down, the lower shutter admits light to the lower Cds cell, lowering its resistance. This provides a fuel turn up signal to the fuel throttling subsystem. There is one more function that the temperature control subsystem must perform. It must shut off the startup subsystem. Across the furnace heat exchanger blowermotor, there is a diode in series with a parallel combination of resistor and capacitor. This is a peak detector that will charge up to the full auxiliary power bus voltage the first time the above blower motor is called upon to operate. This biases the transistor "on", thus furnishing current to the startup subsystem shutoff relay K7 in Figure 2-60. K7 uses control power to seal itself in, thereby locking out the startup subsystem for the remainder of this cycle of operation of the power plant.

The duty cycle motor control is highly desirable for controlling dc motors in fuel cell power plants, since it will give full-off to essentially full-on control with very little wasted power. This is done by "keying" full voltage to the motor in pulse form, with a constant repetition rate and a duty cycle variable from 0 percent to 100 percent. Unijunction transistor Q1,

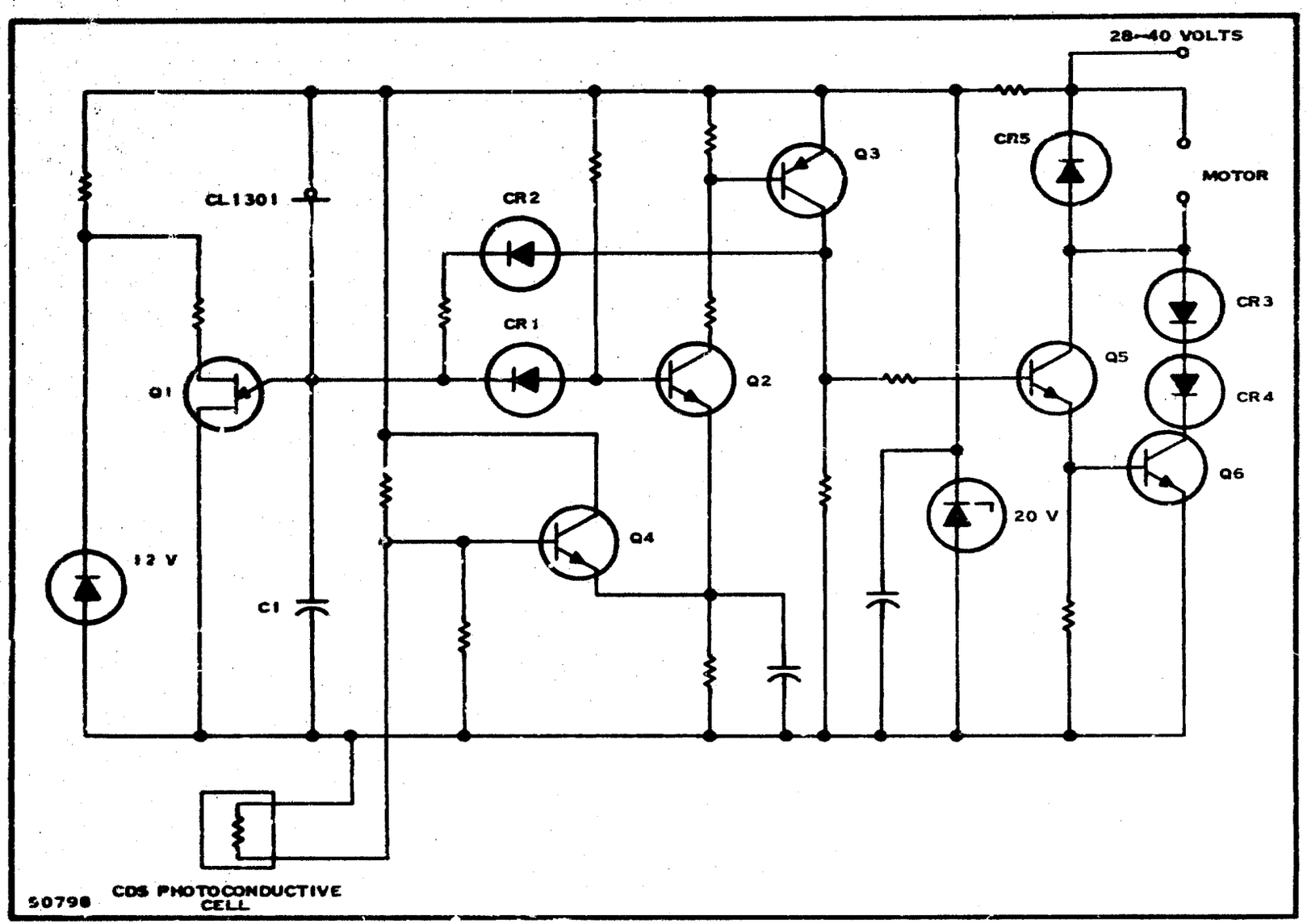

Figure 2-63. Duty Cycle Motor Control

capacitor C1 and the constant current diode CL1301 generator a linear sawtooth at the repetition rate desired. Transistors Q2 and Q3 and their associated components form a two-stage saturating amplifier. This amplifier "clips" a portion of the sawtooth and squares it into a rectangular pulse. Transistor Q4 is controlled by the photoconductive cell. It acts as an emitter-follower to set the "clip" level. Transistors Q5 and Q6 "key" the current into the motor. Even the turn-on base current for transistor Q6 is not wasted since it is also drawn through the motor. This basic circuit will be used in several other places in the control system to control other blowers.

Texas Instruments electrochemists have determined that the theoretical fuel input versus output current for a fuel cell power plant can be approximated by a curve consisting of two straight line segments as shown in Figure 2-64. In Figure 2-65, we show a circuit for generating such a fuel command curve. Total fuel cell output current is sensed by using the voltage drop across a 50-millivolt ammeter shunt. This shunt will be so sized that 50 millivolts will be obtained when the fuel cell is delivering full rated current. This voltage is amplified by transistor Q1. Transistors Q2 and Q3 form a Darlington pair to provide high input resistance and low output resistance. The output of this Darlington pair is applied to transistors Q4, Q6, and Q8. Transistors Q4 and Q5 constitute the overcurrent sensing circuit. Q5 acts as an emitter-follower to set the voltage on the emitter of Q4 to some value below +20 volts. When rated current is exceeded, the base of Q4 goes negative with respect to its emitter, thus turning it "on". Its collector current is drawn through the overcurrent relay K16 (Figure 2-66), thus disconnecting the external load. Transistors Q6 and Q7 are used to form the first straight line segment of the command curve. Potentiometer R2 sets the starting point for this segment. Since, even with no output current, some fuel would be required to keep the furnace up to temperature, the starting point is set to the left of the zero current point. This control can be used to compensate for varying ambient temperatures. R3 sets the gain of Q6. Transistor Q6 draws its collector current through RL, thus generating a command voltage. The gain of Q6 controls the slope of this line segment. Transistors Q8 and Q9 generate the second straight line portion of the command curve. R4 controls the starting point and R5 controls the slope. Since the collector current of transistors is practically independent of collector voltage, these currents can be summed in RL. Transistors Q10 and Q11 provide the fuel turn-up function. If the furnace temperature tends to decrease, the temperature controller supplies a positive signal to Q10. This turns Q11 "on" and it supplied current to RL, thus giving a fuel turn-up command. The gain or rate of turn-up is controlled by the potientiometer in the base of Q11.

To actually accomplish the fuel control, mechanical shaft angle that is proportional to the programmed fuel command voltage will be generated. This is accomplished by a simple followup servo, as shown in Figure 2-67. A

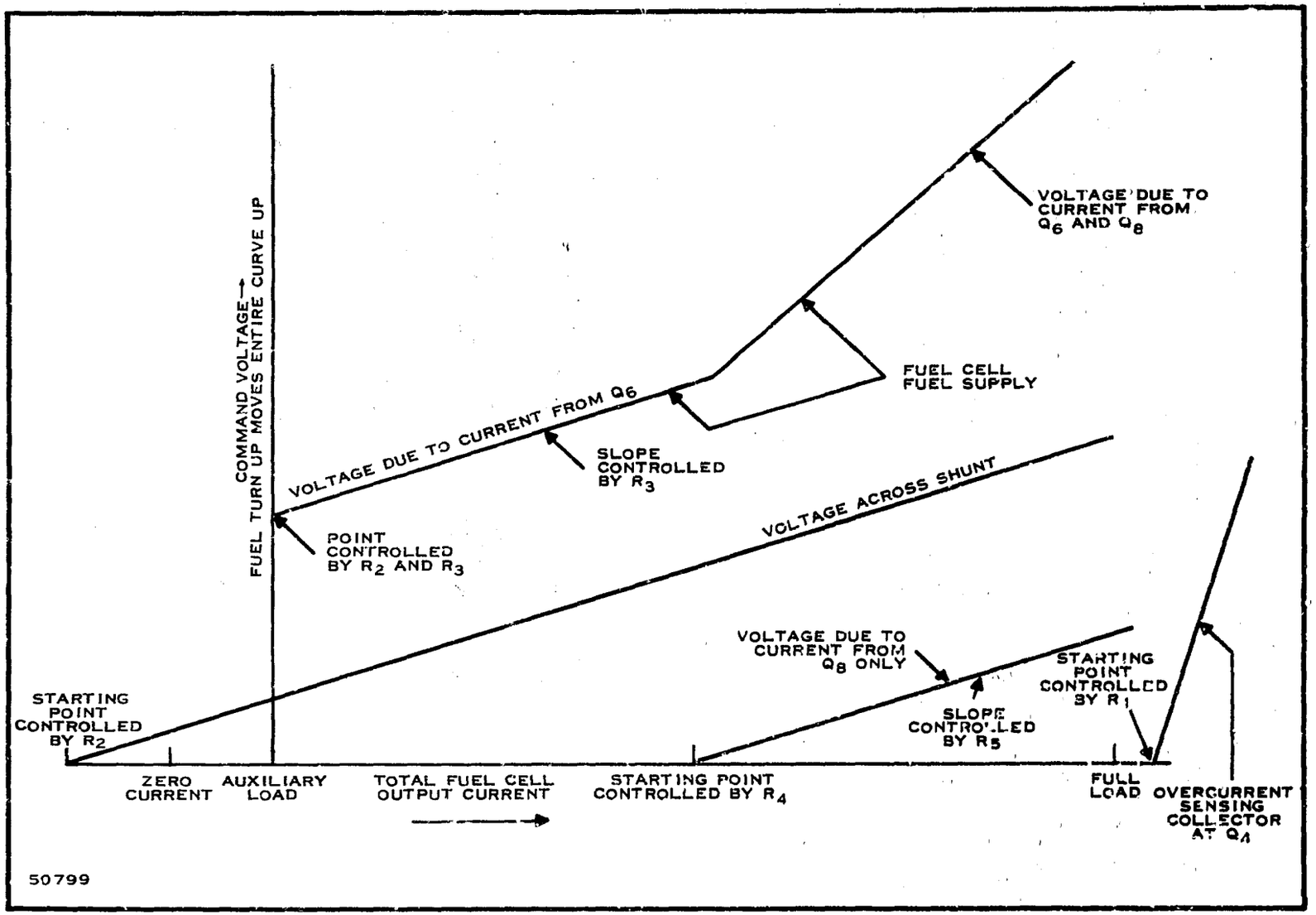

Figure 2-64. Fuel Program Versus Fuel Cell Output Current

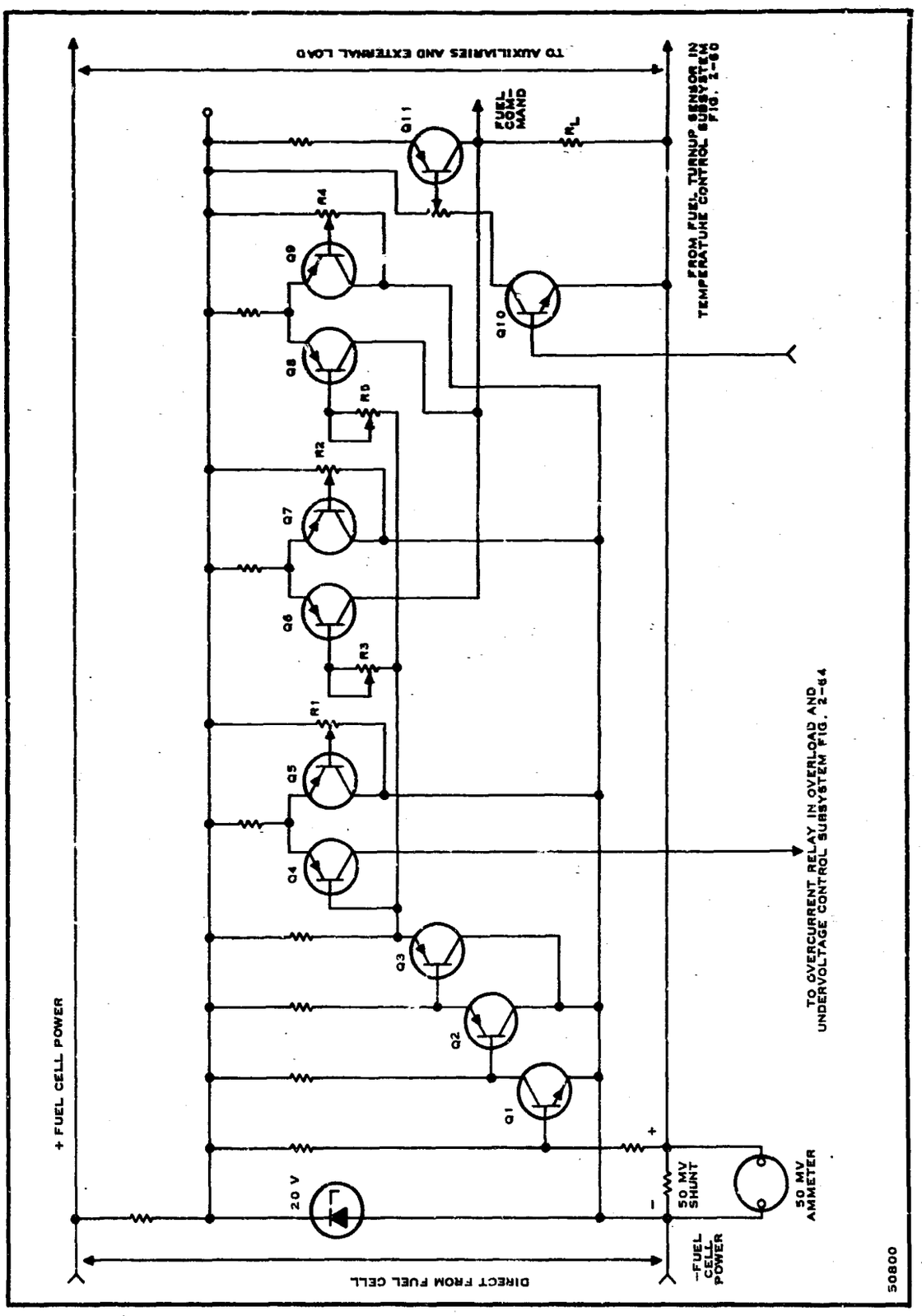

Figure 2-65. Fuel Program Generator

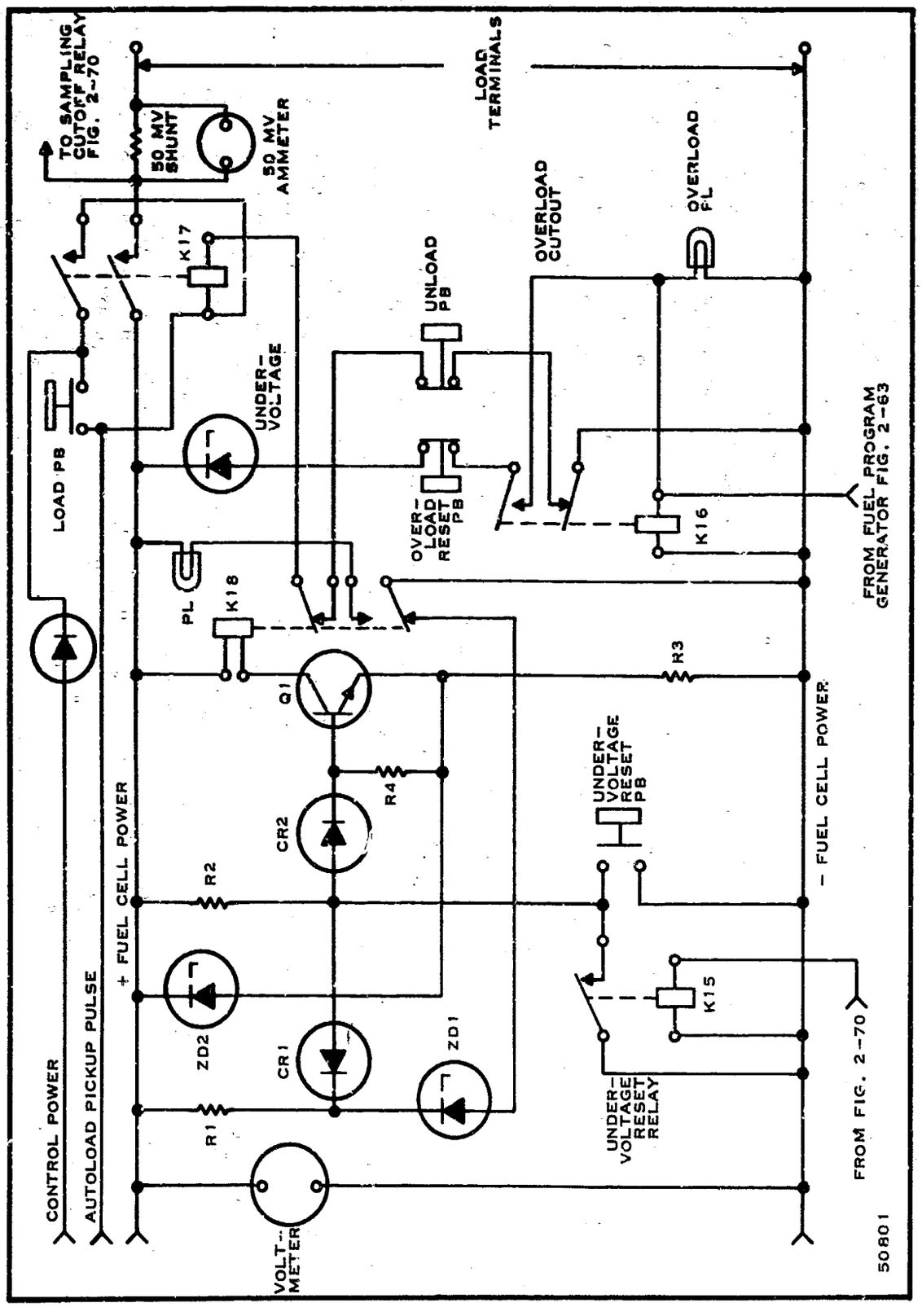

Figure 2-66. Overload and Undervoltage Cutout and Load Contactor

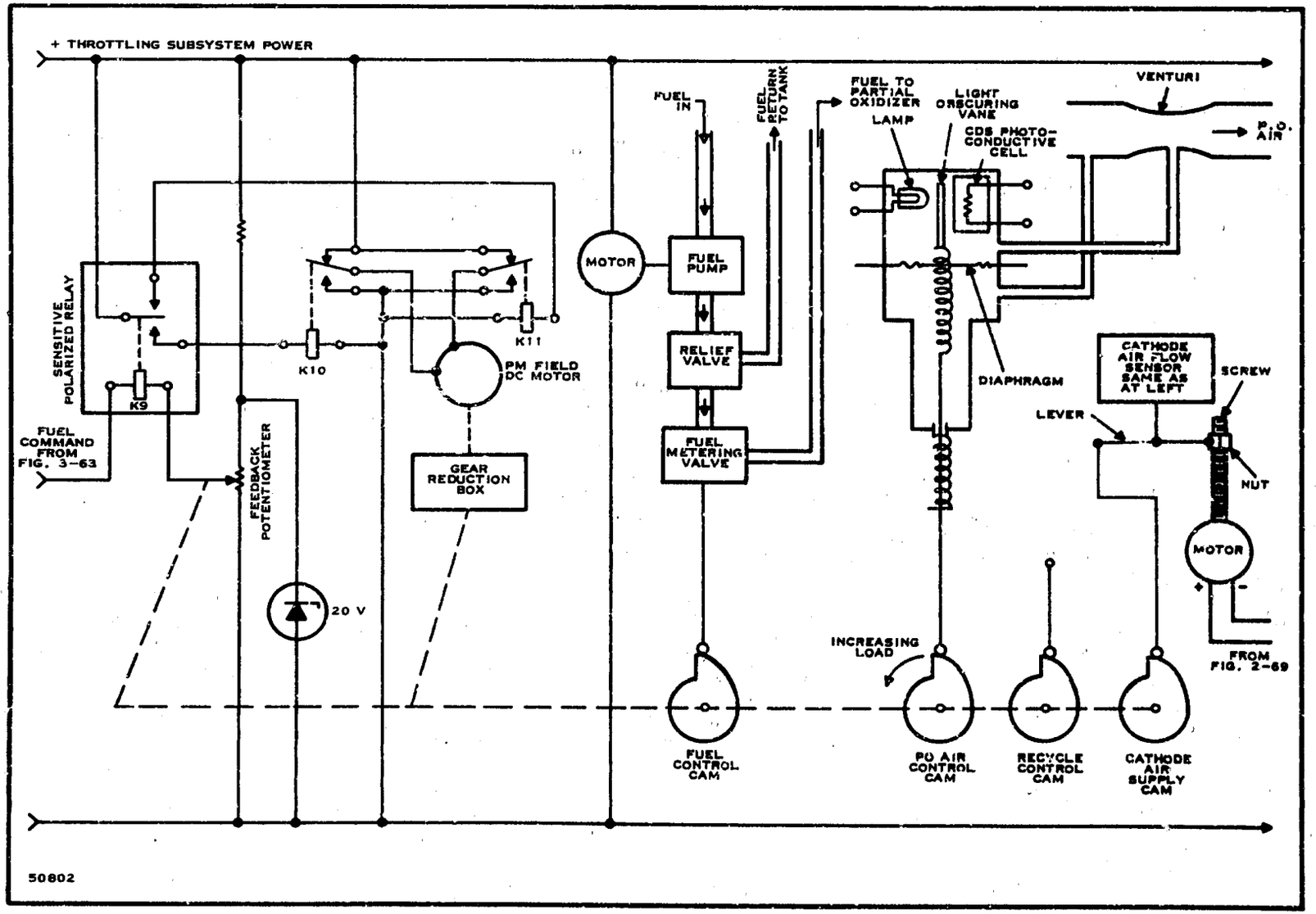

Figure 2-67. Fuel Throttling System

sensitive polarized relay K9, whose coil is connected between the command voltage point and the wiper of the feedback potentiometer, provides error sensing. This relay has form K contacts (both normally open). The polarized relay controls relays K10 and K11. These relays can drive the motor in either direction and in addition provide dynamic breaking by shorting the armature. The motor drives the fuel control shaft through reduction gears at a speed of about 6 revolutions per minute.

Liquid fuel is supplied by a motor-driven pump, followed by relief valve, so that constant fuel pressure is applied to the fuel metering valve. The fuel metering valve will consist of an orifice and a long tapered needle such as is used in some automotive carburetors. The needle need not be contoured since the cam can be cut to the correct rise from empirical measurements. The changeover from combat gasoline to CITE fuel will be made by lifting the cam follower and sliding the appropriate cam into place. Three air flow controls are required: partial oxidizer, cathode air, and recycle. All of these will use the same basic metering technique as shown in detail for the partially oxidized air. Air flow is measured by a venturi connected to a diaphram differential pressure sensor. The diaphram spring is tensioned by the partial-oxidation air control cam. Position of the diaphram is sensed by a lamp and Cds photoconductive cell. This cell controls a duty cycle motor control as shown in Figure 2-63. This control drives the partial-oxidation air blower motor. The recycle blower and cathode air supply blower are controlled in the same way. Since the cathode air supply will have to be adjusted to achieve the correct CO_2 to O_2 ratio in the furnace atmosphere, an additional function is added to this control. The cam follower is coupled to the diaphram unit through a lever. The "fixed" end of this lever is connected to a nut on a motor-driven screw. This will be covered in more detail in the section on furnace atmosphere control.

The partial-oxidation reactor temperature control is shown in Figure 2-68. Partial-oxidation reactor temperature will be sensed by a thermocouple (rod and tube type sensor is not applicable because of its bulk). Thermocouple output will be supplied to one side of a differential amplifier. The other input will be a reference voltage in series with a compensating thermocouple. A sensitive polarized relay will be connected between the collectors. This relay will actuate motor control relays similar to K10 and K11 of Figure 2-67. To avoid shunting and overcontrol, the motor will be geared down so that control time is greater than reactor response time. The motor drives an air proportioning valve which varies the fraction of air bypassing the preheater.

The cathodes of a molten carbonate fuel cell require CO_2 and O_2 in the ratio of two parts of CO_2 to one part O_2. It has been shown that it is highly desirable that the furnace atmosphere contain CO_2 and O_2 in the above ratio.

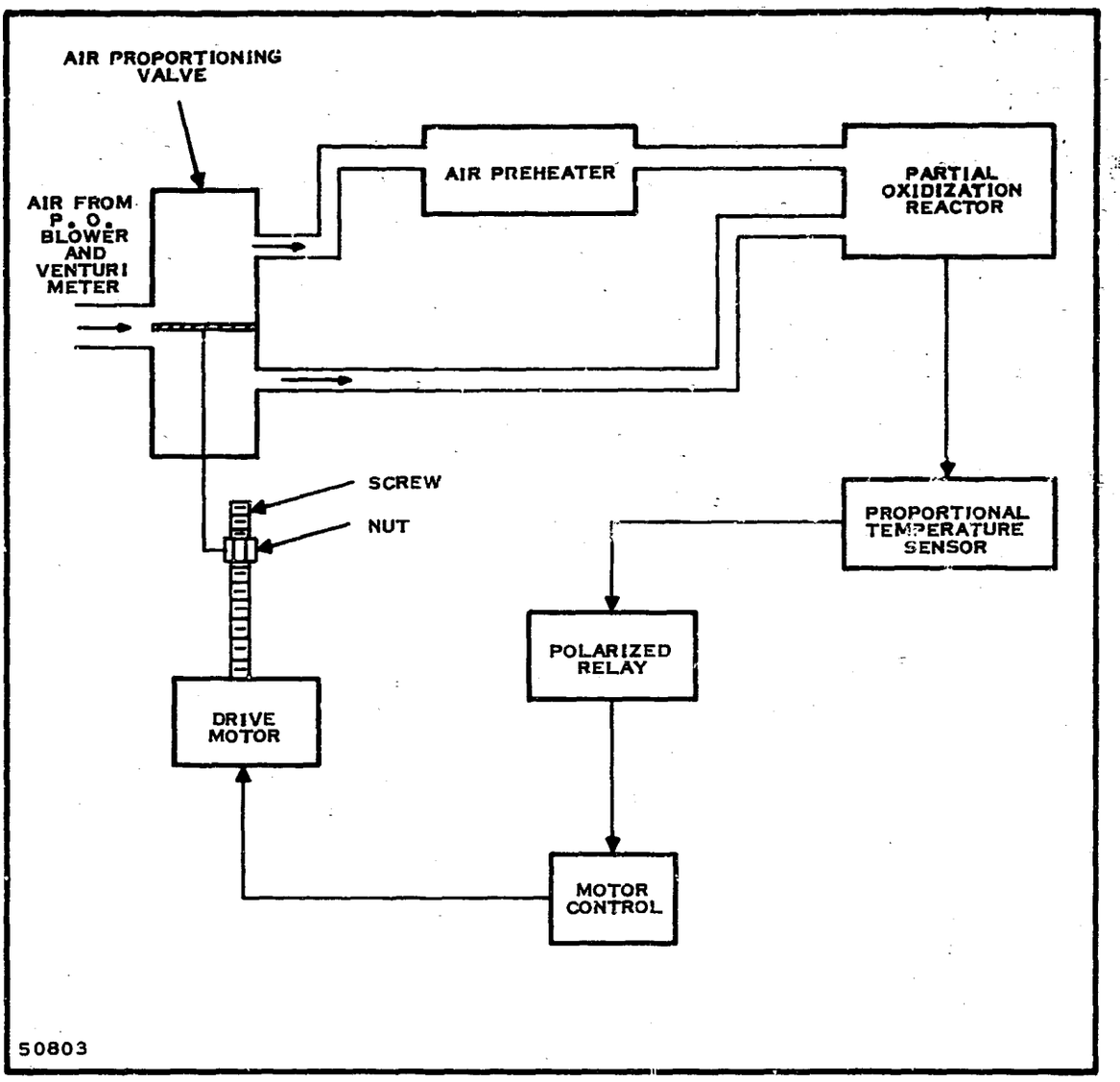

Figure 2-68. Partial-Oxidation Reactor Temperature Control

For the purpose of this discussion, we will assume that the fuel input is constant and that all the fuel is oxidized either in the fuel cells or in the burnoff flame. If we assume that only the exact stoichiometric requirement of air is present, we have the following reaction:

$$CH_2 + 1\text{-}1/2\ O_2 + 6N_2 \text{ ---> } CO_2 + H_2O + 6N_2 \ .$$

Total
8

This gives 12.5 percent CO_2 and 0 percent O_2.

If we increase the air to 1-1/3 times stoichiometric ($2O_2 + 8N_2$) we have

$$CH_2 + 2O_2 + 8N_2 \text{ ---> } CO_2 + H_2O + 1/2O_2 + 8N_2 \ . \qquad \text{Total } 10.5$$

This gives 9.5 percent CO_2 and 4.75 percent O_2, which is the desired ratio.

If we increase the air to 1-2/3 stoichiometric ($2\text{-}1/2O_2 + 10N_2$) we have:

$$CH_2 + 2\text{-}1/2O_2 + 10N_2 \text{ ---> } CO_2 + H_2O + O_2 + 10N_2 \ . \qquad 13$$

This gives 7.7 percent CO_2 and 7.7 percent O_2.

Thus, if we can maintain a 9.5 percent concentration of CO_2 in the furnace atmosphere we will get our required CO_2 to O_2 ratio. To do this, we plan to sense the CO_2 concentration and develop an error signal that will control the cathode air supply blower. A suitable technique for sensing the CO_2 concentration is that of the Luft type infrared analyzer. An instrument of this type is sold by Mine Safety Appliance Company. This instrument, while suitable for laboratory work really is not suitable for use in a fuel cell power plant. An adaptation of this technique suitable for power plant use is described below.

The physical principle used is that of selective absorption of infrared radiation. Since the furnace atmosphere contains CO_2, H_2O, O_2, and N_2, it is necessary to find a wavelength where CO_2 has a high absorption and the other constituents have low absorption. A wavelength of 4.3 microns is suitable, since CO_2 absorbs it strongly and H_2O, O_2, and N_2 have very little absorption.

A schematic of the CO_2 monitor is shown in Figure 2-69. The two infrared sources consist of coils of nichrome wire heated to about 1000°C (something like an automobile cigarette lighter element). The motor-driven shutter (shown in Figure 2-70) permits the infrared radiation to pass alternately through the reference cell and the sample cell. A sample of the furnace atmosphere is cooled and passed through the sample cell. The reference cell will be filled with 9.5 percent CO_2 and 90.5 percent N_2. The cells are tubes about 1-1/2 inches in diameter and 8 inches long with suitable 4.3-μ transmitting windows at either end. The radiation passing through the two cells is directed into the detector cell. This detector cell is a cavity filled with pure CO_2. It has a 4.3-μ transmitting window in one face, through which the radiation can enter, and a flexible metallic membrane in one wall. To describe

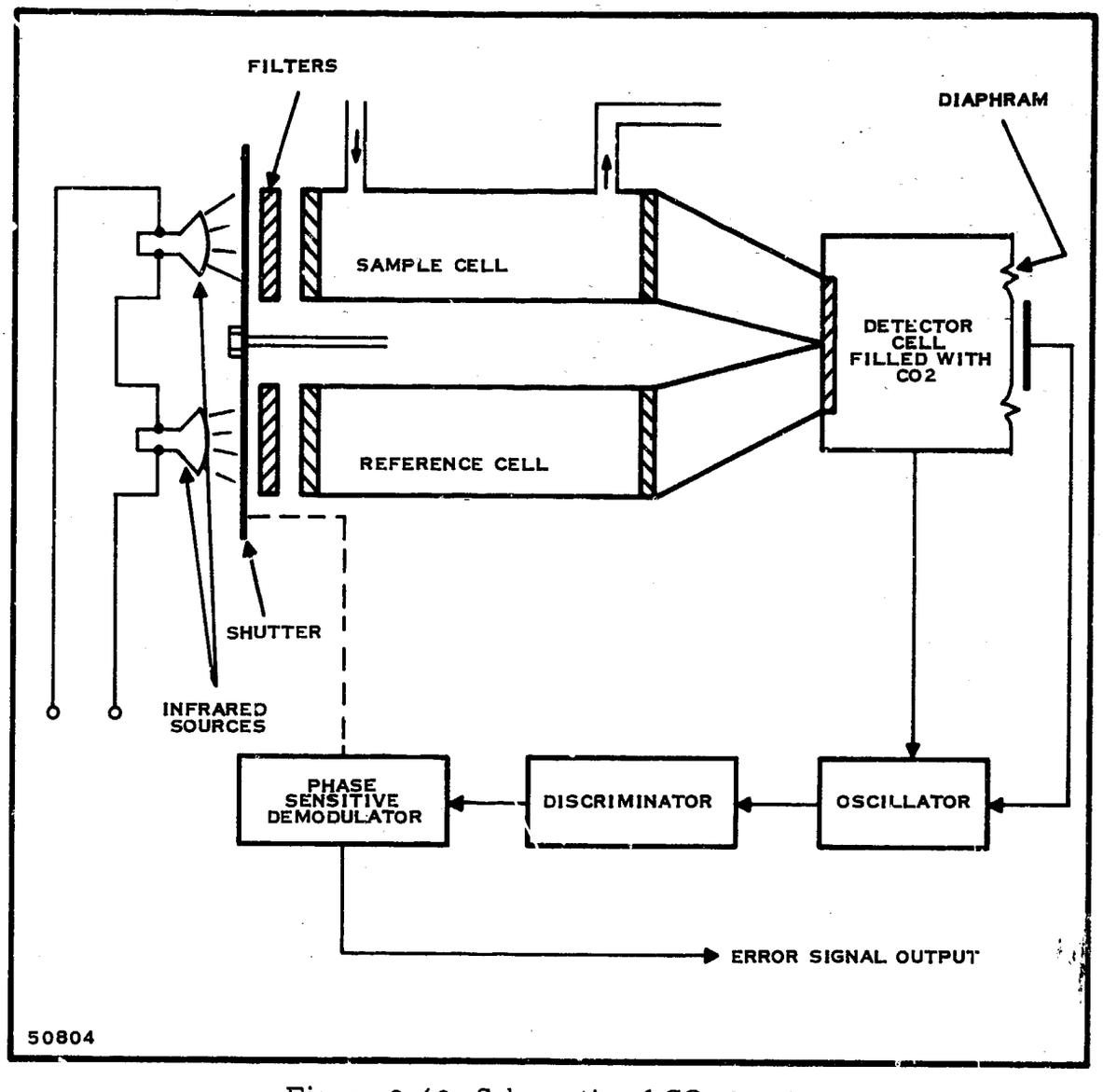

Figure 2-69. Schematic of CO_2 Monitor

this technique, one must assume that the concentration of CO_2 in the sample cell is less than in the reference cell. Therefore, the sample cell will have less absorption of the 4.3-μ radiation than the reference cell. The intensity of radiation entering the detector cell, therefore, fluctuates in synchronism with the shutter rotation. In the detector cell, the 4.3-μ radiation is totally absorbed and, consequently, heats the gas. The heated gas expands and pushes the diaphram outward. Thus, as the intensity of the 4.3-μ radiation fluctuates, the diaphram moves in and out.

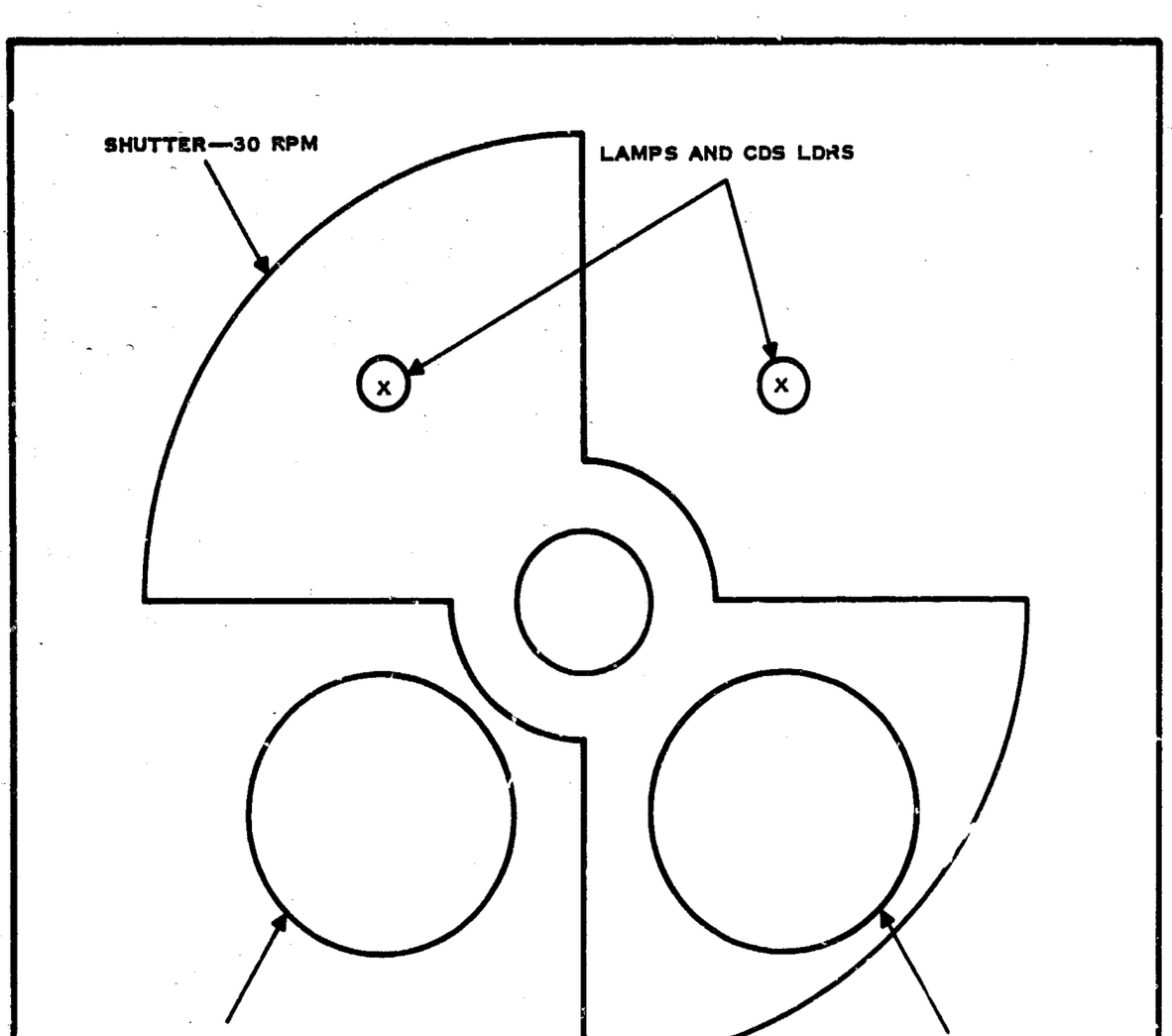

Figure 2-70. Shutter for CO_2 Monitor

If the concentration of CO_2 in the sample cell is more than in the reference cell, the phase of the diaphram movement will be opposite to that above. It only remains to sense the diaphram motion and compare it to the shutter rotation.

In Figure 2-69, we show how this can be accomplished. The diaphram is used as one plate of a condenser microphone. A possible circuit is shown in Figure 2-71. The condenser microphone is connected across the coil of an oscillator. As the diaphram moves, the oscillator frequency will be varied. This frequency variation is detected by a frequency discriminator. This frequency discriminator has two outputs of opposite polarity. In order to get

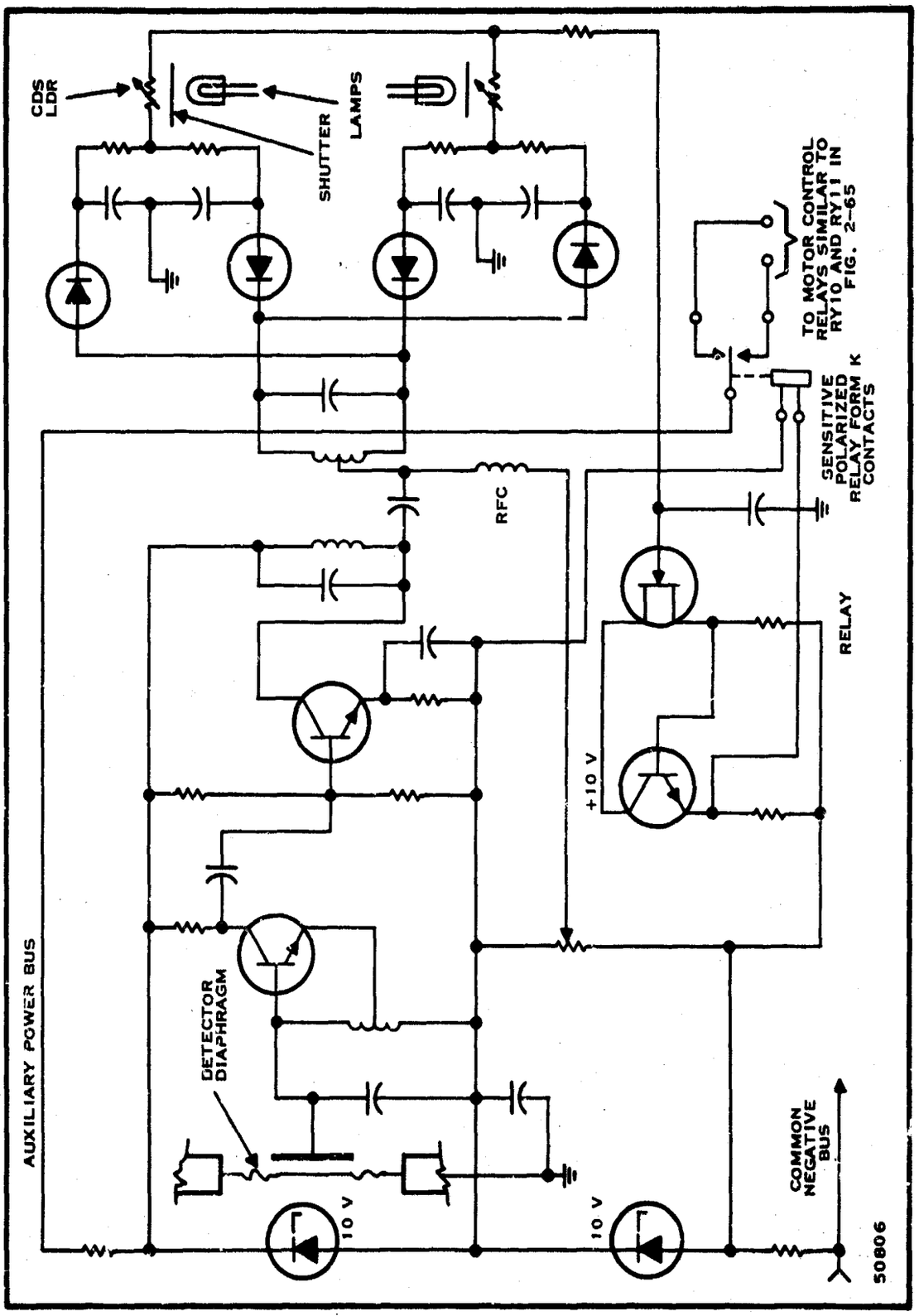

Figure 2-71. Circuit of CO_2 Monitor

a dc error signal, the fluctuating outputs of the discriminator must be synchronously demodulated. This is easily accomplished by using two lamps and two cadmium sulfide photo cells. These are placed so that the shutter alternately interrupts the light from the lamps to the Cds cells. The output from these goes to a long time constant filter and an output amplifier.

In the actual operation of a fuel cell power plant, the primary control signal for the cathode air blower will come from the throttling control system and will be proportional to the fuel input. The CO_2 monitor output operates a sensitive polarized relay. This relay will actuate two motor control relays similar to K10 and K11 in Figure 2-67. The motor will vary the "fixed" end of the combining lever shown in Figure 2-67. The gear ratio will be such that the drive rate is slower than the furnace and monitor response rate.

When used in a fuel cell power plant, a small continuous sample of the furnace atmosphere will be drawn off and cooled to approximately 150°F before passing through the sample cell.

The output verification and automatic load pickup circuit is shown in Figure 2-72. This circuit works in conjunction with the overload undervoltage cut out and load contactor circuit shown in Figure 2-66. The technique used is somewhat similar to that used in the auxiliary power verification circuit. It is unthinkable, however, to place a 15-kilowatt output verifying load across the fuel cell output on a continuous basis. Therefore, a technique of sampling the fuel cell output has been adopted.

When the furnace first reaches 700°C, a signal is received from the voltage sensor (Figure 2-61) which is applied to the sampling keyer. The sampling keyer consists of a 1-revolution per minute dc timing motor, a cam and a snap action switch. This actuates relay K14 for one second every minute. When K14 operates, it does two things; it connects the fuel cell output to the power verifying resistors and it connects C_1 to the fuel cell output. The output verifying resistors can be switched to preset loads of 2.5, 5, 10, and 15 kilowatts. When this load is applied, the undervoltage sensor will latch up if the voltage falls below its set point. This breaks the hold circuit of contactor K17, thus preventing connection to the external load. The undervoltage sensor is similar to the voltage sensor of Figure 2-61, with the zener diodes and resistors interchanged, thus making it operate the relay K18 when an undervoltage condition exists.

When K14 releases, it does three things; it disconnects the output sampling load, applies voltage to the undervoltage reset delay circuit, and connects C_1 to the top end of the coil of the load contactor K17.

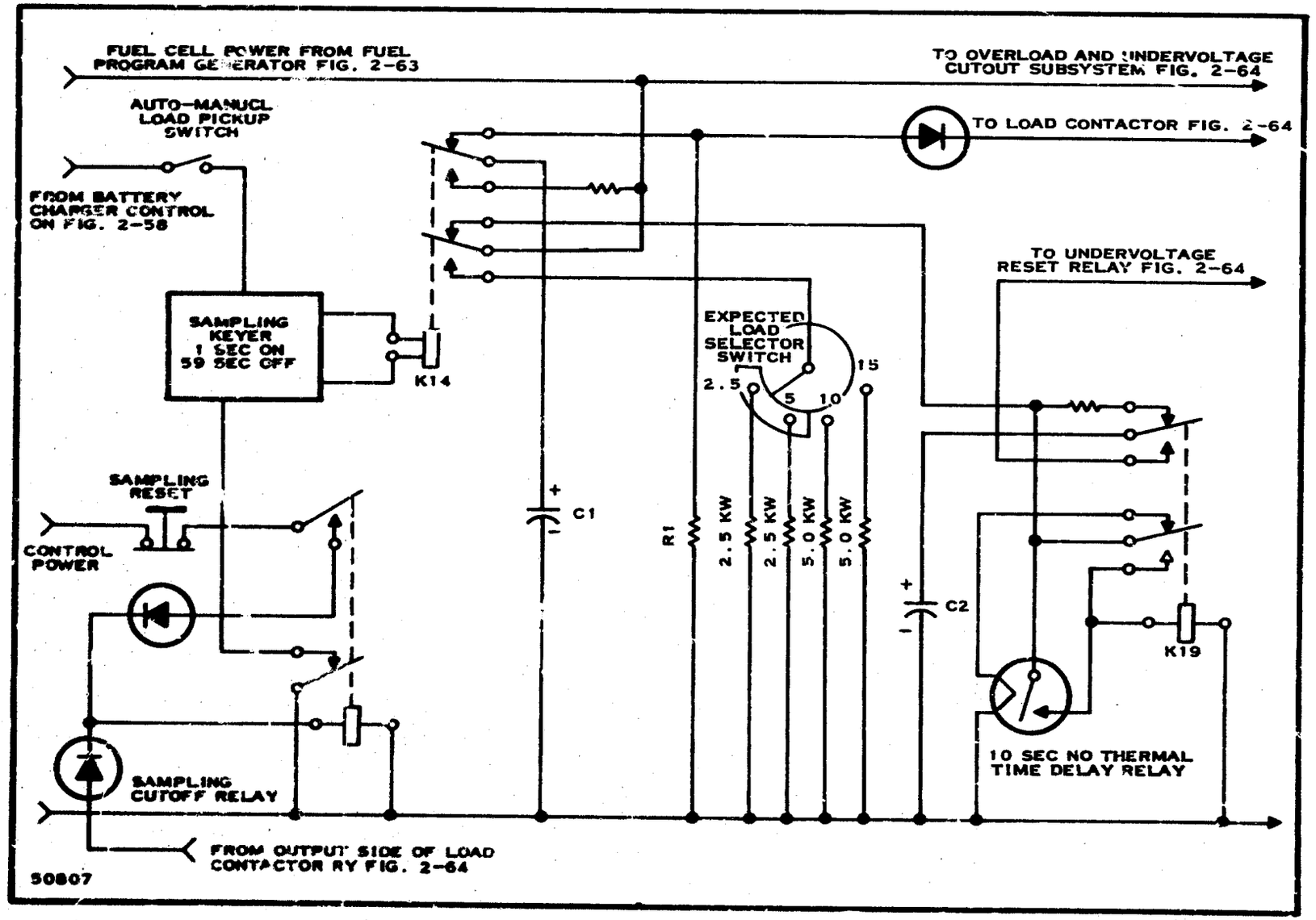

Figure 2-72. Output Verification and Automatic Load Pickup Circuit

There are two things that could happen. If the undervoltage sensor did not trip, the holding circuit would be complete and K17 would operate and seal itself in, thus connecting the external load. If the undervoltage sensor did latch up, the holding circuit for K17 would be incomplete and the charge on C_1 would be dissipated in R_1. To prepare for the next sampling, the undervoltage cutout circuit must be reset. Relay K19 and the 10-second time delay provide a 10-second delayed reset pulse to K15, the undervoltage reset relay, in Figure 2-66. The 10-second delay is to make certain that all the charge has been drained from C_1 by R_1. The circuit is now ready for another sampling interval. If the external load has successfully picked up, voltage from the output side of K17 is applied to relay K13 (Figure 2-72). This relay latches down and thereby stops the sampling process.

Some of the functions of Figure 2-66 have already been covered. There are pushbottons for manually picking and disconnecting the external load and to reset the undervoltage and overcurrent cutouts. It also contains the external load voltmeter and ammeter. There are pilot lights to indicate whether the load was dropped due to undervoltage or overcurrent. It is to be noted that the load contactor K17 holding current is supplied from the control power bus so that when the plant is shutdown, K17 will drop out.

A possible startup battery charging circuit is shown in Figure 2-73. It is imperative that the charger be capable of rapidly recharging the battery and that it have very low internal power loss. It is conceivable that under heavy load the fuel cell output voltage would be too low to provide a fast charge rate. If this proves to be so, we can use a silicon controlled rectifier (SCR) inverter to provide an add-on voltage. The output of this inverter is full-wave rectified by a bridge circuit in series with the fuel cell output plus voltage. The square-wave output of the inverter is a distinct advantage in this application. Charging current regulation is accomplished by a switching type regulator. The SCR'S TY1 and TY2 are fired together. TY1 delivers current to the battery. C_1 is charged through TY2 and L_1 to approximately twice the supply voltage. To terminate the current pulse, SCR TY3 is fired. This momentarily back-biases TY1, thus shutting it off. L_2 permits the voltage on the cathode of TY1 to be back-biased. The details of the SCR firing controller have not been worked out, since they depend upon the type of battery to be used. However, several things can be pointed out. If the inverter boost is not needed, it can be shut off. The bridge diodes will carry the charging current. Since the charging occurs in pulses, it is possible, by a gating technique, to sense the open circuit battery voltage and use this for charge control.

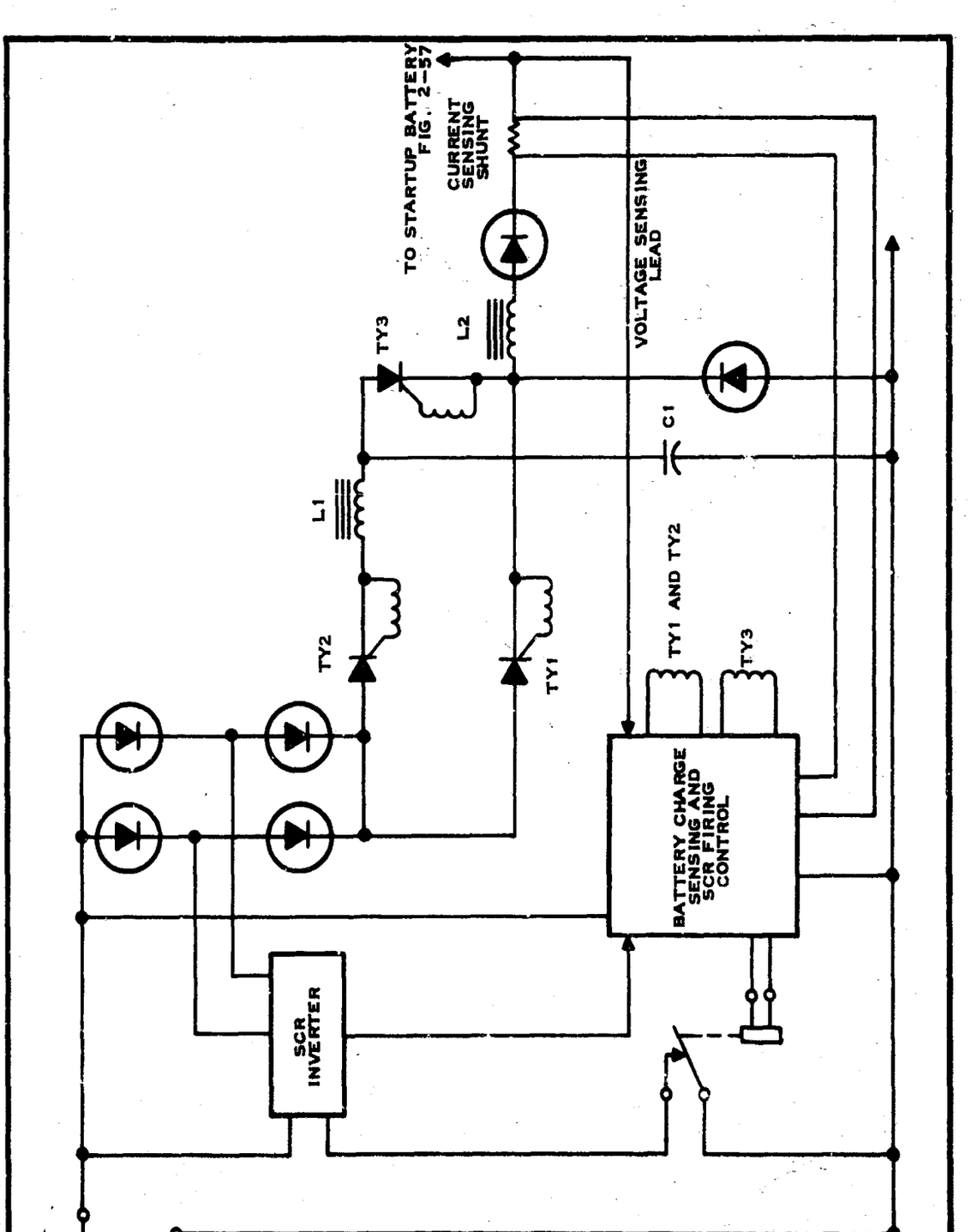

Figure 2-73. Battery Charger

SECTION III

15-KILOWATT POWER PLANT DESIGN

A. GENERAL

A pictorial view of the 15-kilowatt system is given in Figure 3-1. It will be noted that the inverter is not included, since its size and shape are not yet established. The system consists of four parts:

The insulated enclosure, containing the fuel cells, fuel preparation unit, and other hot components

The fan drives, mounted on top of the enclosure

The panel section, containing the auxiliaries, control, etc

Supports, skids, lifting eyes, and tie-downs.

The interior of the enclosure is shown in Figures 3-2 and 3-3. The arrangement of the auxiliaries behind the control panel is depicted in Figure 3-4.

The insulated enclosure is 46 by 42 by 45 inches, or 50 cubic feet. The fan drives and panel section add 1 and 4 cubic feet, respectively. The total weight of the entire package is estimated at 2900 pounds.

At rated load, the efficiency (into the inverter) is expected to be 28 percent. The maximum efficiency will be 33 percent at 57 percent of rated load.

Texas Instruments considers this design to be realistic. It is ambitious; however, considerable development work is needed if it is to succeed. Above all else, attainment of the stipulated performance and lifetime depends upon the fuel cell itself. Discussion of that matter was presented earlier in this report.

B. DESCRIPTION OF SUBSYSTEMS

1. Fuel Cell Stack

This design is based on an average cell performance of 30 watts per square foot at rated load. (Actually, it works out to 28 watts per square foot, since the number of cells must be the product of convenient integers.) It is assumed that the voltage varies linearly from 1.0 volt at open circuit to 0.7 volt (average) at rated load.

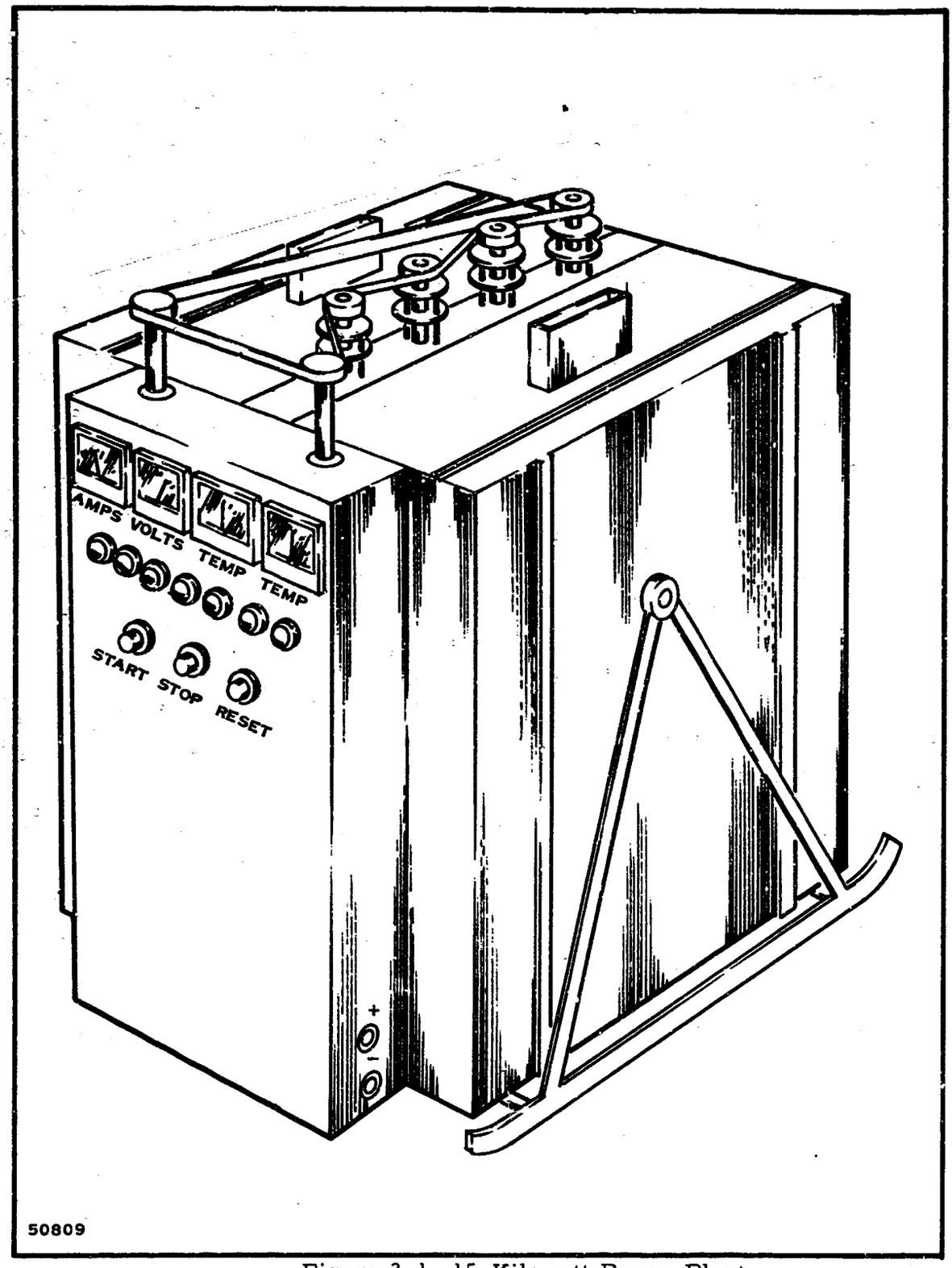

Figure 3-1. 15-Kilowatt Power Plant

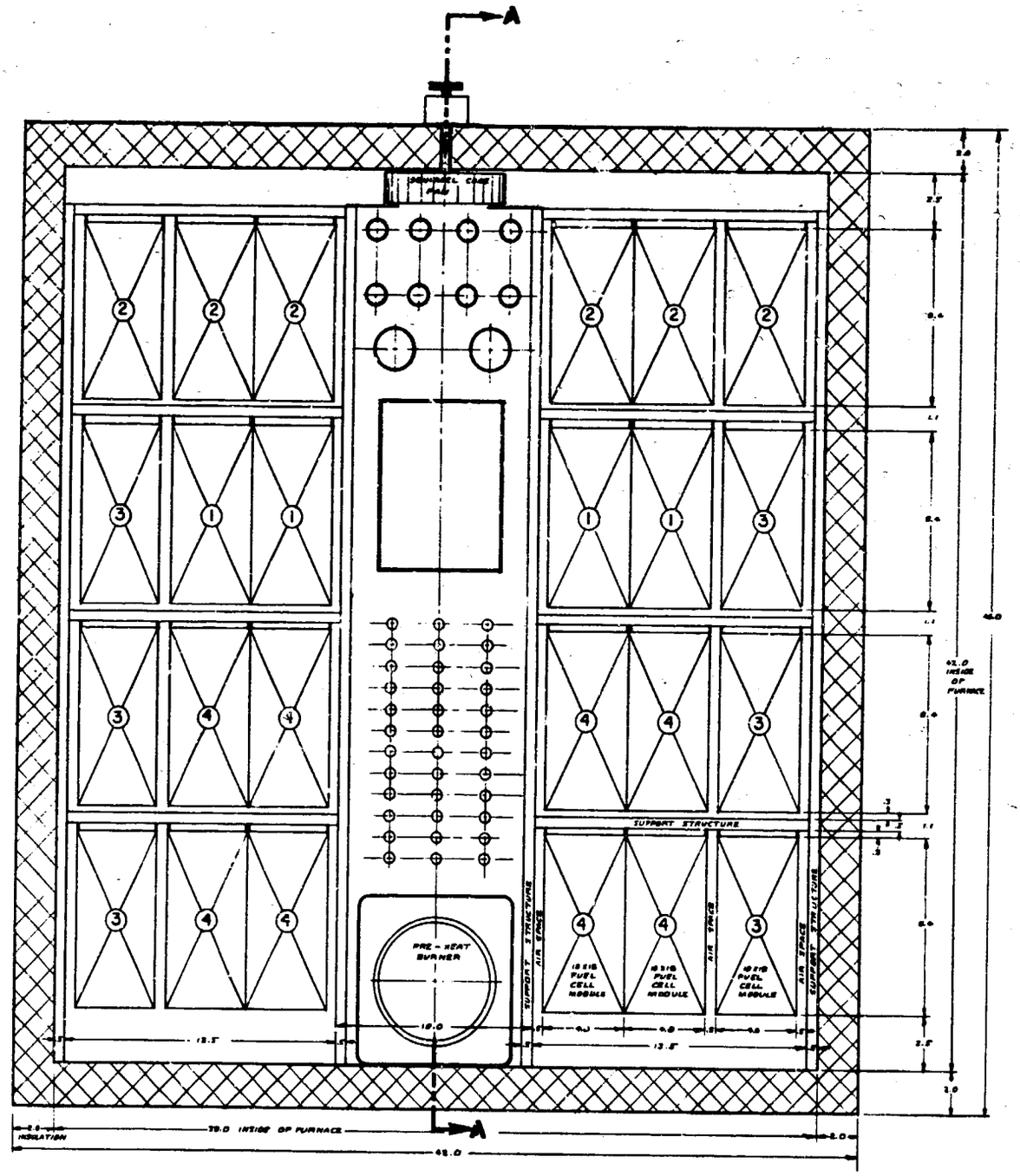

50810

TYPICAL CROSS SECTION
15 KW SYSTEM
HALF SIZE

Figure 3-2. Front Section of Enclosure

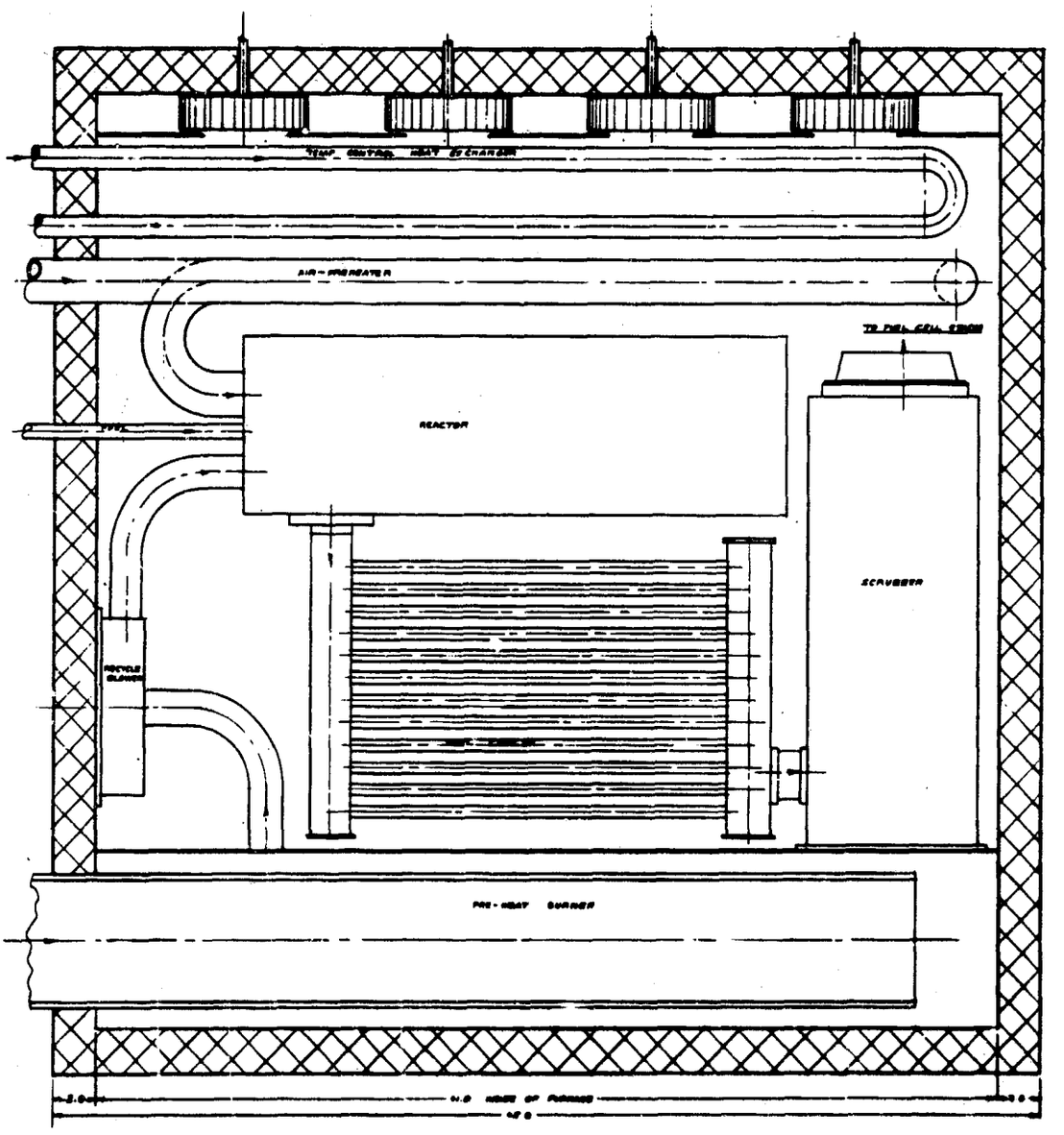

50811

SECTION A-A

Figure 3-3. Side Section of Enclosure

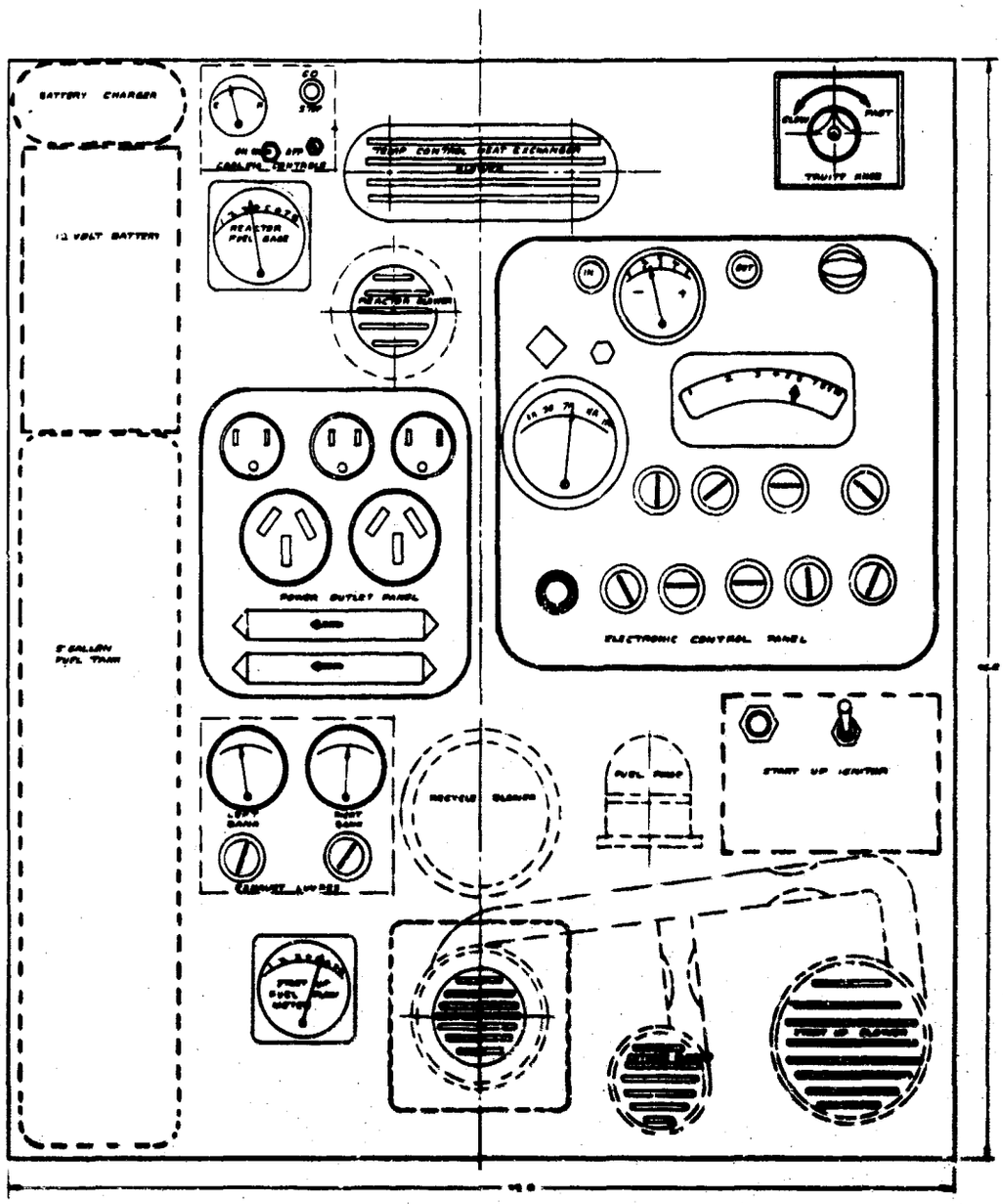

50812

Figure 3-4. Auxiliary Arrangement—Front View

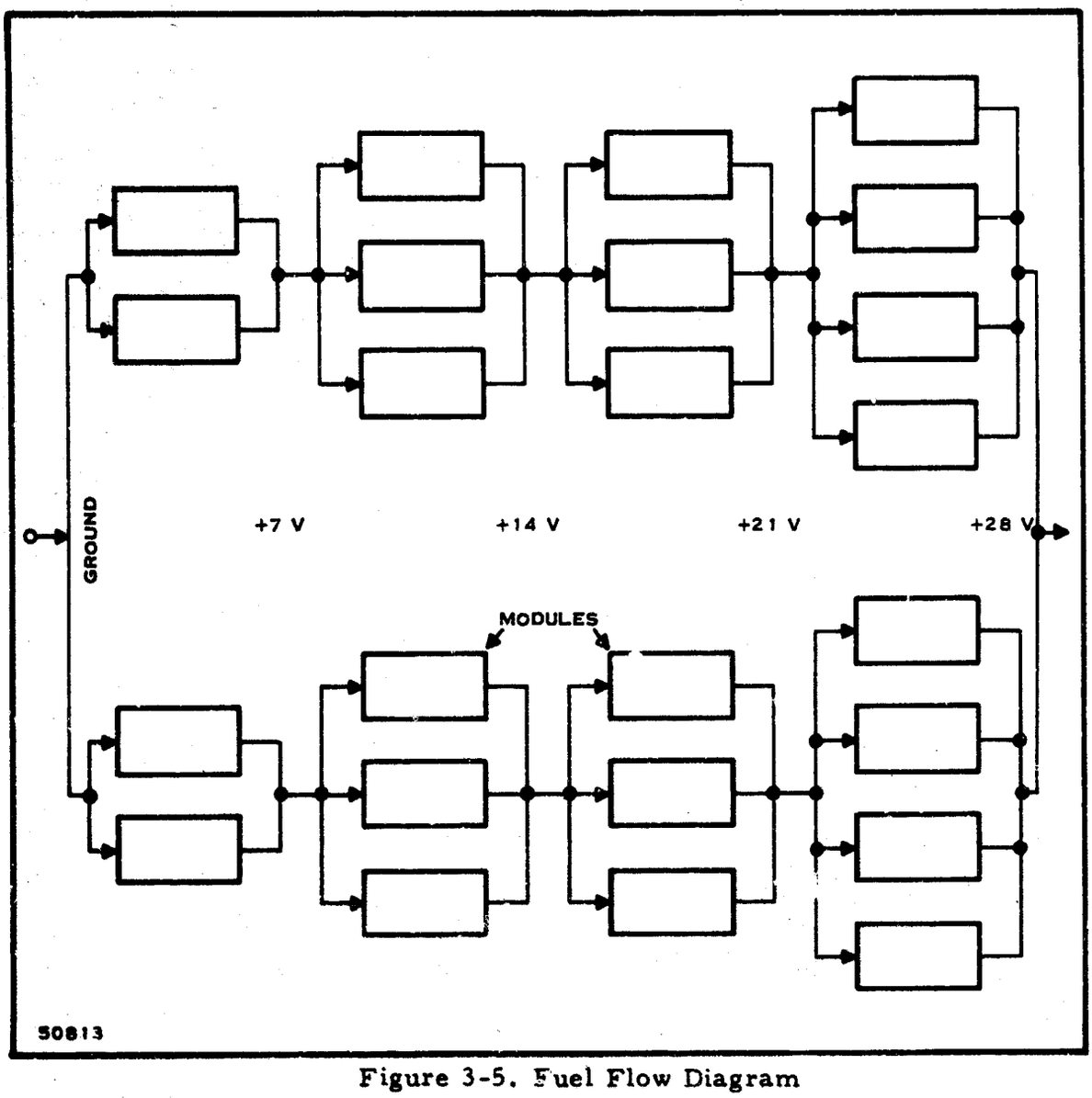

Figure 3-5. Fuel Flow Diagram

The individual cell will resemble those discussed earlier, except that it will be 8 inches high and 3 inches long (nominal). Modules will be 10 cells in series and 18 cells in parallel. Twenty-four such modules will be used. The modules will be grouped in two stacks as shown in Figure 3-2.

Fuel will be conveyed through the modules as shown in Figure 3-5. This arrangement provides 40 cells in series, with the number of cells in parallel increasing as the fuel is consumed. Thus, the cells which receive poorer fuel are permitted to operate at a lower current density. Space is allowed for the manifolds needed for this. The manifolds will connect to headers, affixed to each end of the modules, designed so that all modules will be identical and interchangeable.

It is very desirable that the connection between header and manifold provide electrical contact as well as a gas seal. This will probably require a connector designed and made expressly for the purpose. Current leads will be required to connect the module ends to the terminals at the panel. These will be stainless-clad copper rods.

Means of supporting the modules will be incorporated into the individual cell, a feature not present in cells built previously. Each cell will have a tab which can be welded to a bar carrying two studs. These studs will fasten to, but be insulated from, a beam which will traverse the three modules in a horizontal row. The beams will fasten to the vertical structure.

Each 10 by 18 module will be 33.3 inches long, 8.5 inches high, and 4 inches thick. Allowances for headers, manifolds, isolation, supports, and cathode-side flow bring the space required for the entire stack to 42 inches high by 28 inches wide by 41 inches long.

The 10-inch space in the middle contains the other hot components. These include the partial oxidizer, preheater, fuel cooler, corrosive removal unit, startup burner, cooling heat exchanger, recycle blower, circulation fans, and temperature and composition sensors.

2. Fuel Preparation System

For the partial-oxidation reactor, vaporizer, corrosive removal unit, and recycle blower, design considerations for the 15-kilowatt unit have been discussed earlier in this report and will not be repeated here. The other significant items are the air blower, fuel pump, flower meters, and controls.

The air supply required is moderate in both quantity and pressure; one blower which is more than adequate is a garment ventilation unit made by Globe.* Fuel pumps of the type used on aircraft cabin heaters have been used in development work. They have performed quite satisfactorily. However, in the 15-kilowatt unit it is necessary to vary the fuel flow rate. To do this, it is easier to change the supply pressure automatically than the control valve. Therefore, a centrifugal or gear pump probably will be selected.

3. Cathode Composition System

This system consists of the cathode air supply blower, circulation fans, and appropriate baffles. The baffles are thin sheets of stainless steel which are attached to the module racks.

---

*Part number 19A1189

The circulation fans will be centrifugal design, 6-inches in diameter and 2-inches wide. Their operating speed will be 3000 revolutions per minute, during startup and at all loads. The fans will be driven by a motor and belt drive. Fans of this type were used in the 1-kilowatt module breadboard.

4. Temperature Control (Heat Rejection) System

This will consist of a sensor, probably a thermocouple, a heat exchanger of ample size to handle the requirements of full load, a blower, and a controller. The location of the components may be seen in Figure 3-2, 3-3, and 3-4. The controller and its relation to other functions will be discussed in connection with Controls and Operation.

5. Startup System

The design of a burner suitable for a 15-kilowatt system was covered earlier in this report.

The burner will discharge into a box 8 inches square and 41 inches long, the interior length of the enclosure. Holes in the top of the box will distribute the hot gases along the length. In flowing upward and through the fans, the burner gases become well mixed with the interior stream before passing through the module. Note (Figure 3-2) that the exhaust is taken from the circulating gas after it passes through the module.

A battery and charging control are required to provide auxiliary power during startup.

6. Enclosure

The insulation, on all six sides, will be 2 inches thick. The outer shell will be thin sheet metal, embossed for stiffness. The enclosure will not be a simple box with a single closure line, but will be composed of a number of removable panels. Screening to protect personnel from hot surfaces will be provided as required.

The weight of the components within the enclosure can be borne by the insulation, provided it is distributed. The bottom of the box must be supported, however, this will be done with a honeycomb-type structure. Shock mounts will connect this platform to the skid rails.

The auxiliaries will be mounted in a rack between the control panel and the enclosure. Lifting eyes and tie-downs will be incorporated into the skid structure.

7. Controls and Instruments

The control system must serve two principal functions:

a. Startup and shutdown of the power plant. This entails performing the required actions in proper sequence and at the correct time. Safety devices must be provided to initiate shutdown in the event of malfunction or hazard.

b. Varying the operating condition of the power plant according to the load. This includes controlling the fuel and air rates to the partial oxidizer, the spent fuel recycle, cathode air supply, and the temperature of the enclosure.

In this section, the required sensors and controllers will be described. Operation of the control system will be covered in a later section.

The following items are associated entirely with startup:

The burner fuel pump and solenoid valve

A flame sensor in the burner (This will be a light-sensitive resistor.)

A check valve in the burner air line, to prevent back flow after startup

A load-verifying resistor to determine that the auxiliaries can be run by internal power.

Other items are primarily for operational control, but are also used during the startup period. They are:

The main fuel pump, solenoid valve, and flow meter. The flow meter will be a pressure-drop device.

Flow meters for the partial-oxidizer air and spent fuel recycle. These will be orifice or venturi meters. The chief problem here is to locate or develop sensors for the small pressures.

A thermocouple to measure the temperature of the partial oxidizer.

For control of the cathode gas composition, either a flow meter or composition indicator is required, depending on the method selected. This will be amplified later.

A low-voltage cutout.

Temperature control has already been mentioned.

In each of the control functions which require variation in flow rate, the speed of the drive motor will be controlled by a duty-cycle pulse technique. An experimental control unit of this type has already been operated.

8. Miscellaneous

The fuel tank will have a capacity of 0.7 cubic foot. This will provide a 3-hour supply of gasoline at rated load.

The control panel will contain an ammeter and voltmeter, indicators for enclosure and reactor temperature, and readout devices for the fuel, air, and recycle rates. Signal lights will indicate the operational mode. The only controls presented to the operator will be three buttons labeled START, STOP, and RESET.

9. Weight (Pounds)

Fuel Cell Stack:	
Modules	1500
Headers and manifolds	32
Connectors	16
Supports	185
Fuel Preparation System:	
Reactor	20
Preheaters	26
Vaporizer	2
Corrosive remover	50
Fuel cooler	23
Blower, meter	30
Fuel pump	5
Ignitor	1
Recycle blower and motor	20
Plumbing	15
Cathode Composition System:	
Blower	10
Circulation fans	60
Baffles	28

Temperature Control System:	
Temperature sensor	2
Heat exchanger	23
Blower	10
Control	2
Startup System:	
Burner	30
Blower	50
Ignitor	2
Fuel pump	4
Battery and charger	110
Enclosure:	
Outer shell	180
Insulation	177
Personnel protection	5
Supports and skid frame	96
Controls and Instruments	62
Miscellaneous:	
Fuel tank	5
Control panel and frame	58
Wiring, electrical items	35
TOTAL	2874 Pounds

NOTE

Calculations are presented in Appendix D.

10. Auxiliary Power

	AMPS AT 28 V	
	Startup	Operating
Combustion blower	40	-
Startup fuel pump	5	-
Burner solenoid	0.5	-
Burner ignitor	1 ‡	-
Circulation fans	15	15
Partial-oxidizer blower	6*	6
Partial-oxidizer fuel pump	1*	1
Partial-oxidizer solenoid	0.5*	0.5
Partial-oxidizer ignitor	1*	-
Control circuit	2	2
Cathode air blower	-	3
Recycle blower	-	10
Cooling system blower	-	5
TOTAL	71	42
WATTS	1990	1180

C. OPERATION

The sequence of events in starting and using the 15-kilowatt power plant will be described in this section. The various control and safety functions will be included.

---

‡ Turns off at 500°C
* Turns on at 500°C

1. Startup and Shutdown

a. When the operator pushes the START button, the following take place:

The startup battery is connected

Control circuits are turned on and/or reset from RUN mode to START mode

Combustion blower is turned on

Circulation fans are turned on

Fuel pump is turned on

Burner ignitor is turned on

Start light is turned on.

Three seconds later, the fuel valve to the burner is opened. If the flame sensor does not respond within one second after that, the entire plant shuts down. (In effect, the control system will push the STOP button.)

b. When the enclosure reaches 500°C, the sequence control will:

Turn on the partial-oxidizer blower

Switch the ignitor to the partial oxidizer

Open the fuel valve to the reactor

Turn on the cathode air blower

Turn on the recycle blower.

c. When voltage across the load verifying resistor indicates that the stack is capable of powering the auxiliaries, they are switched to internal power. Simultaneously, the resistor is disconnected, and the BATTERY light goes out. If the voltage drops below an acceptable value the process is reversed.

d. When the enclosure temperature reaches 700°C:

The startup system will be shut off and locked out until the START button is pushed. The START light goes out.

The fuel preparation control system will be switched from START to RUN mode, and locked in until the START botton is pushed.

If the stack voltage is greater than 28 volts, the RESET light will go on. This notifies the operator that the unit is ready to accept a load.

If the voltage is less than 28 volts, the LOW VOLTAGE light will turn on, notifying the operator that the unit is not ready. If this condition persists, he should push the STOP button.

e. When the RESET light goes on, the operator may push the RESET button. This will connect the stack to the output terminals. The RESET light will go out and the OPERATING light will turn on. No other action will connect the terminals to the stack.

f. If the load imposed on the power plant lowers the voltage to 24 volts, the unit will revert to the RESET condition, that is, the terminals will be disconnected and the RESET light will come on. The operator should reduce the load and push the RESET button.

g. If the enclosure temperature rises to 715°C or falls to 690°C, the controller will push the STOP button. The lower limit is bypassed when the startup system is on.

h. If the reactor temperature goes above 1250°C or below 1100°C, the unit is shut down. Again, the lower limit is bypassed during startup.

i. When the power plant is to be shutdown, the operator pushes the STOP botton.

The terminals are disconnected

The battery switch is opened

Main power switch to all auxiliaries is opened

All blowers and pumps stop

Solenoid valves close.

It is possible that a manual override could be provided to turn on some of the blowers, to hasten the cooling of the unit.

j. The power plant is now ready to be started again, at any time, at any temperature.

The time required for the power plant to reach operating temperature from a cold start depends upon the burner fuel rate.

Flow Rate (Pounds per hour)	Time (Minutes)
35	34
40	29
45	26
50	24

A rate of 40 to 45 pounds per hour will be used in this design.

The time required for the contents of the enclosure to cool to 250°F, if none of the fans are used for cooling, will be about 20 hours.

2. Normal Operation

It is assumed that the fuel cell stack can utilize electrochemically 68.2 percent of the fuel fed to it from the partial oxidizer, and that the partial oxidizer can operate properly if the fuel and air (not counting recycle) are supplied in the ratio of one atom of oxygen per atom of carbon.

With this basis, the fuel consumption and efficiency of the powerplant may be computed as a function of output. This analysis is presented in Figure 3-6. The efficiency is seen to rise quickly from zero to a maximum, then decrease slowly as the load is increased. This reflects the fact that at very light loads extra fuel must be supplied to keep the enclosure up to temperature. At high loads, the lower voltage of the fuel cell stack accounts for the lower efficiency.

The maximum efficiency is obtained at the point at which the fuel is exactly that required for the output and the heat losses through the insulation and exhaust. At higher loads, additional waste heat must be removed to prevent the enclosure temperature from rising.

The fuel rate shown in Figure 3-6 is the minimum rate consistent with the design assumptions. It is desired to approach this as closely as possible.

To see how this is to be done, consider Figure 3-7, which shows the fuel rate in terms of gross fuel cell current. The two distinct parts correspond to the two segments (high and low power) of Figure 3-6. Above

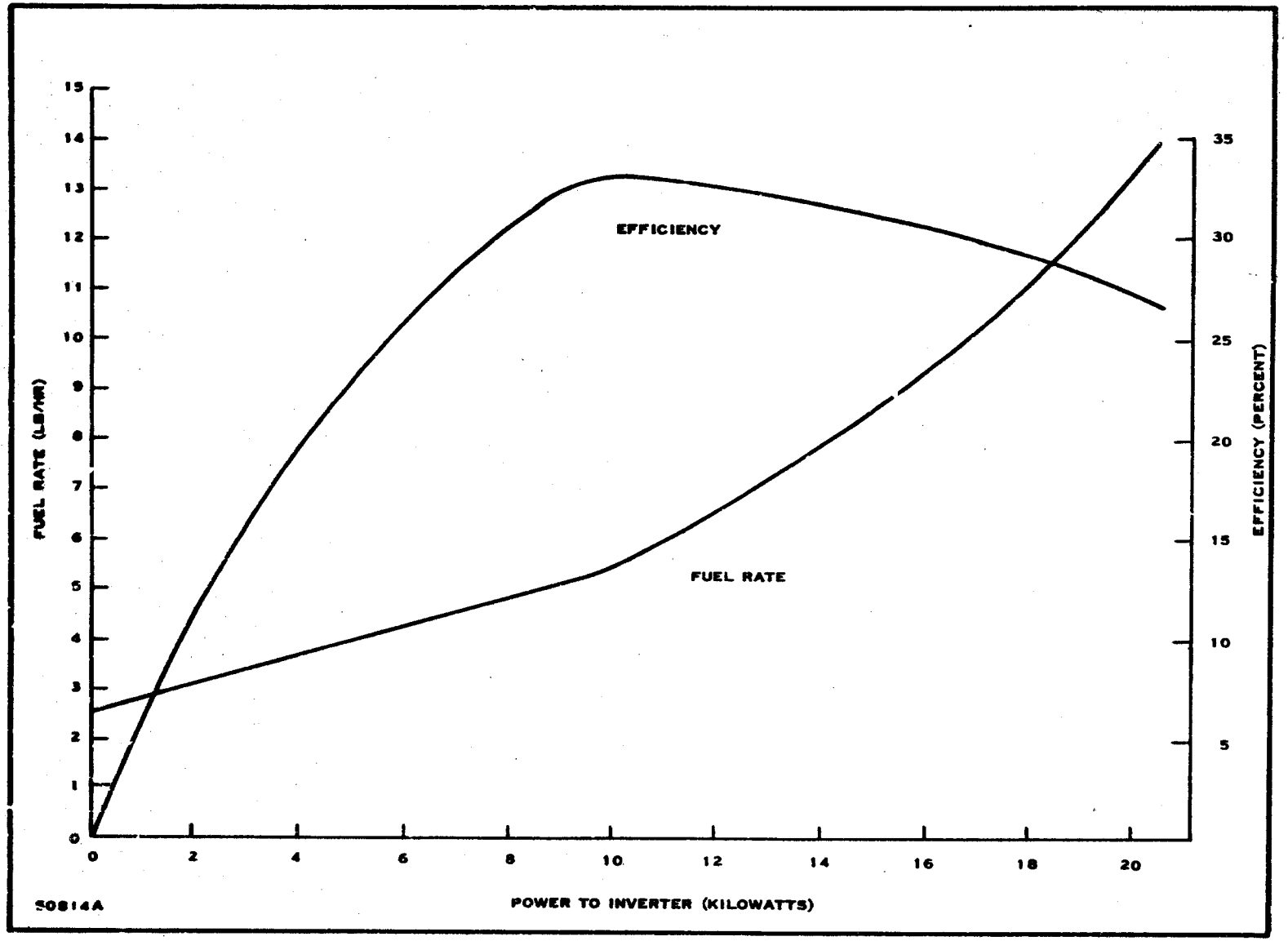

Figure 3-6. Power Plant Characteristics

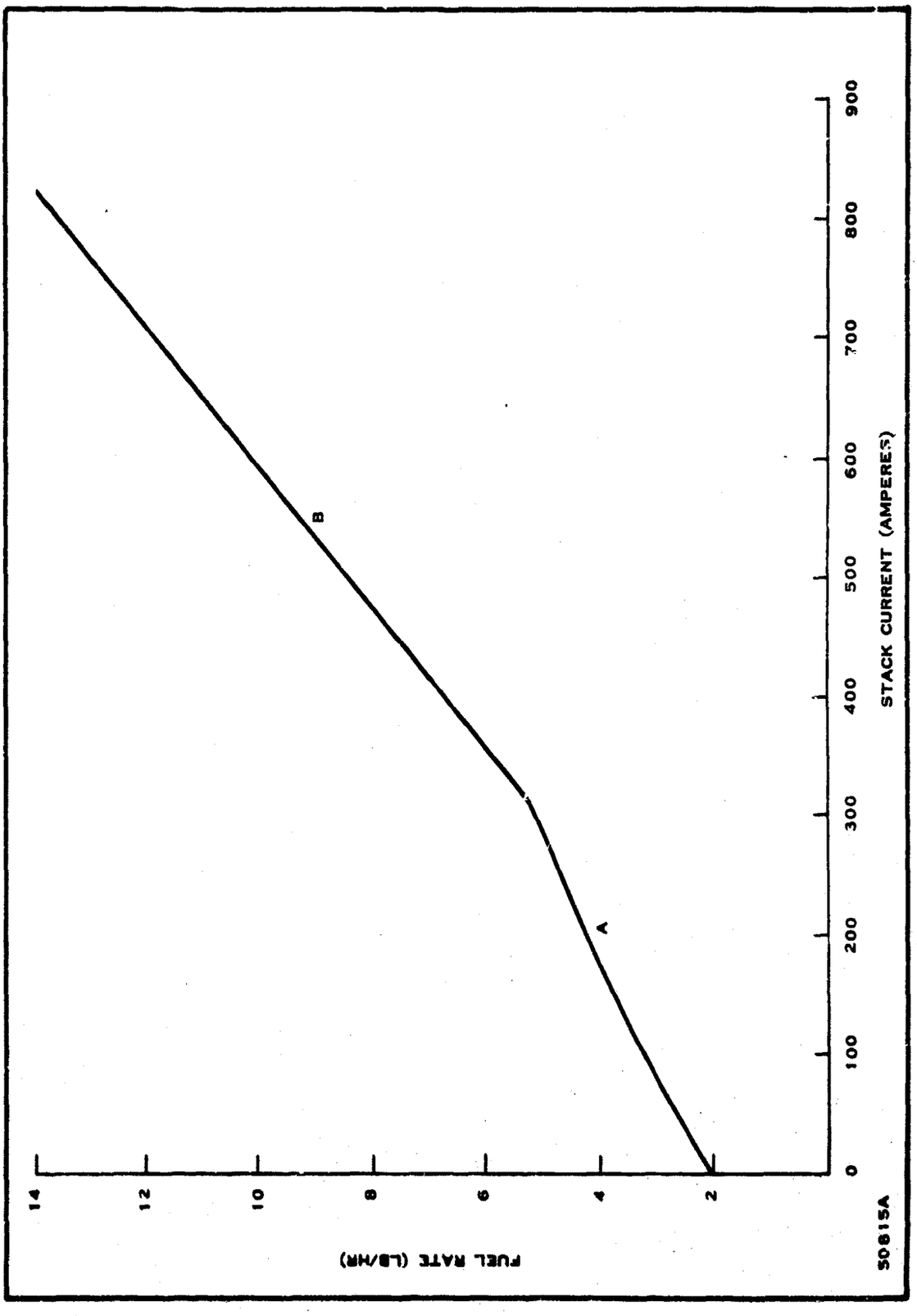

Figure 3-7. Fuel Rate

300 amperes (B) the utilization is always 68.2 percent. (The fuel consumed electrochemically is proportional to current, not power.) Line B is exactly a straight line through the origin. Curve A is very nearly straight, except at very low power.

The throttling control is derived from this graph. The curve will be approximated by two straight line segments. The current through the stack will be sensed and a programming circuit will call for a certain fuel rate. If the unit is in region A, it is necessary that the rate be great enough to keep the enclosure up to temperature. The simplest method is to set the command rate slightly above the minimum value and remove the excess heat with the cooling system. One could allow the rate to be controlled by the temperature in this region, but the savings in fuel are not considered to be worth the complications that this would introduce in the rest of the control circuitry.

In region B this is never a problem, because it is always necessary to remove excess heat. The enclosure temperature will be sensed, and the speed of the cooling blower varied accordingly.

It is also necessary to control the rates of the air and recycle spent fuel. In region B they will be varied in exact proportion to the fuel, since the utilization, and therefore all stream compositions, remain constant. In region A, it is desirable to increase the ratio of air to fuel for two reasons. First, the lower utilization requires it to prevent carbon precipitation. Second, it will be helpful to maintain temperature in the reactor. Therefore, the air rate will be programmed along a line that will provide an oxygen/carbon ratio of 1.25 at zero current. The recycle rate meanwhile will be kept constant. This is illustrated in Figure 3-8, which depicts the variation of these rates with current.

It will be necessary to control the air preheat in order to maintain the temperature in the reactor. This will be done by dividing the air into two streams, one to be preheated, one not. Varying the proportion will accomplish the control.

The cathode air supply must be regulated in accordance with the fuel rate to maintain the optimum composition. Two methods are possible. In the first, the rate will be programmed according to the current. Figure 3-9 shows the relationship of cathode air to fuel and partial-oxidizer air. Note that in region B all rates remain in strict proportion, and in region A the <u>total</u> air rate is in exact porpotion to the fuel.

The control schemes described above will prevail only when the powerplant is in its operating, or RUN mode (that is, after the enclosure reaches 700°C). During startup, the fuel preparation system will be controlled at a single point, selected for optimum starting.

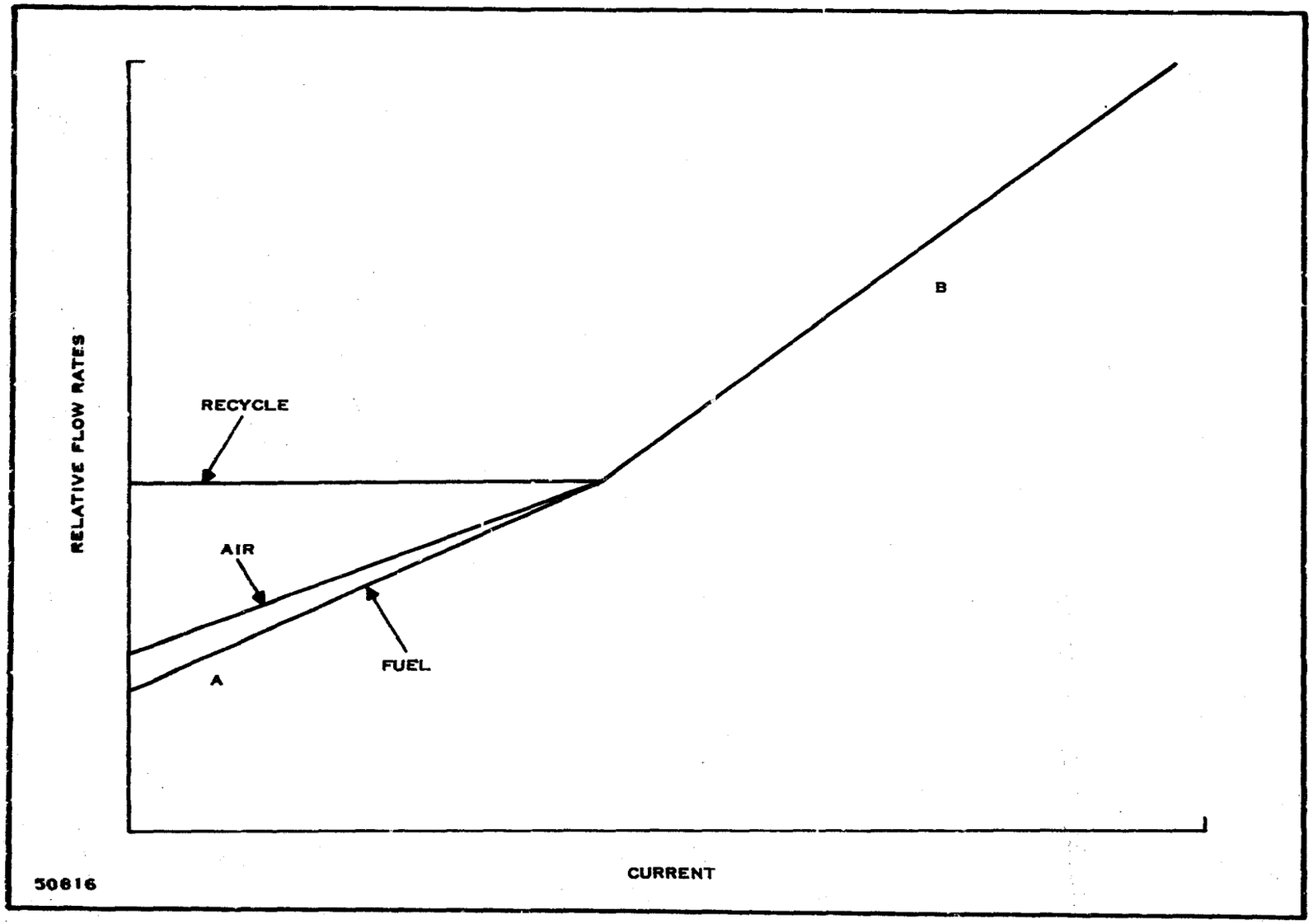

Figure 3-8. Variation of Flow Rates

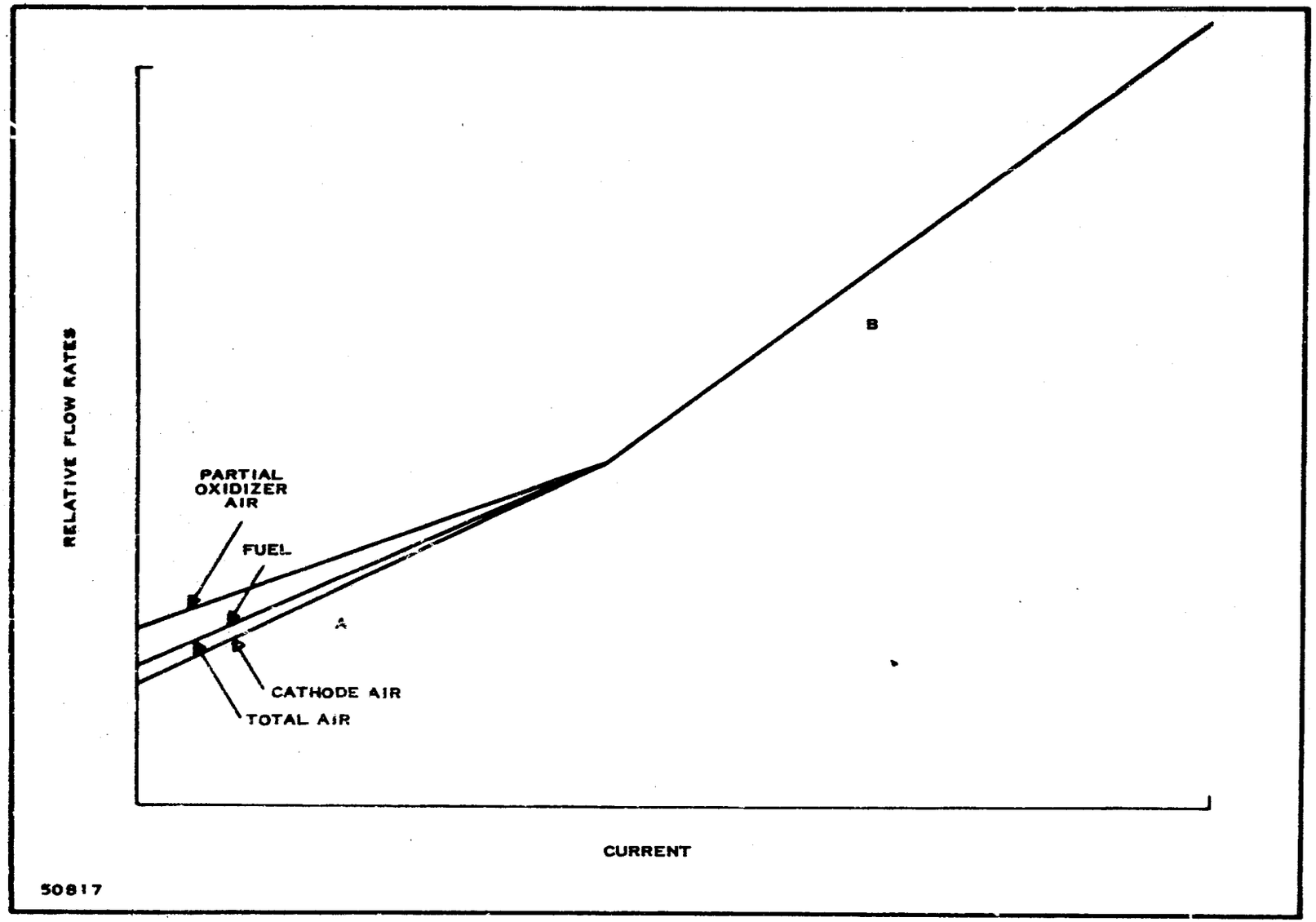

Figure 3-9. Cathode Air Control

An alternative method of handling the cathode air supply is to sense the composition and adjust the air rate appropriately. As this would be independent of the programming controls, it is the superior method if a suitable composition indicator can be found or developed.

When the load on the powerplant is changed, the time required to stablize the new condition will depend upon the new value of the current. The reason for this is that the controlling element is the flow of fuel through the anodes. The time required for replacement of the entire fuel stream is given in Figure 3-10.

D. DEVELOPMENT WORK

As stated earlier, Texas Instruments believes that the 15-kilowatt powerplant can be built. The evidence in support of that view is presented in this report, which is the result of a program to determine the feasibility of such a system. It was also stated that considerable development work remained to be done. The purpose of this section is to amplify this point. Only the major items will be covered; the list of topics should be considered illustrative rather than exhaustive.

The most important and obvious component is the fuel cell itself. The electrochemical aspects of the cell, and the advances necessary to attain the desired performance, have been discussed earlier. Here it may be noted that the following problems must be solved in order to combine the cell into the system. Means of supporting and isolating the cells (modules) must be developed. Headers and manifolds must be made to obtain the proper gas flow and electrical connection. Connectors probably will have to be developed expressly for this use, either in-house or by a vendor experienced in the field.

The fuel preparation system presents several areas that require additional work. Apart from building reactors which will operate at the specified fuel rate, two topics of importance are starting and throttling. The reactor must operate over a wide range (about four to one) of fuel rates, and still be compatible with the required air and recycle flows. Startup must be accomplished more quickly and smoothly than it is at present, and the reactor must be characterized so that startup may be controlled automatically.

It was said earlier that the corrosive removal unit was not yet ready. In fact, work still needs to be done on testing various techniques before one of them can be selected for development.

A startup burner for a 1-kilowatt system was obtained by modification of an existing unit, and it is not doubted that it can be done for the 15-kilowatt system. However, considerable experimentation will be necessary and the demands on a test facility will be compounded by the size of the burner.

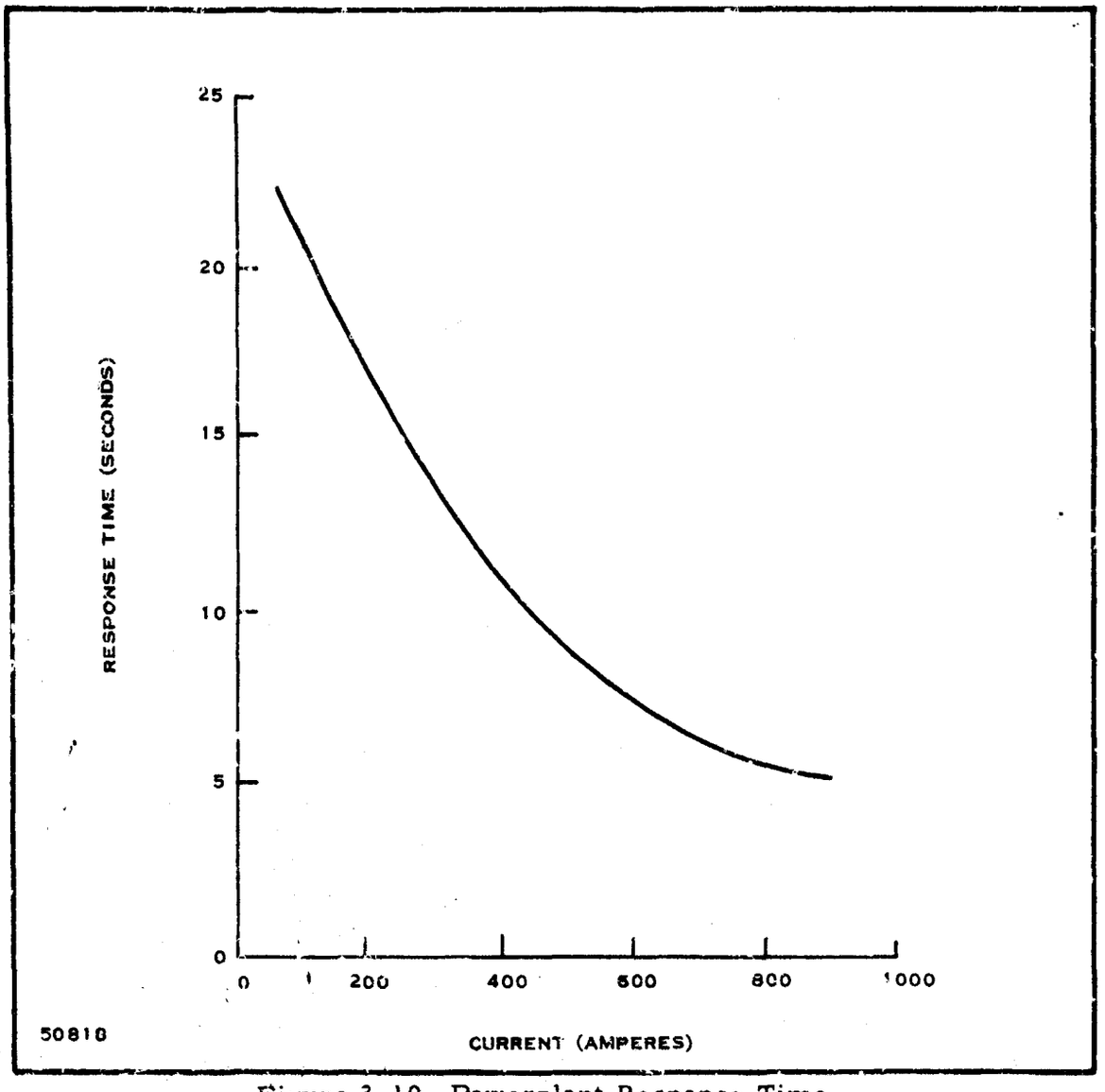

Figure 3-10. Powerplant Response Time

The enclosure, simple box though it may be, offers challenges such as to provide access to parts, attain strength without increasing weight, retain the insulation, and incorporate exhausts.

Very little work has been done to date on the control system. The program circuits and all of the controlling circuits must be designed, built, and checked out. The sequencing and safety controls will have to be made. A number of sensors must be acquired and tested or else developed; several of these (flow rates, cathode composition) will be difficult.

Finally, it may be mentioned that the auxiliary power requirement is a matter deserving of attention, especially during startup. To supply 2000 watts for 30 minutes would require a lead-acid battery weighing probably 200 pounds or more. That cannot be tolerated. A better battery or lower power is needed, if not both.

To conclude, these are some of the elements requiring further development. None is considered beyond the grasp of current technology. For most, sound approaches are already in hand. Nevertheless, the work still has to be done.

SECTION IV

CONCLUSIONS AND RECOMMENDATIONS

Continued development of the molten carbonate cell and the Texas Instruments module during the period of this contract has improved the confidence level that an average power of 30 watts per square foot of cell area can be achieved or exceeded, thus giving good assurance that the goals of size, weight, and economy for the unit can be reached. Likewise, with recent advances, the operating life can be expected to extend beyond 500 hours in test units in the near future. Of prime significance is the fact that the thin matrix development has not demonstrated any adverse effects to rapid thermal cycling.

The fuel preparation subsystem has progressed considerably with two major design developments. Fuel introduction through controlled vaporization with the input air is a far simpler procedure than either the film boiling or ultrasonic atomization techniques envisioned at the outset of the contract experimental phase. Reactor design incorporating internal recycle was demonstrated as having a dramatic effect on smoothing the reaction, as evidenced by quiet operation and virtual elimination of carbon deposition problems. Performance of both these subsystems in combination was demonstrated with both combat gasoline and CITE fuel.

Likewise, modification of a commercial gasoline burner has been demonstrated as a suitable startup heat supply, using both fuels. No difficulties are expected in obtaining a suitable burner for larger units because of the existing related technology. Further investigation is indicated to explore methods of obtaining quieter operation.

Removal of corrosive materials following fuel processing still requires more study. Promising results were obtained using molten carbonates and also finely divided nickel on an inert support.

A recycle blower to be operated hot was designed and satisfactorily demonstrated. No significant problems were encountered.

Results of the testing reported have been applied to the development of plans for 15-kilowatt units that would constitute advanced design demonstration units. It is recommended that such units be constructed while work on module development continues. A detailed proposal to carry out this work has been submitted.

SECTION V

DISTRIBUTION LIST

Commanding General (1)
Headquarters, U. S. Army Materiel Command
ATTN: AMCRD-DE-MO-P,
Mr. Marshall Aiken
Washington, D. C. 20315

Commanding General (1)
Headquarters, U. S. Army Materiel Command
ATTN: AMCRD-RF-CM,
Mr. Joseph Kaufman
Washington, D. C. 20315

Commanding General (1)
Headquarters, U. S. Army Mobility Command
ATTN: AMSMO-PE
Warren, Michigan 48090

Commanding General (1)
Headquarters, U. S. Army Mobility Command
ATTN: AMSMO-RR,
Mr. Otto Renius
Warren, Michigan 48090

Commanding Officer (1)
U. S. Army Electronics Research and Development Laboratory
ATTN: Dr. G. Frysinger
Power Sources Division
Fort Monmouth, New Jersey

Commanding Officer (1)
Army Research Office
3045 Columbia Pike
ATTN: R. Heaston
Arlington, Virginia 22204

Commanding Officer (1)
U. S. Army Transportation Research and Engineering Command
Fort Eustis, Virginia

Chief of Research and Development (1)
Office, Chief of Staff
Department of the Army
Washington, D. C. 20310

Chief (1)
U. S. Army Security Agency
Arlington Hall Station
Arlington, Virginia 22212

Commanding General (1)
Headquarters, U. S. Army Combat Developments Command
ATTN: CDCMR-E
Fort Belvoir, Virginia

Office of the Assistant Secretary of Defense (R&D) (1)
Department of the Army
ATTN: Technical Library
Washington, D. C. 20310

Office of Assistant Director (1)
Defense Research and Engineering
ATTN: 3D-1048
Mr. G. B. Wareham
Pentagon
Washington, D. C. 20301

Power Information Center (1)
103 Moore School
200 South 33rd Street
Philadelphia, Pennsylvania 19104

Institute of Defense Analysis (1)
400 Army-Navy Drive
ATTN: Dr. George Szego
Arlington, Virginia 22202

Director (1)
National Aeronautics and Space Administration
ATTN: Code RNW, Mr. E. M. Cohn
Washington, D. C. 20546

Director (1)
George Marshall Space Flight Center
ATTN: M-ASTR-E
Huntsville, Alabama

Director (1)
Manned Spacecraft Center
Farnsworth Chambers Building
2001 Brock Road
Houston, Texas

Commanding Officer (1)
Aeronautical Systems Division
Wright-Patterson Air Force Base
ATTN: ASRMFP,
Mr. George W. Sherman
Ohio

Director (1)
Lewis Research Center
National Aeronautics and Space Administration
ATTN: Mr. H. J. Schwartz
21000 Brook Park Road
Cleveland, Ohio 44135

National Aeronautics and Space Administration (1)
Head, Operations Section
Scientific and Technical Information Division (SAK/DL)
Post Office Box 5700
Bethesda, Maryland 20014

Commanding Officer (1)
Air Force Cambridge Research Laboratories
L. G. Hanscom Field
ATTN: CRXL-R
Bedford, Massachusetts

Commanding Officer (1)
Rome Air Development Center
Griffiss Air Force Base
ATTN: RASSM,
Mr. F. J. Mollura
Rome, New York

Commanding Officer (1)
U. S. Air Force Security Service
ATTN: DCS/Communications-Electronics (ESO)
San Antonio, Texas 78241

Chief, Naval Research (1)
Department of the Navy
ATTN: Code 429,
Dr. Ralph Roberts
Washington 25, D. C.

Chief (1)
Bureau of Ships
Department of the Navy
ATTN: Code 340,
Mr. B. B. Rosenbaum
Washington 25, D. C.

Office of Naval Research (1)
ATTN: Code 425,
Dr. Harry W. Fox
Washington, D. C.

Commanding Officer (1)
Naval Ordnance Test Station
China Lake, California

Director (1)
U. S. Naval Research Laboratory
ATTN: Code 2027
Washington, D. C. 20390

Commanding Officer (1)
U. S. Naval Electronics Laboratory
San Diego 52, California

Commanding Officer (1)
U. S. Naval Marine Engineering Laboratories
ATTN: Code 841
Annapolis, Maryland

Defense Documentation Center (20)
Cameron Station
Alexandria, Virginia

Commander (30)
U. S. Army Mobility Research
Equipment and Development Center
Fort Belvoir, Virginia 22060

APPENDIX A

BATELLE REPORT ON FUEL PROCESSING

APPENDIX A

BATELLE REPORT ON FUEL PROCESSING

Mr. Ed Orzada
Texas Instruments Incorporated
P. O. Box 5936
Mail Station 144
Dallas, Texas 75222

Dear Mr. Orzada:

This is our Summary Report on the project "Development of an Ultrasonic Atomizer for High Temperature Use in a Partially Oxidizing Fuel Cell" and covers work done from the beginning of the contract on November 1, 1966 through February 10, 1967. The contract was terminated on February 10, 1967 by Texas Instruments Incorporated.

INTRODUCTION

Previous work at Battelle has established the feasibility of using small ultrasonic devices for the atomization of liquid fuels. Ultrasonic atomizers have the advantages of small size, long life, low power consumption and silent operation. In the past the ultrasonic atomizers have been used to atomize liquid fuels directly for combustion. The present application was directed toward atomization of a liquid fuel into a high-temperature reactor where the fuel could be decomposed into gases which could be used directly in a fuel cell where the energy would be converted into electricity.

OBJECTIVES

The objectives of this project were:

(1) Design and fabrication of one or more experimental atomizers. Design flow rates of these units were 3 pounds per hour of gasoline.

(2) Design and fabrication of an electronic driver for the ultrasonic atomizer. A power output to the atomizer of 20 watts was assumed and was used for the initial design.

(3) Design of a suitable atomizer mounting for use in a partial oxidizer. This included heat-transfer studies directed toward cooling the atomizer.

(4) Experimental studies of atomizer operation in an operating partial oxidizer.

Summary

The first three objectives were largely accomplished before the project was ended on February 10, 1967. The work indicated a high probability for success in using ultrasonic atomization of liquid fuel in a partially oxidizing fuel cell. Preliminary measurements of the first stainless steel atomizer showed that its throughput was close to that required. A breadboard version of the electronic driver operated well. Thermal studies indicated that it would be practical to provide the cooling necessary for the atomizer to survive and operate in the high-temperature environment of an operating fuel cell.

It is our recommendation that at an appropriate time work be continued on the use of ultrasonic atomization of liquid fuel in a partially oxidizing fuel cell.

EXPERIMENTAL WORK

Previous work at Battelle using ultrasonic atomization of liquid fuels for combustion has involved introduction of the atomized fuel directly into a combustion chamber. Except for the tip of the atomizer, the remainder of the atomizer system operated at or near ambient temperature. Because of thermal conduction from the heated atomizer tip, it was necessary to provide some atomizer cooling, but the amount of cooling needed was not great, and was determined empirically. The atomizers were aluminum and were good thermal conductors.

To use an ultrasonic atomizer with a partial oxidizer, it is necessary that the atomizer system operate in an environment having a temperature of about 700 C. This in turn requires cooling and thermal insulation for the atomizer itself and the fuel line which supplies it. Because of the elevated temperature, it was decided to use stainless steel rather than aluminum for the atomizer structure.

The electronic driver, required to provide the high-frequency electrical power needed to operate the atomizer, could be operated at ambient temperature and presented no particular problems.

System Requirements

Requirements of the ultrasonic atomizer system included:

(1) The ultrasonic atomizer must atomize gasoline at a rate of at least 3 pounds per hour.

(2) The atomizer and its fuel feed tube must be sufficiently well thermally insulated and cooled that it can survive and operate in a temperature environment of 700 C.

(3) The electronic driver must operate from a primary power source of 12 volts d-c and supply sufficient high-frequency electrical power to operate the atomizer.

Experimental work aimed at satisfying these system requirements is described below.

Atomizer Development

The ultrasonic atomizer developed on this project is similar to one developed previously[1] at Battelle. The atomizer consists of two cylindrical metal structures with a pair of piezoelectric discs mounted between them. The entire unit is one wavelength long at the operating frequency of 85 kHz, and the junction between the piezoelectric discs is mounted at a displacement node in the structure.

Figure 1 is a photograph of the atomizer. The two metal cylinders are made of type 304 stainless steel. The entire structure is about 2-3/8 inches long and weighs about 8 ounces. The two piezoelectric discs[2] are mounted between the clamping flanges of the cylinders. The insulated electrical lead in the left portion of the photograph connects to the electrode between the two piezoelectric discs. To operate the atomizer, electrical driving power is applied between this lead and the two cylinders. The small tube leading off to the right in the photograph is the fuel feed tube. During the assembly of the atomizer, each of the 12 clamping screws is torqued to 36.3 inch pounds to provide the clamping pressure required for proper operation of the piezoelectric discs.

---

[1] Hazard, H. R. and Hunter, H. H., "Multifueled Thermal-Energy-Conversion Systems", Battelle Memorial Institute, Final Technical Report, AD 474540, Contract No. DA 28-043 AMC-00431 (E), August 31, 1965.

[2] The piezoelectric discs are a lead-zirconate-titanate material and are type 12100-4, manufactured by the Piezoelectric Division of Clevite Corporation, 232 Forbes Road, Bedford, Ohio.

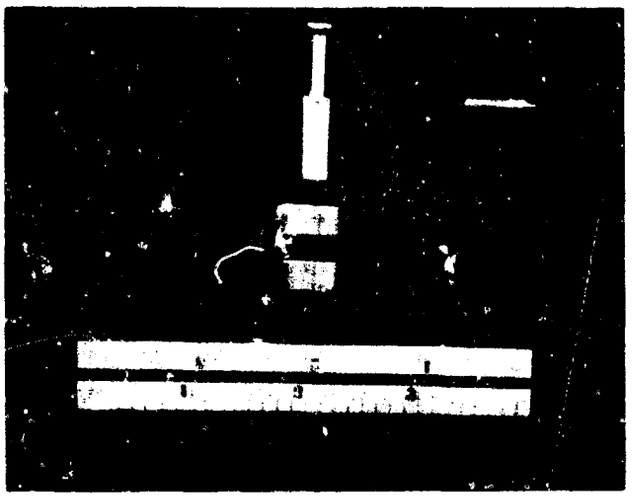

FIGURE 1. PHOTOGRAPH OF THE ULTRASONIC ATOMIZER

Figure 2 is a drawing of the ultrasonic atomizer and provides sufficient information that the atomizer can be duplicated. It is important that a good surface finish be obtained when the cylinders are machined as this prevents the formation of stress risers in the structure.

The atomizer described here was operated briefly. When driven by a laboratory oscillator which supplied an estimated 20 watts of power, the unit operated well and atomized over 2 pounds per hour of white gasoline. This initial test was performed cursorily; the sprayed gasoline was collected in a beaker for 3 minutes and then weighed. No allowance was made for the fact that not all of the aerosol was collected and that some of the gasoline evaporated during the spraying interval. In one test, the flow rate was 15.6 grams per minute, while in another test, the flow rate was 15.3 grams per minute. Thus, the flow rate was slightly more than 2 pounds per hour, and probably was somewhat higher. The atomizer was operated briefly by the electronic driver described later in this report, but no flow-rate measurements were made. The project was terminated before further tests could be made.

Electronic-Driver Development

The electronic driver developed on this project was a single-transistor power oscillator. Two cascaded T-networks were used to provide impedance matching between the low output impedance of the transistor and the relatively high impedance of the atomizer or transducer. The networks also provided the electrical phase shift of the feedback voltage necessary to allow the circuit to oscillate.

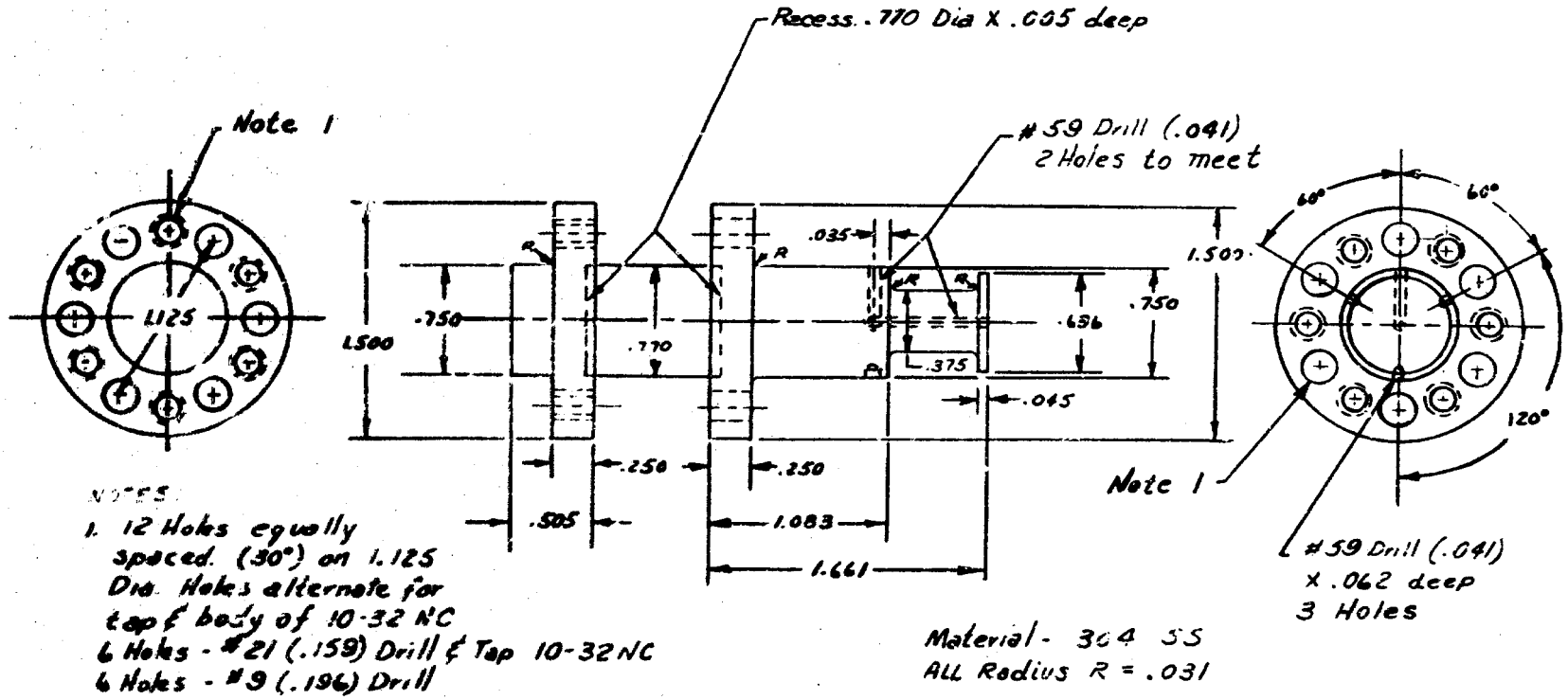

FIGURE 2. ULTRASONIC ATOMIZER

Figure 3 shows the schematic diagram of the initial design of the electronic driver. This circuit was assembled in breadboard fashion and operated with the atomizer shown in Figure 1. This design of the driver was based on an estimate of the electrical properties of the atomizer. After the driver and the atomizer were completed, the electrical properties of the atomizer were measured, using a substitution method. This is a practical technique to optimize the atomizer-driver system. It is a peculiarity of such atomizers that their electrical impedance depends in part upon the operating conditions of the atomizer. Thus, a modified driver was designed, based on the atomizer impedance that was measured. The project was terminated before this new driver was completed.

Partial-Oxidizer Operation

Two partial oxidizers which were needed for this project were received from Texas Instruments Incorporated on January 30, 1967. Included with the oxidizers were an electric furnace and its temperature controller, together with a test panel containing the flow meters needed to operate the unit. This equipment was assembled and was ready for operation early in February, but the project was terminated before the ultrasonic atomizer could be operated in one of the partial oxidizers. The equipment was returned to Texas Instruments Incorporated on March 14, 1967.

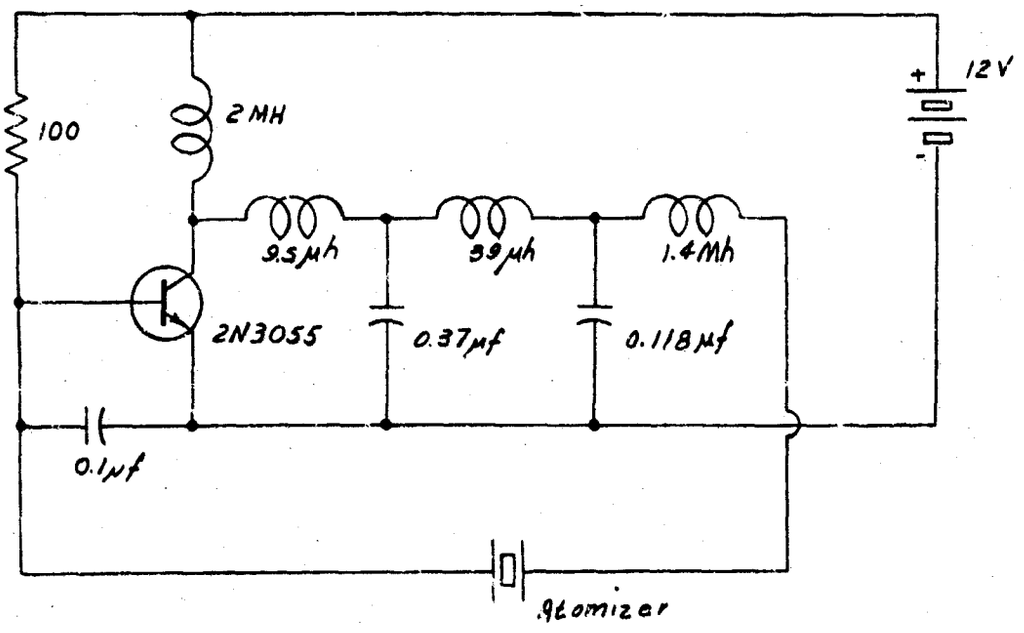

FIGURE 3. SCHEMATIC DIAGRAM OF THE ELECTRONIC DRIVER.

Thermal-System Develcpment

The ultrasonic atomizer included 2 piezoelectric discs which should be kept at a temperature below 65 C to prevent loss of some of their activity. Since the atomizer must operate in the high-temperature environment of 700 C adjacent to the partial oxidixer and spray into the partial oxidizer at a temperature of 1100 C, it was necessary to provide both thermal insulation and cooling for the atomizer. Calculations showed that it was practical to cool the atomizer with room-temperature air.

Figure 4 shows the thermal system designed for use with the atomizer mounted to a 1-1/2-inch-diameter partial oxidizer. The ultrasonic atomizer is mounted to a support ring by means of radial pins. The support ring, in turn, is mounted to the enclosure by means of 6 radial air-cooled tubes extending to the housing. In operation, cooling air would be supplied to the end of the housing opposite the partial oxidizer and would pass through the annular region between the duct and the housing, then enter the radial support tubes and exhaust to the atmosphere. The amount of cooling air required is small, but the pressure within the enclosure must be controlled at a value slightly higher than the pressure within the partial oxidizer to prevent excessive air flow over the atomizer tip and into the partial oxidizer. The design includes a provision for adjusting the enclosure flow resistance to balance these pressures.

Calculations of the heat flow to the atomizer from (1) the 700 C environment adjacent to the atomizer system, (2) the partial oxidizer with an internal temperature of 1100 C, and (3) the 20 watts of electrical power, most of which is dissipated in the atomizer itself, showed that the atomizer system could be suitably cooled by an air flow of 12.3 pounds per hour or 2.7 scfm. These calculations assumed that the cooling air entered the system at a temperature of 37.8 C (100 F) and experienced a temperature rise of 27.8 C (50 F). It was planned that the fuel feed tube would enter the atomizer housing from the outside of the system and not be required to pass through the high-temperature environment.

The thermal system described here was designed but was not fabricated.

CONCLUSIONS AND RECOMMENDATIONS

From the information presented in this report it is concluded that (1) the initial design of the ultrasonic atomizer operated well and its flow rate may be sufficient for use in a partially oxidizing fuel cell, (2) the initial design of the electronic driver for the atomizer operated well and was used to make substitution measurements of the electrical impedance

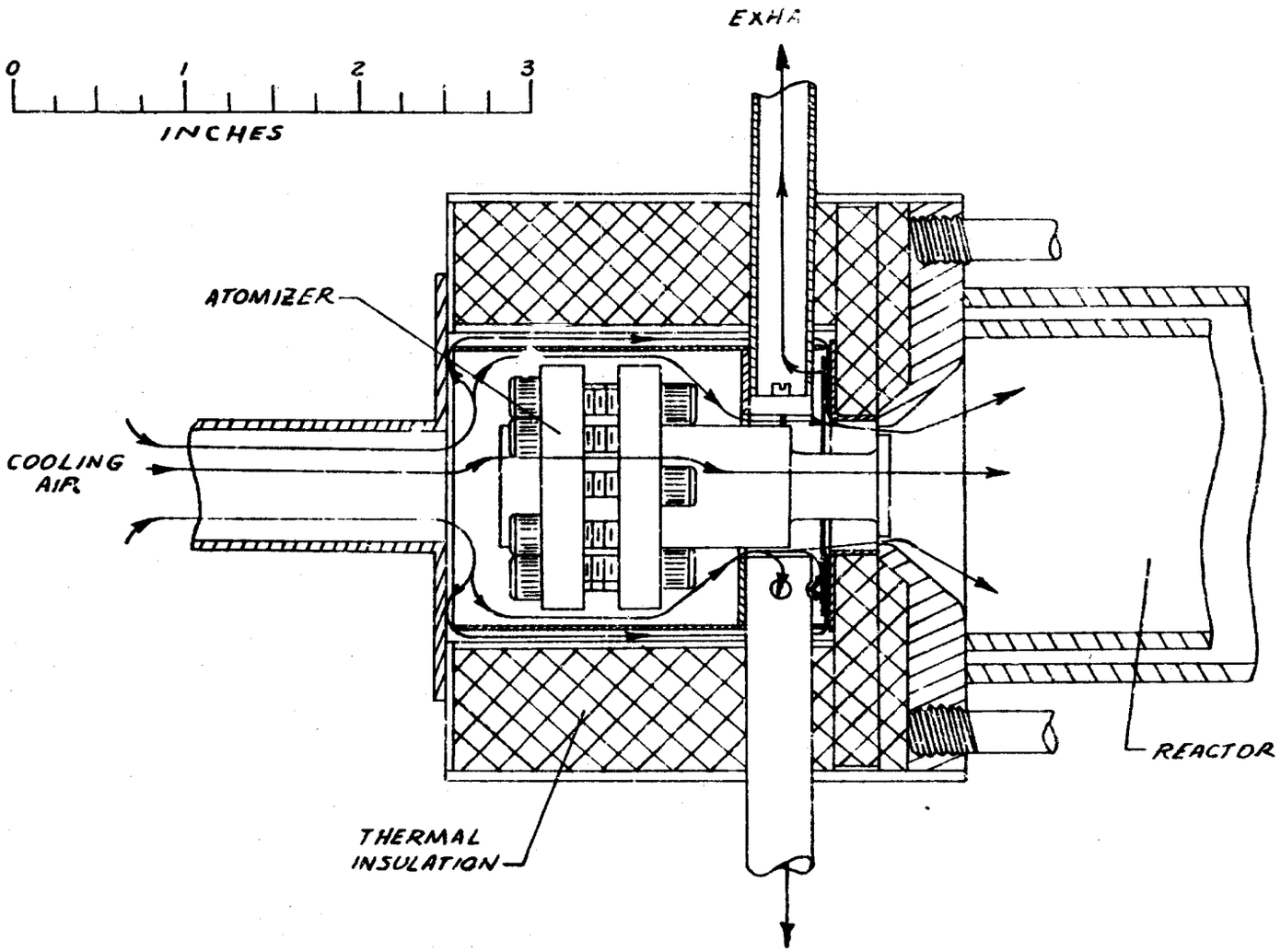

FIGURE 4. THERMAL SYSTEM FOR USE WITH THE ULTRASONIC ATOMIZER.

of the atomizer, and (3) thermal studies indicated that it would be practical to provide the cooling necessary for the atomizer to survive and operate at the required 700 C operating temperature.

It is our recommendation that at an appropriate time work be continued on the use of ultrasonic atomization of liquid fuel for use in a partially oxidizing fuel cell. We feel there is a good chance of success.

The information on which this report is based is recorded in Battelle Laboratory Record Books Number 24205, pages 1 through 38 and Number 24449, pages 1 through 20.

We have enjoyed working with you on this project and hope that at an appropriate time we may be able to continue. Dr. Rodney Wood of the Texas Instruments staff was particularly helpful and we wish to express our thanks to him. If you have any questions or suggestions regarding this work, please call me.

Sincerely yours,

Harvey H Hunter
Senior Electrical Engineer
Systems Engineering Division

APPENDIX B

PERFORMANCE RESULTS

APPENDIX B

PERFORMANCE RESULTS

Performance comparisons of fuel cells are difficult to establish because the variations in important parameters are difficult to assess; e.g., the degree of activation (see Figure B-4) can affect the performance by a factor of 4, but there is no way to measure or control the degree of activation. It is common practice to produce potential-current (E-I) plots of fuel cells. These plots are essentially instantaneous (10 minutes) and, while useful for diagnostic purposes, bear little relationship to the long term (tens of hours) performance of the cell. Figures B-1 through B-5 show E-I plots of a number of cell configurations at different times and with different degrees of activation.

Figures B-6, B-8, and B-10 show the operating histories of three small modules. These performance records are not directly comparable since they reflect the way the module was operated. In general, a change in power accompanied by an inverse change in potential indicates an applied load change. A simultaneous increase in power and voltage results from "activation" procedure. Another possible way of comparing performance results is shown in Figures B-7, B-9, and B-11. These graphs show the fraction of time the cells operated at or above a given power. For graphs B-6 through B-11, a better comparison would result if the cells had been operated at a fixed potential (or results corrected to a fixed potential). This procedure is not considered practical at this stage of development.

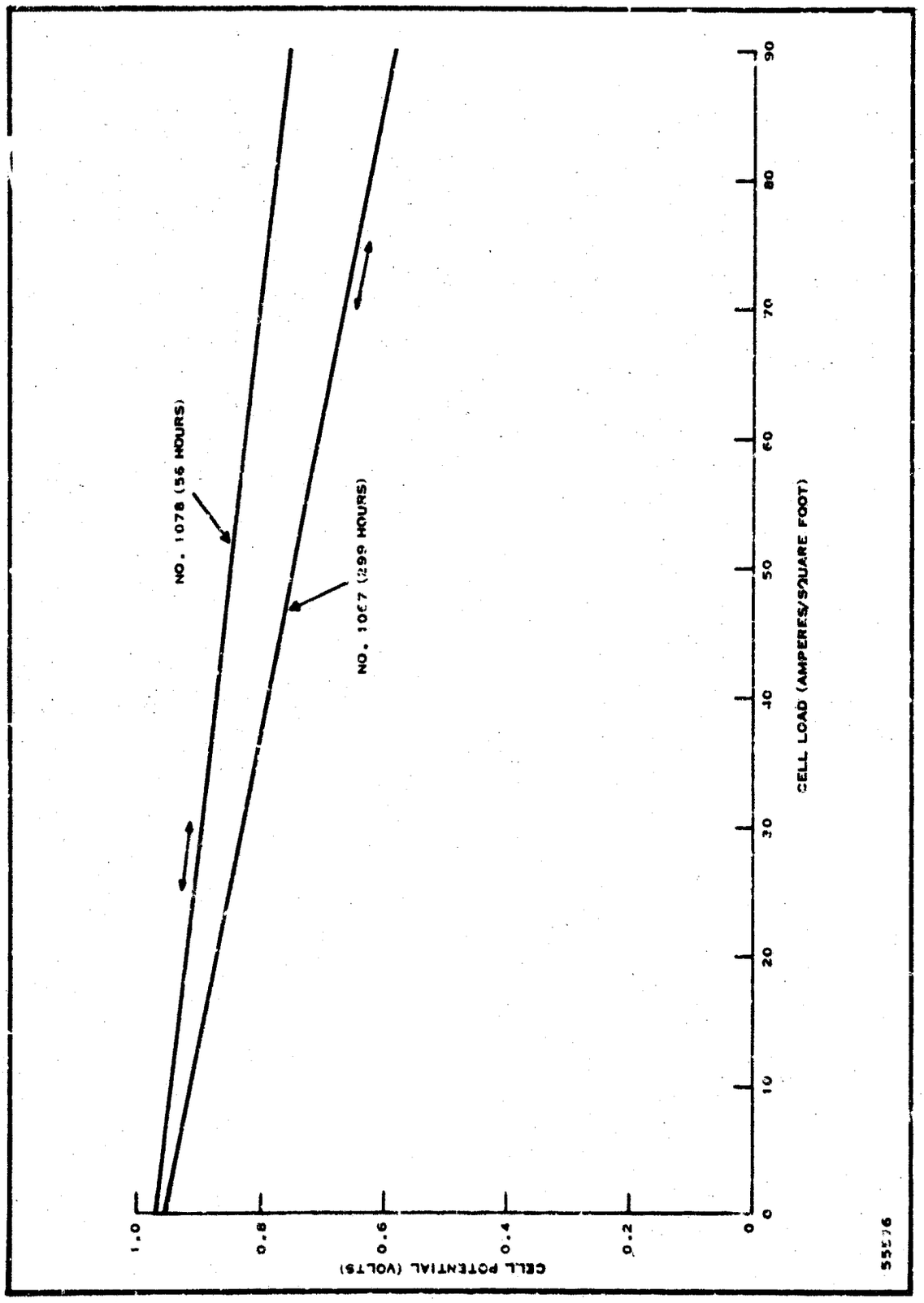

Figure B-1. Performance of Two Cells (1 X 2) with "Candy Ribbon" Anodes

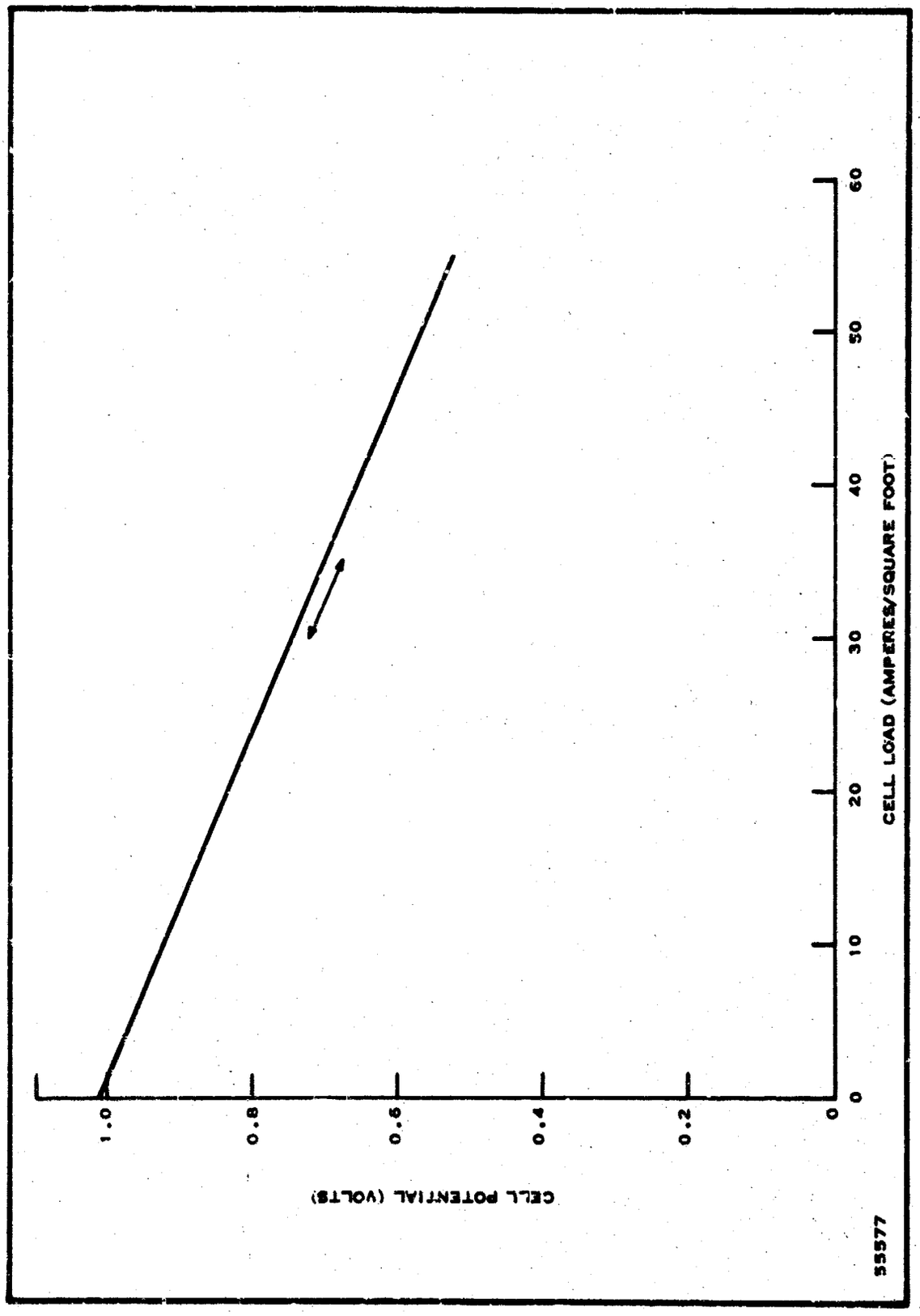

Figure B-2. Performance of No. D-54 (1 X 2) at 341 Hours

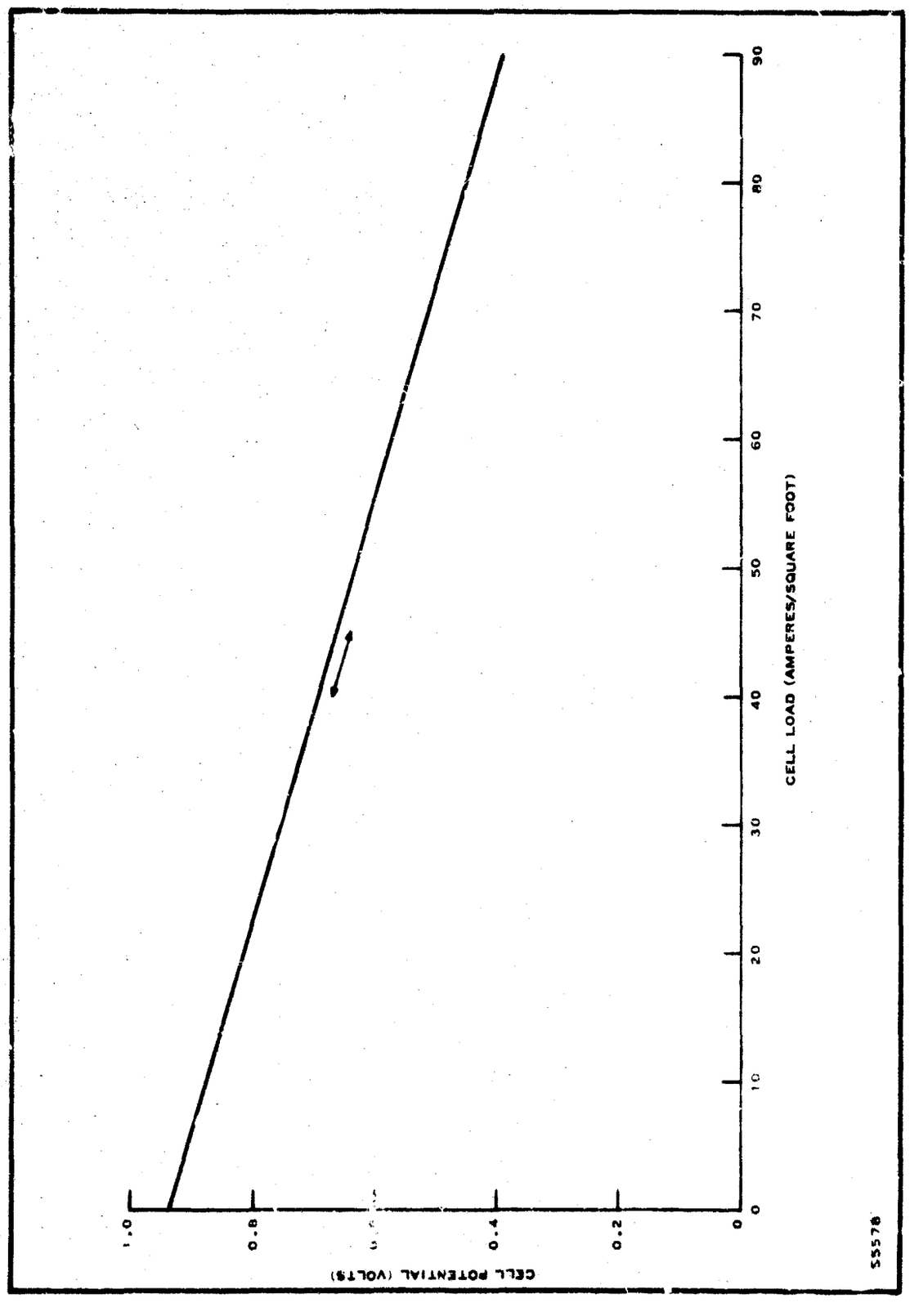

Figure B-3. Performance of No. 1037-A at 144 Hours (1 X 4)

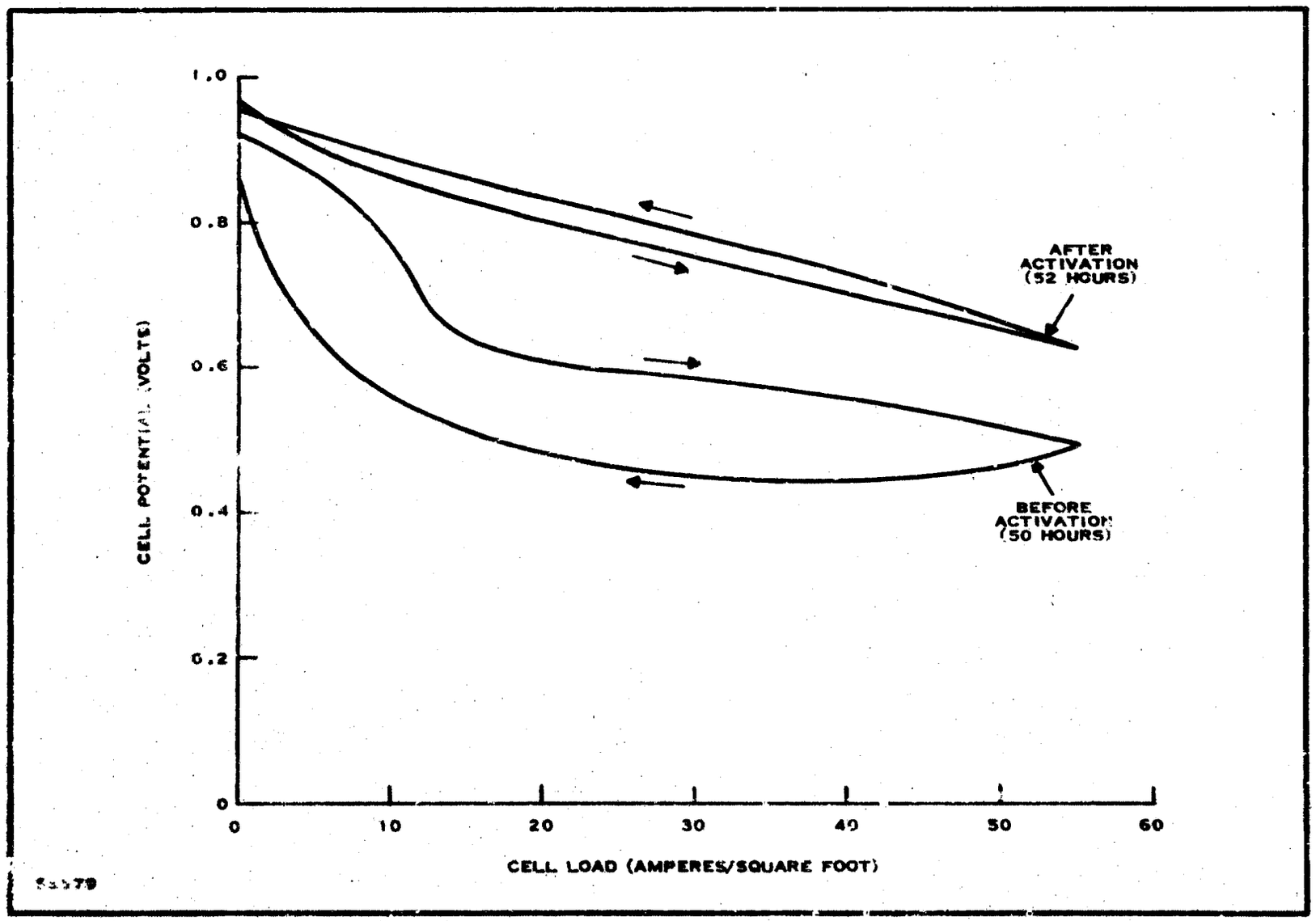

Figure B-4. Performance of No. 1057 (1 X 10) at 50 and 52 Hours

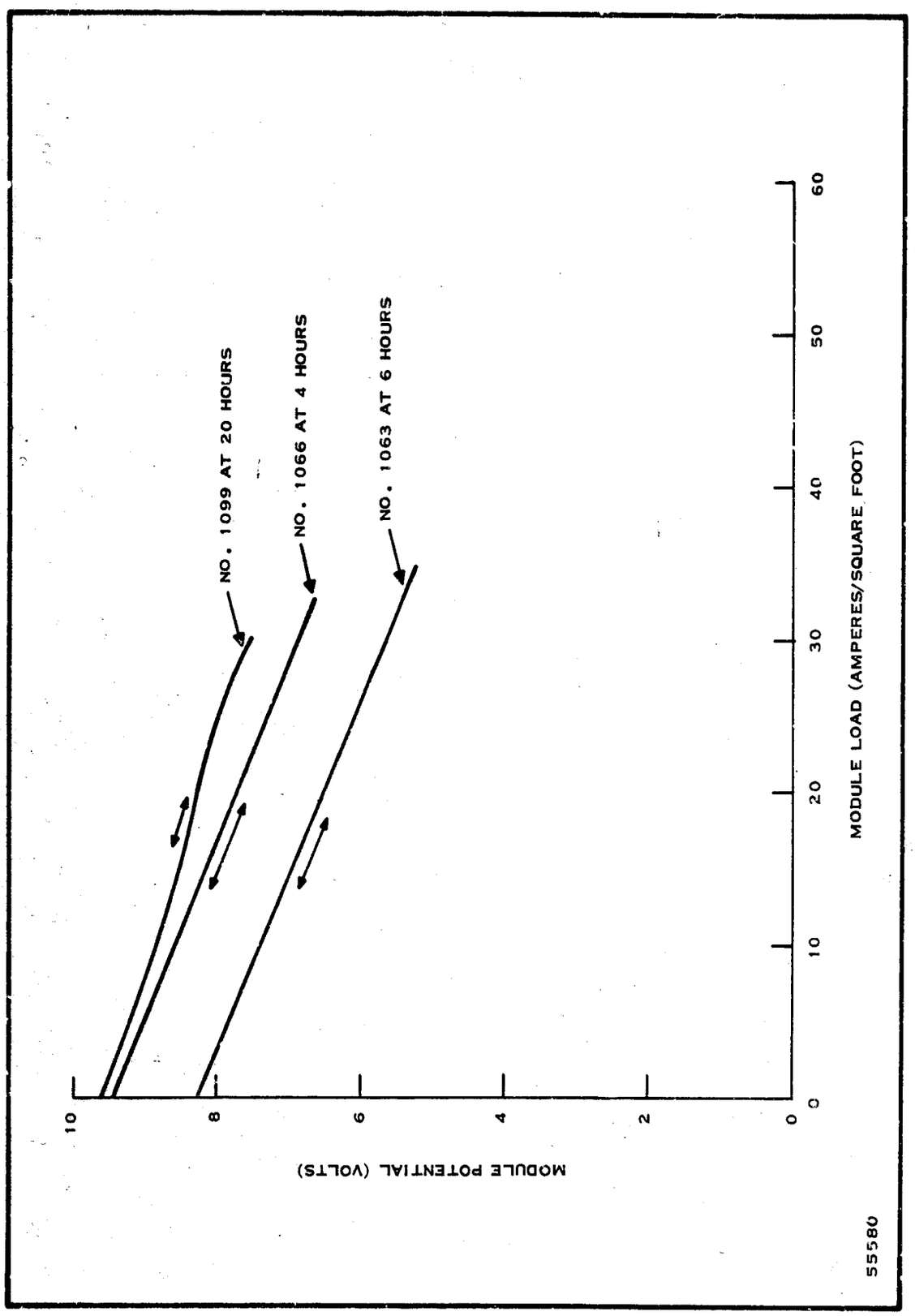

Figure B-5. Performance of Three (10 × 10) Modules

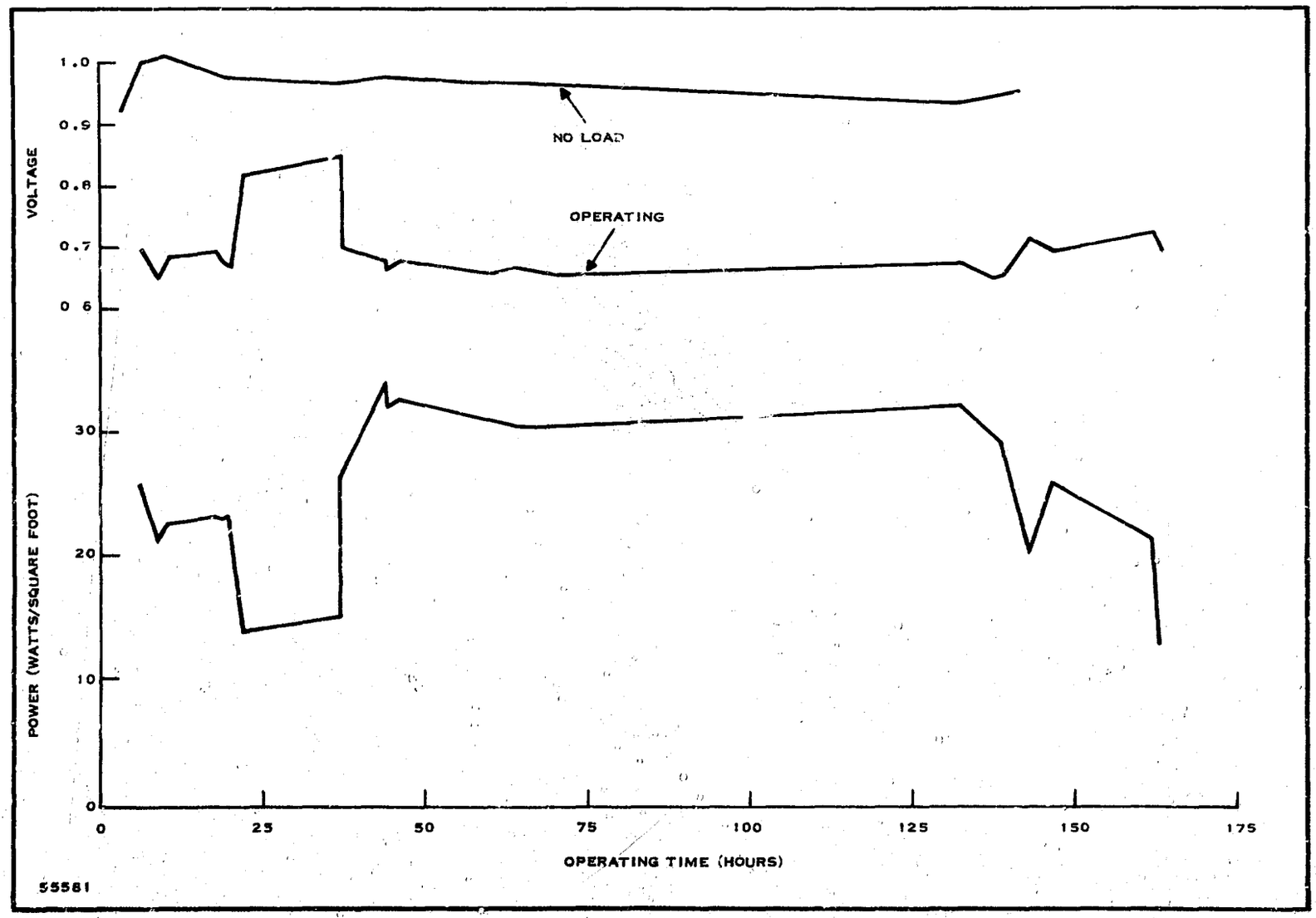

Figure B-6. Operating History of No. 1037-A (1 × 4)

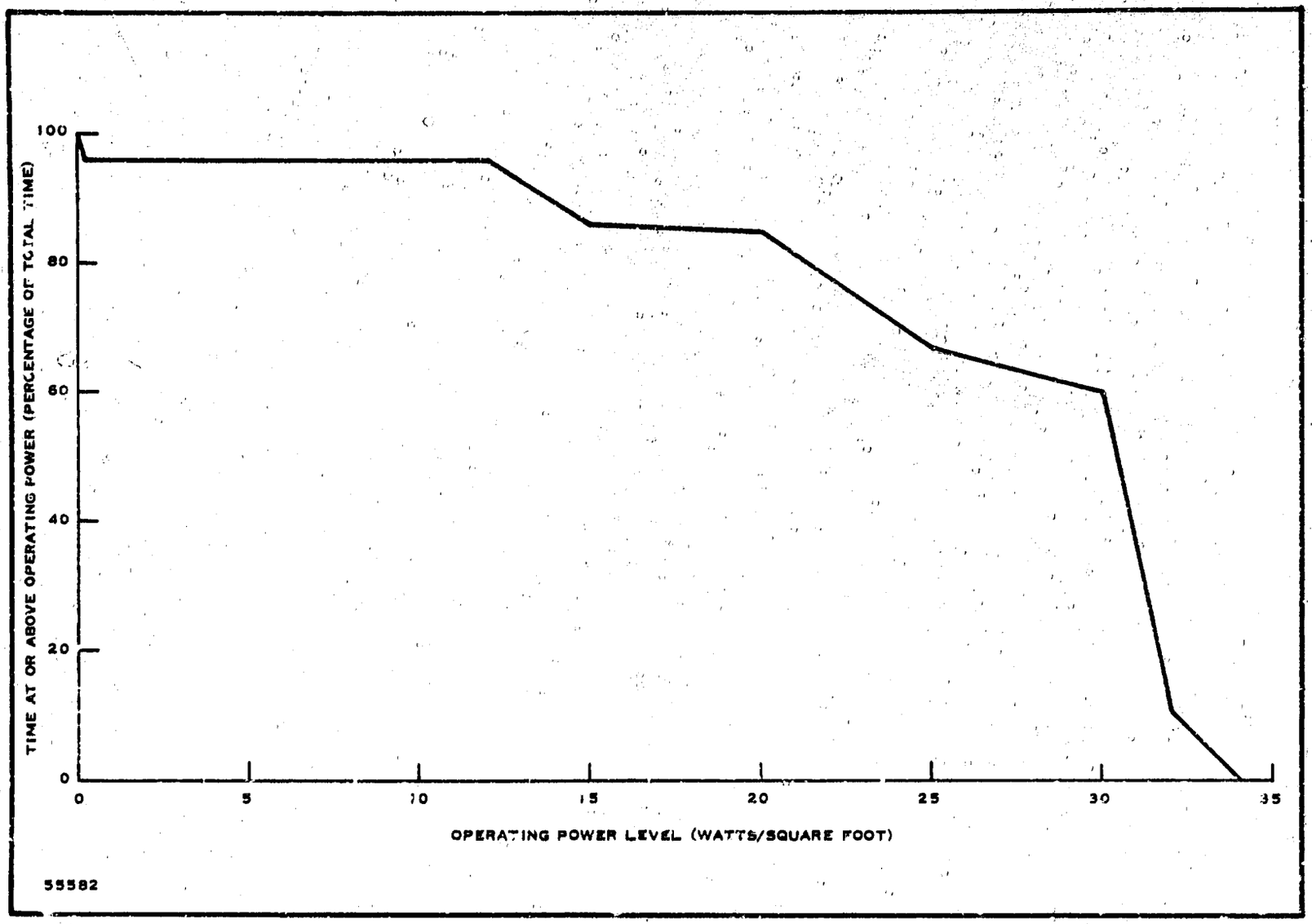

Figure B-7. Performance of 1037-A (1 X 4) (Operating Time: 166 Hours)

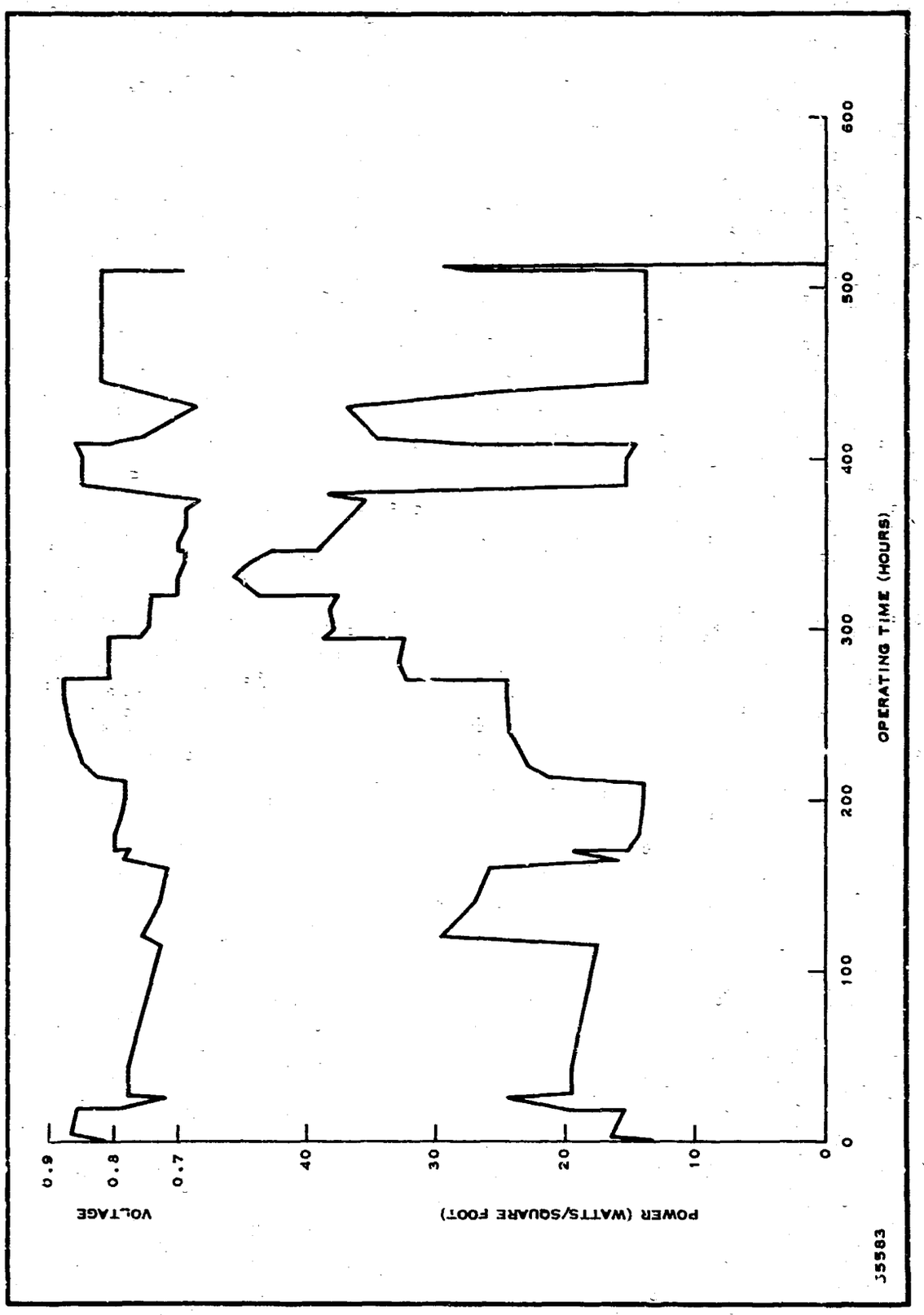

Figure B-8. Operating History of No. 1067 (1 X 2) (First Candy Ribbon Anode)

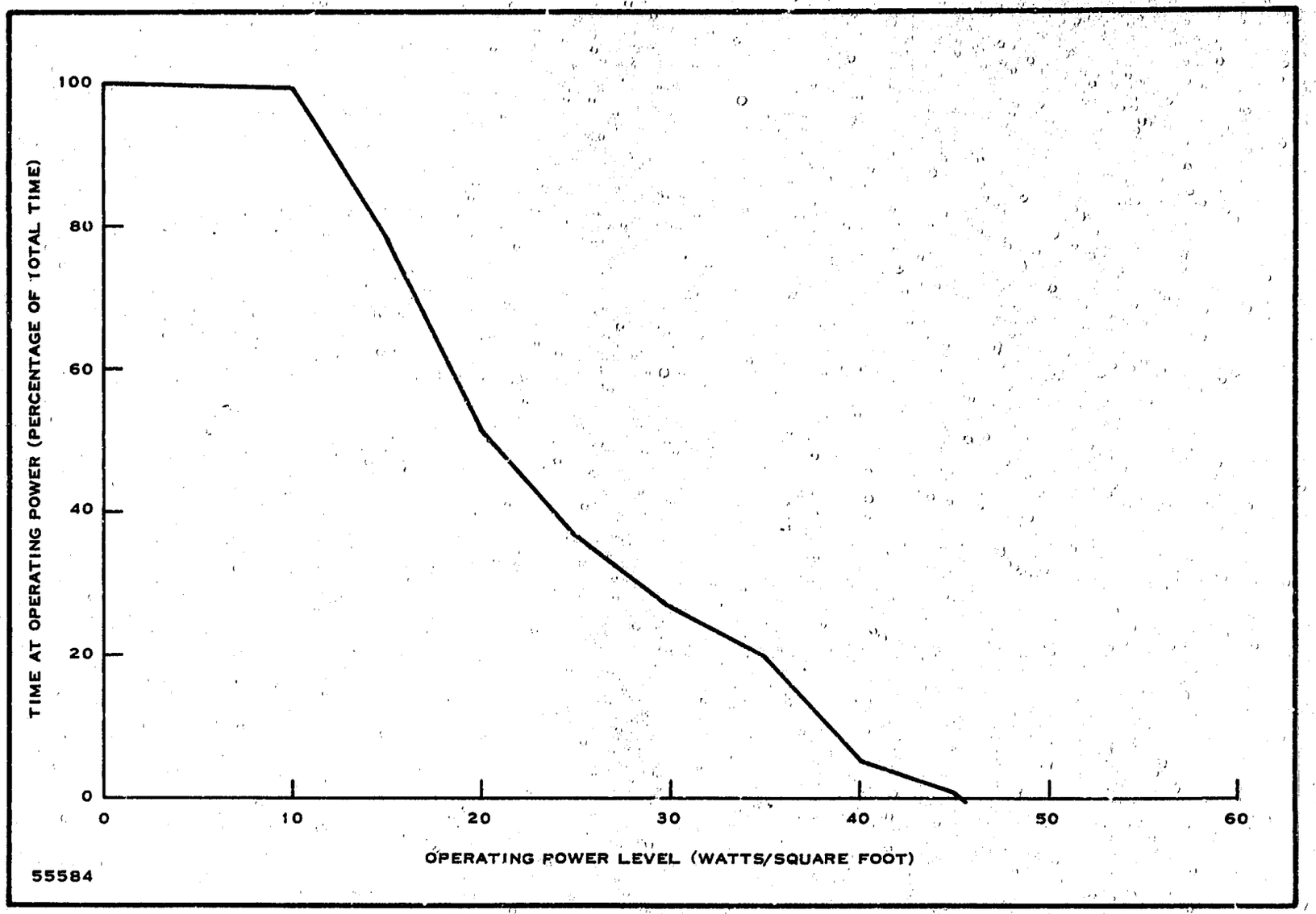

Figure B-9. Performance of No. 1067 (1 X 2) (Operating Time: 512 Hours)

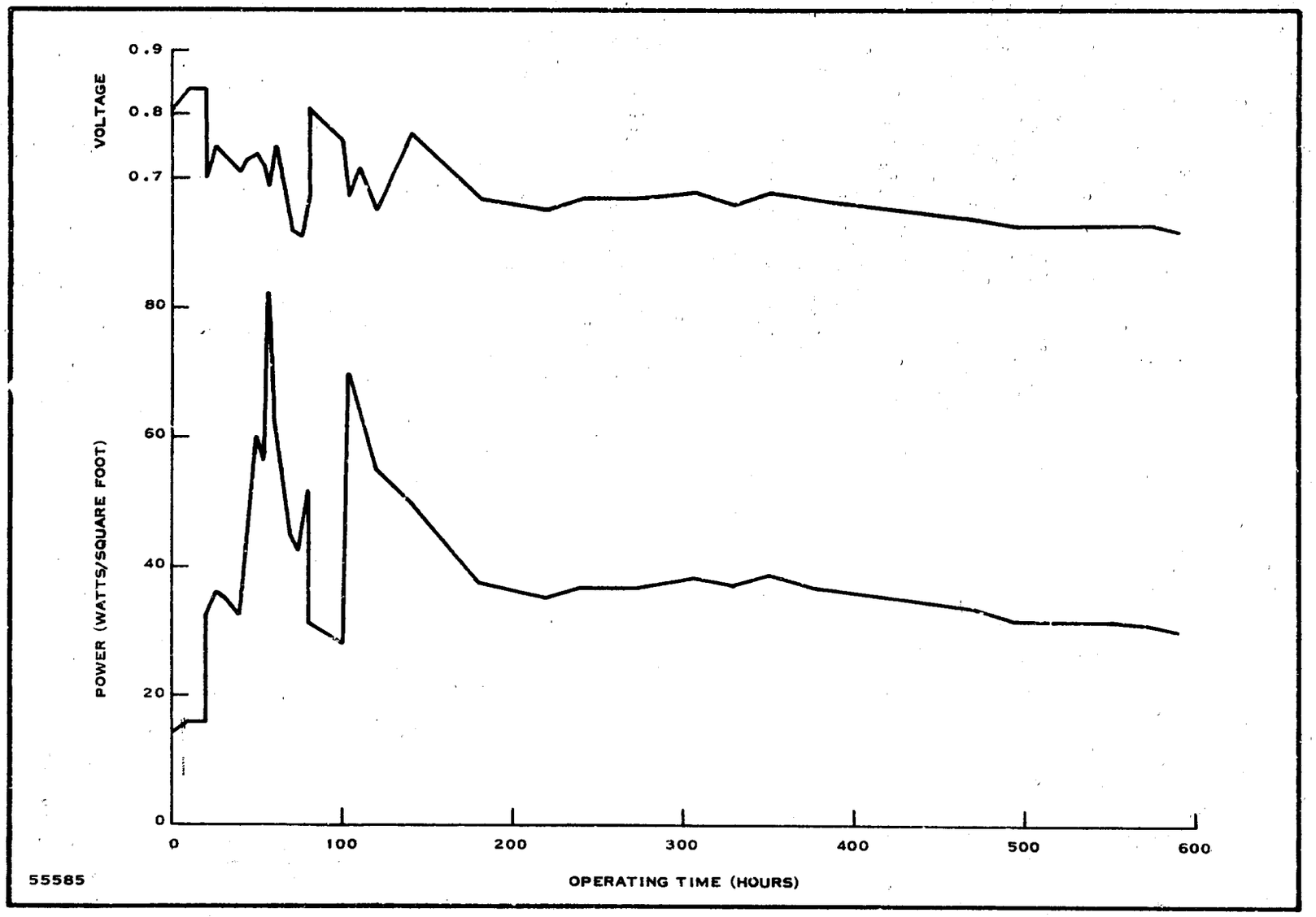

Figure B-10. Operating History of No. 1078 (1 × 2) (Candy Ribbon Anodes)

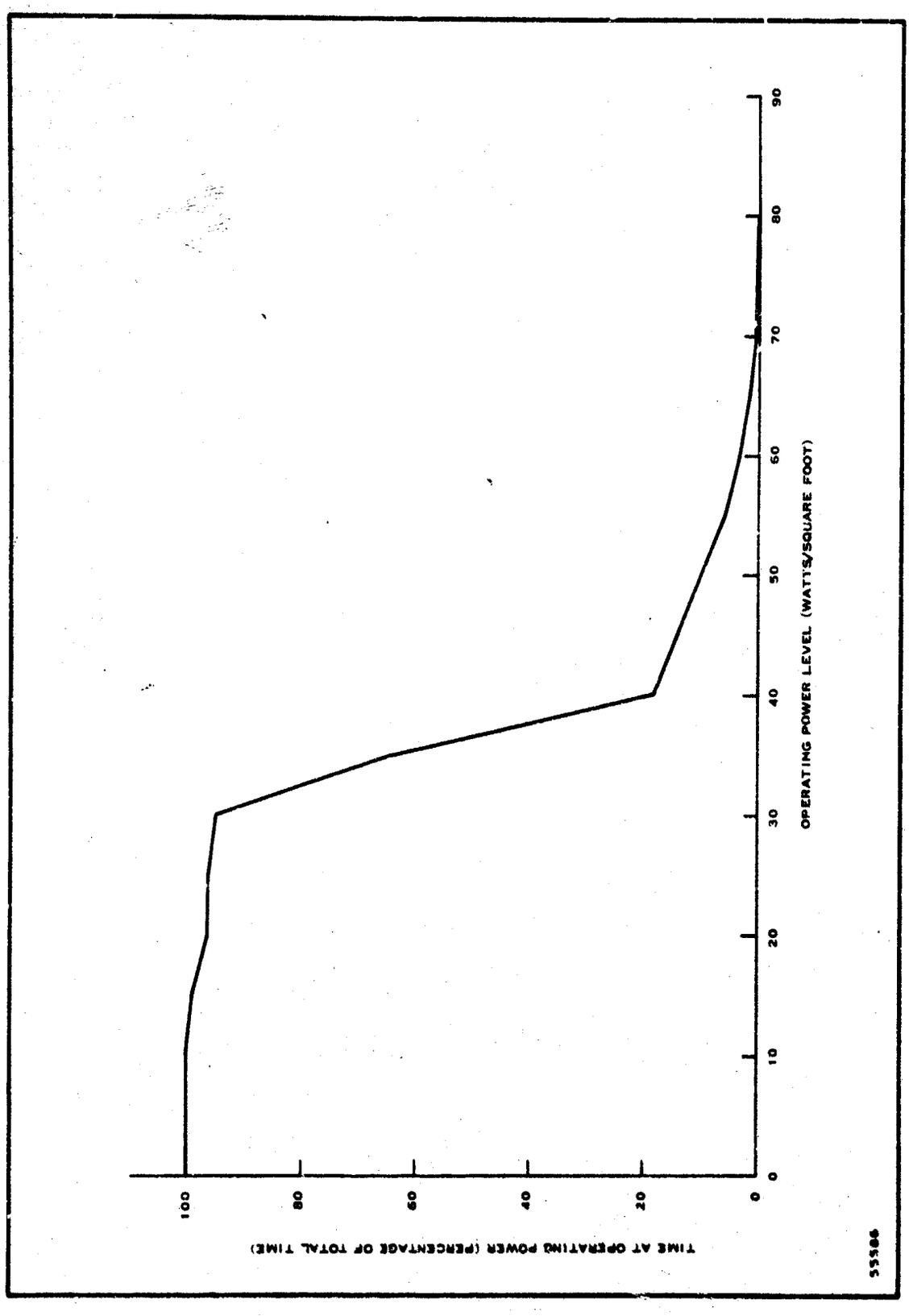

Figure B-11 Performance of No. 1078 (Operating Time: 590 Hours)

APPENDIX C

HEAT AND MASS BALANCE CALCULATIONS

APPENDIX C

HEAT AND MASS BALANCE CALCULATIONS

Presented in this appendix are the design basis and detailed calculations of heat and mass balances for the proposed 15-kilowatt fuel cell system. The process flow schematic shown in Figure C-1 summarizes the results of these calculations. Presented in Table C-I are process stream flow rates and compositions. Energy balances and overall efficiency of the 15-kilowatt system are tabulated in Table C-II at various power levels.

The design basis for the 15-kilowatt system is presented in Table C-III. The computer program reproduced in Table C-IV was used to calculate the anode exhaust composition, accounting for the effects of CO_2 diffusion, recycles, and fuel utilization as limited by H_2/H_2O ratio. The detailed calculations which follow show the derivation of the 15-kilowatt fuel cell system design.

1. Calculate required fuel consumption.

$$\frac{20{,}000 \text{ watts}}{0.7 \text{ volt}} = 28{,}571 \text{ amperes.}$$

$$28{,}571 \text{ amp} \times \frac{\text{gm mol } H_2}{(2)(96{,}500) \text{ amp sec}} \times \frac{\text{lb}}{454 \text{ gm}} \times \frac{3600 \text{ sec}}{\text{hr}} =$$

1.17387 lb mol H_2/hr.

2. From computer results, the following is derived.

Composition	Partial-Oxidizer Product (mole-percent)	Anode Exhaust (mole-percent)
H_2	22.386	9.193
CO	19.352	8.241
CO_2	5.067	12.833
H_2O	3.840	18.172
N_2	49.355	51.561
	100.000	100.000

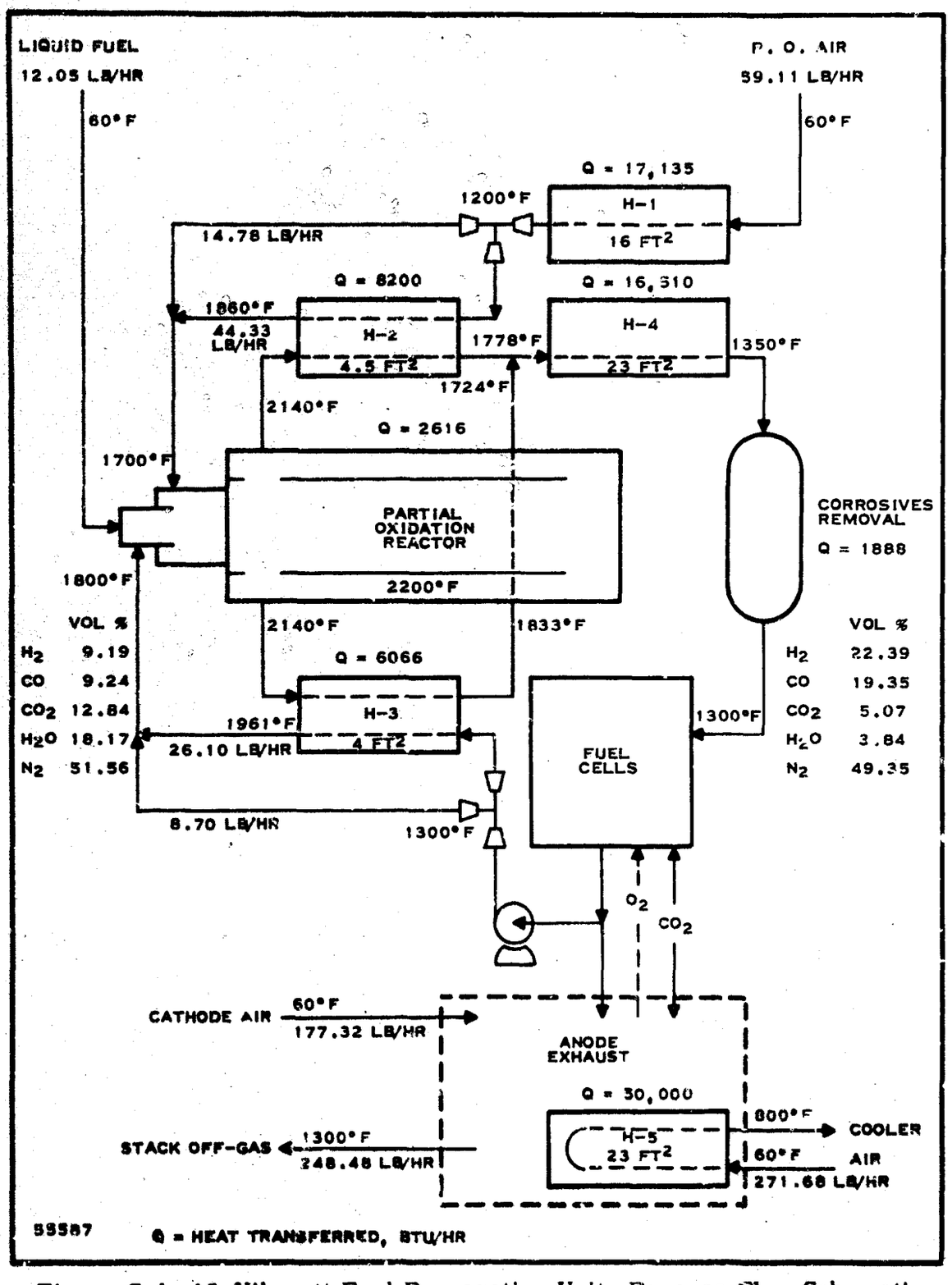

Figure C-1. 15-Kilowatt Fuel Preparation Unit, Process Flow Schematic

Table C-I. 15-Kilowatt Process Stream Flow Rates and Compositions

Component (lb moles per hr)	MW	PO Fuel	PO Air	Anode Exhaust Recycle	PO Product	Anode Exhaust Burnoff	Cathode Air	Stack Exhaust	Cooler Air
H_2	2			0.124	1.049	0.289			
CO	28			0.111	0.907	0.259			
CO_2	44			0.173	0.238	0.403		0.861	
H_2O	18			0.244	0.180	0.571		0.861	
N_2	28		1.619	0.694	2.313	1.619	4.857	6.476	7.45
O_2	32		0.430				1.291	0.430	1.98
$\cdot CH_2 \cdot$	14	0.861							
Total		0.861	2.049	1.346	4.687	3.141	6.148	8.628	9.43
Lbs/Hr		12.05	59.11	34.80	105.96	81.20	177.32	248.48	271.68

Table C-II. 15-Kilowatt System Energy Balance

A	F	V	VA	VA+Q_{box} (BTU/hr)	HV (BTU/hr less exhaust)	Total [lb (·CH_2·)/hr]	P_{net} = VA-1,250	Efficiency (Percent)	Q_{cooler} (BTU/hr)
0	--	--	0	25,000	--	2.115	--	--	--
32	0.540	39.46	1,250	29,268	--	2.476	0	0	--
50	0.844	39.16	1,958	31,685	9,976	2.681	708	4.8	--
100	1.687	38.32	3,832	38,084	19,940	3.222	2,582	14.6	--
150	2.531	37.48	5,622	44,196	29,916	3.739	4,372	21.2	--
200	3.374	36.64	7,328	50,021	39,881	4.232	6,078	26.1	--
250	4.218	35.80	8,950	55,559	49,857	4.700	7,700	29.8	--
300	5.061	34.96	10,488	60,811	59,821	5.145	9,238	32.6	--
325	5.483	34.54	11,226	63,330	64,809	= F	9,976	33.0	1,479
350	5.905	34.12	11,942	65,775	69,797	↓	10,692	32.9	4,022
400	6.748	33.28	13,312	70,453	79,761	↓	12,062	32.5	9,308
450	7.592	32.44	14,598	74,844	89,737	↓	13,348	31.9	14,893
500	8.436	31.60	15,800	78,948	99,714	↓	14,550	31.3	20,766
550	9.279	30.76	16,918	82,765	109,678	↓	15,668	30.7	26,913
600	10.123	29.92	17,952	86,296	119,654	↓	16,702	30.0	33,358
650	10.966	29.08	18,902	89,540	129,618	↓	17,652	29.2	40,078
700	11.810	28.24	19,768	92,496	139,594	↓	18,518	28.5	47,098
750	12.653	27.40	20,550	95,166	149,558	↓	19,300	27.7	54,392
800	13.497	26.56	21,248	97,550	159,535	↓	19,998	26.9	61,985
850	14.340	25.72	21,862	99,646	169,499	↓	20,612	26.1	69,853
900	15.184	24.88	22,392	101,456	179,475	↓	21,142	25.3	78,019

Q_{box} = 25,000

Table C-III. Design Basis

Air rate is adjusted to give 1.0 atomic ratio oxygen/carbon.
30 percent of anode exhaust is recycled to control carbon deposition.
Electrochemical fuel utilization is limited by the requirement that $H_2O/H_2 \leq 2.0$.
Assume a matrix thickness of 0.020 inch.
Gross output of 20 kilowatts is required to supply a 18.75-kilowatt load to inverter.
Average cell voltage decreases linearly from 1.0 volt at open circuit to 0.7 volt at rated load.
Hydrocarbon fuel is effectively $(\cdot CH_2 \cdot)_n$ and can be simulated by a blend 70 mole-percent n-heptane and 30 mole-percent toluene for calculation purposes.
Water-gas reaction ($CO + H_2O \rightleftharpoons CO_2 + H_2$) is at 700°C equilibrium during electrochemical reaction.
Assume zero methane and higher hydrocarbons in partial oxidizer exhaust.
Assume liquid fuel and air enter the fuel cell system at 60°F.
Assume a furnace temperature of 1300°F.
Assume a partial oxidizer adiabatic reaction temperature of 2200°F.

Table C-IV. Computer Program for the Effect of CO_2 Diffusion and Fuel Utilization on Anode Exhaust Composition (Sheet 1 of 2)

```
M195  M S 9AM3        36  90          FORTRAN SOURCE LIST                    10/17/67
      ISN      SOURCE STATEMENT

     0 $IBFTC
       C      PROGRAM WIOS BAN4,FTH IS MATRIX THICKNESS IN CMS.R IS FRACTION
       C      RECYCLED,J MULTIPLIED BY 2 IS PERCENT FUEL UTILIZED,Y IS INLET
       C      CARBON DEPOSITION EQUILIBRIUM,Z REPRESENTS H2O/H2 RATIO AND TCH2
       C      IS LBS. OF CH2 TO GIVE 100 CUFT. OF FUEL GAS,CAP IS CARBON EQUIL
       C      EXCLUDING CO2 TRANSPORT
              DIMENSION PH2(50),PCO(50),PCO2(50),PH2O(50),PN2(50),E(50),Z(50)
              DIMENSION CAP(50), FGAS(50)
            1 READ 10,PPH2,PPCO,PPCO2,PPH2O,PPN2,FTH,R
           10 FORMAT (7F10.5)
              PRINT 11,PPH2,PPCO,PPCO2,PPH2O,PPN2,FTH,R
           11 FORMAT (7F10.5)
            5 X=((1.54*PPCO*PPH2O)-(PPCO2*PPH2))/(PPH2+PPCO2+1.54*(PPCO+PPH2O))
              PH2(0)=PPH2+X
              PCO(0)=PPCO-X
              PCO2(0)=PPCO2+X
              PH2O(0)=PPH2O-X
              PN2(0)=PPN2
              Y=PCO(0)*PCO(0)/PCO2(0)*.01
              ARG=2.236*PH2(0)/(PH2O(0)*PCO2(0))
              E(0)=1.005+.04192*ALOG(ARG)
              PRINT 20,PH2(0),PCO(0),PCO2(0),PH2O(0),PN2(0),Y,E(0)
           20 FORMAT (7F10.5)
              FGAS(0)=100.
              J=0
              FU=.02
              AH2=PH2(J)*FU
              ACO=PCO(J)*FU
              FH2=PH2(J)
              FCO=PCO(J)
              FCO2=PCO2(J)
              FH2O=PH2O(J)
              FN2=PN2(J)
            2 FH2=FH2-AH2
              FCO=FCO-ACO
              FCO2=FCO2+AH2+2.*ACO
              FH2O=FH2O+AH2
              SUMA=FGAS(J)+AH2+ACO
              GCO2=FCO2/SUMA*100.
              ACO2=22.9*((GCO2-PCO2(J))/ALOG(GCO2/PCO2(J))*.01-.1)*.075/FTH
              J=J+1
              FGAS(J)=SUMA-ACO2
              FCO2=FCO2-ACO2
              PH2(J)=FH2/FGAS(J)*100.
              PCO(J)=FCO/FGAS(J)*100.
              PCO2(J)=FCO2/FGAS(J)*100.
              PH2O(J)=FH2O/FGAS(J)*100.
              PN2(J)=FN2/FGAS(J)*100.
              X=1.54*PCO(J)*PH2O(J)-PCO2(J)*PH2(J)
              X=X/(PH2(J)+PCO2(J)+1.54*(PCO(J)+PH2O(J)))
              SUMB=PH2(J)+PCO(J)+PCO2(J)+PH2O(J)+PN2(J)
              PRINT 15,ACO2,SUMA,FGAS(J),SUMB,X
           15 FORMAT (5F10.5)
              PH2(J)=PH2(J)+X
              PCO(J)=PCO(J)-X
```

Table C-IV. Computer Program for the Effect of CO_2 Diffusion and Fuel Utilization on Anode Exhaust Composition (Sheet 2 of 2)

```
MLOS   M S PAVS        16  NB            FORTRAN SOURCE LIST                 10/17/57
              SOURCE STATEMENT

              PCO2(J)=PCO2(J)+X
              PH2O(J)=PH2O(J)-X
              ARG=2.236*PH2(J)/(PH2O(J)*PCO2(J))
              E(J)=1.006+.04192*ALOG(ARG)
              CAR(J)=PCO(J)*PCO(J)/PCO2(J)*.01
              Z(J)=PH2O(J)/PH2(J)
              PRINT 40,PH2(J),PCO(J),PCO2(J),PH2O(J),PN2(J),CAR(J),E(J),Z(J),FGA
             1S(J),J
           40 FORMAT (9F10.5,1I10)
              IF (Z(J).GT.2.)GO TO 30
              IF (J.GT.40) GO TO 30
              GO TO 2
           30 J=J-1
              VOLR=R*FGAS(J)
              W=VOLR*.01
              TPH2=W*PH2(J)+(100.-VOLR)*.25767
              TPCO=W*PCO(J)+(100.-VOLR)*.25767
              TPCO2=W*PCO2(J)
              TPH2O=W*PH2O(J)
              PPN2=W*FN2(J)+(100.-VOLR)*.48466
              TF=TPH2+TPH2O
              PF=PPH2+PPH2O
              AF=ABS(TF-PF)
              CF=TPCO+TPCO2
              QF=PPCO+PPCO2
              BF=ABS(CF-QF)
              IF (AF.LT..01.AND.BF.LT..01) GO TO 60
              PPH2=TPH2
              PPCO=TPCO
              PPCO2=TPCO2
              PPH2O=TPH2O
              PRINT 12,W,VOLR
           12 FORMAT (2F10.5)
              GO TO 5
           60 TCH2=.0092*(100.-VOLR)
              PRINT 80,TCH2,R,VOLR
           80 FORMAT (3F10.5)
              GO TO 1
              END
```

NOTES

Anode exhaust represents 95.758 mole-percent of anode inlet flow.

Anode exhaust recycled is 30 percent of anode exhaust or 30 (0.95758) = 28.727 percent of partial-oxidizer product.

3. Calculate fuel utilization.

Basis: 100 moles to cell stack

Fuel to cell stack	= 22.386 + 19.352	= 41.738 moles.
Fuel in anode exhaust	= 0.95758(9.193 + 8.241)	= 16.694.
Fuel recycled	= 0.3(16.694)	= 5.008.
Fuel burned	= 0.7(16.694)	= 11.686.
Fuel consumed	= 41.738 − 16.694	= 25.044.
Once-through fuel utilization	$= \frac{25.044}{41.738} \times 100$	= 60.000%.
Total fuel utilization	$= \frac{25.044 \times 100}{41.738 - 5.008}$	= 68.184%

4. Calculate flow rates for process streams.

$$\cdot CH_2 \cdot \text{ rate} = \frac{1.17387 \text{ lb mol fuel (consumed)}}{\text{hr}} \times \frac{1}{0.68184 \text{ (consumed)}} \times \frac{\text{lb mol} \cdot CH_2 \cdot}{2 \text{ lb mol fuel}} =$$

0.86079 lb mol/hr.

O_2 rate = 0.5(0.86079) = 0.43040 lb mol/hr.

N_2 rate = $0.5(0.86079)\left(\frac{79}{21}\right)$ = 1.61915 lb mol/hr.

$$\text{Scale factor} = \frac{1.17387 \text{ lb mol } H_2 \text{ (consumed)}}{25.044 \text{ lb mol } H_2 \text{ (consumed)}} = 0.046872.$$

Recycle = 0.3(95.758)(0.046872) = 1.34651 lb mol/hr.

Burnoff = 0.7(95.758)(0.046872) = 3.14186 lb mol/hr.

5. Calculate process stream enthalpy, BTU/hr.

Enthalpy data are from catalog GC-245 published by Girdler Catalyst, Division of Chemetron Corporation or API Project 44. Enthalpy is defined as $H^\circ + H_o^\circ + \Delta H_{fo}^\circ$ where $H^\circ - H_o^\circ$ is the heat content, and ΔH_{fo}° is the heat of formation of the compound from its elements at 0°K. Gas stream enthalpies are shown in Table C-V at various temperatures.

6. Calculate adiabatic reaction temperature.

$$CH_2 + PO\ air + Recycle \rightarrow PO\ product$$

Temp, °F	60(L)	1,700	1,800	T
ΔH, BTU/hr	−4,651	32,736	−35,261	−7,176

$$T = 2200 + \frac{7,338 - 7,176}{15,337 - 7,338} \times 200 = 2204°F.$$

This is sufficiently close to the desired 2200°F.

7. Calculate PO reactor heat loss based on 2200°F outer skin temperature and 1300°F furnace temperature.

Reactor size: 5-inch diameter by 24 inches long

$$\text{Heat transfer area} = \frac{5 \times 24}{144} = 2.62 \text{ square feet.}$$

$$\Delta T = 2200 - 1300 = 900°F;\ T_{avg} = 1750°F.$$

$$K = 1.85 \frac{\text{BTU in.}}{\text{hr ft}^2\ °F} \text{ for Fiberfrax Lo-Con Blanket.}$$

$$Q = \frac{1.85}{2} (900)(2.62) = 2,180 \text{ BTU/hr.}$$

Increase by 20 percent for conduction, giving 2180 × 1.2 = 2616 BTU/hr.

Table C-V. 15-Kilowatt Process Stream Enthalpies at Various Temperatures

	Partial Oxidizer			Anode Exhaust		Cathode Air	Stack Exhaust
	Fuel	Air	Product	Recycle	Burnoff		
Flow, Lb Mol/Hr	0.8608	2.0496	4.6872	1.3465	3.1418	6.1484	8.6284
Enthalpy, BTU/Hr at:							
60°F	−4651*	7,401	–	–	–	22,202	−202,245
700°F	1064		–	−48,140	–	–	–
1000°F	3589	21,365	–	−44,806	–	–	–
1200°F	–	24,536	–	–	–	–	–
1300°F	6415	26,146	−42,456	−41,327	–	–	−118,145
1400°F	–	–	−38,680	–	–	–	–
1500°F	–	–	–	–	–	–	–
1600°F	–	31,050	−31,023	–	–	–	–
1700°F	–	32,736	–	–	–	–	–
1800°F	–	34,415	−23,236	−35,261	–	–	–
1900°F	–	36,104	–	–	–	–	–
2000°F	–	–	−15,337	−32,756	–	–	–
2100°F	–	–	–	–	–	–	–
2200°F	–	–	− 7,338	–	–	–	–

*Liquid is standard state. ΔH_v = 150 BTU/lb (Nelson-Petroleum Refinery Engineering).
Based on 70 mole-percent n-Heptane and 30 mole-percent toluene.

8. Calculate PO product temperature at reactor exit.

$\Delta H_{2204°F}$ − Heat loss → ΔH_T

−7176 − 2616 → 9792

$$T = 2000 + \frac{15,337 - 9,792}{15,337 - 7,338} \times 200 = 2139°F.$$

9. Size air preheater H-1.

PO Air	60°F	→	1200°F
Furnace Gas	1300°F		1300°F
ΔT, °F	1240		100
LMΔT		400	

$$Q = -H_{1200°F} - \Delta H_{60°F} = 24,536 - 7,401 = 17,135 \text{ BTU/hr.}$$

Estimate U = 2.5 BTU/hr ft^2 °F.

$$A = \frac{Q}{U\Delta T} = \frac{17,135}{(2.5)(440)} = 15.6 \text{ ft}^2.$$

Use 16 ft^2 of heat transfer surface.

10. Size air heater H-2

The desired air temperature entering the partial oxidizer is 1700°F. For control purposes, design H-2 to preheat 75 percent of the partial oxidizer air to a temperature such that, after mixing with the 25-percent air bypassing the heater, the combined stream will be at 1700°F.

	0.25 PO Air	+ 0.75 PO Air	→ PO Air
°F	1200	T	1,700
ΔH	0.25 (24,536)	0.75 (ΔH_T)	32,736

$0.75\ \Delta H_T = 32,736 - 0.25(24,536) = 26,602.$

$\Delta H_T = 26,602/0.75 = 35,469.$

$Q = 26,602 - 0.75(24,536) = 8,200$ BTU/hr.

$$T = 1800 + \frac{35,469 - 34,415}{36,104 - 34,415} \times 100 = 1862°F.$$

Assume use of 50 percent of partial-oxidizer product at 2139°F in H-2.

	(0.5) PO Product − Q	→	(0.5) PO Product
°F	2139		T
ΔH	0.5(−9,792) − 8,200		0.5 (ΔH_T)

$$\Delta H_T = \frac{0.5(-9,792) - 8,200}{0.5} = 26,192.$$

$$T = 1600 + \frac{31,023 - 26,192}{31,023 - 23,236} \times 200 = 1724°F.$$

Air	1200°F	→	1862°F
PO Product	1724°F	←	2139°F
LMΔT	390		

Estimate U = 5.

$$A = \frac{8200}{(5)(390)} = 4.2 \text{ ft}^2.$$

Use 4.5 ft^2 of heat transfer surface.

11. Size recycle heater H-3.

For temperature control, heat 75 percent of recycle to a temperature sufficient to give the desired temperature of 1800°F after recombination.

	0.25 Recycle +	0.75 Recycle →	Recycle
°F	1300	T	1,800
ΔH	0.25 (−41,327)	0.75 (ΔH_T)	−35,261

$$Q = 41,327 - 35,261 = 6,066.$$

$$\Delta H = \frac{-35,261 - 0.25(-41,327)}{0.75} = -33,239.$$

$$T = 1800 + \frac{33,239 - 35,261}{32,756 - 35,261} \times 200 = 1961°F.$$

Assume use of 50 percent of partial-oxidizer product at 2139°F in H-3.

	0.5 PO Product − Q	→	0.5 PO Product
°F	2139		T
ΔH	$0.5(-9,792) - 6,066$	→	$0.5\ (\Delta H_T)$.

$$\Delta H_T = \frac{0.5(-9,792) - 6,066}{0.5} = -21,924.$$

$$T = 1800 + \frac{21,924 - 23,236}{15,337 - 23,236} \times 200 = 1833°F.$$

Recycle	1300°F	→	1961°F
PO Product	1833°F	←	2139°F
LMΔT	320		

Estimate U = 5.

$$A = \frac{6066}{(5)(320)} = 3.8.$$

Use 4 ft^2 of heat transfer surface.

12. Size partial-oxidizer product cooler H-4.

Assume the product cooler outlet is 1350°F and that the partial-oxidizer product is cooled from 1350° to 1300°F in the corrosives removal vessels and lines.

	0.5 PO Product +	0.5 PO Product − Q	→	PO Product
°F	1724	1833		1,350
ΔH	0.5 (− 26,192)	$0.5\ (-21,924) - Q$	→	−40,568

$Q = 40,568 - 13,096 - 10,962 = 16,510$ BTU/hr.

PO product temperature at H-4 inlet = $\frac{1724 + 1833}{2}$ = 1778°F.

PO Product	1778°F	→	1350°F
Furnace	1300°F		1300°F
LMΔT	178		

Estimate U = 4.

$$A = \frac{16,510}{(4)(178)} = 22 \text{ ft}^2.$$

Use 23 ft^2 of heat transfer surface.

13. Calculate heat transferred in corrosives removal vessel and lines.

	PO Product − Q	→	PO Product
°F	1,350		1,300
ΔH	−40,568		−42 456

Q = 42,456 − 40,568 = 1,888 BTU/hr.

14. Calculate cathode air rate for CO_2/O_2 = 2.0.

$$CH_2 + O_2 + N_2 \rightarrow CO_2 + H_2O + O_2 + N_2$$

PO + cathode	0.8608	1.7216	6.4764	0.8608	0.8608	0.4304	6.4764
− PO		0.4304	1.6192				
Cathode, lb mol/hr		1.2912	4.8572				

15. Calculate box heat losses.

Eagle-Picher Insulation Conductivity, $\frac{\text{BTU-in.}}{\text{Hr ft}^2\ ^\circ\text{F}}$

Mean Temperature (°F)	Ceramic Fiber Block	Superglas 1800
400	0.39	0.27
600	0.48	0.37
800	0.58	0.48
1000	0.70	0.59
1100	0.76 (est)	
1150	0.80 (est)	

Assume: 1-inch ceramic fiber inside exposed to 1300°F furnace atmosphere with 1-inch Superglas 1800 between ceramic fiber and outside shell. Estimate outside shell temperature as 200°F.

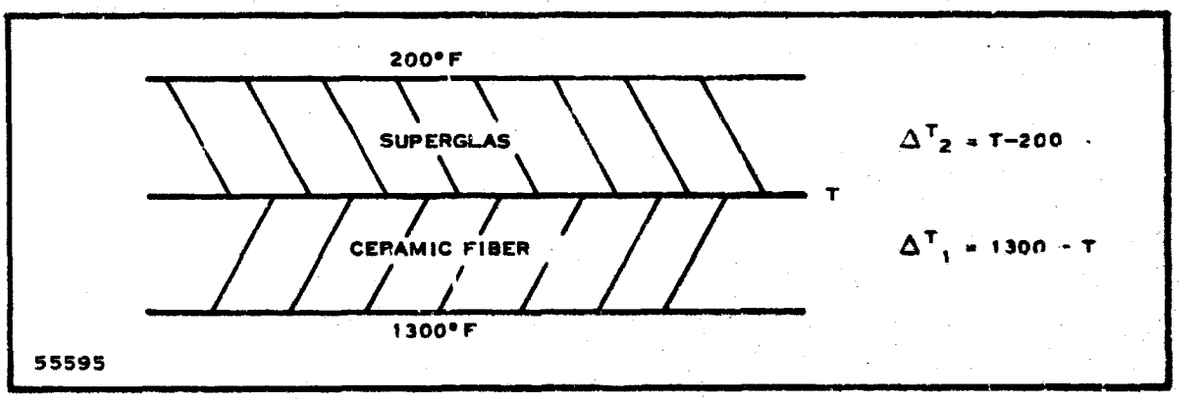

Estimate heat loss of 275 BTU/hr ft^2 and T of 950°F.

$$Q_{ceramic} = 275\ \frac{\text{BTU}}{\text{hr ft}^2} = K\Delta T_1 .$$

$$K = 0.78 \text{ at } 1125^\circ\text{F mean.}$$

$$\Delta T_1 = 275/0.78 = 352^\circ\text{F versus } 350^\circ \text{ estimated.}$$

$$Q_{Superglas} = 275 \frac{BTU}{hr\ ft^2} = K\Delta T_1 .$$

$K = 0.36$ at 575°F mean.

$\Delta T_2 = 275/0.36 = 764°F$ versus 750° estimated.

Therefore, Q of box is 275 BTU/hr ft^2. Outer box dimensions are 46 by 42 by 45 inches giving an outer area of 81.7 ft^2.

$Q = 275(81.7) = 22{,}500$ BTU/hr.

Plus 2500 BTU/hr estimated leakage through plumbing and voltage taps gives a total box heat loss of 25,000 BTU/hr.

17. Calculate cooling air rate.

Based on 1 lb mol air,

Component	Lb Mol/Hr	BTU/Lb Mol	
		800°F	60°F
O_2	0.21	9101	3607
N_2	0.79	8863	3612
BTU/lb mol air		8913	3611

$$\frac{50{,}000 \text{ BTU/hr}}{(8913 - 3611) \text{ BTU/lb mol air}} = 9.43 \text{ lb mol air/hr.}$$

18. Calculate system energy balance.

U = Fuel utilization

F = Lb ($\cdot CH_2 \cdot$)/hr required at 68.184 percent utilization

V = System voltage

A = System amperes

P_{net} = Kilowatts to inverter

$$\cdot CH_2 \cdot + 1/2\ O_2 \rightarrow CO + H_2.$$

$$14\ \text{lbs}\ \cdot CH_2 \cdot \rightarrow 4\ \text{lb eqv of fuel as}\ H_2.$$

$$\frac{96{,}500\ \text{amp sec}}{\text{gm eqv}} \times \frac{454\ \text{gm}}{\text{lb}} \times \frac{\text{hr}}{3600\ \text{sec}} = 12{,}170\ \frac{\text{cell amp hr}}{\text{lb eqv}}.$$

$$\text{System amperes} = \frac{\text{cell amp}}{40\ \text{series cells}}$$

$$F = \left[\frac{40}{(12{,}170)}\right]\left[\frac{14}{4(0.68184)}\right] \times A = 0.01687 \times A.$$

The lower heating value of $\cdot CH_2 \cdot$ is 18,800 BTU/lb. Heat carried out by stack exhaust is

$$\frac{202{,}245 - 118{,}145}{(0.8608)\ (14)} = 6{,}980\ \text{BTU/lb}\ (\cdot CH_2 \cdot).$$

Therefore, heat liberated into enclosure including electrical equivalent is 18,800—6980 = 11,820 BTU/lb ($\cdot CH_2 \cdot$).

Assuming that system voltage decreases linearly with current from 40.0 volts at 0 amperes to 28 volts at 714 amperes,

$$V = 40 - \frac{12}{714} \times A$$

$$V = 40 - 0.0168 \times A.$$

$$\text{Efficiency} = \frac{P_{net}\ (3414)100}{F(18{,}800)} = 18.162\ \frac{P_{net}}{F}$$

The results of these calculations are tabulated in Table C-II.

APPENDIX D

DESIGN WEIGHT CALCULATIONS

APPENDIX D

DESIGN WEIGHT CALCULATIONS

This section presents the basis and calculations involved in estimating the weight of the 15-kilowatt fuel cell system. Obviously, these weights are only approximate since many individual components are not completely defined and a detailed engineering design would be required for accurate weight analysis. However, these weight estimates represent our best judgments based on 1-kilowatt system experience and preliminary design calculations.

Fuel cell module weight will be reduced as power density increases. At increased power density, the number of modules will be reduced as well as the enclosure volume. Reductions in weight of system components will require detailed engineering evaluation and analysis with respect to the system goals.

The basis and calculations of weight are summarized below.

1. Fuel Cell Stack:

   a. Modules, 24 Required.

Item	Component	Ft^2/Cell	Lb/Cell	Lb/Module
1	Cathode channel	0.0291	0.0122	2.20
2	Cathode electrodes	0.367	0.0620	11.10
3	Cathode silver	0.367	0.0033	0.60
4	Anode flange	0.0252	0.0106	1.91
5	Anode electrode	0.515	0.0725	13.07
6	Matrix	--	0.1010	18.20
7	End channels	0.0115	0.0048	0.86
8	$NaLiCO_3$	--	0.0590	10.62
9	End plates	--	--	0.50
10	Plenums	--	--	2.45
11	Couplings	--	--	0.46
12	Sealant	--	0.0031	0.56
13	Total (Pounds) =			62.53

NOTES

Each fuel cell module consists of 18 3- by 8-inch cells arranged in parallel and 10 blocks of 18 each connected in series. Total effective area per module is 30 square feet.

Items 1, 4, and 7 are made of 10-mil (0.010 inch) 446 S.S. strip.

Item 2: It is assumed that the cathode electrodes can be successfully made of thin (0.004 inch) strip stock which has been perforated with many slits in an expanded metal punch press.

Item 3: It is assumed that a silver "strike" on the dual cathode will operate as well as the silver plate now used. A silver strike will require only 10 percent of the silver used for a silver plate.

Item 5: It is assumed that the anode screen can be replaced with electroformed nickel strip 4 mils (0.004 inch) thick and containing 25 percent openings.

Total weight of modules = 24 × 62.53 = 1500 lbs

b. Headers and Manifolds

Inlet and intermediate = 8 × 3 lbs ea (est) = 24 lbs

Burnoff = 2 × 4 lbs ea (est) = 8 lbs

Total weight for headers and manifolds = 32 lbs

c. Connectors

Current leads: 12 ft of 1/2-inch copper rod at 0.759 lbs/ft = 9.1 lbs

Other internal connections = 6.9 lbs

Total weight for connectors = 16 lbs

d. Supports

Bracket or side panels - 4 required

Make in 4 stacked sections with 3/4 by 3/4 by 1/8 316 S.S. angle frame 41 inches long and stacked height of 40 inches. Use two intermediate supports of 3/4 angle. Face with 1/32 316 S.S. sheet

Angle at 0.59 lbs/ft:

$8 \times 41 + 4 \times 40 = 488 \div 12 \times 0.59$ 24 lbs/panel

Sheet at 1.31 lbs/ft^2:

$(41 \times 39) \div 144 \times 1.31 = 14.6$ lbs/panel

Weight per system:

4 (38.6) = 154.4; use 155 lbs

Hangers - 32 required

1/8 by 5/8 bar, 316 S.S. at 0.213 lbs/ft:

Use 23 inches of bar/hanger or 0.5 lb/hanger; 32×0.5 = 16 lbs

Hanger rods - 32 required

3/16-inch S.S. rod at 0.094 lbs/ft^2:

Each uses 48 inches of rod

$32 \times 48 \times 0.094 \div 12$ = 12 lbs

Miscellaneous (nuts, ceramic, etc.) = 2 lbs

Total weight for supports = 185 lbs

2. Fuel Preparation System

a. Reactor: 0.062 Inconel at 2.62 lbs/ft^2.

Three tubes, 5-inch dia by 24-inch length, 4- and 3-inches dia by 21-inch length; require 840 in.^{2} of sheet.

Two ends require 40 in.^{2} of sheet.

Use $880 \times 2.625 \div 144 = 16$ lbs sheet.

Inlet and outlet connection = 4 lbs.

Total weight for reactor = 20 lbs

b. Preheaters, air and recycle (est 1 lb/ft^2 of surface)

H-1: 16 ft^2 surface at 16 lbs
H-2: 4.5 ft^2 surface at 5 lbs
H-3: 4.0 ft^2 surface at 5 lbs

Total weight for preheaters = 26 lbs

c. Vaporizer, estimated at — 2 lbs

d. Corrosive remover

Basis is 50 hours operation between changes at 12 lbs/hr of CITE at maximum of 0.4 weight-percent sulfur.

$50 \times 12 \times 0.004 = 2.4$ lbs sulfur.

Assume adsorbent capacity of 6.0 weight-percent.

$2.4/0.06 = 40$ lbs adsorbent required.

Estimated 10 lbs for container.

Total weight for corrosive remover = — 50 lbs

e. Fuel cooler

H-4: 23 ft^2 surface at 1 lb/ft^2, estimated at — 23 lbs

f. P.O. blower and meter, estimated at — 30 lbs

g. Fuel pump, estimated at — 5 lbs

h. Ignitor — 1 lb

i. Recycle blower and motor, estimated at — 20 lbs

j. Miscellaneous plumbing, estimated at — 15 lbs

3. Cathode Composition System

a. Blower, estimated at — 10 lbs

b. Circulation fans, mounts, drive — 60 lbs

c. Baffles - 316 S.S. sheet 1/16 inch at 2.625 lbs/ft^2. Esimated area equal to base of system, $38 \times 41 \times 2.625 \div 144 =$ — 28 lbs

4. Temperature Control System

a. Temperature sensor, estimated at — 2 lbs

b. Heat exchanger, box cooler

H-5: 23 ft^2 surface at estimated 1 lb/ft^2 = — 23 lbs

c. Blower, estimated at — 10 lbs

d. Control, estimated at — 2 lbs

5. Startup System

a. Burner, estimated at 30 lbs

b. Blower, estimated at 50 lbs

c. Ignitor, estimated at 2 lbs

d. Fuel pump, estimated at 4 lbs

e. Battery and charger

Charger, estimated at 10 lbs

Battery - must supply 2000 watts for 30 minutes or 1000 watt-hours. Assume NiCd batteries with 10 watt-hours per lb. Battery weight is 100 lbs

Total weight of battery and charger = 110 lbs

6. Enclosure

a. Outer shell:

Base—42 × 45 in. of 3/32 steel sheet at 0.293 lbs/in.^{3}:

$42 \times 45 \times 0.094 \times 0.293$ = 52 lbs

Sides and Top—0.10 aluminum sheet at 1.41 lbs/ft^2:

$2 \times 45 \times 46 = 4130$

$2 \times 42 \times 45 = 3780$

$1 \times 45 \times 42 = \underline{1890}$

$9800 \div 144 \times 1.41$ = 96 lbs

Reinforcing rib—0.10 aluminum sheet, 3 per face and 4 on top:

$16 \times 46 \times 3 \div 144 \times 1.41$ = 22 lbs

Connectors, bolts, etc., estimated at 10 lbs

Total weight of outer shell = 180 lbs

b. Insulation:

Base—1 in. glasrock at 25 lbs/ft^3:

$1 \times 42 \times 45 \times 25 \div 1728$ = 27 lbs

1 in. Eagle Picher Superglas at 11 lbs/ft^3:

$1 \times 42 \times 45 \times 11 \div 1728$ = 12 lbs

Sides–2 in. of Eagle Picher Superglas 1800 at 11 lbs/ft^3:

$2 \times 45 \times 46 \times 2 = 8300$

$2 \times 38 \times 46 \times 2 = 7000$

$38 \times 41 \times 2 = 3200$

$18,500 \div 1728 \times 11 = 118$ lbs

Insulation Supports–1/16 316 S.S. at 2.625 lbs/ft^2:

$1 \times 46 \times 1/16$-inch strips

4 strips per side and top

$20 \times 1 \times 46 \times 2.625 \div 144 = 17$ lbs

316 S.S. bolts at 2 lbs/100 = 3 lbs

Total weight of insulation = 177 lbs

c. Personnel protection esimated at 5 lbs

d. Support and skid frame

2 5-ft I-beams, 5-inch (0.210 × 3.00) aluminum at 3.42 lbs/ft = 34 lbs

2 steel wear plates - 5 ft by 1/4 inch by 4 inches at 0.293 lbs/cu. in. = 35 lbs

X-frame - 110 inches of 3-inch (0.170 by 2.33) aluminum I-beam at 1.96 lb/ft = 18 lbs

2 crossties - 3 ft of 3-inch (0.170 by 1.41) aluminum channel at 1.42 lbs/ft = 9 lbs

Total weight of support and skid frame = 96 lbs

7. Controls and Instruments

Instruments, estimated at 7 lbs

Transformers, 2, estimated at 5 lbs

Control Circuitry, estimated at 50 lbs

Total weight of controls and instruments = 62 lbs

8. Miscellaneous

a. Fuel tank, estimated at — 5 lbs

b. Control panel and frame

Size: 42 × 46 × 8 inches

Frame of 3/4 × 3/4 × 1/8 angle aluminum at 0.2 lb/ft:

$4 (42 + 46) \div 12 \times 0.2 = 5.9$ lbs

Sides of 0.1 aluminum sheet at 1.41 lb/ft^2:

$8 \times 2(42 + 46) \div 144 \times 1.41 = 14.0$

$2 \times 42 \times 46 \div 144 \times 1.41 = 37.8$

Total weight of control panel and frame — 57.7 lbs use — 58 lbs

c. Wiring, electrical items, estimated at — 35 lbs

Total weight of fuel cell system = 2874 lbs

DEPARTMENT OF THE ARMY
U. S. Army Mobility Equipment
Research and Development Center
Fort Belvoir, Virginia 22060

Postage and Fees Paid
Department of the Army

Official Business

THIRD CLASS MAIL

Security Classification

DOCUMENT CONTROL DATA - R&D

(Security classification of title, body of abstract and indexing annotation must be entered when the overall report is classified)

1. ORIGINATING ACTIVITY (Corporate author)	2a. REPORT SECURITY CLASSIFICATION
Texas Instruments Incorporated, Dallas, Texas	Unclassified
	2b. GROUP

3. REPORT TITLE

Engineering Design and Development Study of 15-kW Hydrocarbon-Air Fuel Cell Electric Power Plant

4. DESCRIPTIVE NOTES *(Type of report and inclusive dates)*

Final Report, September 1966 to July 1967

5. AUTHOR(S) *(Last name, first name, initial)*

Truitt, James K.; Bawa, Mohendra S.; Goodman, Robert C.; Gray, Foster L.; Kroeger, Henry R.; Kuehne, Walter (NMI); and Wood, Rodney R.

6. REPORT DATE	7a. TOTAL NO. OF PAGES	7b. NO. OF REFS
January 1968	230	

8a. CONTRACT OR GRANT NO.	9a. ORIGINATOR'S REPORT NUMBER(S)
DA-44-009-AMC-1806(T)	U2-202452-2
b. PROJECT NO.	
c.	9b. OTHER REPORT NO(S) *(Any other numbers that may be assigned this report)*
d.	

10. AVAILABILITY/LIMITATION NOTICES This document is subject to special export controls and each transmittal to foreign governments or foreign nationals may be made only with prior approval of Mobility Equipment Command Research and Development Center, Power Equipment Div., SMEFB-EP; Ft. Belvoir, Va. 22060.

11. SUPPLEMENTARY NOTES	12. SPONSORING MILITARY ACTIVITY
	United States Army Mobility Equipment Research & Development Center Ft. Belvoir, Virginia

13. ABSTRACT

Critical subsystems and components representing elements of a 15-kilowatt partial-oxidation molten carbonate fuel cell power generating system were designed, fabricated and tested to establish overall feasibility of the 15-kilowatt design. Testing was carried out generally at the 1-kilowatt size. The elements tested were the fuel cell module or stack, partial-oxidation fuel preparation subsystem including fuel vaporization using combat gasoline and CITE fuel, startup burner on both fuels, corrosives removal from the fuel gas stream, and the spent fuel recycle blower. Results of testing these units indicate that the design concept is feasible and attainable.

DD FORM 1 JAN 64 1473

Security Classification

14. KEY WORDS	LINK A		LINK B		LINK C	
	ROLE	WT	ROLE	WT	ROLE	WT
Molten carbonate						
Fuel cells						
Partial oxidation						
Hydrocarbon fuel						
Power generator						

INSTRUCTIONS

1. ORIGINATING ACTIVITY: Enter the name and address of the contractor, subcontractor, grantee, Department of Defense activity or other organization *(corporate author)* issuing the report.

2a. REPORT SECURITY CLASSIFICATION: Enter the overall security classification of the report. Indicate whether "Restricted Data" is included. Marking is to be in accordance with appropriate security regulations.

2b. GROUP: Automatic downgrading is specified in DoD Directive 5200.10 and Armed Forces Industrial Manual. Enter the group number. Also, when applicable, show that optional markings have been used for Group 3 and Group 4 as authorized.

3. REPORT TITLE: Enter the complete report title in all capital letters. Titles in all cases should be unclassified. If a meaningful title cannot be selected without classification, show title classification in all capitals in parenthesis immediately following the title.

4. DESCRIPTIVE NOTES: If appropriate, enter the type of report, e.g., interim, progress, summary, annual, or final. Give the inclusive dates when a specific reporting period is covered.

5. AUTHOR(S): Enter the name(s) of author(s) as shown on or in the report. Enter last name, first name, middle initial. If military, show rank and branch of service. The name of the principal author is an absolute minimum requirement.

6. REPORT DATE: Enter the date of the report as day, month, year, or month, year. If more than one date appears on the report, use date of publication.

7a. TOTAL NUMBER OF PAGES: The total page count should follow normal pagination procedures, i.e., enter the number of pages containing information.

7b. NUMBER OF REFERENCES: Enter the total number of references cited in the report.

8a. CONTRACT OR GRANT NUMBER: If appropriate, enter the applicable number of the contract or grant under which the report was written.

8b, 8c, & 8d. PROJECT NUMBER: Enter the appropriate military department identification, such as project number, subproject number, system numbers, task number, etc.

9a. ORIGINATOR'S REPORT NUMBER(S): Enter the official report number by which the document will be identified and controlled by the originating activity. This number must be unique to this report.

9b. OTHER REPORT NUMBER(S): If the report has been assigned any other report numbers *(either by the originator or by the sponsor)*, also enter this number(s).

10. AVAILABILITY/LIMITATION NOTICES: Enter any limitations on further dissemination of the report, other than those imposed by security classification, using standard statements such as:

(1) "Qualified requesters may obtain copies of this report from DDC."

(2) "Foreign announcement and dissemination of this report by DDC is not authorized."

(3) "U. S. Government agencies may obtain copies of this report directly from DDC. Other qualified DDC users shall request through _____."

(4) "U. S. military agencies may obtain copies of this report directly from DDC. Other qualified users shall request through _____."

(5) "All distribution of this report is controlled. Qualified DDC users shall request through _____."

If the report has been furnished to the Office of Technical Services, Department of Commerce, for sale to the public, indicate this fact and enter the price, if known.

11. SUPPLEMENTARY NOTES: Use for additional explanatory notes.

12. SPONSORING MILITARY ACTIVITY: Enter the name of the departmental project office or laboratory sponsoring *(paying for)* the research and development. Include address.

13. ABSTRACT: Enter an abstract giving a brief and factual summary of the document indicative of the report, even though it may also appear elsewhere in the body of the technical report. If additional space is required, a continuation sheet shall be attached.

It is highly desirable that the abstract of classified reports be unclassified. Each paragraph of the abstract shall end with an indication of the military security classification of the information in the paragraph, represented as *(TS), (S), (C), or (U)*.

There is no limitation on the length of the abstract. However, the suggested length is from 150 to 225 words.

14. KEY WORDS: Key words are technically meaningful terms or short phrases that characterize a report and may be used as index entries for cataloging the report. Key words must be selected so that no security classification is required. Identifiers, such as equipment model designation, trade name, military project code name, geographic location, may be used as key words but will be followed by an indication of technical context. The assignment of links, rules, and weights is optional.